THE EFFECTS OF HYDROGEN, OXYGEN AND WATER VAPOUR ON THE WORK FUNCTION AND RESISTANCE OF TITANIUM FILMS

A thesis submitted for the degree of
Doctor of Philosophy at the
University of Keele

by

K. Kandasamy B.Sc.(Cey)

Physics Department
University of Keele,
Keele, Staffordshire,
England

July 1980

The following was redacted from this digital copy of the original thesis at the request of the awarding university:

Appendix I (journal articles)

Appendix J (journal article)

ACKNOWLEDGEMENTS

The Author wishes to express his gratitude to Professor W. Fuller for the provision of laboratory facilities, Dr. N. A. Surplice for his excellent supervision, invaluable assistance and constructive guidance throughout this work, Professor K. Kunaratnam* for his interest and encouragement, Mr. F. Rowerth and his technical staff for their constant assistance throughout this work; in particular Mr. G. Dudley and the staff of the workshop for their helpful assistance in design works.

My colleagues and friends for their helpful discussions and suggestions.

The University of Keele for providing financial support in the form of a departmental studentship and part-time demonstratorship.

The University of Jaffna, Sri Lanka for the study leave, and to Mrs. S. Cooper and Mrs. B. Haywood for their care and cooperation in typing this thesis.

* Professor of Physics, University of Jaffna, Jaffna, Sri Lanka.

Preface

Technologists have recently become interested in metallic hydrides because these substances can be used to store hydrogen which could possibly be used as a fuel. Physicists are mainly interested in the thermodynamic and electronic properties of metallic hydrides, but many of these properties are of prime importance for the storage of hydrogen. Examples of such properties are: density of H atoms in the hydride, the temperature and enthalpy for hydride formation and dissociation, the kinetics of the hydrogen exchange reaction and its sensitivity to impurities, and the electronic nature of the metal-hydrogen bonding (Physics Bulletin 1977 June). One of the most promising hydrides for technological purposes is TiFeH and many of its properties depend on its base hydride which is titanium hydride. Titanium hydride might also be used for a neutron moderator, and for electrodes in fusion reactors. The interaction of hydrogen with titanium is technologically useful as a vacuum getter, but a nuisance in the embrittlement of Ti-based metal alloys. Interest in the fundamental electronic properties of metallic hydrides has recently been stimulated by the publication of band structure calculations with which they can be compared. Previously workers used only the rigid band approximation for the solid and an anionic or protonic model for the hydrogen in it. However Switendick recently calculated the band structures for several metallic hydrides, including titanium hydride. All these characteristics led to the author's interest in working on the titanium-hydrogen system.

It has been recognized in previous work that an impurity either on the surface or in the bulk of titanium samples, has a significant effect on hydrogen sorption. Titanium is a very active element and it is normally covered with oxygen and other impurities. A complete removal of oxygen impurities from titanium single crystals is a very difficult problem. Further, little or nothing in experimental

information would have been gained by using single crystals in this titanium-hydrogen study because after a small amount of hydrogen sorption they would become polycrystalline due to the difference in crystal structure of titanium hydride (F.C.C.) from titanium (H.C.P.). It is also noteworthy here that excellent agreement was observed between the resistivity curves obtained by hydriding single crystal and polycrystalline samples of Ce (Libowitz, 1972) [the structure of cerium (F.C.C.) is the same as in cerium hydride up to the composition CeH_3]. Therefore films of titanium were used in this work and they were prepared by evaporating titanium from high purity (99.9%) titanium filaments onto glass substrates in ultra-high vacuum ($< 5 \times 10^{-9}$ torr). The surface cleanliness of titanium films which had been prepared in exactly the same way was confirmed previously by A.E.S. (Surplice et al., 1978).

Later, this study was extended to include the interaction of oxygen with titanium films and water vapour with titanium films. Previous studies of oxygen interaction with titanium had been limited to low exposures and low pressures. In this work therefore a large range of exposures and the effect of high pressures were investigated. The water vapour study is a new entry in the field, and has scientific interest because water vapour is the major residual gas in high vacuum.

In this thesis, an outline of the physics which is relevant to the field of research is given in chapter one. In the second chapter the apparatus used, and the experimental methods are described. The next two chapters are about the hydrogen study; chapter three describes the previous work on metal/hydrogen and titanium/hydrogen systems; chapter four describes the author's work on titanium/hydrogen systems. Oxygen/titanium and water vapour/titanium studies are described in chapter five and chapter six respectively. Final remarks are given in chapter seven.

CONTENTS

ABSTRACT

The changes of work function; ϕ and resistance; R of titanium films were measured in U.H.V. at room temperature, when hydrogen, oxygen and water vapour interacted with them. The interaction of hydrogen reduced R by 30% after an initial increase of 1% of its initial resistance R_0. The initial increase of ϕ by 50meV was followed by a decrease of 300meV and then by an increase of 125-150meV. It was found that the high composition hydride ($> TiH_{1.9}$) was unstable in high vacuum and the dissociation pressure of TiH_2 was 2×10^{-3} torr at room temperature. The F.C.T/F.C.C. transition of the high composition hydride was investigated within the temperature range 20-75°C and the transition temperature of TiH_2 was deduced as 110°C. The correlation and variation of ϕ and R are explained qualitatively from features of the conduction band and crystal structures. The chemical boundaries of titanium-hydrogen alloy are deduced, and a phenomenological model is proposed to account for the electronic nature of titanium hydride. The experimental results are compared with the predictions of the theoretical models available and general agreement is observed.

The interaction of oxygen with titanium films gave a maximum increase of ϕ 1.2eV and a large increase of R (> 20%) and an equilibrium pressure $P \sim 10^{-4}$ torr. When P was raised above 10^{-4} torr R increased slowly but ϕ decreased by 0.5-0.8eV. An explanation for these changes of ϕ and R is given which is consistent with the different chemical phases of Ti-O alloy, and a mechanism is proposed for the diffusion of oxygen atoms into the titanium lattice. The interaction of water vapour reduced ϕ by 950meV and increased the R by $\sim$ 10-20% at an equilibrium pressure $P \sim 10^{-2}$ torr. Above this pressure the resistance increased slowly but ϕ increased by 500-600meV. An explanation is given in terms of dissociative chemisorption of water molecules, solution of oxygen atoms in the titanium lattice, and the formation of an hydroxyl complex at the surface. The work function of 60 clean titanium films was distributed in the range from 4.0eV to 5.3eV; the nature of this distribution is discussed.

CHAPTER 1

Field of Research and Theory of Technique

1.1 Surface Science

The electronic, mechanical and chemical properties of solid surfaces are important for physicists, chemists, metallurgists, material scientists and electronic engineers. However it is only recently that these studies started to have great attention from scientists. The reasons for the delay are understandable. Primarily scientists have been interested in the bulk properties of solids, therefore they ignored the surface effects, since the amount of surface atoms is negligible e.g. 1 cm^3 solid has only one surface atom for each 10^8 bulk atoms. Secondly only in the last decade have experimental surface studies become reproducible, [probably] due to the advancement of vacuum technology.

What is the speciality of a solid surface? What is the difference between the bulk and surface positions of an atom? Fundamentally an atom at the surface misses half of its neighbours and is influenced by the surrounding atoms or molecules in the gas phase. This different and asymmetrical neighbourhood is the reason for the surface having different electronic properties from the bulk and a more active nature in forming a bond with foreign atoms. Even if we are interested only in bulk properties we are still forced to deal with surface whenever a measurement removes an electron from solid. The energy required to extract an electron even, one which originates deep in the interior, is determined by the surface as well as bulk. This is because there are distortions in the electronic charge distribution near the surface that, because of the long range of the coulomb potential, affect the energies of levels far inside. Such effects are critical to the understanding of contact potential, thermionic emission, photoelectric effect and any other phenomena in which electrons are removed from a solid, such as electron spectroscopy. In describing

such a phenomena an important part is played by the work function. The main aim of this work is determination of changes of work function, therefore a critical discussion about it is presented in the next section.

The activity of the surface in forming bondswith foreign atoms leads to the studies of adsorption, catalysis and metallic corrosion. Adsorption means that a foreign atom or molecule becomes bound at the surface. This phenomena has been investigated both experimentally and theoretically. Most of these studies are of the geometrical and electronical structures of adsorbed layers and the correlation of this information with other parameters like bond energy, charge transfer etc. At present the developments in theory lag far behind the experiments. The theoretical study started with Lennerd-Jones's (1932) classical model for adsorption. Three years later Gurney (1935) proposed a quantum mechanical treatment for gas adsorption. Modern chemisorption theories try to account mainly for the electronic nature of the surface. There are at present two principal quantum mechanical approximations, which are molecular orbital theory (Grimley, 1967; Newns, 1970) and valency bond theory (Schrieffer et al., 1971). However these theoretical calculations are expensive in computing time. Some simplified models, the so called cluster calculations were developed by various workers but because of the simplification these calculations are not exact. Recently a third approach the so called density functional analysis was developed by Lang et al. (1975). They have succeeded in describing adsorption on the jellium model of a metal; however the application of their method to a complex metal like a transition metal is questionable.

There has recently been a rapid advance in experimental studies, mainly due to advances in technology. The basic idea of monolayer adsorption was introduced by Langmuir in 1916, and the importance of surface contamination was shown by Roberts in 1935, but the low pressures needed to avoid rapid contamination, were not measureable before the

invention of the Bayerd Alpert gauge in 1947. The pumping techniques needed to reach ultra high vacuum ($\lesssim 10^{-9}$ torr) were developed by Venema (1959), who showed the importance of baking the traps of mercury diffusion pumps, and by Jepsen et al. (1960), who developed the sputter ion pumps. Small, sensitive, mass spectrometers were also developed to measure the partial pressure of each component gas in the ultra high vacuum (U.H.V.) apparatus. During the same time a major part of surface science studies was the preparation of clean surfaces and monitoring their cleanliness. Clean surfaces were obtained first on the tungsten wires (Roberts, 1935). Later they were prepared by evaporating a thin film of it on glass and finally by cleaning single crystals of tungsten and some other metals, by high temperature flashing in U.H.V., ion bombardment (Eggleton & Tompkins, 1952) and oxidation-reduction procedures (Eley & Norton, 1966). The Auger effect had been known about 1930, but the electronic technology needed to study the Auger spectrum of metal was not ready until 1968, when Harris introduced it for monitoring purposes. It is now a highly sensitive tool for monitoring surface cleanliness. However due to difficulties in the theory it is mainly a qualitative tool for identifying adspecies and its quantitative interpretation is often questionable. Single crystal planes were just studies at the tips of fine wires by field emission and field ion microscopy, then advances in the technology of crystal growth led to geometrical studies of single crystal surfaces by L.E.E.D. However the theory of L.E.E.D. is very difficult, because of multiple scattering and some phenomena like surface reconstruction seem to be unresolvable. Infra-red spectroscopy, microbalances and flash desorption studies are also used to study the adsorbed species; however the theoretical interpretation of their data can be ambiguous.

During the last decade there has been a tremendous growth in experimental methods for studying the electronic energy states of the adsorbed species, by various electron, photon and ion spectroscopies. A

Table 1.1

Technique	Exciting Probe	What is analysed	Information
1. A.E.S.	3 Kev electrons	Auger electrons	Surface composition
2. S.I.M.S.	Ions 1-4 kev	Mass selected ions	Surface composition
3. I.S.S.	Inert gas ions 2-40 kev	Elastically or inelastically scattered electrons	Surface composition
4. E.L.S.	Electrons $\sim$ 3 kev	Inelastically scattered electrons	Surface composition
5. X.P.S.	X rays $\sim$ 1.5 kev	Photo electrons	Surface composition and electronic structure
6. U.P.S.	u.v. light 20-40 ev	Photo electrons	Electronic structure
7. F.E.S.	High electric field	Tunnelling electrons	Electronic structure
8. I.N.S.	Ion beam few ev	Auger electron	Electronic structure
9. A.P.S.	Electrons 0-1.5 kev	X ray photons	Electronic structure of unfilled band.

short comparison of these spectroscopies is given in table 1.1.

As seen previously most of these studies depend on the electron emitting property of a surface and so in turn on work function even though their complexity usually prevents them from being used for the determination of work function.

Absolute work functions are very difficult to measure (Rivière, 1969). Work function differences however, are much easier to measure. If the work function of the reference electrode is known then determination of the average work function of the other electrode is straight forward, by Kelvin probe. The Kelvin method has proved to be particularly useful for gas adsorption studies (Culver et al., 1959; Fain et al., 1976). It is as sensitive as A.E.S. for the state of surface cleanliness (Christman, et al., 1974) and can provide useful information about the state and quantity of adsorbed particles of a known gas (Jewsbury, 1977). The main advantage of the method is, the measurement cannot disturb the state of the adsorbed gas. The main disadvantages, compared to the spectroscopies shown in the table are that it cannot identify the adspecies and only measures an average property of the surface.

1.2 Work function

The work function is one of the fundamental electronic properties of solid surfaces. Since 1949 interest in the work function has been stimulated by ultra-high vacuum technology, by new experimental technique of surface science and by technological interest. Progress has been very rapid both on the theoretical and experimental sides and there are several reviews available (Holze et al., 1979; Rivière, 1969; Gundry et al., 1968; Kaminsky, 1965; Hayward, 1964; etc.)

The work function of a metal is defined as the minimum energy required to remove an electron from the metal to a position just outside. Alternatively it can be defined as the energy difference between two states of

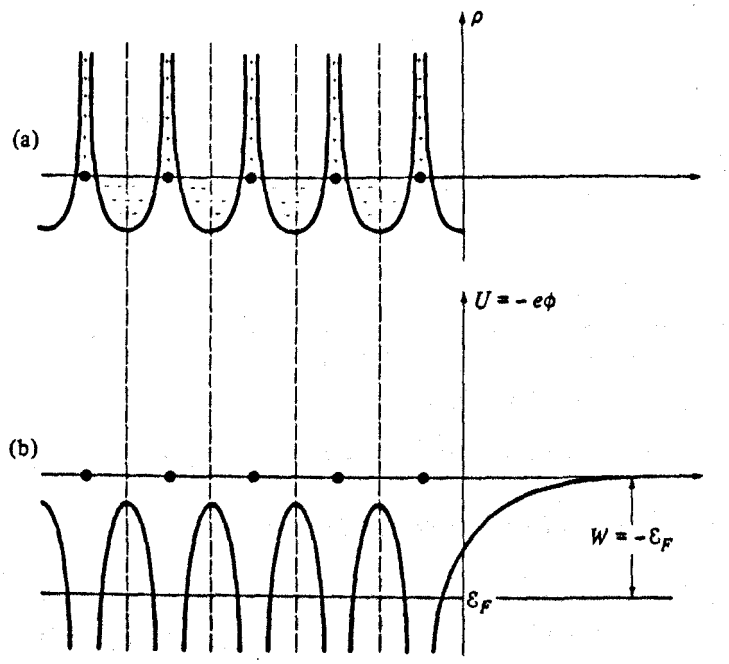

FIG 1-a

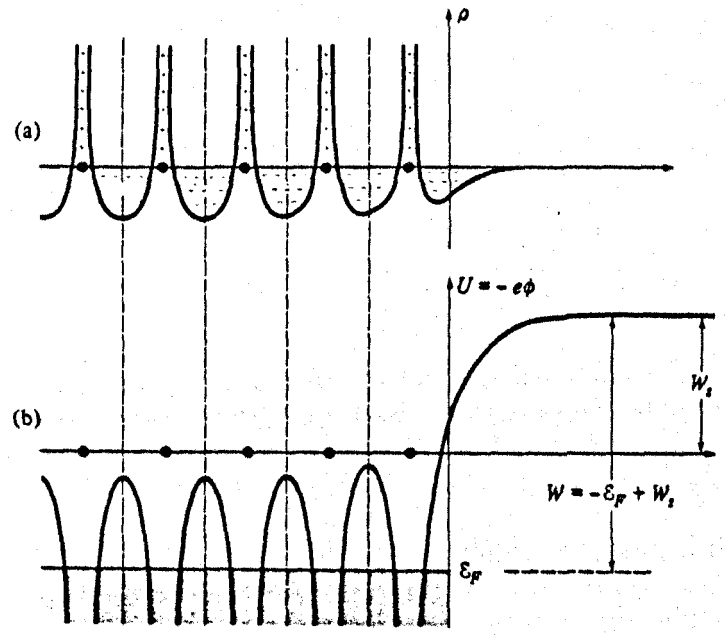

FIG 1-b

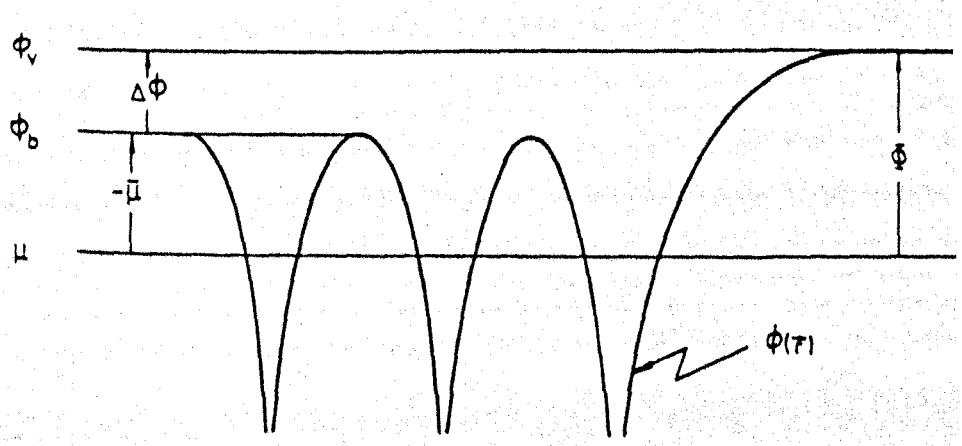

the whole crystal at zero temperature. In the initial state the neutral crystal containing N-electrons is assumed to be its ground state with energy-E_N. In the final state one electron is removed from the crystal to a region just out side; there the electron is at rest and the remaining N-1 electrons in crystal are at ground state. The second definition is a simple way to correlate the thermo-dynamical parameters, like electro-chemical potential, with work function. However in both definitions "just outside" means a distance from the surface that is large on the atomic scale but small compared with linear dimensions. For example in the case of a single crystal face it is the distance from the face at which the image force is negligible (typically 10^{-4} cm), otherwise energy will not be minimum. At the same time it should be small compared with the distance from other faces with different work functions. If the distance from the surface is very large then it is not possible to dis-criminate between the work functions of different faces.

Consider one Wigner-Seitz (W-S) cell well within the solid (here coulomb contribution of surface W-S cells is negligible). The highest occupied electronic level in this cell at 0° K would be the Fermi level (E_F). The lowest energy of an electronic level just outside the crystal would be zero. Therefore the minimum energy difference for an electron inside and outside the crystal is $-E_F$. However the electron emission process has to take place via the surface. If the surface had a uniform charge distribution like the bulk, then the minimum energy required to remove an electron would be just $-E_F$. But the actual charge distribution near the surface of a finite crystal differs from the uniform charge distribution of the bulk due to the slight displacement of the lattice points at the surface, a typical situation is shown in the figure 1.a. The electronic charge distribution in a W-S cell near the surface therefore need not have the symmetry of a Bravais lattice. Such cells will in general have non-zero electric dipole moment, they may even have

a non-vanishing electrical charge.

The particular way in which the surface charge distribution differs from the bulk depends on whether the surface plane is smooth or rough, also on the orientation of the plane with respect to the crystallographic axes. For the simplest model let us ignore any effect due to the characteristic of the surface plane. Then we can assume equal charge density in a plane parallel to the surface. In other words we can represent the charge density of a plane parallel to the surface as a function only of distance from the surface plane. For example; we can write the charge density distribution as follows

$$\rho(x) = \rho_0 - \tfrac{1}{2}\rho_0 e^{\beta x} \quad \text{for } x < 0$$

$$= \tfrac{1}{2}\rho_0 e^{-\beta x} \quad \text{for } x > 0$$

where the distance variable x measured from the surface plane, perpendicularly away from the bulk, and ρ_0 is the density of the charge distribution in the bulk. β is a constant, depends on the property of the metal. The surface layer, which includes two or three lattice planes, (depends on the value of constant β), in which the distribution deviates from the bulk will give rise to an appreciable electric field E(x). During the electron emission process we have to work (W_s) against this electric field.

where $W_s = \int e \cdot E(x)dx$.

Therefore the minimum energy (ϕ) required to remove an electron from a solid is given by

$$e\phi = -E_F + W_s, \text{ where } \phi \text{ is the work function.}$$

Normally a surface has got many different crystal planes. Fundamentally they differ from one another in charge distribution, therefore their surface contribution (W_s) to the work function is different. In other words different crystal planes at the surface will have different work functions. This behaviour is obvious from the table 1.2 (selected from

Table 1.2

Plane	Work function in ev.
W(001)	4.60
(119)	4.56
(116)	4.36
(115)	4.35
(229)	4.34
(114)	4.40
(227)	4.43
(113)	4.55
(112)	4.71
(025)	4.55

the review paper of Holze et al., 1979). As the result of this, there is an electrostatic field between these patches of different planes in a polycrystalline surface, however usually this field is very small and known as patch field.

The treatments described above cannot really offer a fundamental insight into the theoretical subject, however this approach can certainly be used as a starting point in the explanation of experimental observations. For quantum mechanical calculation of the work function in principle one has to start with Schrodinger equation for a system of N-mutually interacting electrons which are moving in a potential V(r) caused by the ion cores. For computation, this many-body problem has to be reduced to a one-body form. The basic ideas were developed by Wigner et al. (1935) and they employed Hartree-Fock approximation; but in all modern calculations the density functional formalism (Hohenberg et al., 1964; Kohn et al., 1965; Sham et al., 1966) has been used. In any case, to obtain reasonable results, it is necessary to take the individual coulomb interaction between the electrons into account via exchange and correlation potentials. In general these methods divide the work function into two parts with respect to zero of a muffin tin potential (potential at the interstitial region), as shown in the figure 1.b. The part below the muffin-tin zero is purely due to the bulk, and can be obtained from the band structure calculation. The part above the muffin-tin zero is mainly

due to surface properties and needs a self consistent calculation of the dipole barrier at the surface. However wave mechanical self consistent calculations cost a large amount of computer time, therefore extensive use has been made of the conceptually simple uniform background model (Lang, 1973). For simple free electron metals, this methods shows reasonable agreement, and it can be improved further by considering lattice effects (Monnier et al., 1978); however, for d-band metals it is not suitable method.

In principle a work function measurement can be used to understand the nature of a process which could alter the surface part (W_s) or bulk part ($-E_F$) or both. The surface part is very sensitive to the adsorption and desorption of foreign atoms, positions of the sites at which foreign atoms interact, and nature of the adspecies. A work function study with suitable calibration can therefore be used to monitor surface coverage and sticking coefficient (Christmann et al., 1974), it also can be used to detect surface diffusion (Butz et al., 1977). The bulk part i.e. the position of the Fermi level, would be shifted due to any kind of phase transformation. This can therefore be used to detect crystallographic phase transitions (Hill et al., 1971); chemical phase transitions (Muller et al., 1977), super/normal conductivity transitions (Schodt et al., 1977) and ferromagnetic/paramagnetic transitions (Holze et al., 1975). Also it can be used for elastic deformation studies (Mints et al., 1975) and for studies of alloys (Djubua et al., 1966; Bouwman et al., 1972).

1.3 Contact potential difference (C.P.D.)

Suppose two metals at the same temperature are connected ohmically. Electrons start to flow from one to another until an equilibrium is reached. At equilibrium, the electrons in both metals must be at the same chemical potential, in other words the Fermi levels of both metals are equal. This has been attained by charge flow from one surface to another. The surface charge on each metal gives rise to a potential in

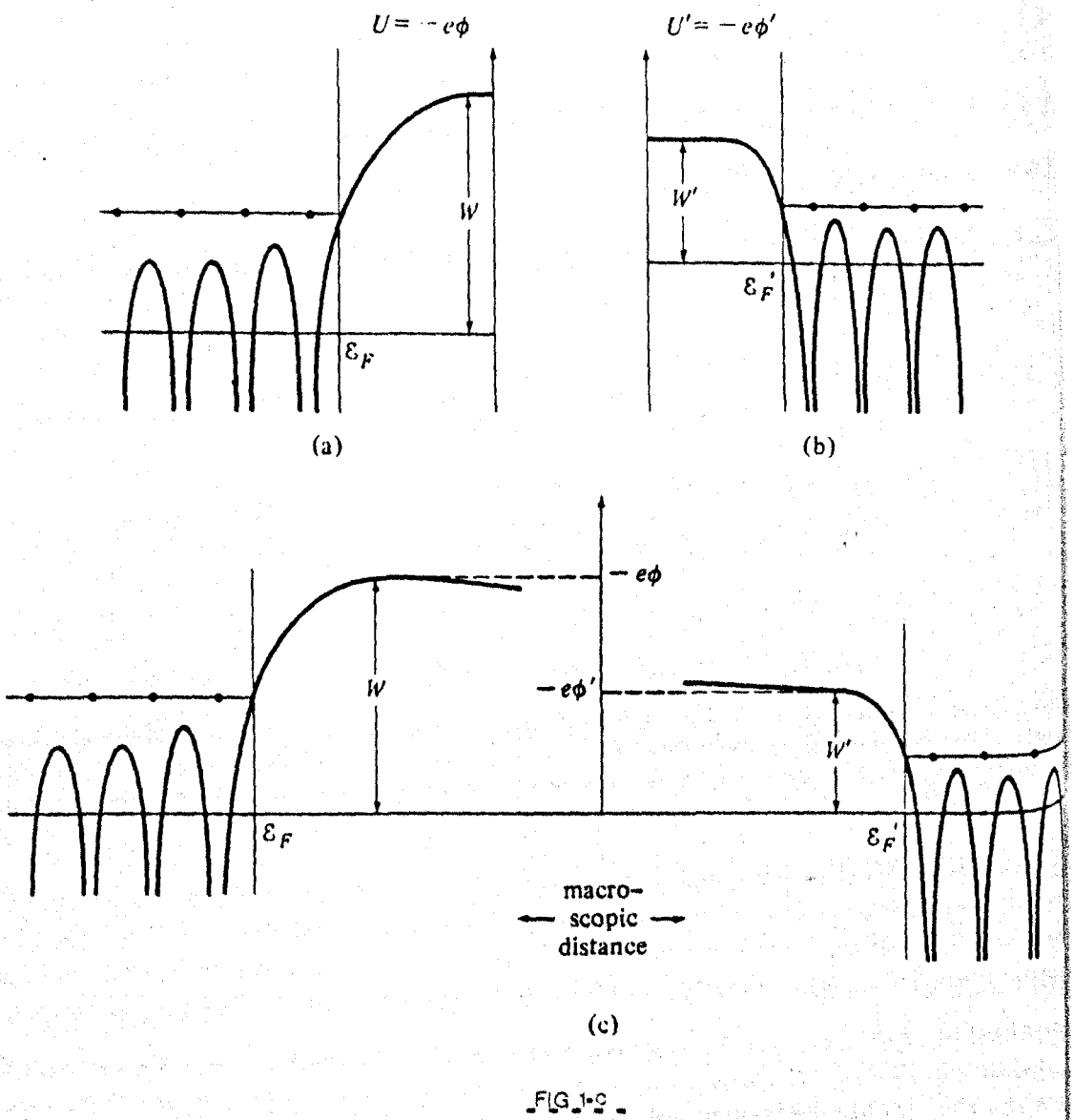
$U = -e\phi$
W
$\mathcal{E}_F$
(a)
$U' = -e\phi'$
W'
$\mathcal{E}_F'$
(b)
$-e\phi$
$-e\phi'$
W
W'
$\mathcal{E}_F$
$\mathcal{E}_F'$
macro-
scopic
distance
(c)

FIG. 1-c

the interior that uniformly shifts all of the bulk energy levels together with the Fermi level. The two metal surfaces are not at the same potential because of the charge transfer, and the potential difference between the two metal surfaces is known as C.P.D. The situation is shown in the figure 1.c. Suppose an electron from the Fermi level of the one metal (1) is extracted through its surface and introduced to the Fermi level of other metals through its surface. In this process, energy is conserved, therefore there must be work $e(\phi_1 - \phi_2)$ done against some external field. This field exists due to the presence of C.P.D., therefore C.P.D. is equivalent to $(\phi_1 - \phi_2)$, the work function difference of the two metals which are in contact ohmically. This effect can be used to measure the work function of one metal if the work function of another metal is known, or it can be used to measure a work function change due to some physical process if the work function of another metal is unchanged. However C.P.D. cannot be measured simply by connecting a galvanometer between the metals, because this system cannot be a source to produce a continuous current flow. Practical ways of measuring C.P.D. are described later in 1.5 and 1.6.

1.4 Adsorption and surface potential

In the vapour stage of matter, the atoms or molecules are free to move in all directions. However when they collide with solid surfaces, some of them can become bound with the loss of their degree of freedom. This effect is known as adsorption. Adsorption is a pure surface effect and could influence all phenomena related to the surface such as electron emission, chemical reaction etc. In general adsorption can alter the strength of the surface barrier, therefore in turn alter the work function of the metal surface. The change in work function on adsorption of an adsorbate is loosely defined as the surface potential of the adsorbate on the particular adsorbent. If the work function of the surface increased

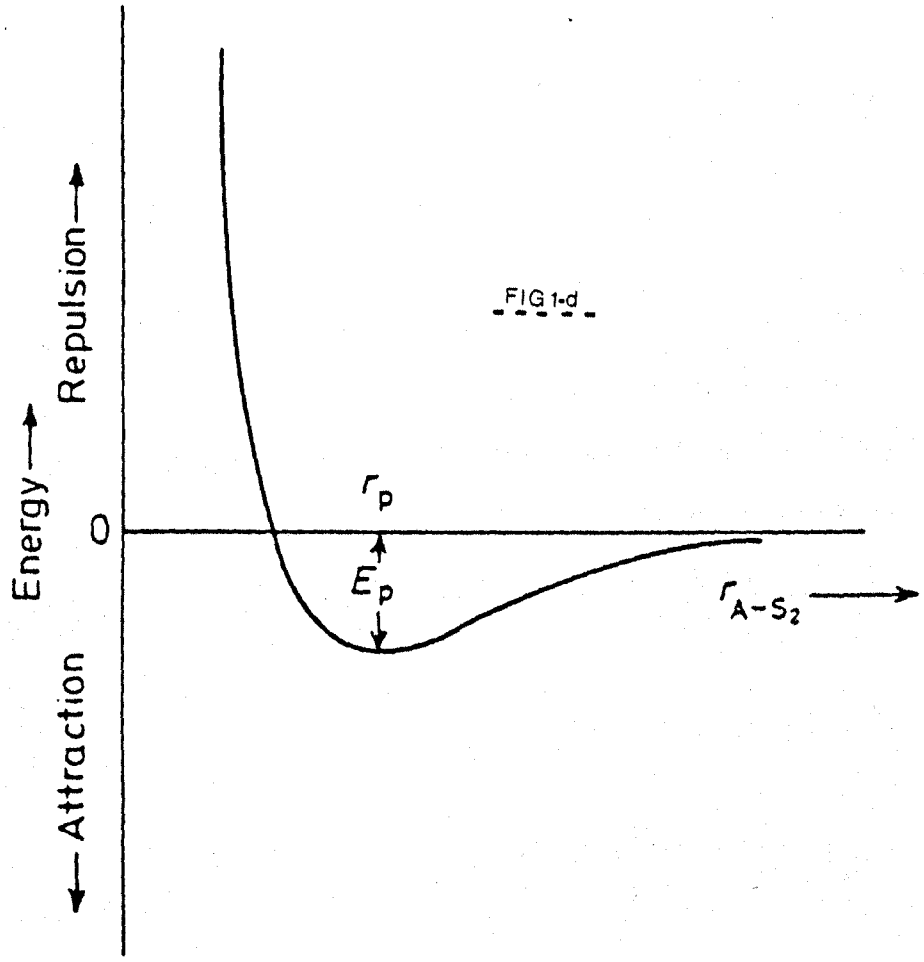
Repulsion
Energy
0
Attraction
r_p
E_p
r_{A-S_2}

FIG 1-d

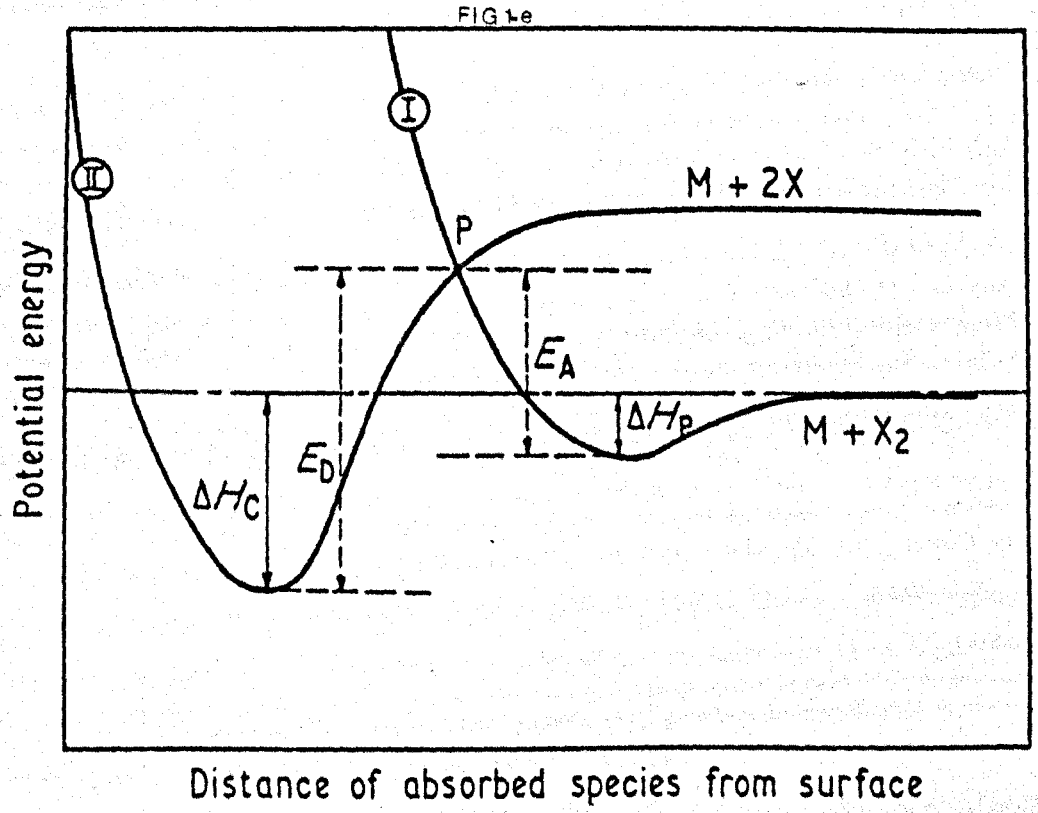
I
II
M + 2X
P
E_A
ΔH_p
M + X_2
E_D
ΔH_c
Potential energy
Distance of absorbed species from surface

FIG 1-e

on adsorption then the adsorbate has negative surface potential, in contrast if the work function decreased then the surface potential of the adsorbate is positive. In addition to the adsorption at the surface, if the adsorbate diffuses into the bulk, the new process is known as absorption, which is a bulk process. Both processes without distinction are called a sorption process.

Thermodynamically the adsorption process is exothermic, because of entropy loss or loss of degrees of freedom when the adsorbate becomes bound to the adsorbent. The energy released is known as heat of adsorption (ΔE). In early days if the heat of adsorption is large ($\gtrsim$ lev) then the process is recognised as strong adsorption, in contrast if the heat of adsorption is very small ($<<$lev) then the process is weak adsorption. But later works shows a whole range of values of heat of adsorption. So the processes are categorized into chemisorption, weak chemisorption and physisorption, in the descending order of heat of adsorption. In principle the forces responsible for the adsorption are the same as those operating between two atoms in a molecular bonding. But a theoretical description of adsorption is made more difficult by one partner being an atom which is incorporated in a solid. However we can distinguish two different contributions to the total force, which are a long range attractive force (dispersive forces) and a short range repulsive force (electron orbital overlap or valency, forces). Therefore the potential diagram figure 1.d of the adsorption process can be represented by Lennard-Jones's relationship

$$E = -ar^{-m} + br^{-n} \qquad m = 6, \qquad n = 12$$

This type of potential diagram can be accounted for wave-mechanically by anti-parallel and parallel bonding states of adsorbate and adsorbent. A parallel bonding state has small energy and large bonding distance therefore corresponds to physisorption. Physisorption is not specific

to the nature of the absorbent. Very often chemisorption behaviour differs even between the different crystal faces of same adsorbent. Chemisorption is often, but not always accompanied by dissociation of polyatomic adsorbate molecules (H_2, O_2, CO_2, H_2O). The corresponding potential diagram is shown in the figure 1.e for diatomic molecules (H_2, O_2). Then clearly dissociative chemisorption is more stable than molecular adsorption.

In the case of dissociative adsorption of a diatomic molecule, the molecular chemisorption energy ΔE_m is given by $\Delta E_m = 2\Delta E - E_{dis}$

where E_{dis} is the dissociation energy.

Therefore if $\Delta E < \frac{E_{dis}}{2}$, then dissociative chemisorption is thermodynamically unfavourable. In other words molecular chemisorption is more favourable.

The real surface has various kinds of defects which can be represented by a terrace-ledge-kink model (Stranski, 1928). Further even an ideal single crystal face has different coordination sites (single coordination or atop site, double coordination or bridge site etc.). These sites could influence the dissociation probability, and in turn chemisorption process is a complicated fashion. In general the phenomena associated with a chemisorption process are a bit complicated. The variation of the work function of a surface on adsorption was qualitatively explained by Langmuir's (1932) classical model. He explained the observed work function changes on a metal due to the adsorption of alkali atoms by the equation

$$\Delta\phi = -4\pi\, e\, p\, N_a \qquad \text{(C.G.S. unit)}$$

$$= -\frac{e\, p\, N_A}{\epsilon_o} \qquad \text{(SI unit)}$$

where N_A is the number of adsorbed alkali atoms per unit area and p is the dipole moment of ionized alkali ion on adsorption.

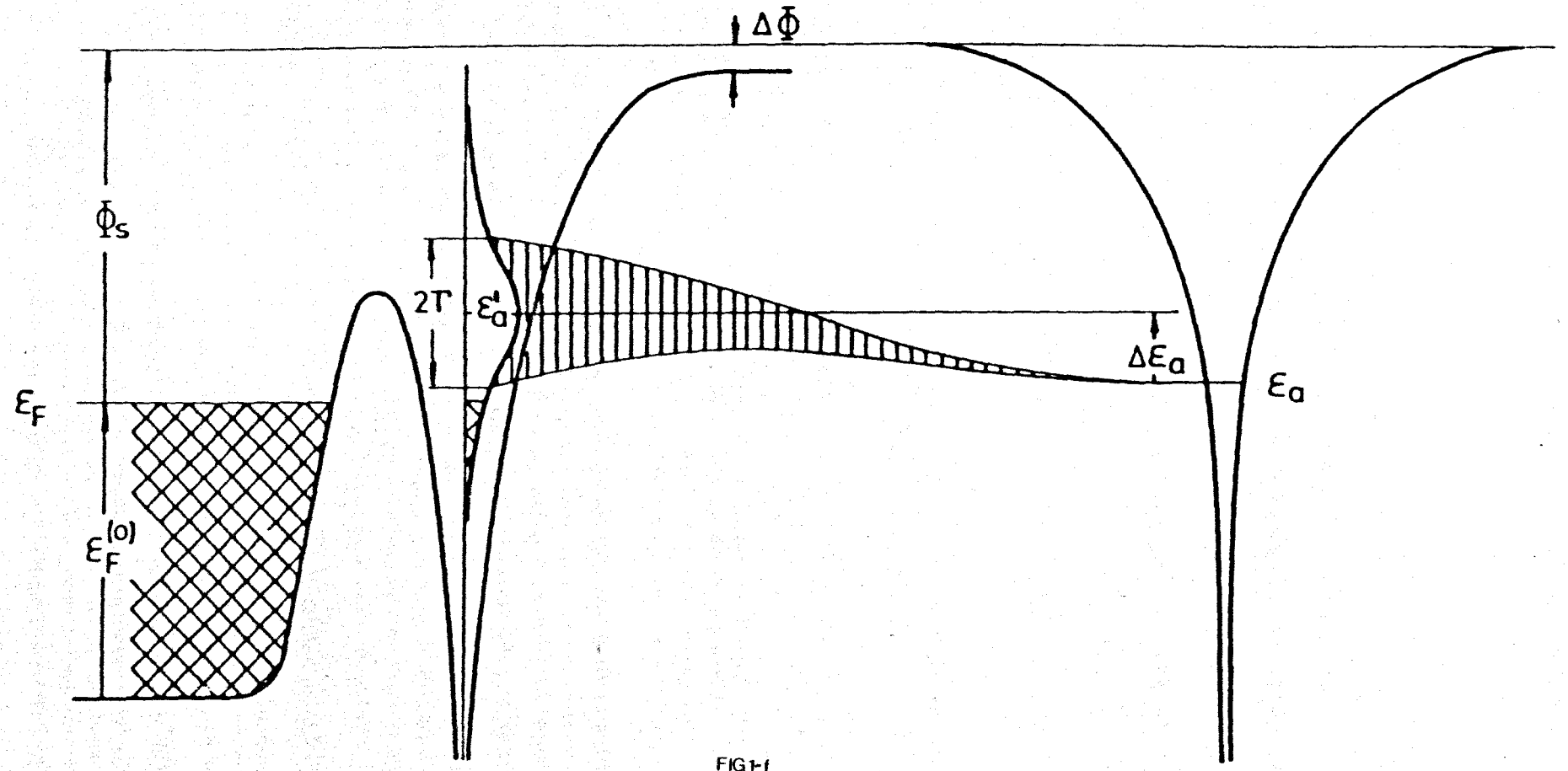

FIG 1

In general the polarity and strength of the dipole moment depends on the nature of adsorbed atom and the position of the adsorption sites with respect to the surface plane. In the case of alkali atom adsorption, negative charge is transferred to the metal, and position of the adion is above the surface plane, therefore the dipole moment is positive. Hence the adsorption will give work function reduction. This relationship predicts a linear work function change with coverage i.e. no. of adsorbed atoms. Practically this is not observed at high coverage. In the expression the value of p is independent of N_A but it is really not so, because of a depolarizing effect of other adsorbed dipoles, or adatom-adatom repulsive forces. The practical observation i.e. the deviation nature of work function variation from the linearity, was explained by Hewson et al. (1974), by considering the depolarizing effect.

However the physical origin of the charge transfer is not clear in classical models. Gurney (1935) gave a quantum mechanical model to explain this phenomena and the model is shown in the figure 1.f. He showed the well defined atomic energy level E_a gets broadened when the atom approaches the metal surface due to the overlap of metal and atom wave functions, also the mean energy E_a^1 of the broadened atom becomes shifted. In this situation the electron can tunnel with a time constant τ given by $h/2\Gamma$ where 2Γ is the width of the broadened atomic energy level. Due to electron tunnelling the broadened atomic level can be filled only partially and so the adatom can be characterized by fractional charge. The amount and the polarity of the charge is determined by the relative location of the metal's Fermi level and the position of the broadened band. The combination of the charged adatom with the electron cloud screening it (which is concentrated in the region near the metal surface) behaves like a dipole, and changes the work function of surface. Methods of calculating the work function change differ in their way of determining the charge and the length of the dipole. The effective

charge can be determined from the occupied portion of the broadened band, i.e. local density of electrons on the adatoms, and Newns (1969) - Anderson (1961) formalism has been used extensively for this purpose. In this formalism the adatom-adatom direct interaction at high coverage is included; but indirect interaction (via substrate) is neglected. Density-functional formalism has also been applied for the calculation of work function change, and Lang et al. (1975) obtained a reasonable agreement with measurement for transition metals.

1.5 Methods of work function measurements

In general these methods can be divided into two groups, which are direct methods and indirect methods. Using direct methods one can measure absolute work functions but by indirect methods one can only measure relative values (with respect to a reference electrode). However the correct interpretation of the results from both methods mainly depends on the assumptions and approximations taken in the theoretical descriptions of the physical process involved in the methods, and the experimental conditions which are in operation during the experiment. For example in the definitions of the work function we have assumed 1.infinite half space of surface, 2.single crystal face, 3.field free space, 4.absolute zero temperature. Clearly every experiment which can be conducted in a laboratory is far from these assumptions. Therefore in the interpretation it is important to recognize the effect of these differences which are, 1.stray field effect due to finite size, 2.patch field effect due to polycrystalline nature, 3.Schottky effect due to applied field, 4.correction for finite temperature. An excellent review about these problems was given by Rivière (1969).

The direct methods basically depend on the emission of electrons either thermionically or photoelectrically or by field excitation. There are two well knwon experimental arrangements for the thermionic

emission measurements, which are planar diode, and cylindrical diode. Both are theoretically based on the Richardson-Dushman equation, and involve high temperatures and accelerating fields. In the case of a polycrystalline sample the effect of patches depends on the strength of applied field. Obviously this method is unsuitable for low temperature work and for substances which give little emission below their melting point. The photoelectric method is theoretically based on the Fowler (1931) expression, it also has limitations because of the application of an accelerating field and patches in the case of a polycrystalline sample. For adsorption studies there might be a possible disturbance of adsorbate due to the irradiation. The field emission method is based on the tunnelling probability of electrons through the Schottky barrier due to the application of a strong electric field and it is generally limited to the refractory metals. The measurement of the individual work function of a single crystal face is possible by using "probe hole" (Muller, 1943); it has also been a very useful technique for diffusion studies, but there may be disturbances due to the very high electric field. The application of these direct methods to adsorption studies is limited to low pressure of adsorbate to avoid scattering of electrons and gaseous breakdown.

Indirect methods can be divided further into two subgroups which are diode method and condenser method. The precision of these methods depends mainly on the accuracy of the detector, this varies from 0.1 to 10 mev. These methods are theoretically based on the contact potential between the sample and the reference electrode, when they are connected ohmically. The diode method depends onthe characteristic curve of the diode being displaced along the voltage axis by an amount equal to the C.P.D. and assumes that it is not altered in any other way. According to the working point in the characteristic curve, the diode techniques can be divided further into two types which are charge limited diode and retarding field diode. The development of these methods for the measurements of surface

potentials were excellently reviewed by Knapp (1973). In practice, the work function changes can be obtained from the additional voltage necessary to maintain the constant anode current. The retarding field diode technique is basically equivalent to thermionic emission technique. In this method the electron beam can be focussed strongly to a diameter less than that of the size of a patch therefore a study over individual patches is possible. Different versions of the retarding field diode are available for different purposes. Spherical and cylindrical diodes (Pritchard, 1965; Mignolet, 1955) are suitable for gas adsorption studies on evaporated films. Crossed filament diodes (Hayes et al., 1965) are suitable for refractory metals and simultaneous flash-desorption studies. The electron beam technique (Anderson, 1941; Nathan et al., 1974) is suitable for adsorption studies on single crystals. The scanning beam diode (Haas, 1966) is suitable for gas adsorption and diffusion studies. However for all these diode methods, gas adsorption studies are limited to a maximum pressure of 10^{-3} torr due to the effect of gas on the electron beam and to the possible chemical reaction of gases (O_2 H_2 etc) with hot cathode.

The condenser method can be divided into two types which are static and vibrating capacitor methods, which differ only in the method of detection. In static capacitor (Delchar et al., 1963) the tendency for charge flow due to the change in C.P.D., is detected and then compensating potential is applied immediately until charge ceases to flow. The static capacitor allows only to measure the change in C.P.D. The essence of the method is the quick application of compensating potential; in contrast to vibrating capacitor, in static capacitor both electrodes are stationary. The vibrating capacitor technique is the one employed in this work, therefore a detailed description is given in the next section.

1.6 Vibrating capacitor method

This method was originally proposed by Thomas (Kelvin, 1898) and is currently used in the form due to Zisman (1932). In this method two electrodes A and B are electrically connected through high resistance $R(> 10^{+8})$.

From the section 1.3, the contact potential difference V_{AB} given by

$$V_{BA} = \phi_B - \phi_A$$

where V_{BA} measured with respect to A. The value of V_{BA} and polarity is detected by vibrating one of the electrodes (either electromagnetically or electrostatically or mechanically) or by other means of changing the capacitance between the electrodes.

Suppose Q is the charge on the condenser due to the potential difference V between the electrodes then

$$Q = CV$$

$$\frac{dQ}{dt} = V \frac{dC}{dt}$$

If there is no other form of voltage between the electrode then

$\frac{dQ}{dt} = V_{BA} \frac{dC}{dt}$ $\qquad V = V_{BA}$

Suppose there is an additional voltage V_C between the electrodes, then

$$V = V_{BA} + V_C$$

$$\text{Therefore } \frac{dQ}{dt} = (V_{BA} + V_C) \frac{dC}{dt}$$

This charge variation will develop a current flow and is detected in the form of voltage across the resistance R. The value of V_{BA} is determined by adjusting the value and polarity of V_C until the charge flow ceases. Then the value of $V_{AB} = - V_C$, (when $\frac{dQ}{dt} = 0$).

In practice, the voltage across R is detected in the amplified form by means of a phase sensitive detector or cathode ray oscilloscope. The

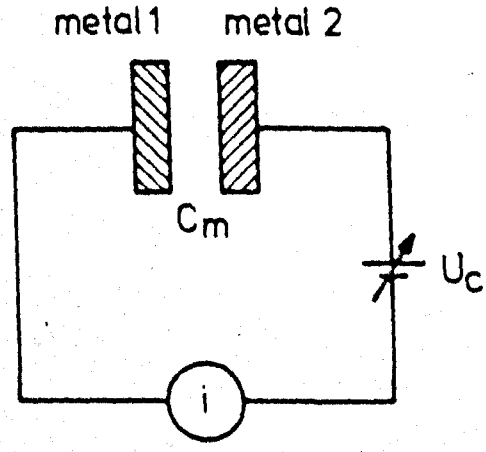

(a)

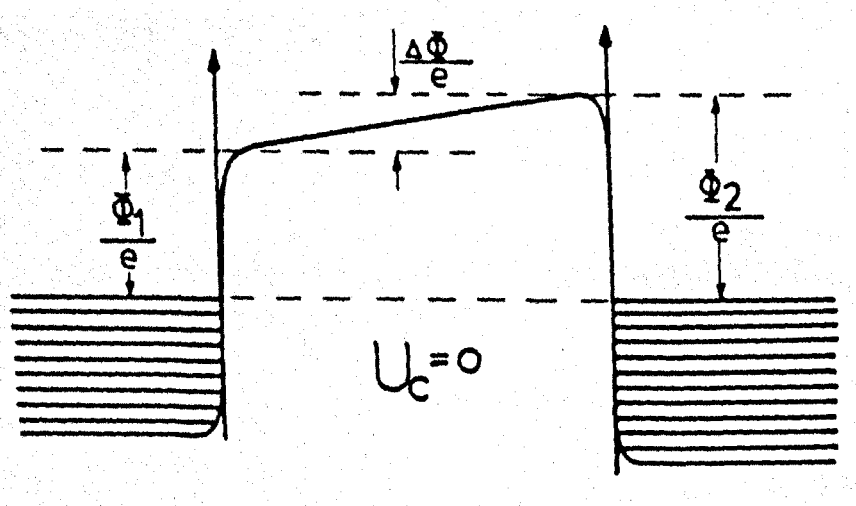

(b)

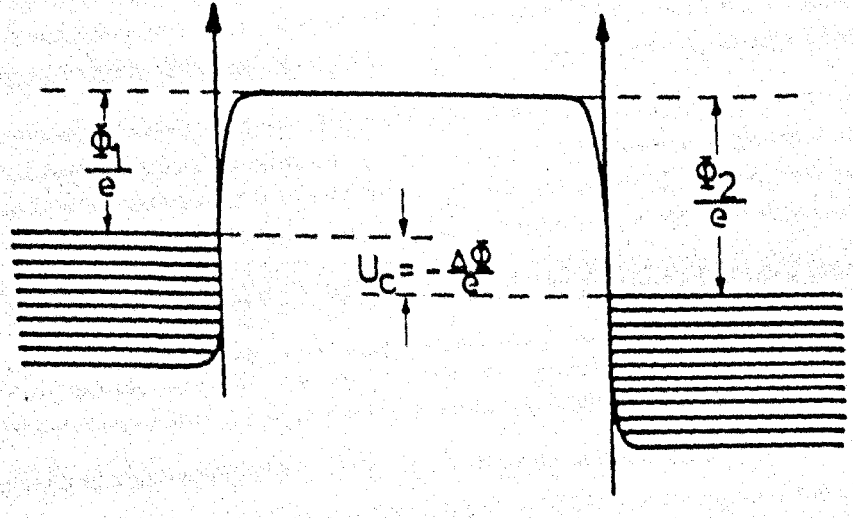

(c)

FIG 1g

description of electronic circuit is given in the next chapter. The basic principle of the technique is given in figure 1.g. The capacitor modulation, in turn the voltage developed across the resistor, is not strictly sinusoidal. This contains higher order harmonics. The harmonic content increases with the amplitude of the modulation, the reciprocal time constant and non-parallelism of the electrodes. If the geometrical size of the condenser is large compared with the size of the patches of the electrode surfaces, then the C.P.D. measured by this method is arithmetic mean of the individual C.P.D. of all the patches. The reliability and reproducibility of the results are basically limited by any changes of the work function of reference electrode (e.g. due to gas adsorption on it) and the effect of stray capacitance. The stray capacitance effect on C.P.D. has been thoroughly investigated by Surplice et al. (1970) and de Boer et al. (1973). Investigation shows that a variation of vibration amplitude or variation of the electrode separation can alter the C.P.D. by several hundred mv. It seems also necessary to have vibrating electrode as reference and connect the detection system to other electrodes, for further reduction of stray field effect. The use of detector system with high input resistor is also important to achieve sufficiently high voltage input at the detector. Now, in addition to the A.C. version of Zisman (1932), there are some other versions which have been developed by Holzl et al. (1974), Fain et al. (1976) and Butz et al. (1977), specially to satisfy particular experimental requirements (e.g. sampling very small areas).

Clearly this method has an advantage over other methods because it does not involve an emission process; also it does not probe the surface with high energy particles. Therefore it has no risk of changing the surface condition of the sample during the measurement. Finally it can be used for a large range of pressure and temperature. The main disadvantage of this method is the requirement of the reference electrode with known and unchanged work function.

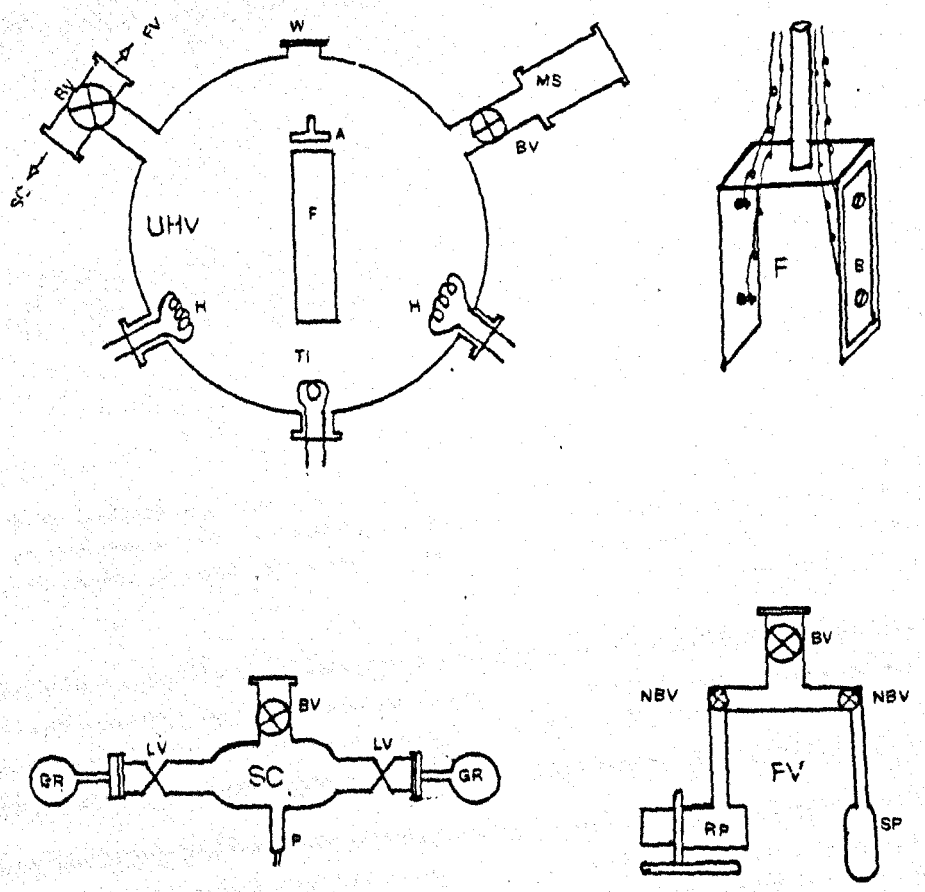

Fig 2.8

UHV = Ultra High Vacuum

W = Window

H = Heater

MS = Mass Spectrometer

T = Titanium Filament

RP = Rotary Pump

SC = Sample Chamber

BV = Bakeable Valve

A = Gold Electrode

B = Glass Substrate

F = Ceramic Frame

P = Pirani Gauge

LV = Leak Valve

GR = Gas Reservoir

SP = Sorption Pump

FV = Fore-Vacuum

NBV = Non Bakeable Valve

CHAPTER 2

Apparatus and Method of Experiment

2.1 Vacuum System

The entire system was made of grade 304 stainless steel (Type EN38E), its general features are shown in figs 2.a and 2.b. The main chamber has a cylindrical shape and capacity of about 5000 c.c. The walls of the chamber are coated with a gold layer formed by thermal decomposition in the air of an organo-metallic compound (Johnson-Mathey, Bright gold G.B.V. 27650). The top flange carries a rotary motion drive which supports a frame (F.) 5 B.N.C. sockets and a rod (L.) A port at the bottom of the cylinder is connected to the ion pump (I.P.) via a bakeable valve (B.V.). Around the circumference of the chamber there are six other ports placed at 60 degrees to each other which are for windows (W.) tungsten heaters (H.) (or a tungsten wire resistance thermometer), mass spectrometer (M.S.), titanium filament (Ti.) and a tee-piece to the fore-vacuum (F.V.) and gas sample chamber (S.C.). The rod (R.) is projected vertically through the top flange, its upper end is connected to the vibration transducer (T.) (fig. 2.b) and its lower end to electrode A, vibrating electrode. The vibrating electrode A, and the fixed electrodes B are positioned in the vacuum chamber as shown in fig. 2.a. The vibrating electrode is electrically insulated from rod (R) and the main chamber.

One end of the tee-piece is connected to the fore-vacuum (F.V.) side via bakeable valve (B.V.). The fore-vacuum side consists of one sorption pump and one rotary pump with a liquid nitrogen trap and these two pumps are isolated from one another by non-bakeable valves (N.V.). The other end of the tee-tube is connected to the gas sample chamber (S.C.) via a bakeable valve. This chamber has one Pirani gauge (type M9B) and two leak valves (L.V.) and its capacity is about 250 c.c. The Pirani

FIG 2-b

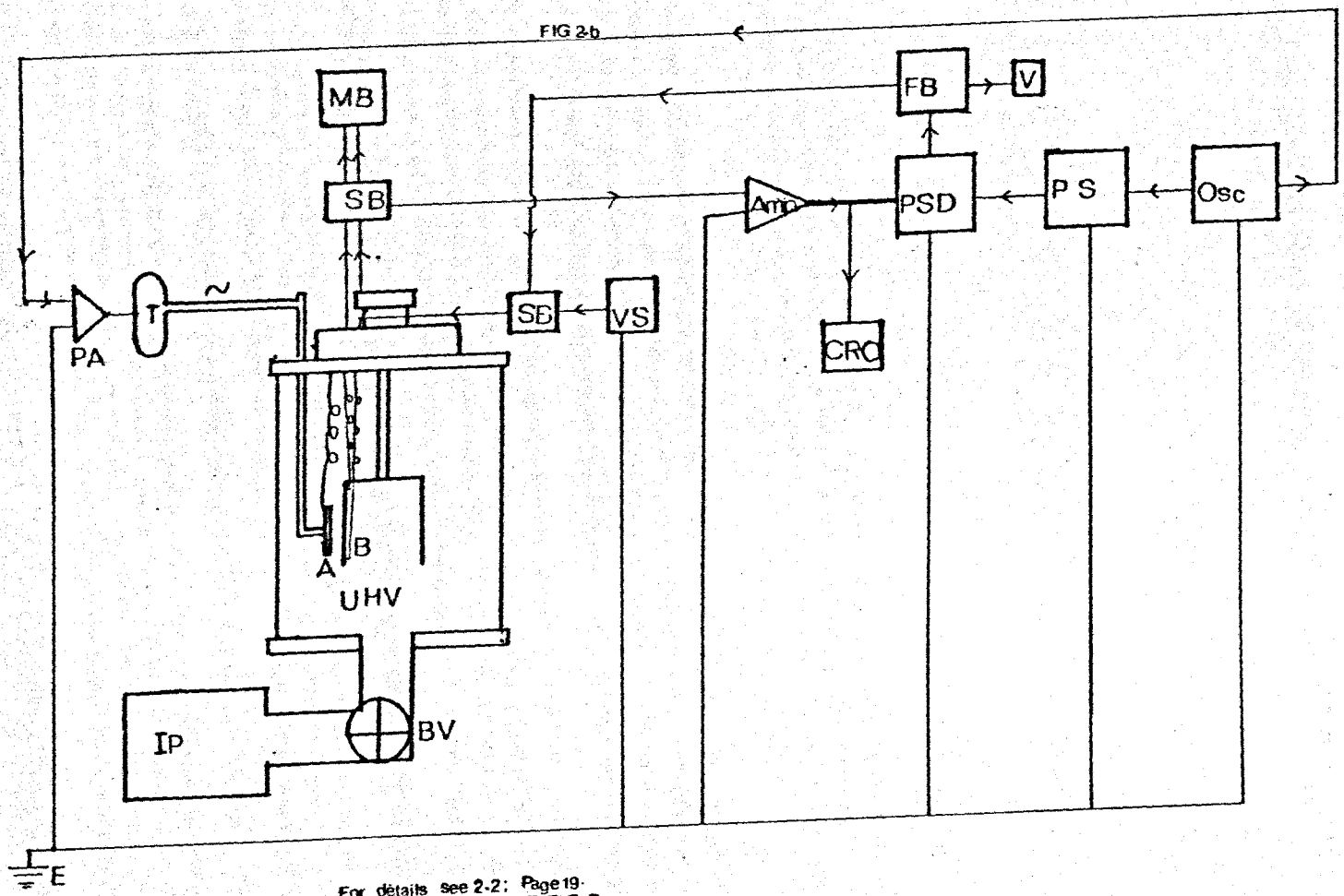

For details see 2-2; Page 19.

gauge measures pressure within 10% over the range 10^{-3}-10 torr, and the leak valves are connected to the different gas reservoirs (G.S.)

A ceramic frame (F.) of inverted U shape is supported at the centre of the vacuum chamber from the rotary drive. The two arms of this frame are the bases for the glass substrates B. By this arrangement each glass substrate can be rotatable about a vertical axis in a semi-circular path (of radius nearly 1.85 cm) between the titanium filament and the vibrating electrode, and the separation between A and other electrode (evaporated metal film on B) can be kept equal to 1.5 mm. During the evaporation the two arms of the frame protect the vibrating electrode completely from the stream of evaporated metal vapour. A glass window allows us to see the inside of the chamber and to adjust the position of the substrate B. For further details about the vacuum chamber see D'Arcy's thesis (1971).

2.2 Electronic system

The general arrangement of the electronic system is shown in fig. 2.b. This can be classified in two groups: The first is the vibrator driving group, and the second is the detector group. An oscillator (OSC.), Type TF2100 Marconi Instrument Ltd, is common to both groups. In addition, the first group consists of a power amplifier (P-amp.) type 440B Dawe Instruments Ltd, and vibration transducer (T.). The second group consists of a phase sensitive detector (P.S.D.), type 411 Brookdeal Ltd. A phase-shifter (P.S.), type 451 Brookdeal Ltd, a low noise amplifier (amp.) with high input impedance, type 451 Brookdeal Ltd, a universal bridge (U.B.) type TF2700, Marconi Instruments Ltd; a feed-back system (F.B.), Cathode ray oscilloscope (C.R.O.), backing voltage source (B.V.) and two switch boxes (S.B.). Screened coaxial cables are used for the electrical connections, all earth leads are taken to one common point E to avoid earth-loops, connectors in the detector side are kept as short as possible, and unnecessary movement of the cables is avoided

during the experiment to reduce the charging by friction. According to the experimental needs, a pen recorder can be included in the detector side to record the voltage output of the phase sensitive detector or the feed-back system. In some experiments a bridge was used for the recording of the resistance variation of the titanium film.

2.3. Reference electrode

The reference electrode was made of sheet gold, which had been polished with diamond paste, cleaned ultrasonically in distilled acetone to remove the paste, and baked in air to remove the acetone. The work function of this electrode had previously been studied by Surplice et al., 1975. Its work function was less than for a freshly evaporated gold film on a glass substrate by an average amount of 0.925 ± 0.03 eV. The work function of fresh gold film can be taken as 5.32 ± 0.10 eV (Riviere, 1969). Therefore the work function of our reference electrode can be assumed as 4.4 ± 0.1 eV.

It is well known that the pressure of H_2 up to 1 torr does not affect the work function of pure gold (Culver et al., 1959, Reviere, 1965). This was further checked in the present work from the constant value of the C.P.D. within the experimental range of pressure between the reference electrode and a layer of gold, which had been formed on a glass substrate from the thermal decomposition in air of an organometallic compound (Johnson Mathey) Bright gold G.B.V. 27650). All the literature on the subject agrees that at room temperature gold does not adsorb molecular oxygen for pressure up to at least several torr (Hopkins et al., 1959, Satcher et al., 1966, Eley et al., 1978, Legare et al., 1980) and probably up to 100 torr (Kirk et al., 1968) although it slowly absorbed it at above 100°C (Eley et al., 1978). It has also been confirmed by (Kirk et al., 1972) that gold repeatedly baked in a vacuum is stable up to a pressure of 4.58 torr of water vapour.

In the present work the following steps are adopted to check this further:

(a) The system was baked thoroughly and a newly evaporated titanium film was investigated on exposure to water vapour.

(b) The system was internally baked at a medium temperature (125°C) and experiment (a) was repeated.

(c) The system was pumped up to base pressure without any baking just by evaporating more titanium on the substrate and the experiment (a) was repeated.

In all cases the same result was reproducible quantitatively as well as qualitatively. Therefore we confirmed that within our range of experimental conditions the gold reference electrode was stable on exposure to water vapour.

2.4 Preparation of substrate

Pieces of glass four cm long and one cm wide were cut from a glass microscope slide.

The edges were smoothed by emery paper. Two holes of 2 mm diameter were drilled symmetrically in the glass piece at a separation 3 cm from one another by means of an ultrasonic driller, then they were cleaned thoroughly by means of ultrasonic agitation in a distilled water bath. For the electrical contact round the holes the two ends were painted with "liquid gold" (Johnson Mathey, Bright gold G.B.V.27650) and a gap of 2.5 cm length was left without gold in the middle of the substrate (see fig. 2.a). The gold was formed on glass pieces by baking at up to 350°C. Each substrate had two leads screwed into the holes so that it could be used for resistance monitoring as well as contact potential difference measurement. At the start of this work several substrates were prepared as described and used for titanium films. Later on the films which had been studied were removed by dissolving in

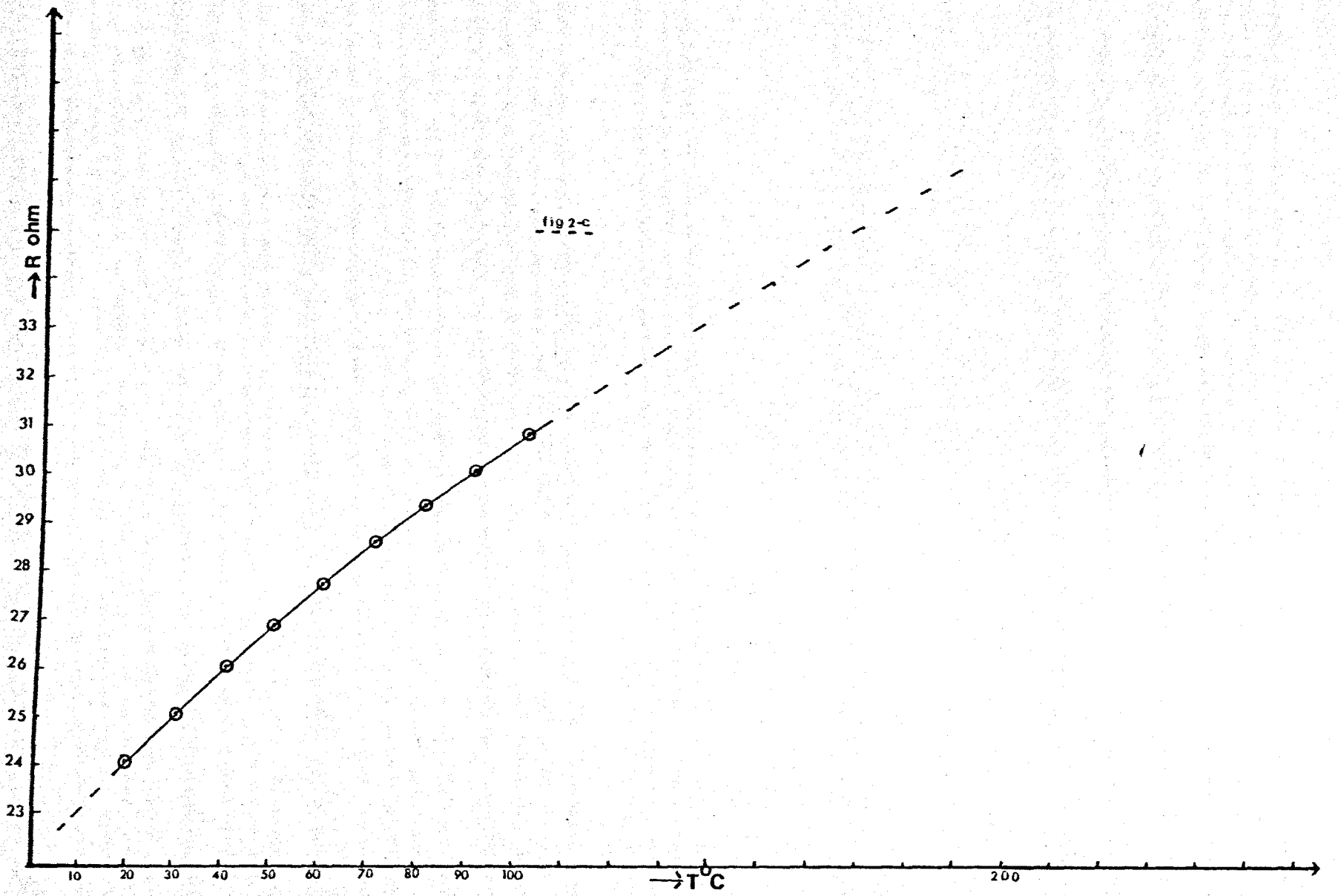
fig 2-c
→R ohm
33
32
31
30
29
28
27
26
25
24
23
10
20
30
40
50
60
70
80
90
100
→T°C
200

"100 volume" hydrogen peroxide at 50°C and substrates used again after cleaning them ultrasonically in distilled water.

2.5 Preparation of resistance thermometer

Fine tungsten wire was wound over a mica base. The terminals of the wire were spot welded on the nickel feed-through. The resistance variation of the coil with temperature change was calibrated over the temperature range 20-100°C using a water bath. The calibration curve shown in the fig. 2.c. The stability of the resistance was checked in the ultra high vacuum and in hydrogen atmosphere for these temperatures and found to be very steady.

2.6 Preparation of water vapour

A clean stainless steel container was filled with freshly distilled water and connected to the sample chamber via one of the leak valves. At the start, it was pumped by rotary pump and pressure reduced to 10^{-1} torr. Then the rotary pump was isolated and the sorption pump used for pumping while freezing the container in a liquid nitrogen bath for 15-20 minutes. Particular attention was taken to keep the temperature of the water container above the liquification temperature of the carbon dioxide (-150°C, 10^{-1} torr), since CO_2 is the only part of air that dissolves easily in water, and mass spectra taken during the course of preparation showed a large amount of CO_2, when the container was frozen at very low temperature. With sorption pump in use the air pressure over the water was lower than 10^{-3} torr. Later a volume sharing technique with ultra high vacuum chamber was employed to reduce the pressure further. Finally the water container was isolated from other parts and allowed to warm. After reaching the room temperature the procedure described above was repeated more than ten times and the mass spectrum of the purified water vapour recorded to check the improvement.

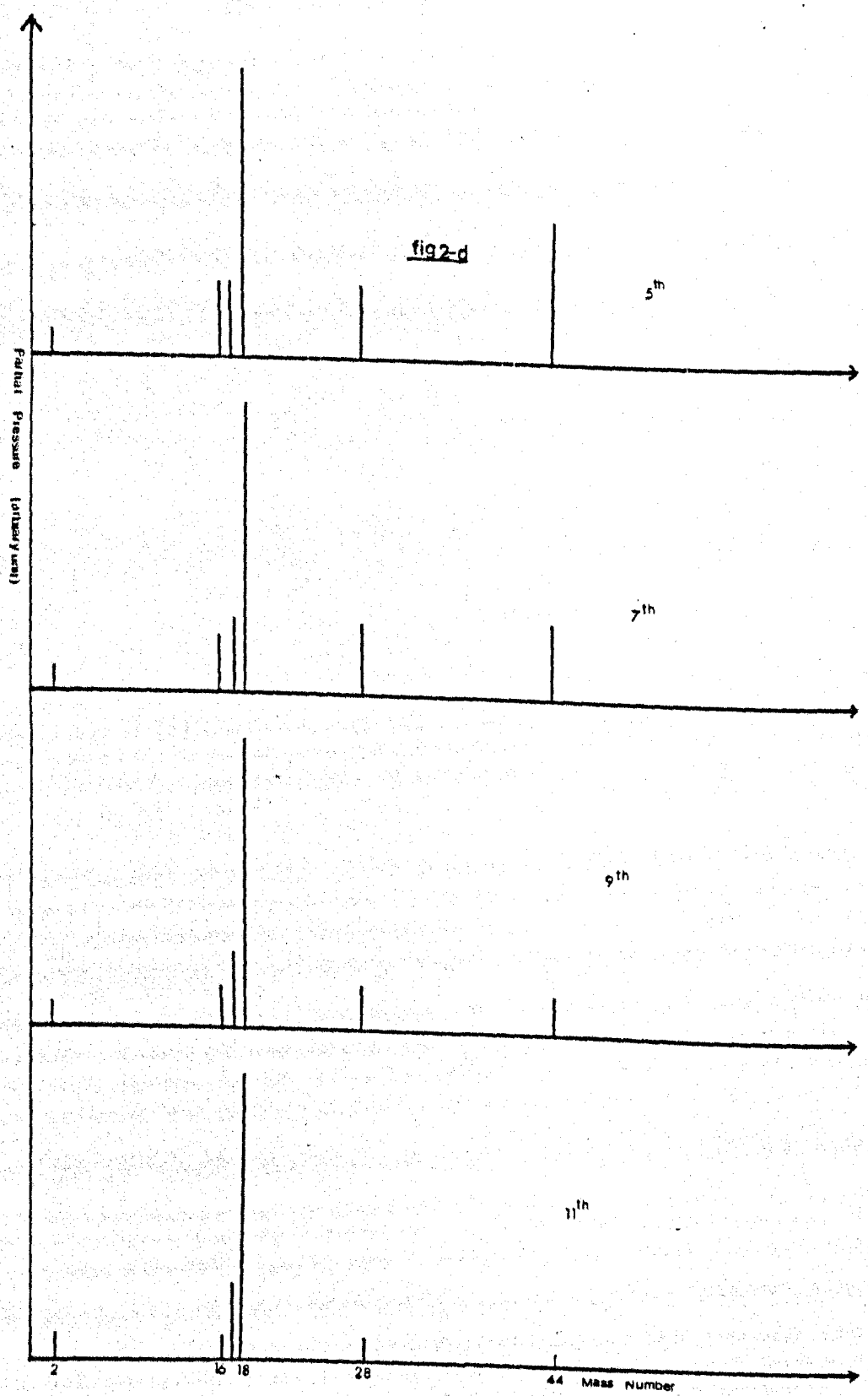
fig2-d
5th
7th
9th
11th
Partial pressure (arbitrary unit)
2
16
18
28
44
Mass Number

After the tenth repeated freezing and pumping the improvement was negligibly small. A simple estimate shows that at the end of the tenth pumping a purity of about 93% is attainable. However this calculation is not exact because water vapour has greater adsorption probability on the chamber wall, but in calculation equal adsorption probability is assumed for water vapour and other impurities. Therefore it is reasonable to expect better purity than estimated. For the comparison of the improvement, the mass spectrum of the prepared water vapour after the 5th, 7th, 9th and 11th pumping is shown in the fig. 2.d. They show that the main impurities are carbon monoxide and dioxide. The origin of the carbon monoxide is recognized as the mass spectrometer itself (by a series of subsidiary experiments), probably filament, therefore the major impurity in the water vapour is carbon dioxide, its maximum percentage is presently estimated at about 5%

Previously only few authors (Krueger et al., 1972, Fort et al., 1972, Huber et al., 1966, Tompkins, 1977) have prepared water vapour by means of repeated freezing methods and the impurity of their prepared water vapour is unknown. However, recently Tompkins(1977) published a mass spectra of the water vapour prepared by the above method and there is good qualitative agreement of our spectrums with his spectrum.

2.7 Preparation of ultra high vacuum

Three stages of pumping were employed. In the first stage the rotary pump with liquid nitrogen trap was used to pump the system to 10^{-3} torr, which normally took 15 minutes. In the second stage the rotary pump was isolated and the sorption pump used for the pumping while the chamber was externally baked at moderate temperature for about one hundred minutes until at the end a pressure of 10^{-5} torr was attained. At this level the last stage was brought into operation in which the

fig-2-e

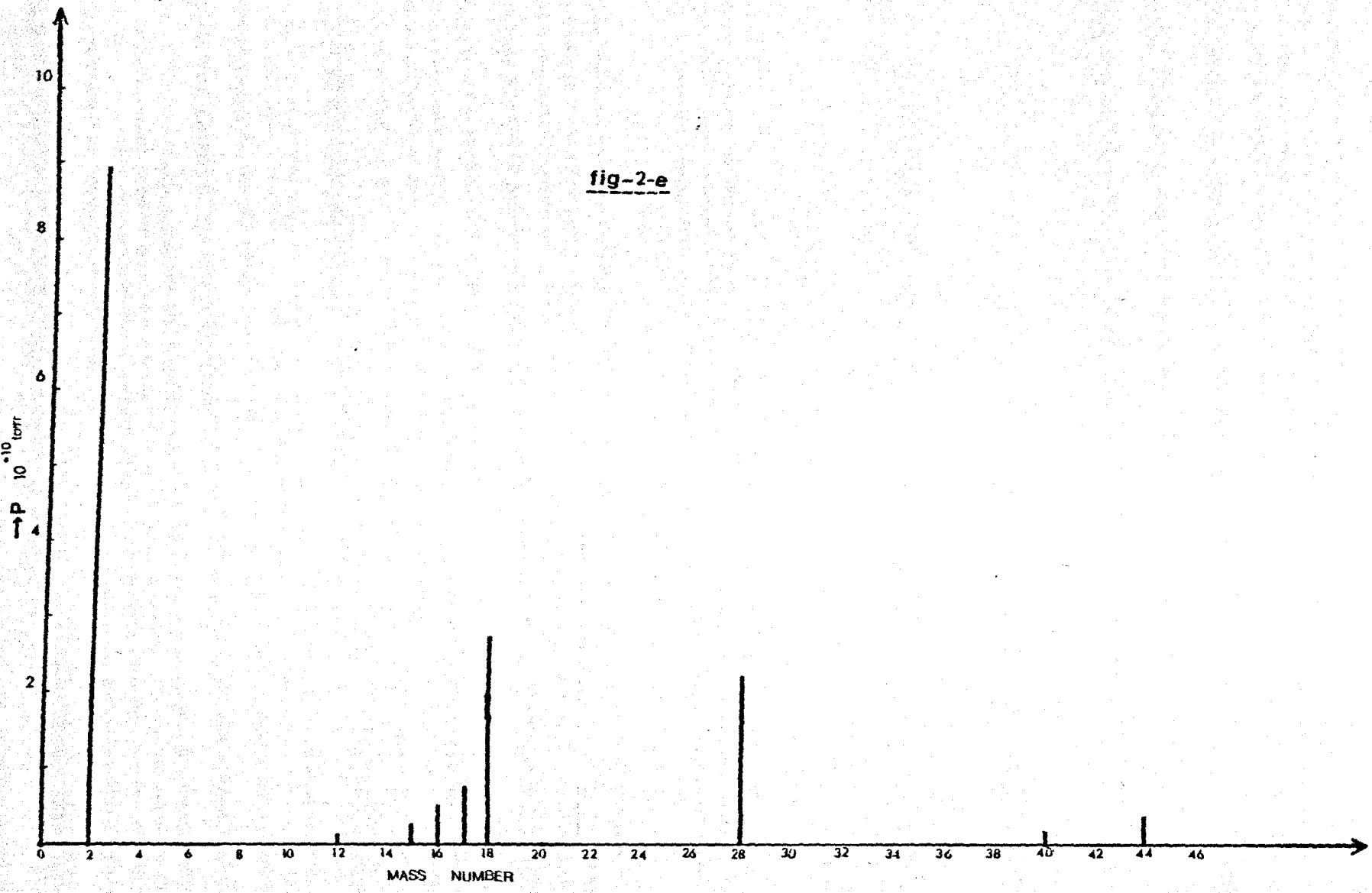
10
8
6
4
2
P
10^{-10} torr
0
2
4
6
8
10
12
14
16
18
20
22
24
26
28
30
32
34
36
38
40
42
44
46
MASS NUMBER

fore-vacuum side was isolated from the main chamber and the ion pump used for pumping. In this state the whole ultra high vacuum side was baked externally and internally at high temperature, about 275°C, for more than 24 hours. At the end of this procedure a pressure of 10^{-7} torr was readily attained, while the system was hot. Then the system was allowed to cool while degassing the titanium filament at 3 amp current for two days. At this stage the base pressure dropped to 10^{-9} torr or less. Usually the characteristic of the base pressure was checked by recording the mass spectrum. The mass spectrum commonly observed is shown in the fig. 2.e.

The spectrum contains mainly peaks, 2, 17, 18 and 28, with a small amount of 16 and 15, but the partial pressure of each peak is less than 10^{-9} torr. The hydrogen came mostly from the titanium filament. When the current in the filament increased from 3 amp to 4 amp, the mass 2 peak height increased by five times, while other peaks remained unchanged (this agrees with Riviere's work (1965)). Therefore particular attention was taken to degass the filament thoroughly just below its temperature, before evaporation. The height of the peak 17 and 18 depends on the baking procedure and to reduce these peaks a uniform baking without cool spot was employed, also the inside of the chamber had been coated with gold to reduce the probability of water vapour being formed by the reaction of the hydrogen with stainless steel (Beavis, 1973). Previously the origin of the carbon monoxide peak 28 has been suggested to be hot filament inside the ultra high vacuum (Somarayai, 1968, Kirk et al., 1968, Banker, 1965, Singh, 1976). In the present work this problem was investigated to some extent according to the experimental interest. The mass spectrometer was tuned to the peak 28, the ion pump valve and mass spectrometer valves were closed simultaneously, the variation of the peak 28 recorded for a

few minutes ; when the mass spectrometer valve was suddenly opened to the chamber, the height of the peak and its rate of increase with time dropped by the same factor as the volume had been increased. However when a small dose of research grade oxygen was introduced in the chamber the CO peak suddenly increased to many times its former height and similar effect was noted when a dose of water vapour was introduced into the system. We concluded therefore that the origin of the carbon monoxide was in the mass spectrometer, probably its filament, and that gases which contain oxygen can activate the generation of this carbon monoxide. In all experiments (except those in which the mass spectrum was studied) the mass spectrometer valve and ion pump valve were kept closed to avoid the generation of carbon monoxide.

The origin of peaks 15 and 16 was also investigated according to our experimental need. In some of our experiments one of the internal heaters was carrying 5.5 amp to keep the system at 50°C in an hydrogen atmosphere. The heater at this current is at dull red heat stage. For the investigation a thoroughly degassed heater was kept at 6 amp and the mass spectrometer turned to the 15 peak (selected to avoid confusion of other gases at 16). When a dose of 10^{16} molecules of pure hydrogen was introduced, the rate of increase of the peak height increased by many times but it did not decrease when the heater was switched off. In a second experiment the heater was off at the start and hydrogen introduced again the rate of increase of peak height increased many times, but no effect was observed when the heater was switched on. In a third volume - sharing experiment (as described above for carbon monoxide) the peak height dropped by more than five times. Therefore we concluded that the CH_4 was coming from hot MS 10 filament due to the reaction of hydrogen gas there. But in those experiments at 50°C, where we used W-heater with 5.5 amp, it was not

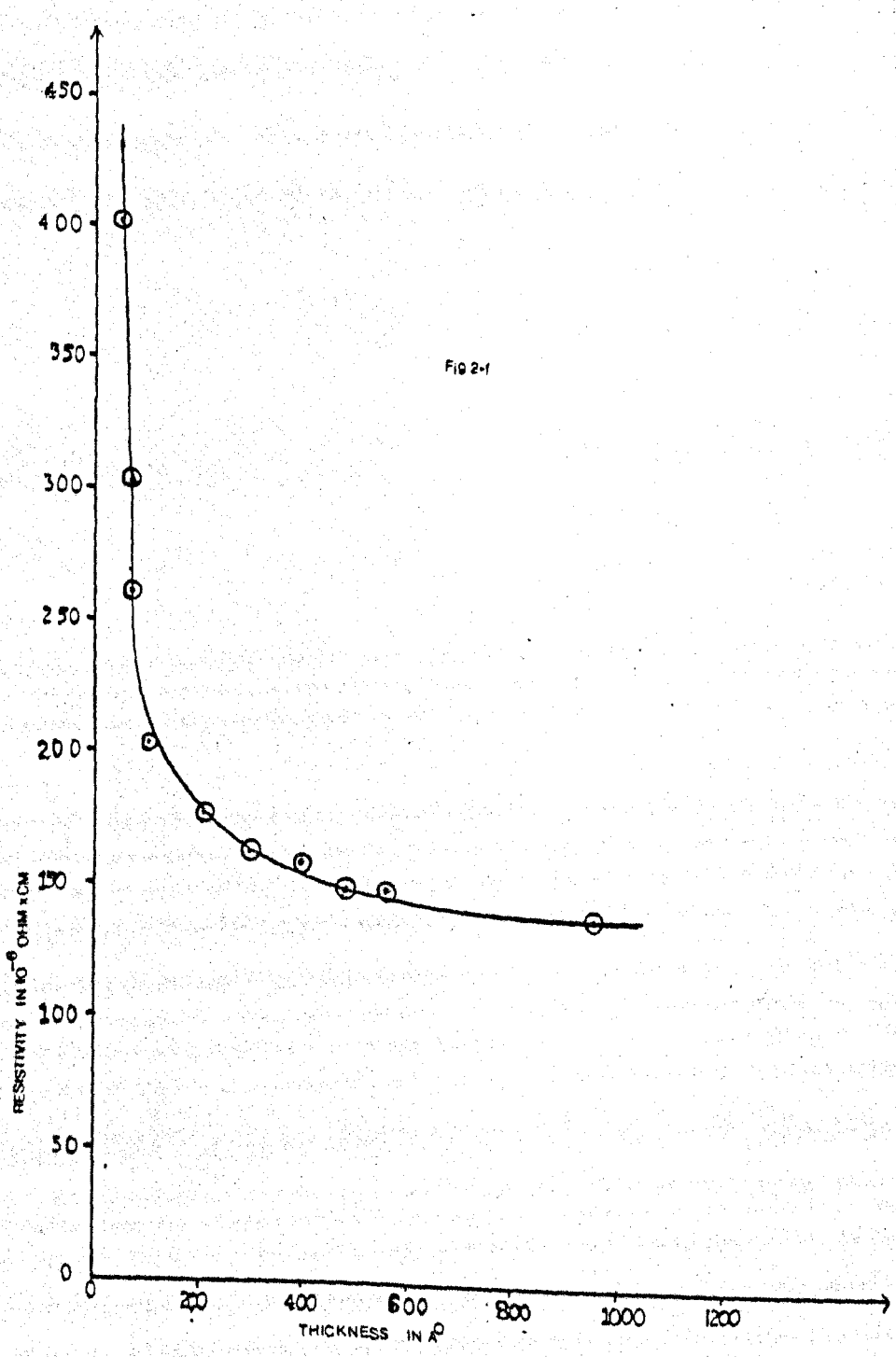
450
400
350
300
250
200
150
100
50
0
0
200
400
600
800
1000
1200
RESISTIVITY IN 10^{-6} OHM x CM
THICKNESS IN Å

Fig 2-1

hot enough to activate the generation of the CH_4.

Therefore in all our experiments (except in a few water vapour experiments) the base pressure is mainly due to the hydrogen gas. In water vapour experiments, H_2O proportion is slightly more.

2.8 Preparation of thin film

A titanium wire of diameter 0.25 mm and purity 99.7% (quoted impurities in PPM were C-95, Fe-30, Si-20, Al-20, other metals 130; Metal Research Ltd, London) was well degassed at a temperature just below the evaporation point by passing current for two or three days. Then by slightly increasing current the titanium evaporated over the glass substrate. During the evaporation, pressure rose to nearly 5×10^{-9} torr and substrate temperature rose to nearly 50°C. The thickness of the film was estimated from a calibration curve of thickness against film resistivity, this plot was established previously by Singh (1971) for titanium film prepared in a very similar situation, and it is shown in the fig. 2.f. The rate of evaporation was slow and varied from 3 to 5 Å per minute. For each experiment a film of thickness 100 Å was prepared. The stability of the film was checked by observing stability of resistance and work function after evaporation. Twenty minutes seemed to be enough to reach a steady state for these two parameters. (After the evaporation, pressure and temperature dropped quickly to their initial values. It has also been shown previously by Surplice et al., (1978) that the Ti-films prepared by this method (a) have good surface cleanliness as shown by their Auger spectrum (b) have a randomly oriented H.C.P. structure (when examined in air) (c) have a grain size of 50 Å.

In this way more than one film could be deposited on each substrate. The first Ti-film in each series was deposited on a clean glass substrate and named as fresh film (e.g. Ti 30-1). The notation Ti 30-1, represents

fresh Ti film in 30th series. After the experiment another Ti-film was deposited over the one just studied (now a compound) and named a sandwich film (e.g. Ti 30-2). Again the notation represents 1st sandwich film of the 30th series. In some cases a maximum of six sandwich films were deposited one over another.

2.9 General procedure of experiment

The evaporated Ti-film was placed in front of the vibrating electrode and left for a minimum of twenty minutes to allow it to reach a stable state. The stability was identified from the constant value of C.P.D. and resistance within random experimental error, which were ± 5 mV for C.P.D. and ± 1 ohm for resistance. After attainment of a steady state, the gas CH_4 or O_2 or H_2O) was introduced either in the form of continuous flow or in doses. The hydrogen and oxygen studied were B.O.C. grade X. Water vapour was prepared as described previously. According to the experimental needs the rate of flow varied from 10^{13} to 10^{16} molecules per minute, and also size of the dose varied from 10^{15} to 10^{18} molecules. The doses were introduced at regular intervals and the length of the interval varied from 10 minutes to half an hour. The saturation stage which is mentioned later was identified from the constant value of C.P.D. and resistance within the experimental error for half an hour. Particular attention was taken to reduce other types of error which were stray capacitance error; (For details see D'Arcy's work on the same apparatus), electromagnetic pick-up (described previously) and frictional charge development. To reduce the last, all the parts of the system were kept as rigid as possible during the experiment. Also the main chamber and gas reservoir was isolated from hot filament effects to avoid the generation of gaseous carbon products as described in 2.7.

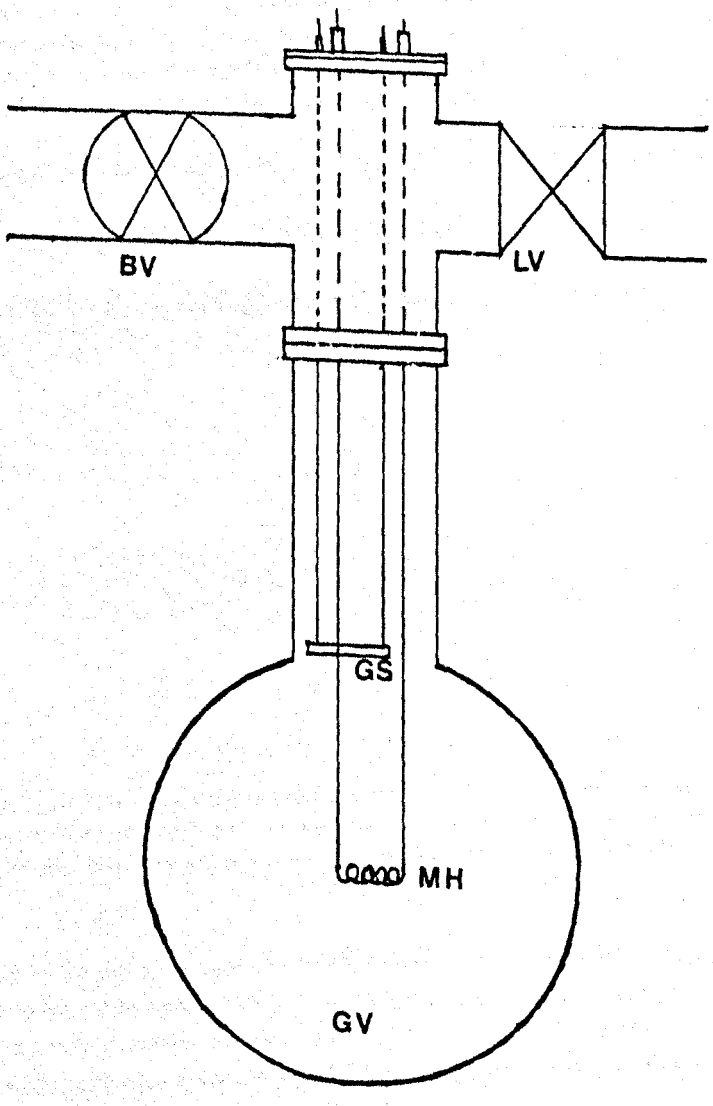

fig-2-g

According to experimental need the C.P.D. and resistance readings were noted one after another but as close as possible. For the C.P.D. measurement two modes of detection were used. On one mode it was measured by applying a backing voltage. In the other mode a feedback system was employed. The C.P.D. or resistance could also be recorded directly on a chart using pen recorders. In a few experiments the mass spectrum was recorded; the C.P.D. and resistance results of these experiments were used for the identification of experimental stages but not added as a result for interpretation, due to possible error due to impurities. All pressure readings were corrected for the sensitivity of the particular gas, using manufacturer's data.

2.10 Calibration of atomic ratio (r) against resistance variation

This experiment was conducted only for the titanium-hydrogen system, in a spherical glass flask (of area 320 cm^2), which was connected to the ultra-high vacuum chamber. The arrangement is shown in the fig. 2.d. A known amount of titanium is evaporated from a W-helix heater. A blank run showed that the vessel, W-helix and leads sorbed a negligible amount of hydrogen. Hydrogen doses of known size were introduced to the titanium film as a slow flow. The variation of film resistance for each dose was measured across a square sample of titanium film on a square glass substrate (described previously) which was placed near the neck of the vessel, facing away from the incoming hydrogen jet. The calibration curve was plotted from the percentage variation of resistance at the end of each dose and the amount of hydrogen atoms sorbed.

CHAPTER 3

Titanium-hydrogen study: Previous work

3.1 Metal-hydrogen system

a) Surface studies: In general the interaction of hydrogen involves three stages which are adsorption, solution and hydride formation. Adsorption is the most important process of these three and always an integral part of the other two. Research on the adsorption of hydrogen on metals is not only important in understanding the other two processes, but is also a test case for understanding the interaction of other gases with metals, because of the chemical simplicity of hydrogen. Consequently there is an enormous literature available, mostly limited to a few metals; however the exact nature of the interaction of hydrogen is not clear. This could be due to theoretical predictions coming from idealized and specialized models, which can obviously differ from experimental results which are conducted on real surfaces.

It is well known that hydrogen is readily adsorbed by metal surfaces (Trapnell, 1955). For many years the adsorption studies have been investigated by means of work function measurements, diffraction experiments, desorption techniques, photo-, ion-, electron- and field-emission spectroscopies. The common observation is that the chemisorption of hydrogen atoms on a clean metal surface needs very little activation energy and even at low temperatures molecular chemisorption can take place. In general on all metals hydrogen first becomes physisorbed and then, if the activation energy is enough becomes dissociatively chemisorbed. The chemisorption behaviour of hydrogen on the metals is given in table 3.1. It is well known that the chemisorption of hydrogen by metals is exothermic (Trapnell, 1955), and dissociation of the hydrogen molecule is of central importance not only in chemisorption but also in all surface processes. A high activity for chemisorption is only apparent in the

Table 3-1

Distribution of H_2 Chemisorption in the Periodic Table. + = H_2 Chemisorption, − = no H_2 Chemisorption at 273 K.

Na	Mg											Al	Si
K	Ca	Sc	Ti	V	Cr	Mn	Fe	Co	Ni	Cu	Zn	Ga	Ge
Rb	Sr	Y	Zr	Nb	Mo	Tc	Ru	Rh	Pd	Ag	Cd	In	Sn
Cs	Ba	La	Hf	Ta	W	Re	Os	Ir	Pt	Au	Hg	Tl	Pb

Table 3-2

Nonactivated chemisorption	Activated chemisorption	No chemisorption up to 0°C
W, Ta, Mo, Ti, Zr, Fe, Ni, Co, Pd, Rh, Pt, Ba, Nb, Cr	Mn, Ge, Ca(?)	Cu, Ag, Au, K, Zn, Cd, Al, In, Sn, Pb

centre of the periodic table (Table 3.1) i.e. among the transition metals. The heat of chemisorption of hydrogen on transition metals is relatively large (20-50 K cal/gmole).

The dissociation of hydrogen molecules on adsorption depends on the electronic (Trapnell, 1955) and geometrical structure (Jones et al., 1975; Lang et al., 1972) of the metal surface. Jones et al. have observed that there is dissociative adsorption of hydrogen on a stepped surface of Cu, but molecular adsorption on a smooth surface of Cu. Baskin et al. (1976) have pointed out that the local bulges on a surface will produce attractive centres for chemisorption. Further, Fassaert et al. (1976) have suggested that stepped surfaces and high index planes are specially active for hydrogen chemisorption due to the availability of active sites such as edges and protrusions. Lang et al. (1972) supposed that the increased activity was caused by the large amount of metal atoms available at a step for interactions with hydrogen. This special activity could be one reason for the difference in theoretical predictions and experimental results conducted on real surfaces, which have all kinds of defects.

It has been well established experimentally that some transition metals can chemisorb hydrogen dissociatively even at low temperatures (Deuss et al., 1973). Also chemical kinetic data indicates that the hydrogen chemisorbs atomically on transition metals (Bagchi et al., 1974). The changes in the U.P.S. spectra (Demuth, 1977) due to the chemisorption of hydrogen on transition metals indicates the participation of d-electrons. The importance of the d-electrons, especially in dissociation, is well illustrated by hydrogen's dissociative adsorption on Ni, but molecular adsorption on Cu (Yoshinori et al., 1977 ; Baloock et al., 1974). This experimental evidence has been supported by theoretical reasons given by Deuss et al. (1973), who pointed out that the unoccupied d-electron orbitals in Ni can cause unactivated dissociation of hydrogen molecules,

and the reason for the different behaviour of Cu is the completely occupied d-band. Further examples are evident in table 3.2.

The nature of the chemisorption bond between a transition metal and hydrogen has received great attention because of its importance in surface processes like catalysis. The role of s and p electrons is less understood than d-electrons but has been postulated to be of some importance (Dowdin, 1958). Recent calculations on Ni (Cuse et al., 1977; Johnson, 1977; Blyholder, 1975; Melius et al., 1976) suggest that bonding occurs predominantly via 4s-electrons, and 3d electrons play an important role in dissociation but a minor role in bonding. This conclusion has been generalized for transition metals (Melius et al., 1976). But the U.P.S. experiments of Demuth (1977) on Ni, Pd and Pt show that the generalization is not correct, he concluded that the interaction of hydrogen with the d-states of Ni is different and probably weaker than with the d-states of Pd or Pt where d-electrons are directly involved in bonding, and also a stronger interaction of s electrons occurs on Ni. than on Pd or Pt. Bullett et al (1977) also concluded for W that the interaction was mainly due to the d-electrons but with a little contribution from s-electrons. The NMR study of Ito et al. (1977) also shows the contributions of 5d and 6s electrons in the case of W and Pt, but only 4s electrons in Cu. However Fassaert et al. (1976) concluded that in the case of hydrogen chemisorption on Ni, the d-electrons play a major role. So the relative importance of the s, p and d-electrons of a metal in chemisorption and bonding is not well understood. However one can speculate that the availability for large overlap and vacancies in the electron lobes are important factors in the determination of the nature of the chemisorption bond and relative importance of d-electrons. For the understanding of these phenomena, the U.P.S. is the only spectroscopic study which seems to be suitable at the present time.

Theoretical models for H adsorption on low index crystal planes were

contradictory. Fassaert et al. (1976) have predicted A site adsorption, but Blyholder (1975) has suggested C site adsorption is the most favourable site. However experimentalists generally suggested random adsorption at room temperature to account for the features of L.E.E.D. patterns (Christman et al., 1979).

Further, L.E.E.D. workers have suggested that coverage dependent adsorption on A, B and four-fold sites, were needed to account for the L.E.E.D. patterns which they observed for H on single planes of Mo and W (Dooley et al., 1970; Madey et al., 1975). It is more difficult with H than with other gases to obtain and interpret L.E.E.D. patterns because of its low scattering cross-section and high rate of diffusion. The L.E.E.D. patterns which have been observed for hydrogen adsorption on a metal have been found to depend on the crystal planes and coverage and temperature. For example at low temperature L.E.E.D. patterns are observed for Ni(100) and Ni(111) but they disappear at room temperature (Christman, 1974), low coverage C(2x2) patterns on W(100) for hydrogen adsorption become P(1x1) at high coverage (Madey et al., 1975). The hypothesis of surface reconstruction and relaxation has also been proposed to account for the difficulty of interpreting the patterns.

Most thermal desorption studies of H from crystal planes indicate that there is more than one binding state and some of them depend on coverage, but they disagree about the number of states (e.g. from two to as many as five have been proposed for H/W(100)) and about the measured adsorption energies. The general outcome from L.E.E.D. and desorption studies is that on any crystal plane there is likely to be a hetereogenity of the adsorption sites whose relative importance depends on the crystal plane, on coverage and on temperature.

It is reasonable to observe several sorts of adsorption sites because of the hetereogenity of available sites at the surface. This idea was proposed by Bond (1969), who suggested that in chemisorption the electron

lobes which emerge outside the surface are important. The nature of the chemisorption bond and possible sites for adsorption could be determined from the nature of the electron lobes and the direction at which they are directed outside the surface. Tamm et al. (1971) have distinguished several different sorts of adsorption for hydrogen, on three main planes of W with different overlaps of metal electron lobes. Madey (1972) has said that the Bond model is consistent with the desorption features of hydrogen on W(100) and W(110) but not on W(111). It is also less successful in correlating work function measurements and L.E.E.D. patterns. This will be due to the simplicity of the model because the presence of chemisorbed atoms will have some effect on the nature of the adsorption sites, and the existence of adatom-adatom interaction forces is evident from the observation of L.E.E.D. patterns at fractional coverages.

Therefore the complicated nature of all these studies indicates that the adsorption of hydrogen on metal surfaces is not a straightforward topic but rather a difficult problem with many effects; some of them are more effective in some situations e.g. surface diffusion of adatoms at high temperature. Some of them are ineffective in some situations e.g. adatom-adatom interaction at very low coverage. So correct understanding requires critical knowledge about all these factors. Bearing these difficulties in mind we will now start to look at the previous studies of work function and conductivity measurements.

Work function measurement was also one of the major techniques used for the study of hydrogen adsorption on metals and there have been an enormous number of measurements. Many polycrystalline samples of metals have been investigated by various workers (Baker et al., 1954; Mignelot, 1957; Lewis et al., 1969; Dus et al., 1976 etc.) and work function measurements have also been made during the adsorption of hydrogen on single crystals in conjunction with L.E.E.D. studies

(Christmann et al., 1979; Taylor et al., 1974; Conrad et al., 1974 etc.). In the interpretation of these results it was mainly assumed that the solution of hydrogen in the metal was negligible, or the work function change due to the solution of hydrogen is negligible. Fortunately this is valid except in a few cases (Sc, Pd) which have become known, in which the solution of hydrogen is accompanied with lattice expansion. In these cases a consideration of the effect of lattice expansion becomes important. Most of the transition metals form hydrides. The hydride formation very often affects the position of the Fermi level (Müller et al., 1977; Dus, 1975). Therefore it is very important to understand about the formation of hydride patches at the surface for a correct interpretation of the observed effects of hydrogen. The work function shows an increase for most metals due to hydrogen adsorption (Holze et al., 1979). Some metals show an increase at the start and then a drop (Christmann et al., 1979; Christmann et al., 1976; Dus et al., 1976; Bradford et al., 1974; Mignelot, 1957). Mignelot (1957) suggested the increase of work function during hydrogen adsorption on Pt (poly) at $77^{\circ}K$ was due to the electronegative form of chemisorbed hydrogen, and the drop due to the electropositive form of molecular hydrogen. This view was generally taken by later workers on the same metal (Satcheler et al., 1960 and Lewis et al., 1969) but not by Christmann et al. (1976). Christmann et al. suggested that the increase was due to the adsorption of hydrogen on the imperfections (defects) of the surface and the drop due to the chemisorption of atomic hydrogen. Dus et al. (1979) explained their result on Co at $78^{\circ}K$ by assuming an atomic electronegative form for the decrease of work function. Christmann et al. (1979) explained their result on Ni(111) by assuming a positive dipole moment state of hydrogen atoms up to $\theta = 0.5$ and a negative dipole moment state of hydrogen atoms on new adsorption sites after $\theta = 0.5$

Barford et al. (1974) observed that some faces [(111), (110)] of

W show a drop in work function at the start, while other faces [(100), (112)] show an increase, but Madey (1972) observed an increase for W(111) [both workers measured C.P.D. changes in their experiments]. Demuth et al. (1974) observed a large increase in work function on the Ni(110) plane but a small increase on the Ni(100) plane due to the adsorption of hydrogen, and Madey (1972) also observed the same type of difference between adsorption on W(100) and W(111) faces. A stepped face of Pd(111) showed a larger increase of work function than a smooth Pd(111) face, on hydrogen adsorption (Conrad et al., 1974). Beaker (1961) observed breaks in the variation of work function with coverage and attributed this to the adsorption of hydrogen on different sites due to the heterogeneity of the single planes of W. However Tamm et al. (1970) and Madey et al. (1970) did not observe any breaks in the variation of work function corresponding to the different desorption states of W(100). However hydrogen adsorption on W(211) face showed an increase at the start corresponding to one desorption state, then an increase corresponding to another desorption state (Rye et al., 1973). The adsorption of hydrogen on Nb(110) showed a small work function increase ($\lesssim$ 100 meV) but no new L.E.E.D. pattern, and this adsorption was described by the authors (Hass, 1968) as an amorphous type. They also pointed out that the adsorption of hydrogen was not affecting the structure of the Nb(110) surface because of the unchanged L.E.E.D. pattern, but in the same chemical group a Ta(110) surface gave a small decrease in work function (Fehrs et al., 1967). Finally it is noticeable that the increase in work function due to adsorption of hydrogen on polycrystalline nickel (Delcher et al., 1968; Crossland et al., 1964) is almost the mean increase of work function for the three low index planes Ni(111), Ni(100), Ni(110) (Christmann et al., 1979). Further, Christmann et al. observed a linear variation of work function with coverage up to half the saturation coverage, and the polycrystalline

Ni also shows a linear variation up to half the saturation coverage, but after that the slope becomes smaller. This data supports the assumption of a predominance of low index planes at the surface of polycrystalline samples.

The results discussed above generally indicate that the work function variation depends on the electronic and geometric nature, and on the relative size of chemisorbed hydrogen and size of adsorption site. Conductivity measurements have also been used for hydrogen adsorption studies (Brocker et al., 1971; Geus, 1964; Suhrmann et al., 1959). These workers observed an increase of resistance due to hydrogen adsorption on metals (Ni, Fe, W) and proposed that an electronegative form of chemisorbed hydrogen atom was the reason for it. The electropositive form of adsorbed hydrogen was believed to be the reason for a resistance drop. However later workers (Singh et al., 1976; Curzon et al., 1979) attributed the increase of resistance to the solution of hydrogen in the bulk.

It seems likely that both processes are possible, but the latter is dominant in a metal which dissolves a reasonable amount of hydrogen e.g. Singh et al. (1976) observed nearly 30% increase of Er film resistance on the sorption of hydrogen at room temperature and this observation can be explained only by the effect of the latter process. Therefore it is important to recognise which is likely to be the dominant process in the resistance changes due to the sorption of hydrogen by a particular metal.

In conclusion hydrogen is chemisorbed dissociatively by most of the metals. The chemisorbed atom is negatively polarized and its effect on the work function of the surface depends on the position of the adsorption site. The site of adsorption varies from crystal plane to plane and depends on the electronic and geometric nature of the surface The temperature of the metal surface and of the chemisorbed hydrogen atoms

have an effect on the chemisorption process. The adsorption effect often overlaps with bulk sorption effects in metals (especially in transition metals) due to the rapid diffusion of hydrogen into the bulk. In the next section we will look more at studies which are affected by the bulk properties.

b) Bulk Studies: Bulk studies of metal-hydrogen systems have intrigued researchers ever since Graham (1866) first observed that Pd could absorb a large amount of hydrogen. These studies normally described the nature of the solution and the hydride states of the metal-hydrogen system. Researchers have mainly studied thermodynamical properties, x-ray, neutron, and electron diffraction, transport and magnetic properties, N.M.R., and positron annihilation. The hydrogen adsorbed on a metal surface in general diffuses into the bulk metal and becomes a solution, and if the amount of it dissolved exceeds the so-called solubility limit of the particular metal, then the hydride starts to precipitate. There are two kinds of absorbers which are classified as endothermic and exothermic ones. Exothermic absorbers include alkali metals, alkaline earth metals, titanium and vanadium group metals, rare-earth metals, actinide metals, Yt and Sc. These metals form stable hydrides and one of their common features is a change in lattice structure on hydrogen absorption; also their solubility limit decreases as temperature increases. Other metals dissolve hydrogen endothermically and generally do not form stable hydrides and their lattices are not changed. However exceptionally a few of them (Cr, Ni, Pd and Cu) form hydrides with a discontinuous lattice expansion.

There are three kinds of hydrides which can be classified from the nature of the bond between the metal and hydrogen, as covalent, ionic, and metallic hydrides. However such classifications is not always completely descriptive e.g. Rare-earth hydrides are usually classified

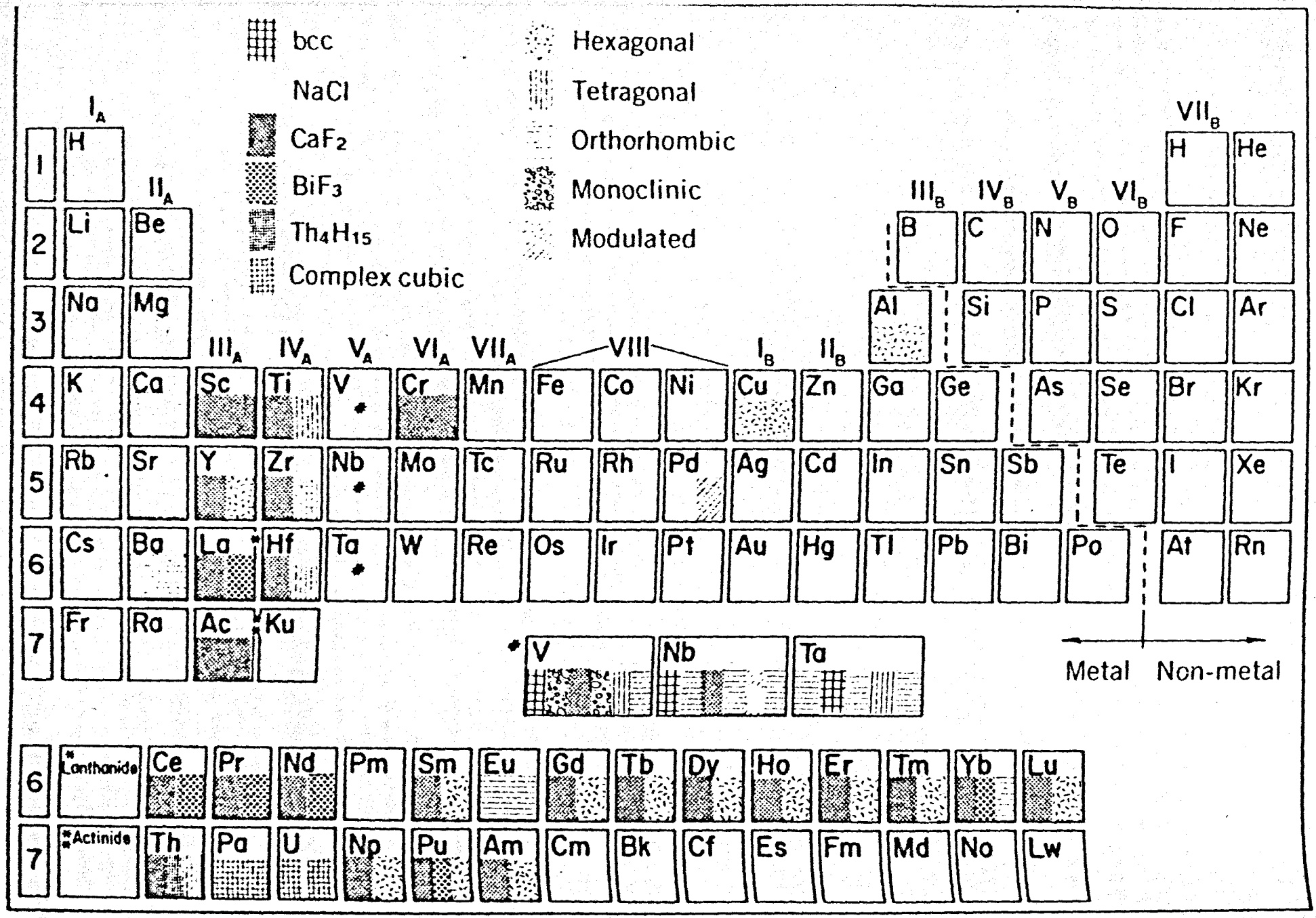

Periodic table of the elements showing occurrence and structure of metal hydrides. Stoichiometries range from $MH_{0.5}$ (for M = V or Ta) to $MH_{3.75}$

these hydrides exhibit more than one crystal structure. For example, Tilman Schober, at KFA Jülich, has proposed the existence of nine hydride

as metallic but they exhibit some characteristics similar to those of ionic hydrides. The strongly electropositive alkali and alkaline earth metals form ionic hydrides. Transition, rare-earth and actinide metals form metallic hydrides. Other metals (Cu, Al etc.) form covalent hydrides.

A complete review of all metal hydrides was given by Muller et al. (1968). Since 1968 there have been large advances in this field. Superconducting hydrides with an inverse isotope effect (Miller et al., 1975) have been discovered, the importance of hydrides in the energy storage problem has been recognized, and theoretical workers have proposed new models to explain some of the experimental data. In other words, not only technological studies but also basic physical studies of this system have been stimulated; an indication of this stimulus was a recent article published by Westlake et al. (1978) in "Physics Today". Because of the wide extent of metal-hydrogen studies this survey is limited to metallic hydrides, especially transition hydrides because the study of titanium hydride is the main interest of this work.

The common features of the metallic hydrides are that they have homogeneous phases of variable composition, properties (e.g. structure) that are different from those of the metal, and a high concentration of hydrogen. The variable composition indicates the possibility of non-stoichiometry. The possible reasons for this are structural defects, impurities in the metal and hydrogen, incomplete hydriding, and the electronic structure of the metal. A complete structural survey of all hydrides is given in Figure 3.a. It is a characteristic of the metallic hydrides to have more than one crystal structure. Most of the metallic dihydrides have CaF_2 structure, however the structure of the trihydrides is either hexagonal or BiF_3 structure. This feature of these hydrides (except PdH_x, CeH_x) makes it difficult to prepare them as single crystals, but PdH_x and CeH_x have been prepared as single crystals.

Neutron diffraction, N.M.R., P.M.R. and internal friction studies indicate that hydrogen occupies interstitial sites in the metal lattice. For an F.C.C. metal lattice it can be visualized that the occupation of all octahedral sites leads to the composition MeH with NaCl structure, whereas occupation of all tetrahedral sites leads to a composition MeH_2 with CaF_2 structure, and the occupation of all octahedral and tetrahedral sites gives the composition MeH_3 with BiF_3 structure. Most of the trihydrides of group three metals have hexagonal structure, and the occupation of all tetrahedral and octahedral sites gives trihydride of the metal. But the situation in a B.C.C. metal lattice is rather complicated due to the large number of interstitial sites.Simultaneous occupation of hydrogen in all interstitial sites would allow a composition MeH_9 which is not experimentally observed. B.C.C. vanadium group metals show only a maximum composition MeH, therefore a random arrangement of hydrogen in these sites is possible. As the result of this, these metal hydrides show order-disorder transition phenomena with the formation of superstructures at low temperature (Wallace, 1961). From N.M.R. studies of B.C.C. NbH, Zamir et al. (1964) and Stalinski et al. (1967) disagreed about whether octahedral or tetrahedral sites were occupied. However the neutron diffraction experiments of Somenkov (1968) suggest only about 10 per cent occupy octahedral sites and the others are in tetrahedral sites. But for Pd and Ni the occupation of octahedral sites was confirmed from the neutron diffraction studies by Worsham et al. (1957) and Wollan et al. (1963) respectively. Tetrahedral sites occupation was confirmed by the neutron diffraction studies of Sidhu et al. (1963) for titanium group hydrides.

We might expect it to be an easy problem to determine the nature of the Me H bond in hydrides owing to the simple electronic structure of hydrogen. But this is not so, even now the nature of the bond is a question for scientific debate. In early days three models were commonly

used to explain the electronic nature of metallic hydrides: the 'protonic', 'anionic', and covalent or 'Interstitial atomic' models. In the interstitial atomic model, H-metal bonding was considered to be either resonating covalent (Pauling et al., 1948) or covalent-metallic (Ubbelohde, 1937), however in both cases hydrogen is considered to be more protonic than anionic. This model can explain some structural features of metallic hydrides (e.g. lattice expansion) (Gibb, 1963).

The first two models are based on the rigid band approximation, in which one assumes no changes in the energy band of the metal during the formation of hydride. They differ in their assumption about the relative position of the metal conducting band and hydrogen 1s band. The protonic model assumes that the hydrogen 1s band lies above the conduction band of the metal, therefore the electron from hydrogen prefers to occupy a vacant d-state of the metal band in order to keep the total energy a minimum, so the hydrogen acquires unit positive charge. The anionic model assumes the reverse situation, therefore the electron flow is from metallic band to hydrogen 1s band, so the hydrogen acquires unit negative charge.

The protonic model has been widely used for transition metal-hydrogen systems, the anionic model seems equally well to describe the physical properties of rare-earth hydrides. Gibb (1963) argued against the protonic model. Heckman (1969) gave experimental support for the protonic model. Stalinski (1972) generally supported the anionic model for rare-earth hydrides, but he was not certain about its validity in transition metals (Ti-group, V-group etc.). Strong support for the protonic model comes from the fast diffusion of hydrogen in metal hydrides and zero paramagnetic susceptibility of Pd $H_{0.7}$ (Oxley, 1922). The high heat of formation of metallic hydrides seems to support the anionic model, but this model is contradicted by the observed sharp rise of Hall coefficient with hydrogen concentration in cerium (Heckmann, 1969). Generally both models explain the conductivity of the rare-earth trihydrides,

fig 3b

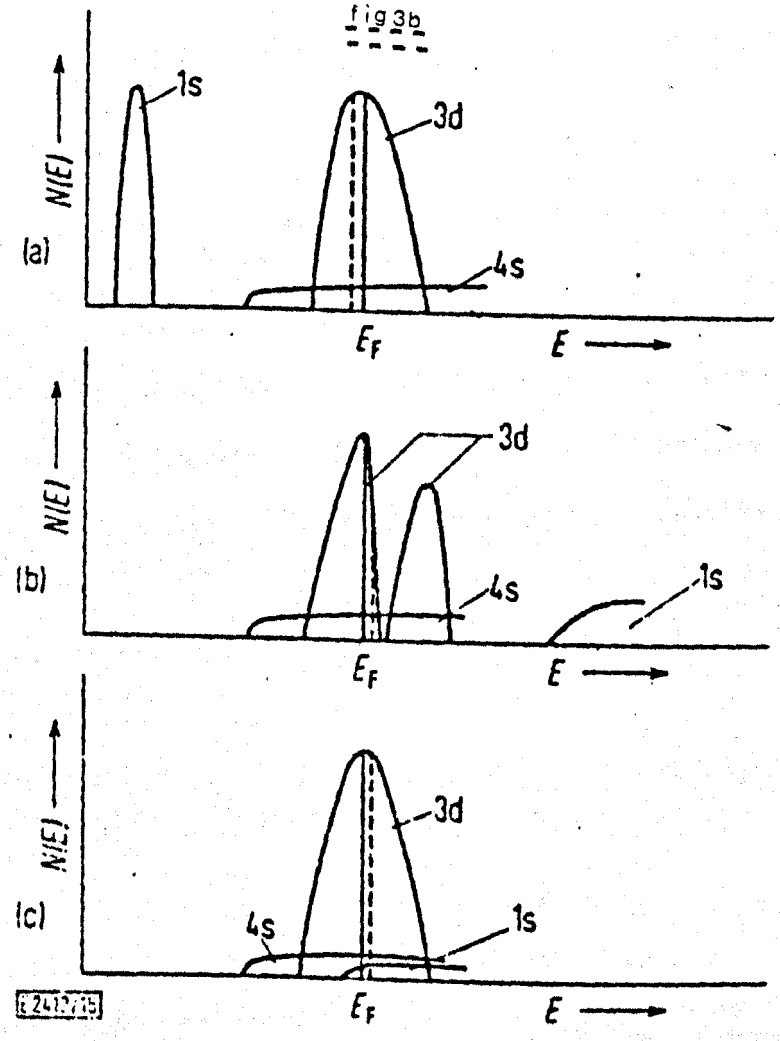

Energy band schema for a) anionic, b) protonic, and c) intermediary model

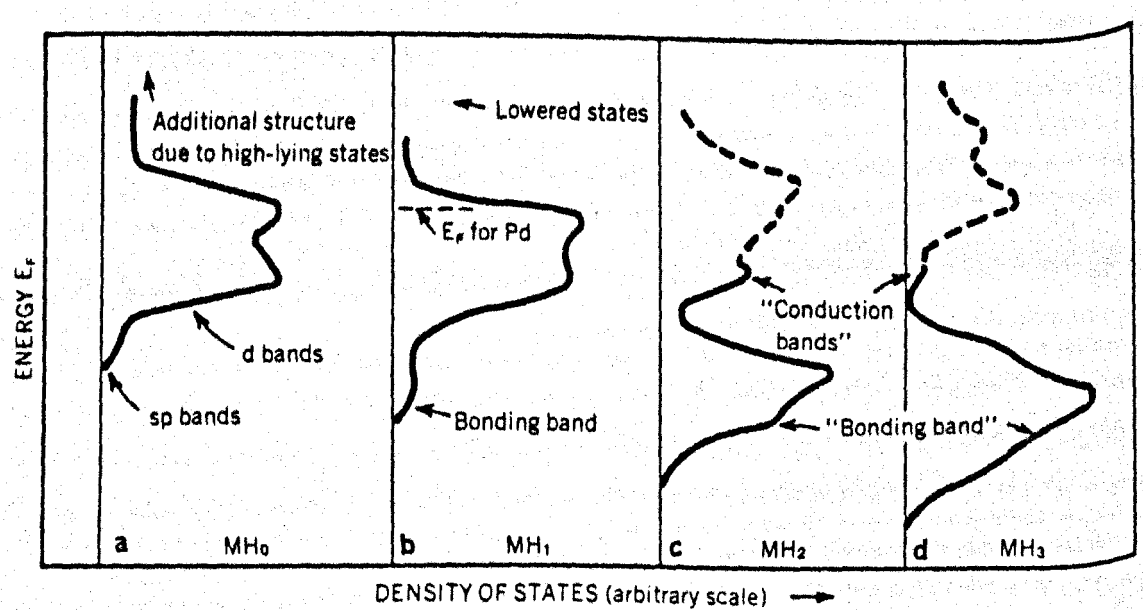

which show a sharp rise of resistance with hydrogen concentration and have a semi-conducting nature. But there is no explanation by the anionic model of why rare earth dihydrides show better conductivity than the corresponding metals. The calculation of Friedel (1972) indicates that in metals with a high density of states like rare earths, there is a large charge pile-up around the protons for screening reasons. Therefore the hydrogen atoms apparently behave like anions in rare-earth metals. Apart from this "dual nature" of hydrogen in rare-earth hydrides, the protonic model is mostly accepted for transition metals. However there are few different opinions concerning the state of hydrogen in transition metal hydrides; e.g. in the explanation of zero paramagnetic susceptibility of $Pd\,H_{0.7}$ (Oxley, 1922; Libowitz, 1958), of Knight shift in vanadium hydride (Stalinski, 1972) and of crystal field splitting in Yttrium dihydride (Parks et al., 1970). The complications showed the need for a new model to explain the electronic nature of the metal-hydrogen bond.

In the early 1970's Switendick (1975) showed the possibility of using a band structure model for metallic hydrides. In contrast to the "rigid band" approximation of the early models, this model allows for the modification and shifting of the density of states of the metallic conduction band, and formation of hybridized bands of metal and hydrogen as well as the hydrogen 1s band, in hydrides. This model has received support from recent experimental studies on metal hydrides (Eastman et al., 1971; Nagel et al., 1975; Weaver & his coworkers, 1979). Photo electron (Eastmann, 1971 and Weaver et al., 1977) and soft x-ray spectra (Fukai et al., 1979) have proved that the bonding state due to hydrogen is below the bottom of the d-band of transition metal hydrides. The general features of this band model for M, MH, MH_2 and MH_3 are given in the figure 3.b (Westlake et al., 1978).

The diffusion of hydrogen in metals has been well studied by N.M.R., quasi-elastic neutron scattering, Mossbauer resonance, and some other

studies like permeation which are subject to surface effects. The generally observed results agree with extremely rapid diffusion; for example the jump rate of hydrogen in vanadium at 100 K is about 2×10^{12} sec^{-1}. The activation energy deduced using the Arrhenius relation shows that hydrogen is relatively weakly bound in palladium hydride and in the vanadium group hydrides, slightly stronger in titanium group hydrides, and most strongly in lanthanide hydrides, if one takes into account the occupancy of tetrahedral sites only.

In general the magnetic susceptibility of metallic hydrides decreases with increasing hydrogen content. This has been explained either by protonic or anionic model; the protonic model requires a splitting of the d-bands into two sub-bands. Positron annihilation studies and Mossbauer spectroscopy have also been used to understand the nature of hydrogen in metallic hydrides. Inelastic scattering of cold neutrons has been used to study lattice dynamics and the bond strength of metal hydrides.

Chemical phase analysis is another major area of study of metal hydrides. Details of the chemical phases of all metallic hydrides have been given by Muller et al. (1968). However most of these studies were conducted at high temperature, so low temperature data very often involves extrapolation. The commonly used techniques are x-ray, neutron and electron diffraction studies, resistivity and susceptibility measurements, Pressure-temperature-composition analysis, N.M.R. studies, optical and electrical microscopy and internal friction measurements. Each technology has a different sensitivity for the determination of the phase boundaries so often they show slight differences in these boundaries. Pryde and his coworkers (Pryde et al., 1971) demonstrated the possibility of studying the phase diagram of metal hydrides (Nb, Ta) by means of resistance measurements. Libowitz (1965) and Gibb (1962) have reviewed the limited experimental and theoretical works on the electrical

properties of metallic hydrides and they conclude that changes in resistance due to hydrogen absorption may be due to at least three causes: 1) scattering of conduction electrons by interstitial hydrogen atoms, 2) changes in the number of conduction electrons and 3) modification of the band structure.

The conductivity studies of actinide hydrides were particularly difficult because of their finely divided form. There is some early literature available on the conductivity of metal hydrides (Ta, Y, Sc, Pd and Zr) but most of these studies were limited to a small range of composition (Hillig, 1953; Bruning et al., 1933; Parker, 1960; Azarkh et al., 1967; Bickel, 1960) and impure conditions. Heckman (1969) gave a collection of conductivity measurements taken during the exposure to hydrogen of polycrystalline samples of rare earth metal slabs (La, Ce, Pr, Nd, Sm, Gd, Tb, Dy, Ho, Er, Tm, and Lu). These slab samples may have had a high risk of containing impurities, also these experiments did not cover full range of composition; however these results reflected the general features of the different phases of hydride. Generally all metals except Yb showed an increase of conductivity in the mixed phase of metal and dihydride, but a drop in the single dihydride phase. However we would also generally expect a drop in conductivity at the start corresponding to solution of hydrogen in the metal, but this was not observed in any sample except Ho. This may have been due to the hydrogen already dissolved in the sample as an impurity, or a negligible amount of solubility hydrogen in these metals. All these features were reflected in the recent studies of Singh et al. (1976) for Er-H system and of Curzon et al. (1978) for Y-H system. However, Yb showed a drop in conductivity in the mixed phase of metal and dihydride, and a slight increase in the single dihydride phase (Heckman, 1969). Resistivity measurements by Libowitz et al. (1969) on single crystal cerium hydride of high composition are in very good agreement with Heckman's data. In

general, rare earth hydrides with high resistivity e.g. [CeH_3, $YbH_{1.9}$] seem to have semiconducting properties (Libowitz, 1972).

Hall effect measurements by Heckmann (1969) indicated that cerium trihydride is a p-type semiconductor, however thermoelectric power measurements indicated an n-type semiconductor (Libowitz, 1972). Savin et al. (1978), using resistivity measurements on various compositions of the Sc-H system, found an initial increase of resistance and then a drop up to the composition MH_2. ZrH_2 is a better conductor than pure Zr metal and F.C.T. ZrH_2 is an n-type conductor in which the resistivity increases with increased deviation from stoichmetry (Libowitz, 1972). Vanadium hydride ($VH_{0.72}$) has higher resistivity than pure V metal. Smith et al. (1970) measurements on the Pd-H system showed an increase of resistance across the solution and mixed phases, but a drop in the single hydride phase. In conclusion, conductivity measurements are suitable to observe the different phases of hydrides especially at low temperatures, and, generally the conductivity variation with hydrogen content reflects the nature of the conduction band and the density of states at the Fermi level.

Recently, Müller et al. (1977) have successfully demonstrated the use of work function measurements for the establishment of the chemical phases of Er hydride. It is reasonable to expect this because the work function depends on the position of the Fermi level, so the formation of different hydride phases (often accompanied by changes in crystal structure) will correspond to some change in Fermi level and in turn to a change in work function. The work function measurement is sensitive for the few top layers of the metallic sample; therefore the success of the experiments mainly depends on the production of a uniform composition throughout the sample, which in turn depends on the rapid diffusion of hydrogen in the metal. There are only a few earlier works available to support this idea; Satchler et al. (1957) study on Ta, Rivière's (1967)

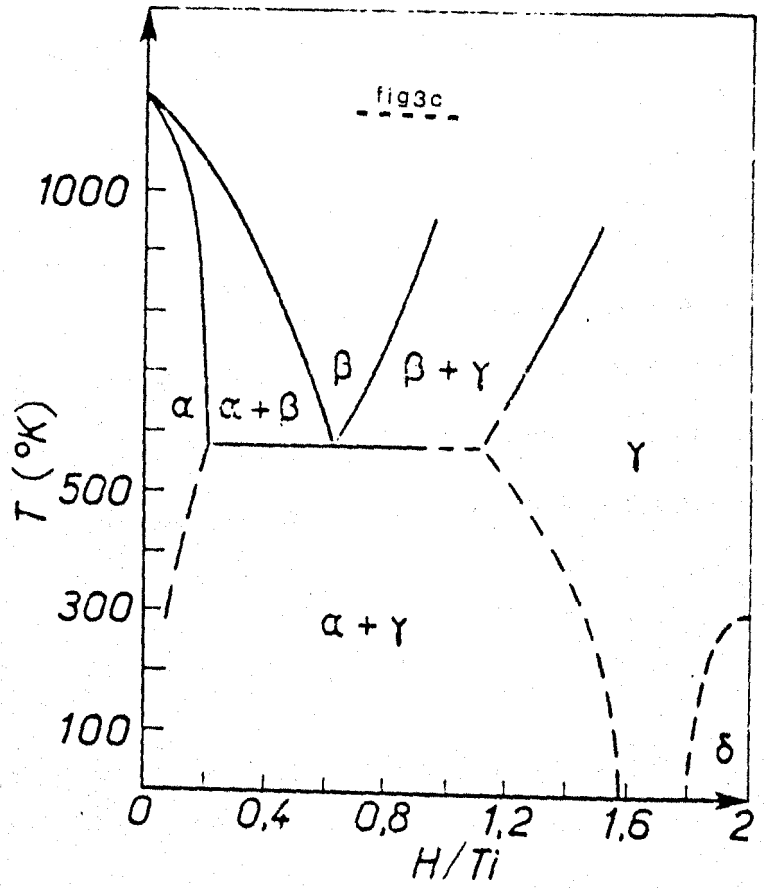
fig3c
1000
500
300
100
T (°K)
α
α + β
β
β + γ
γ
α + γ
δ
0
0,4
0,8
1,2
1,6
2
H/Ti

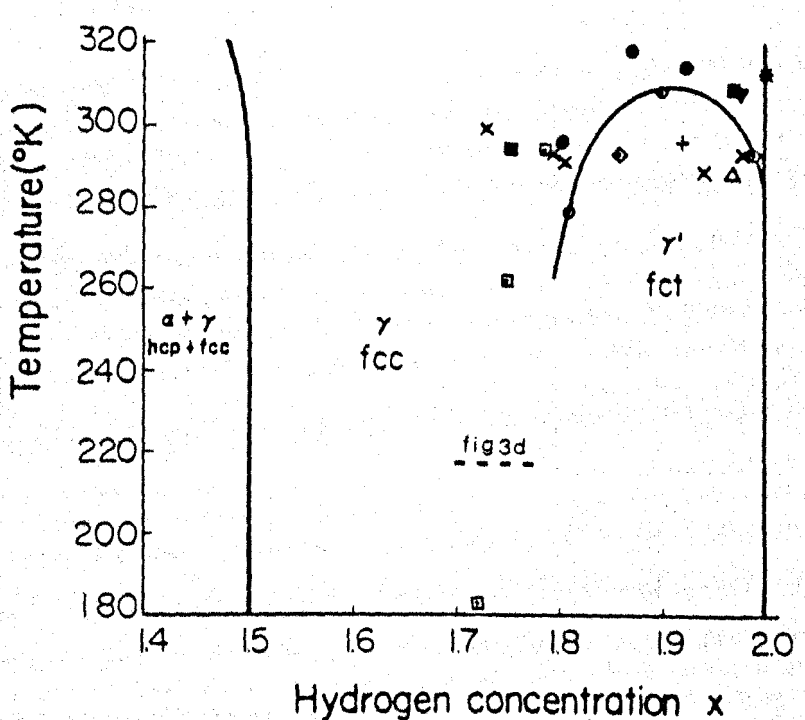
320
300
280
260
240
220
200
180
Temperature(°K)
α + γ
hcp + fcc
γ
fcc
γ'
fct
fig3d
1.4
1.5
1.6
1.7
1.8
1.9
2.0
Hydrogen concentration x

study on U, Dus (1973) work on Pd, Dus (1975) work on Nb, and Müller et al. (1977) work on Er.

The validity of the work function variation in these works in predicting the phase boundaries was discussed by Müller et al. (1977). Recently Kucherov et al. (1978) measured the work function variation with hydrogen content for the Nb-H, V-H, and Ta-H systems. The details of this literature are in Russian, however the general features of the work function variation are in agreement with five or six chemical phases of these systems.

Present day studies of the fundamental, physical and chemical properties of metal hydrides is motivated by discovery of super conductivity and the inverse isotope effect in PdH, and the technological importance of "hydrogen economy" in energy storage. However the complication of the results in many cases is a subject of warm scientific debate and it needs further research in this field.

3.2 The titanium-hydrogen system

There has been an enormous amount of literature on this system because of its technological importance. However certain aspects of it need further investigation. This chapter first describes the properties which are well established and then the areas of disagreement.

Hydrogen has a relatively high sticking coefficient on titanium and it is adsorbed dissociatively. Dissociative adsorption is to be expected from the high heat of adsorption and from the position of Ti in the periodic table. The chemisorption of hydrogen is followed by fast diffusion into the bulk. The diffused hydrogen can form several distinct phases at different compositions and temperatures as shown in the figure 3.c

Phase diagram studies were started many years ago; McQuillan's (1950) study was the first one with relatively high purity titanium

although his work was performed only at high temperatures. Lenning et al. (1954) found that the solubility of hydrogen in α-Ti decreases to less than 0.15 atomic percent at room temperature, but later workers (Vitt et al., 1971 and refs. therein) observed slightly higher values. The x-ray work of Azarkh et al. (1970) shows that the solution phase extends up to a composition with atomic ratio - r (= H/Ti) equal to 0.17 at room temperature. Further, their work confirmed that the lattice parameter of H.C.P. titanium was not affected by the solution of hydrogen. Hydrogen atoms in the solution phase are distributed randomly among the tetrahedral sites of H.C.P. α-Ti (Pinto et al., 1979).

The solution phase is followed by a wide ranging mixed phase of H.C.P. Ti and non-stoichiometric hydride. The x-ray work (Azarkh et al., 1970, and refs. therein) has shown that the lattice of titanium in the hydride of this phase has an F.C.C. structure with a constant lattice parameter of 4.404 A^{o}. The neutron diffraction study of Sidhu et al. (1956) indicated that the hydrogen atoms occupy randomly the tetrahedral voids of the F.C.C. lattice. Further, inelastic neutron scattering showed that there is no population of the octahedral voids by hydrogen in titanium hydride (Zemlyanov et al., 1978). The x-ray work of Azarkh et al. (1970), the neutron work of Sidhu et al. (1956) and the N.M.R. study of Korn et al. (1970) agree that the mixed phase ends at a composition with r = 1.5, at room temperature. Korn et al. (1970) have suggested clusters of hydrogen atoms form in the mixed phase. If so, then in the mixed phase the hydride $TiH_{1.5}$ and Ti patches exist simultaneously but Ti patches gradually disappear as composition approaches r = 1.5

The mixed phase is followed by a single phase titanium hydride. This is the most investigated phase because of many disagreements between experimental results which will be described later. In this single phase the F.C.C. structure of the lattice shows deformation or becomes

F.C.T. at high compositions and low temperatures. But at high temperatures the F.C.C. structure remains unchanged up to the maximum composition with r = 2. In the F.C.T. structure there is a continuous expansion of the crystal lattice in two directions and a continuous contraction in the third. Azark et al. (1970) observed that at room temperature the F.C.C. lattice parameter increases linearly from 4.404 A^{o} to 4.425 A^{o} within the composition r = 1.5 - 1.7, but then becomes distorted with c/a ratio nearly equal to 0.98, this ratio decreases slowly and becomes 0.97 at saturation. The rate of increase of unit cell volume with composition is slightly less in the F.C.T. structure than in the F.C.C. structure. This structural transformation can be described as a rapid and reversible second-order transformation.

All N.M.R. works accept that hydrogen diffusion in titanium hydride is very rapid and takes place via a vacancy mechanism. The generally obtained value for the jump frequency of hydrogen between the tetrahedral sites is of the order of 10^{12} sec^{-1}. The N.M.R. work of Korn et al. (1970) and Stalinski et al. (1961) agree about the nature of the hydrogen distribution in the single phase hydride, which they suggest is a uniform distribution rather than clusters; but they disagree about how the activation energy for diffusion varies with composition.

A few works are available about the effect of hydrogen on the resistance of a titanium film on a spherical substrate. They all are in very good agreement about the general variation of resistance with composition, but they all have disadvantages due to their complicated geometry. Suhrmann et al. (1962) observed a small increase of resistance at the start followed by a large drop of 30% at r = 1.2 at 273°K, but at 90°K only an increase of 20% at r = 0.6. Wedler et al. (1966) found that on exposure to hydrogen the resistance of their titanium films first increased by a small fraction up to an atomic ratio r = 0.06 then decreased by more than 30% at r = 1.8 at room temperature. Surplice

(unpublished) found a small increase of ≤ 1% resistance at r = 0.065, was followed by drop of 30% at r = 2 at room temperature, and at 78°K an increase of 2% up to saturation at r = 0.3 ± .1 [or surface coverage 1.5].

There have been disagreements about the effect of hydrogen on work function, about the details of Ti-H bond and especially about the F.C.C.-F.C.T. transition. They will be discussed in that order.

There have only been two experiments on the effect of hydrogen on the work function of titanium. One said hydrogen increased it, but the other said hydrogen decreased it. Suhrmann et al. (1962) found a maximum increase of 0.25 eV at r = 0.6 at 90°K and 0.35 eV at r = 1.2 at 273°K. They interpreted their results solely in terms of changes of surface potential. Magee (1967) found that the work function decreased by 0.22 eV up to a composition $TiH_{0.05}$ and then remained constant for higher composition, $TiH_{1.62}$, by using photoelectric measurements.

It seems to be accepted that the H-Ti bond is partly ionic, partly covalent, but there have been several different results for the degree of ionization. Stalinski et al. (1961) have mentioned that hydrogen has a net positive charge. Kachalkin et al. (1977) have concluded from their π-meson capture experiments that the nature of the metal-hydrogen bond in titanium hydride was unchanged within the tested composition range from r = 1.65 to r = 2, and over temperatures 25°C to 200°C for $TiH_{1.65}$. The U.P.S. work of Eastman (1972) indicated that the interaction of hydrogen caused a large change in the structure of the d band of titanium especially near the Fermi level. Further he has mentioned that, with a rigid band approximation, a downward shift of Fermi level by 0.7 eV in the d-band is equivalent to having 2 rather than 4 occupied electron states. Kulikov et al. (1978a) stated from their band calculation for TiH_2 that the rigid band approximation and anionic model are inapplicable, but the protonic model is more adequate for the Ti-H

system. Namchenko et al. (1975) concluded from their thermoelectric power measurements, and with the assumption of rigid band approximation, that the ionization of hydrogen in titanium hydride is partial and equal to 0.25 e. Switendick's (1976) band calculation showed that 0.85 electrons of each two atoms of hydrogen added are transferred to higher energy levels [$\Gamma_{2'5}$ L_3] of metal d-band; this indicates an ionization of 0.425 e for hydrogen.

There is a wide disagreement about the concentration range of the F.C.T. structure and about the F.C.C.-F.C.T. transition temperature for a particular composition. The minimum composition for the F.C.T. structure at room temperature was found to be $TiH_{1.75}$ by Azarkh et al. (1970), $TiH_{1.9}$ by Irving et al. (1971), but it had not been observed at all not even for TiH_2 by Malyuchkov et al. (1959). The transition temperature of the F.C.T. structure for Ti H_2 is scattered from 285°K to 310°K for different investigations (Korn, 1978). This interesting problem was investigated with various technologies with the aim of establishing the boundary of the F.C.T. structure. Their scattered results were plotted by Korn (1978) and given in the figure 3.d. Korn (1978) and Azarkh et al. (1970) gave several reasons for the disagreements between the results of these experimentalists. The latter in particular pointed out that the purity of the starting products along with the methods of preparation of the hydrides are reasons for the observed scatter. From the present work Surplice and Kandasamy (1978) have suggested that the dissociation of hydrides of high concentration could be the reason for some of the anomalies observed by the following workers around this temperature and composition. The temperature dependence of magnetic susceptibility (Stalinski et al., 1961), the proton spin-lattice relaxation rate (Korn, 1978), the specific heat (Stalinski et al., 1960) and the Hall coefficient and resistivity (Gesi et al., 1964) of hydrides of high composition all showed anomalies around room temperature.

The dissociation of high composition hydrides at room temperature and low pressure (10^{-3} torr) was observed by Surplice and Kandasamy (1978) and Kasemo et al. (1979). Therefore, the experimental data which are available for hydrides with high compositions have to be treated carefully. For example Namchenko et al. (1975) and Ducastelle et al. (1970) took thermo e.m.f. coefficient measurements which agree for low composition hydrides but disagree for high composition hydrides. This disagreement was ascribed by Namchenko et al. (1975) to a slightly lower composition than the expected value in Ducastelle et al. samples. The microbalance experiments of Kasemo (1977) showed that the equilibrium between adsorption, desorption and diffusion of hydrogen in titanium depends on the hydrogen pressure. More recent work of Kasemo et al. (1979) indicates that the initial sticking coefficient - S of hydrogen on an evaporated titanium film is 0.17 and it decreases monotonically until the atomic ratio r = 0.3, then S remains constant up to r = 1.8 after which it decreases rapidly. Further they have stated that even the partially hydrided samples desorbed hydrogen at room temperature. The desorption kinetics show that the rate is controlled by the combination of H atoms at the surface, and the rate of hydriding is limited by the number of sites available for the dissociation of hydrogen on the surface. Desorption experiments by Schwarz et al. (1977) indicated only one desorption peak for titanium hydride and a desorption process of order 1.5. They ascribed this observation to the formation of a non-stoichiometric hydride $TiH_{1.5}$. Malinowski's (1978), (1976) work indicated that the hydrogen diffuses from a titanium hydride substrate to an overlaid titanium film and forms a homogeneous titanium hydride film; contamination by CO reduces the rate of hydriding, but this effect decreases with the atomic ratio of the titanium hydride film. Further his data support the dissociation of titanium dihydride at room temperature. The kinetics of the thermal decomposition of titanium dihydride

also suggest that the surface-process is rate controlling (Steinberg et al., 1973). Reichardt (1972) has suggested that the kinetics of the hydrogen-titanium reaction indicate that a surface process limits the rate of interaction, and the rate of the reaction is linearly dependent on the pressure of hydrogen. Newns (1963) showed that the chemisorbed hydrogen atom on titanium surface has a negative charge of 0.39 e.

Now let us consider some general features of the studies of high-composition hydrides. The electrical resistivity, susceptibility at $0^{o}K$, and entropy of the F.C.C. dihydride are larger than those of the F.C.T. dihydride. The temperature coefficient of susceptibility is negative for F.C.C. but positive for F.C.T. dihydride, and the Hall coefficient is positive for F.C.C. but negative for F.C.T. structure of TiH_2 (Gesi et al., 1964). From these data Gesi et al. have suggested that the density of states at the Fermi level is larger for F.C.C. than for F.C.T., and the position of the Fermi level is near to the density of states minimum for F.C.T. but away from the minimum for the F.C.C. structure. Further, their band diagram shows that the Fermi level of the F.C.T. structure is lower in energy than for the F.C.C. structure of TiH_2. The variation of spin relaxation constant $(T_{1e}T)^{-\frac{1}{2}}$ and of magnetic susceptibility with composition, is generally ascribed to the variation of the density of states at the Fermi level (Korn, 1978). From a plot of the above two parameters Korn proposed a phenomenological model to explain features of the band structure of the Ti-H system. However it failed to account for the features of Zr-H which belongs in the same group of the periodic table (Korn, 1977). The electronic specific heat, magnetic susceptibility and thermoelectric power were measured by Ducastelle et al. (1970) who have suggested that the density of states increases with composition in the F.C.C. structure, and that a structural transformation from F.C.C. to F.C.T. is accompanied by a

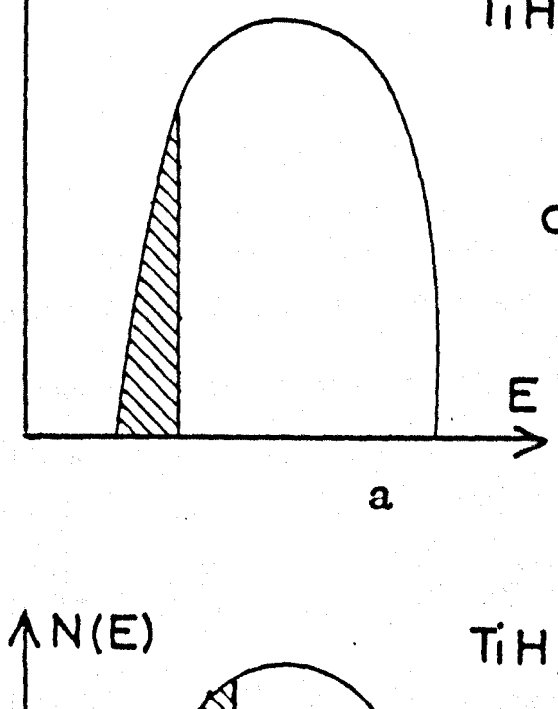

a

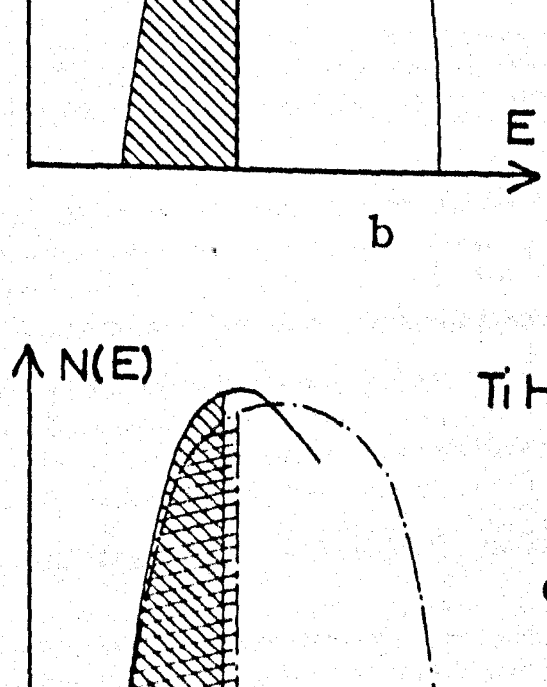

b

c

fig-3e

reduction in the density of states at the Fermi level. Their model is shown in the figure 3.e. Further they estimated that the density of states at the Fermi level is 0.80 states/eV atom for F.C.C. $TiH_{1.75}$, and 0.95 states/eV atom for F.C.T. $TiH_{1.97}$. Band structure calculations by Kulikov et al. (1978b) for F.C.C. and F.C.T. TiH_2 with c/a 0.945 shown in the figure 3.f showed that during the structural transformation from F.C.C. to F.C.T. there was a drop in the position of the Fermi level by 0.02 Ry (= 0.272 eV) and a drop in the density of states at the Fermi level from 0.95 to 0.87 states/atom eV. Gupta's (1979) calculation showed that a flat degenerate band lies at the Fermi level, and the density of states at the Fermi level for F.C.C. dihydride is 1.73 states (bothspin) /eV atom. Switendick's (1976) band calculations for F.C.C. TiH_2 (with c/a = 0.97) also predict a degenerate band at the Fermi level and suggest that the F.C.T. distortion lowers the Fermi level by 0.1 eV.

However the reason for the second-order phase transition of titanium hydride of high composition is not yet well understood. There are several reasons proposed by different workers. Yakel (1958) has suggested the transition may be due to either a gradual change in band character or a change in the Brillouin zone scheme at the Fermi level. The second reason was supported by Gesi et al. (1964). Azarkh et al. (1970) believed that the ordered filling of tetrahedral holes at high composition led to the distortion. Ducastelle et al. (1970) suggested that the reason for the distortion is a Jahn-Teller type effect; this idea was further supported by Switendick (1976) and Gupta (1979) in their band calculation. Kulikov et al. (1978a) suggested that the close position of the sp symmetry state (Γ_2^1) to the Fermi level leads to the phase transformation. Korn et al. (1978) proposed that transformation is due to the presence of a Van Hove singularity in the density of states at the Fermi level.

FIG 3 f

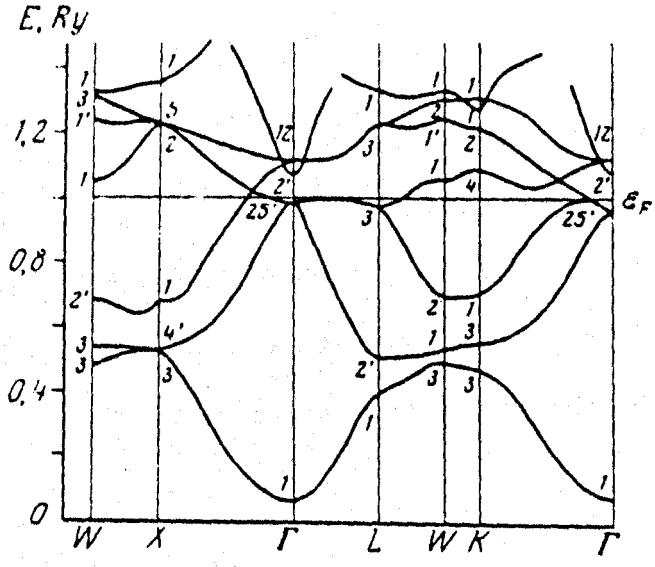

Рис. 1 FCC TiH_2

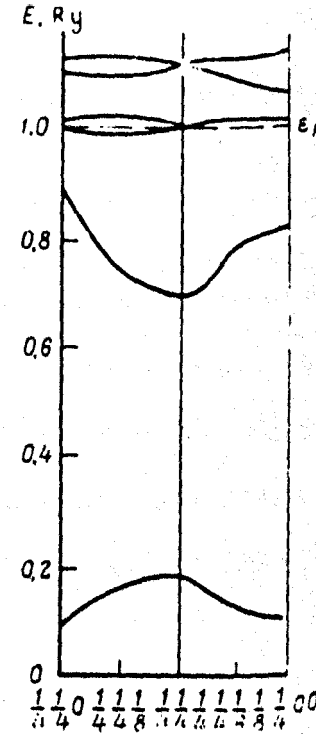

Рис. 3

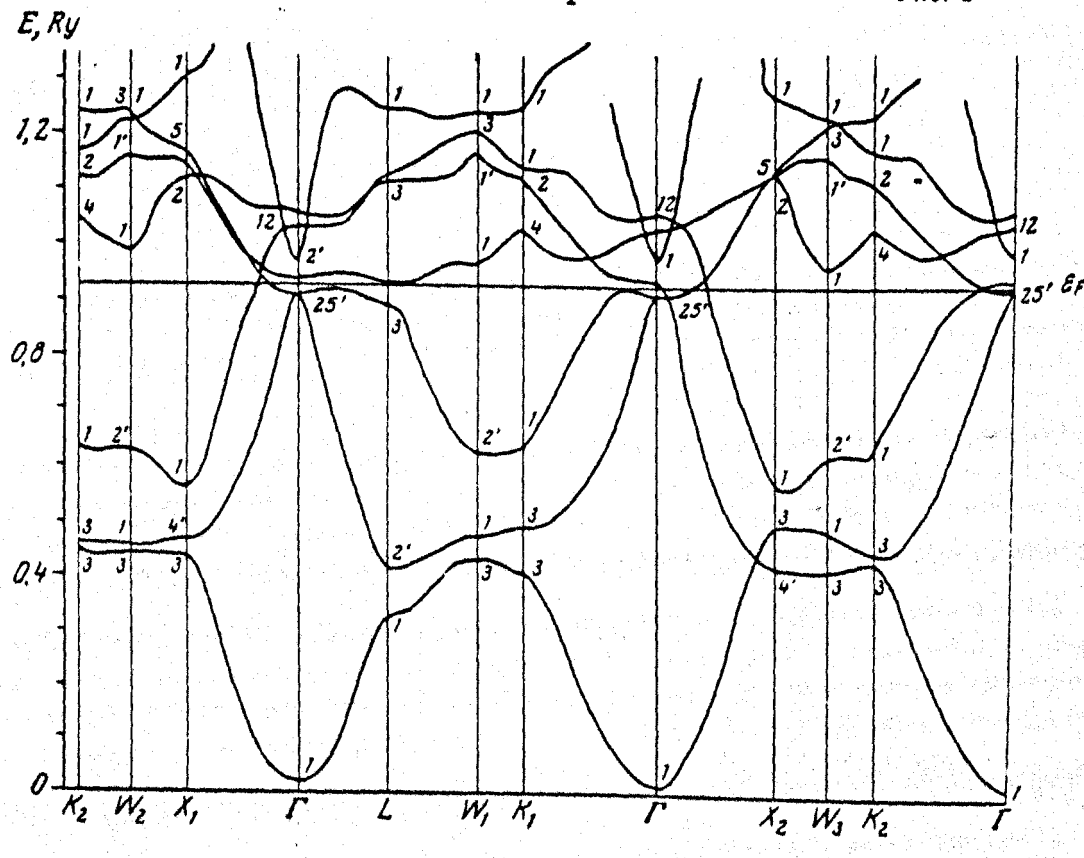

Рис. 2 FCT TiH_2

Рис. 1. Зонная структура кубической фазы дигидрида титана (значения энергии отсчитываются от «МТ – нуля»)

Рис. 2. Зонная структура тетрагональной фазы дигидрида титана (значения энергии отсчитываются от «МТ – нуля»)

$$\Gamma - \frac{2\pi}{a}(0, 0, 0); \quad X_1 - \frac{2\pi}{a}(1, 0, 0); \quad X_2 - \frac{2\pi}{a}\left(0, 0, \frac{a}{c}\right); \quad L - \frac{2\pi}{a}\left(\frac{1}{2}, \frac{1}{2}, \frac{a}{2c}\right);$$

$$K_1 - \frac{2\pi}{a}\left(\frac{3}{4}, \frac{3}{4}, 0\right); \quad K_2 - \frac{2\pi}{a}\left(\frac{3}{4}, 0, \frac{3a}{4c}\right); \quad W_1 - \frac{2\pi}{a}\left(1, \frac{1}{2}, 0\right); \quad W_2 - \frac{2\pi}{a}\left(1, 0, \frac{a}{2c}\right);$$

$$W_3 - \frac{2\pi}{a}\left(\frac{1}{2}, 0, \frac{a}{c}\right)$$

Рис. 3. Законы дисперсии электрона в кубической фазе дигидрида титана для направлений, перпендикулярных к направлению $\Gamma - L$.

In conclusion the Fermi level in titanium hydride lies in a region of high density of states, and the phase transition from F.C.C. to F.C.T. is combined with a reduction of the density of states at the Fermi level. This transition at high compositions could be a reflection of some major change in the electronic structure. However, some of the anomalies observed around the transition temperature may not be due to the phase transition but due to poor experimental conditions.

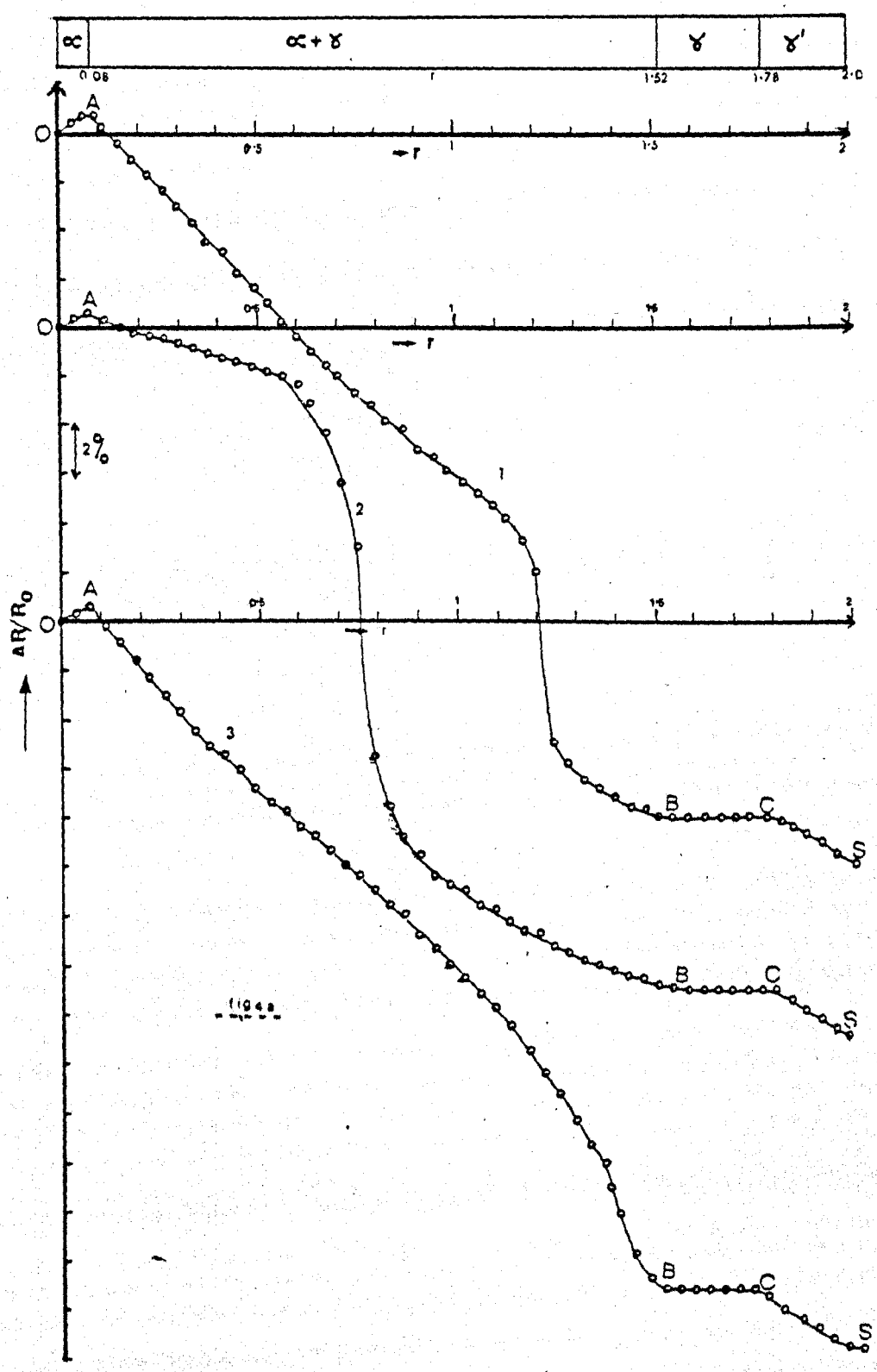

fig 4a

CHAPTER 4

Titanium-hydrogen study: Present work

4.1 Results

a) Resistance variation with atomic ratio - r.

The general features of the change of resistance of films with atomic ratio ($r = {}^{H}/_{Ti}$) are shown in figure 4.a. The letters O, A, B, C and S on the plot identify the different regions in which different resistance variations were observed. At the start about a dozen doses each of size 10^{17} atoms increased the resistance until $\frac{\Delta R}{R_O}$ reached a small maximum (< 1%) at A. Further doses of size 10^{18} atoms reduced the resistance by about 28% up to B. After B the variation was practically zero until C. After that the resistance dropped again slowly about 2% until the film saturated at S at a pressure 2×10^{-3} torr. The maximum at point A was observed around the atomic ratio 0.08. Before A the resistance rose suddenly at each dose and any resistance variation after a dose was smaller than the detectable limit.

For each dose between A and B the resistance dropped rapidly at the dose, then gradually became constant. The time taken to reach a constant value after each dose was about 5 minutes close to A, but about 15 minutes close to B, for equal sized doses. A special feature was observed in the mid part of this region (r = 0.5-1.1) that a single dose was able to drop the resistance by 50% of the total drop from O to B. From B to C each dose made R drop rapidly and then gradually increase back to its initial value; point B was noticeable as the start of this process at about $r = 1.55 \pm .05$. After C, first the resistance dropped for each dose as in the previous region, but then it increased to some value smaller than the initial value. This process continued until S, after which further doses become ineffective (up to 5 torr, or for 12 hours at 10^{-2} torr). The atomic ratios of C and S were about

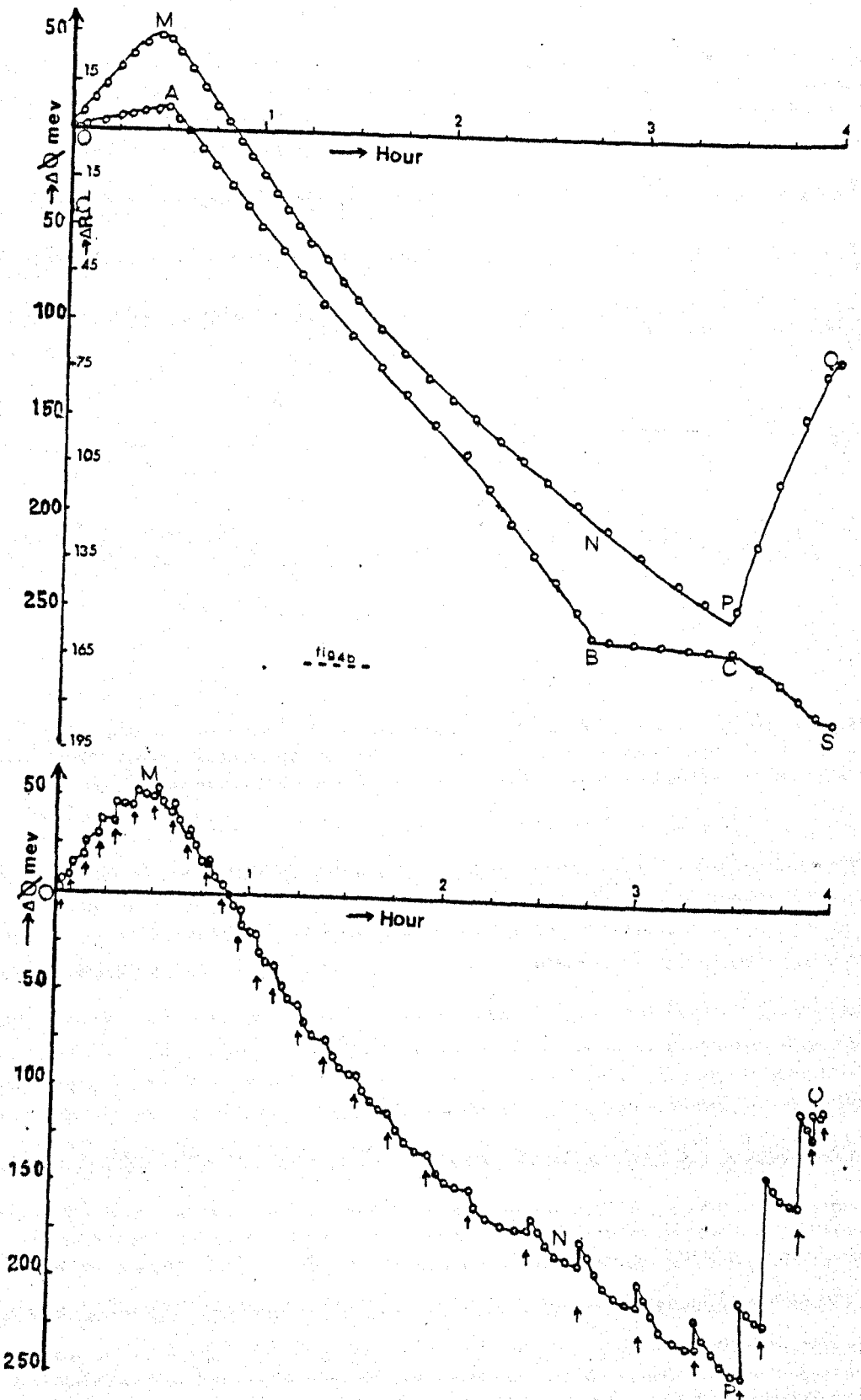
M
A
O
Hour
N
P
B
C
S
Q
fig 4b
M
Hour
N
P
Q

1.78 and 1.97 respectively with an estimated error of 3%. Pumping out gas until the pressure became 10^{-8} torr, increased the resistance again to half way up the portion CS.

b) Correlation of work function-ϕ and resistance-R with exposure.

The general variation of ϕ and R with 'expsoure time' and a summary of the experimental data are given in figure 4.b and table 4.1 respectively. The total exposure time was the time required to conduct an experiment, which varied from 10-15 hours, with various levels of exposure. The amount of exposure (in torr sec) varied from experiment to experiment and depended on the amount of titanium evaporated on the wall of the chamber.

At the start, ϕ increased by 40-60 meV until it reached a broad maximum at M, then it dropped sharply by 275-300 meV until it reached a sharp minimum at P, and finally increased by 120-150 meV until the film saturated at Q, after that ϕ remained constant up to a pressure as high as 5 torr for one hour. In a dose experiment the first few doses each caused a gradual increase of ϕ by 5 to 10 meV within 3 minutes and then it levelled off. Further doses each caused a gradual increase of 10 meV followed by a small drop, until M. After M, a few equal doses each gave a rapid initial increase of 10-15 meV followed by a gradual drop of 20-25 meV and ϕ levelled off after 5-7 minutes. For the later doses, gradually the initial increase disappeared but the time taken to reach a steady state after a dose gradually increased to 15 minutes. This process continued until N. From N to P each dose caused an initial increase of ϕ by 25-30 meV followed by a slow drop of 40-45 meV and finally ϕ became steady after 20-25 minutes. After P the same type of variation continued to operate, for each dose, but the drop of ϕ at the end was smaller than the initial rise. Close to Q these variations became pressure dependent. After Q the doses became ineffective. The variation of resistance was the same as described previously. The

Table 4.1

Film	P_{evap} 10^{-9}(torr)	T_{evap} (hour)	Thickness (A^o)	$\Delta\phi_{OM}$ (meV)	$\frac{\Delta R_A}{R_o}$%	$\Delta\phi_{MP}$ (meV)	$\Delta_{\phi PS}$ (meV)	$\frac{\Delta R_S}{R_o}$%	T_{exp} (hour)	Exposure	$\Delta\phi_{dis}$	$\frac{\Delta R}{R_S}$ dis	
Ti 31/1	1	3	100	45	0.4	300	140	31	4	10A+10B +3C	–	–	
33/1	5	5	80	40	0.3	>50	–	42	3	22B+3C	–	–	*
34/1	5	6	100	60	0.4	>50	–	33	3	A+3B+ 18C	–	–	
35/1	2	4	175	45	1.3	295	130	31	3	10B+6C D	40	4.6	
36/1	5	4	100	0	0	300	70	28	3	10B+400	40	1.0	
37/1	8	5	105	25	–	250	80	23	11	13B+8C	40	1.6	
38/1	5	3	105	40	–	200	80	28	12	10^{16}mol/ sec	–	–	
43/1	6	3	100	50	0.4	–	–	–	–	–	–	–	**
44/1	8	5	100	40	0.2	>220	–	>28	10	51B	–	–	**
45/1	5	2	120	35	0.5	>270	–	>25	12	10^{13}mol/ sec	–	–	**
61/1	5	3	105	35	0.4	>100	–	28	10	11A+12B	–	–	**

* – Very thin film

** – Not saturated

A – 10^{14} atoms

B – 10^{15} atoms

C – 10^{16} atoms

D – Big dose

Fig 4-C

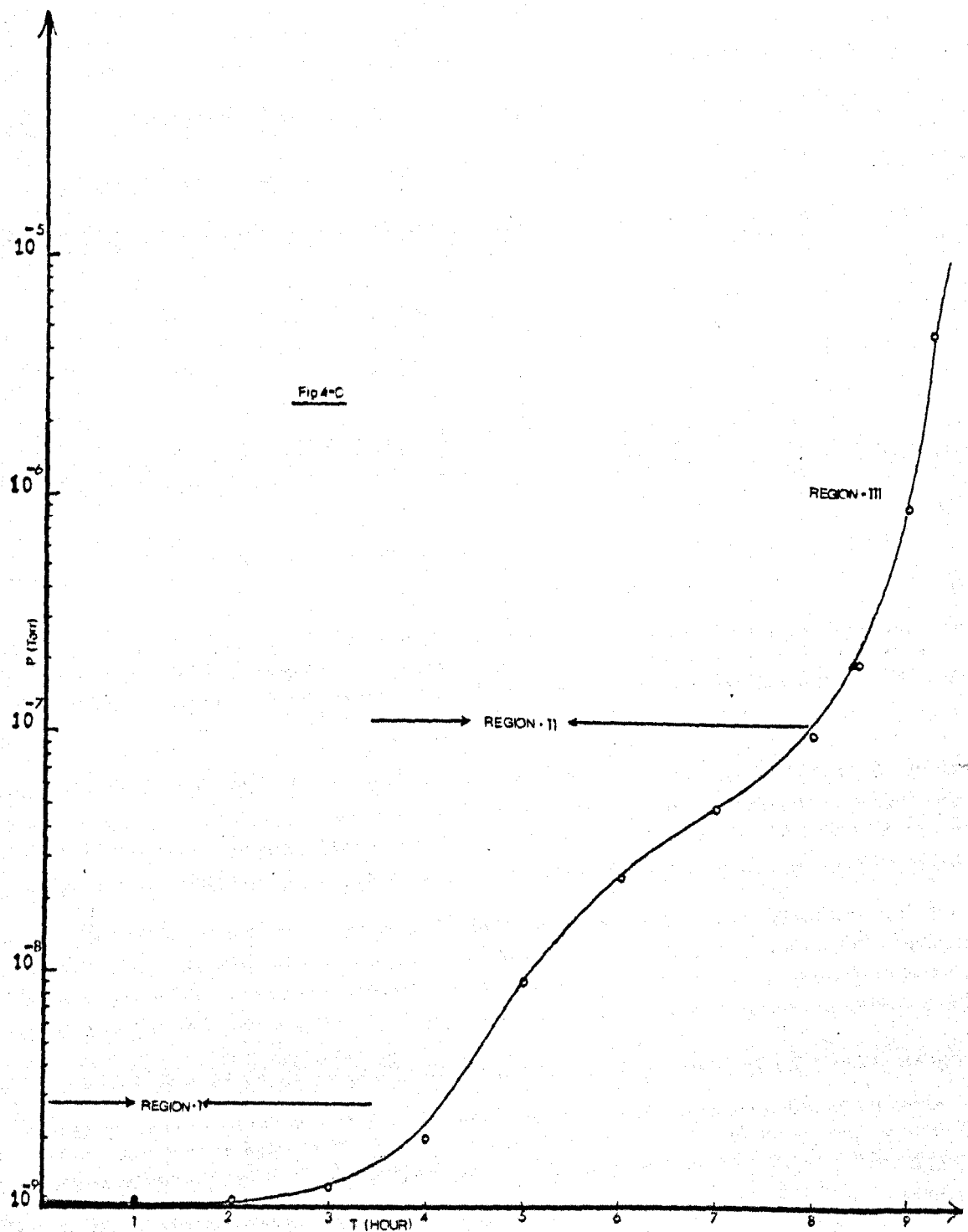
10^{-5}
10^{-6}
10^{-7}
10^{-8}
10^{-9}
P (Torr)
REGION - I
REGION - II
REGION - III
1
2
3
4
5
6
7
8
9
T (HOUR)

coincidence of the positions A with M, of C with P, and of S with Q is excellent; the coincidence of B with N is reasonable. In a few experiments a reasonably linear variation of resistance was observed between A and B.

The observed total drop of resistance was 30 $\pm$ 3% of the initial film resistance. For the correct investigation of the initial part of this study a very good base pressure and careful degassing of the titanium wire are very important, otherwise we can easily miss the initial part, but sometimes still we can observe a small rise (15-20) meV in ϕ without a corresponding increase of R.

c) Pressure variation during the sorption of hydrogen by titanium.

The general features of pressure variation with time, in a continuous flow experiment with a constant rate of flow of 10^{13} molecules per sec, and in a dose method are shown in the figure 4.c. The pressure variation was noted only up to 10^{-5} torr, which was the maximum for detection by the mass spectrometer. Within this range three different regions were identified. In the region 1 the pressure was constant at 10^{-9} torr or had negligible increase. This region continued until the film resistance had dropped by 1.5% (or r = 0.4). In the region 11 the pressure increased with linear rate of increase (with average rate 10^{-8} torr/hour). This region extended until resistance had dropped by 20% (or r = 1.3). The pressure at the end of this region is about 10^{-7} torr. In the region 111 the pressure increased more rapidly and at the end of the region constant part of the resistance curve appeared. In this experiment, for a 120 A^{o} film, 90 minutes were required to reach the maxima of ϕ and R at the base pressure 10^{-9} torr.

In a dose experiment more than 50 doses of 5×10^{16} molecules were sorbed, within the range of the mass spectrometer study. In the first region (described previously) all doses were sorbed almost completely within 0-5 seconds. In the second and third regions the time taken to

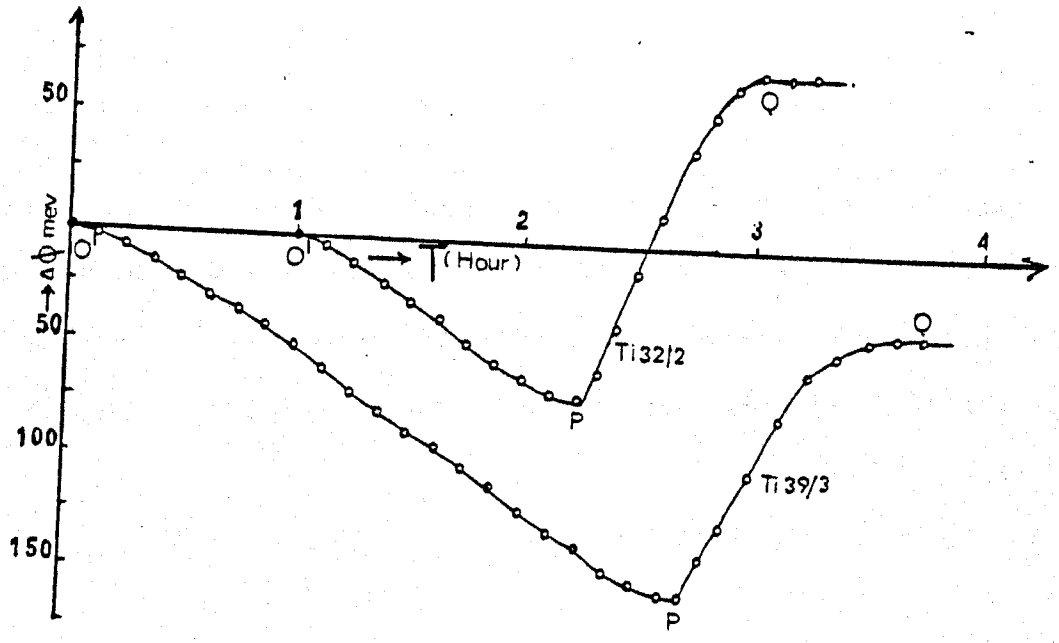
50
100
150
Δ Φ mev
O
1
2
3
4
(Hour)
P
Q
Ti 32/2
Ti 39/3

fig 4d

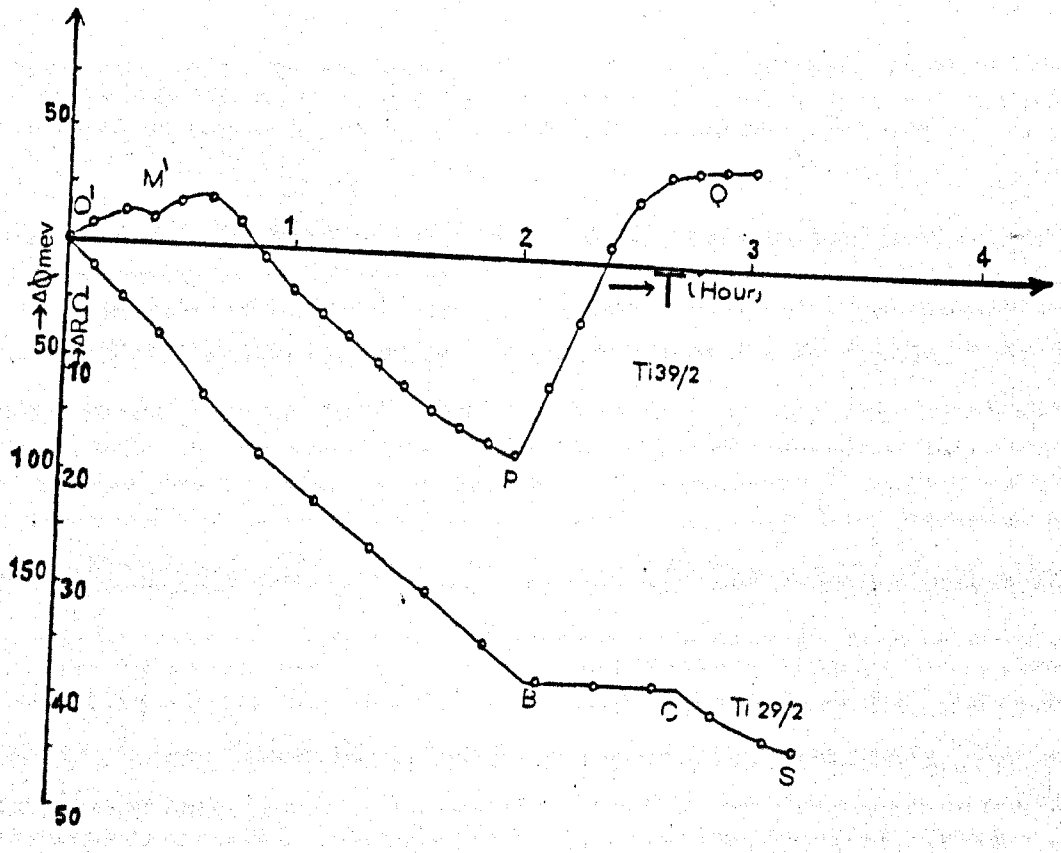
50
100
150
Δ Φ mev
ΔR Ω
10
20
30
40
50
O
M'
1
2
3
4
(Hour)
P
Q
Ti 39/2
B
C
Ti 29/2
S

sorb a dose increased gradually from 5 seconds to 300 seconds. Especially in the third region, each dose started to give a long tail on the partial pressure signal of hydrogen in the mass spectrum, and a finite increase in the base pressure.

In an experiment with 100A^{o} titanium film, the mass spectrum was recorded up to the maximum of ϕ and R in a calibrated pressure-time plot. The total area under the pressure signal was equal to 31 x 10^{-7} torr. sec (3.1 L).

d) Sandwich film study

The general variation of ϕ and R is shown in figure 4.d and the summary of the data is given in table 4.2 for sandwich films. The quantitative features of R and ϕ were completely different from those of fresh films except for the rise of ϕ near the saturation. In contrast to fresh films no increase of resistance at the start was observed. In most of the films even a large rate of flow or large dose did not give any increase in ϕ at the start, but in a few films a small flow showed a small maximum of 10-20 meV, and the amount of increase of ϕ was dependent on the rate of flow. This is clearly shown in the figure. Some experimental data, which are selected for the discussion were given in table 4.3 with calculated information. See the table on the next page, where R_x is the initial resistance of a sandwich film

R_s is the resistance at saturation

ϕ_d is the work function drop

R_o is the calculated valve corresponding pure titanium

d is the estimated thickness of the sandwich film

r_1, r_2 and r_3 are the composition of the sandwich films at start

For more detail see Appendix C.

Table 4.2

Film	P_{evap} (10^{-9} torr)	T_{evap} (hour)	$\Delta\phi_{OM}{}^{1}$ (meV)	$\Delta\phi_{M}{}^{1}{}_{P}$ (meV)	$\Delta\phi_{PS}$ (meV)	$\frac{\Delta R}{R_x}$ %	T_{exp} (hour)	Exposure	$\Delta\phi_{dis}$	$\frac{\Delta R}{R_S}_{dis}$	Temp.
Ti 29/2	1	1.5	–	125	150	26	3	8B+42C	–	–	-20°C
29/3	1	2.5	–	15	150	2.1	2.5	12B+9C	–	–	"
30/2	2	5	No reliable data								
30/3	1	1.5	–	–	–	20	2	10B+22C	–	–	"
30/4	1	3	–	50	140	20	2	9C	–	–	"
30/5	2	2.5	–	–	150	13	3	13B+17C	–	–	"
31/2	1	2	15	180	100	20	8	10A+35B+26C	–	–	"
31/3	1	2	–	125	130	23	4	4A+2B+24C	–	–	"
31/4	1	2	–	105	100	25	3	7B+20C	–	–	"
32/2	5	3	–	70	150	10	2	3A+7B+15C	–	–	"
33/2	2	2	–	80	110	20	6	15B+8C	–	–	"
33/3	1	2	–	140	115	20	2	2B+7C	40	–	"
35/2	5	2	–	150	130	30	10	46B+31C	40	3	"
36/2	9	4	–	40	135	16	2	8B+5C	–	–	"
37/2	9	3	–	20	100	–	7	10^{14} mol/sec	30	–	"
39/2	5	1	20	80	125	20	3	10^{16} mol/sec	–	–	"
39/3	3	1.5	–	160	135	–	4	10^{16} mol/sec	–	–	"
40/2	5	1	–	55	140	27	10	10^{16} mol/sec	40	1.5	"
43/2	–	1	–	10	105	28	4	19B	65	2.2	50°C
43/3	5	1	–	45	95	28	7	10^{16} mol/sec	45	3.8	"
43/4	–	1	25	20	90	25	6	10^{16} mol/sec	40	7	"
45/2	1	2	–	35	125	–	6	10^{16} mol/sec	–	–	20°C

A – 10^{14} atoms B – 10^{15} atoms C – 10^{16} atoms

Table 4.3

Film	Ti/31, T.F.F.=100A°			Ti/33, T.F.F.=200A°		Ti/39, T.F.F.=100A°
	Ti31/2	Ti31/3	Ti31/4	Ti33/2	Ti33/3	Ti39/2
R_x(EXP)Ω	225	117	72	100	60	290
R_s(EXP)Ω	178	90	54	80	48	234
ϕ_d(EXP)meV	180	125	105	80	140	90
R_0(cal)Ω	255	129	77	115	69	335
d(cal)A°	180	325	490	280	535	145
r_1(cal)±.05	0.76	1.07	1.19	1.30	0.98	1.27
r_2(cal)	1.0	0.99	1.19	1.28	0.94	1.24
r_3(aγ)(cal)	0.896 ± 0.160	0.837 ± 0.129	0.566 ± 0.094	0.867 ± 0.148	0.867 ± 0.148	0.913 ± 0.164

r_1 = Estimated from the ϕ variation
r_2 = Estimated from the thickness of the film
r_3(aγ) = Estimated from the R variation
T.F.F. = Thickness of the fresh film

e) Study of dissociation of titanium hydride

Near the saturation the results, especially for ϕ, showed a pressure dependent variation. When the pressure was reduced from the saturation pressure to 10^{-8} torr, ϕ decreased considerably and R increased a small amount (3-4 Ω), as if they were moving back from Q and S along the curves of figure 4.b. The saturation pressures P_s for temperatures 20°C, 50°C and 70°C are given in table 4.4. For a pressure > P_s, ϕ and R remained constant, but for a pressure < P_s they changed with pressure. This effect was reversible, ϕ dropped when pressure < P_s but returned to its saturation value when P was increased again to P_s. Similarly R increased when pressure < P_s but returned to its saturation value when P was increased again to P_s. This pressure dependence was investigated by reducing the pressure of the surrounding hydrogen, either

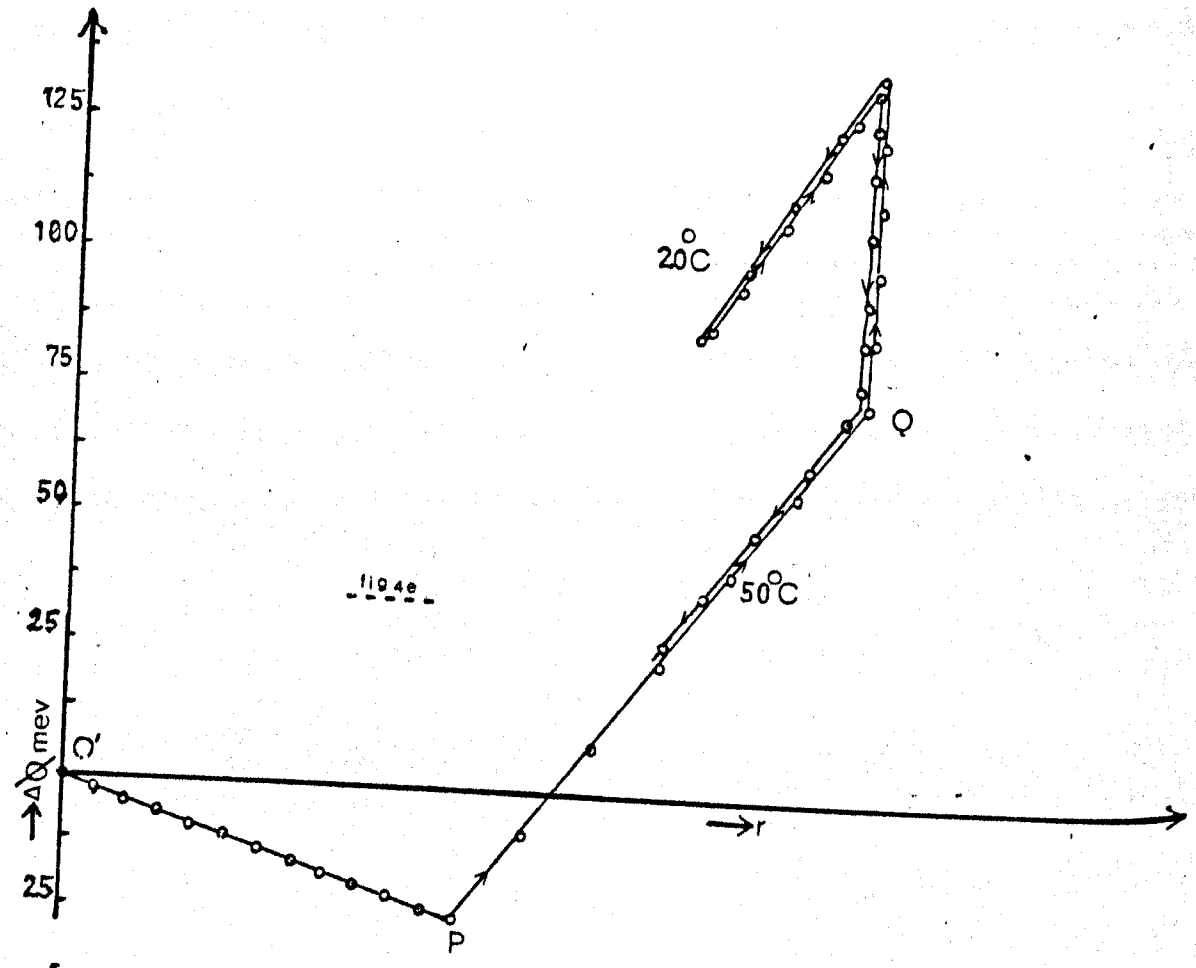
125
100
75
50
25
25
Δ Q mev
O'
P
Q
20°C
50°C
r

fig 4e

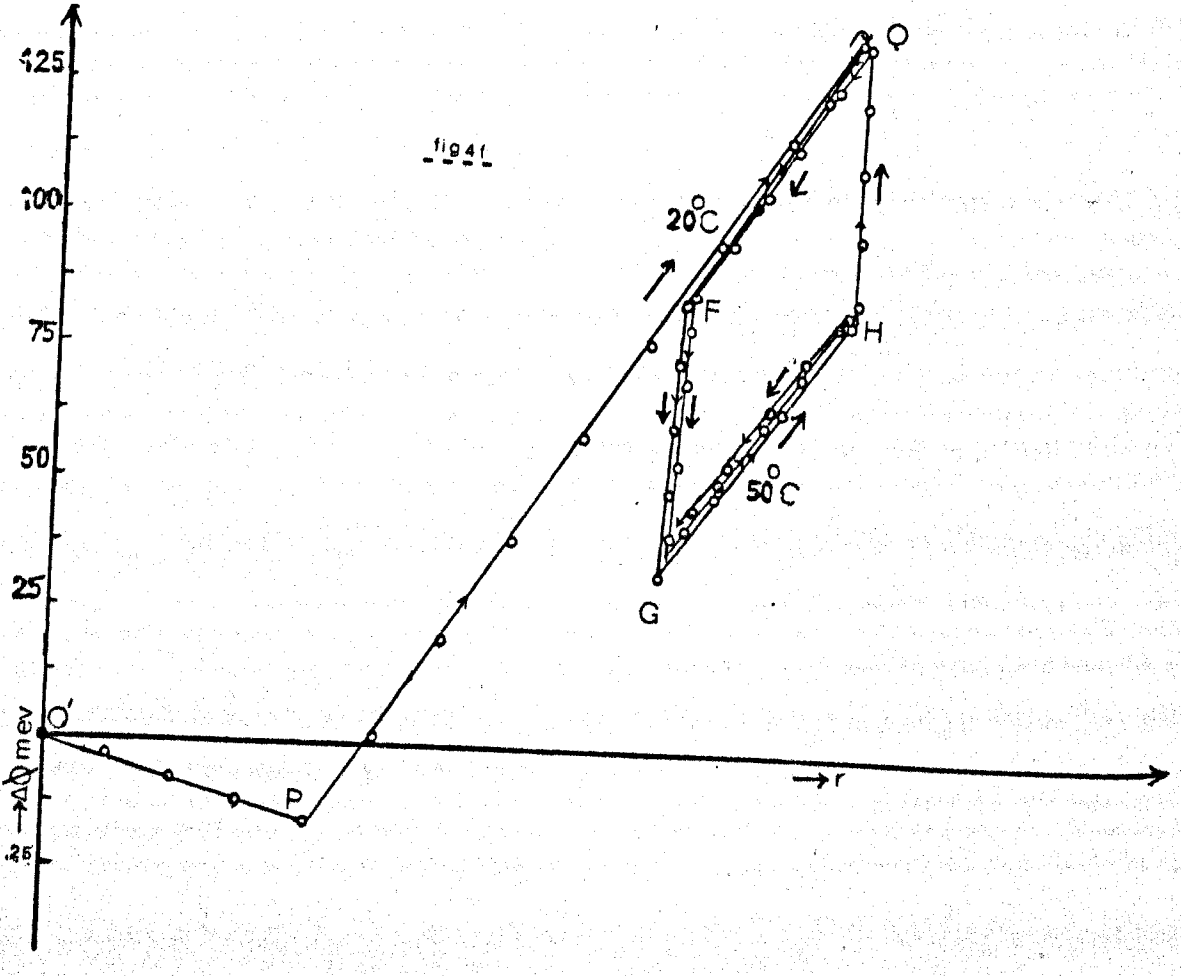
125
100
75
50
25
Δ Q mev
O'
P
Q
20°C
50°C
F
H
G
r

fig 4f

rapidly by slightly opening the valve to the ion pump, or slowly by allowing it to be sorbed by the chamber wall. The minimum pressure attainable without internal baking was 10^{-8} torr. In the first case ϕ decayed rapidly at first then decayed slowly and gradually to reach a constant value after 30 minutes. In the second case ϕ decayed very slowly and gradually over 5 hours until ϕ dropped by 35-45 meV, which was a $^1/_3$ of the rise which had been observed during the high composition part at 20°C. However in both cases the variation of ϕ with time was non-linear. In contrast to this the variation ϕ with time was when the pressure was increasing slowly. At 50°C the drop of ϕ due to the dissociation was 50-60 meV which was about $^2/_3$ of the rise near saturation at this temperature. At 70°C, ϕ dropped to the minimum - P.

Table 4.4

Dissociation pressure of titanium hydride

Atomic ratio, r	Temp T°C	Dissociation pressure P_s torr
2.0	20	1.2×10^{-3}
2.0	50	1.2×10^{-2}
2.0	70	4×10^{-2}
≈ 1.9	20	$\lesssim 10^{-8}$
≈ 1.9	50	$\lesssim 10^{-8}$

f) Comparative study at 50°C and 20°C

A few experiments were conducted with sandwich films at different temperatures to investigate the variation of ϕ near saturation. In the first experiment (procedure clearly shown in figure 4.e) a sandwich fulm was saturated at 50°C and a rise of 100 meV in ϕ was obtained (after the minimum P). At the saturation pressure the film was allowed to cool and a gradual increase of 60 meV in ϕ was obtained while the film reached room temperature. It was left at room temperature until a steady state of ϕ was ensured, and then the gas was pumped off to allow the film to dissociate until the pressure became steady again at 10^{-8} torr.

A gradual drop of 45 meV in ϕ was observed due to dissociation. After ϕ reached a steady value the pressure was increased once again up to 2.0×10^{-2} torr, meanwhile ϕ increased by 45 meV until the pressure was 1.2×10^{-3} torr and then it became constant. At this pressure the film was warmed up to 50°C at a rate of 10°C per hour. During this step ϕ gradually dropped by 55 meV as the temperature increased. The film was left at 50°C for half an hour until a steady state of ϕ was ensured and then allowed to dissociate. During the dissociation there was a drop of 55 meV until the pressure became steady at 10^{-8} torr.

In a second experiment (procedure is clearly shown in figure 4.f) a sandwich film was saturated at 20°C and a rise of 150 meV in ϕ was obtained at Q after the minimum at P. Then the film was allowed to dissociate until the pressure became 10^{-8} torr and a gradual drop of 45 meV in ϕ was observed at F. At 10^{-8} torr the film was warmed up to 50°C at a rate of 10°C per hour. During this step there was a gradual drop of 55 meV in ϕ with the temperature increased to G. The film was left half an hour at 50°C until a steady state was ensured, and the pressure increased up to saturation 1.2×10^{-2} torr. Meanwhile an increase of 50 meV in ϕ to H was observed at this pressure. There was a further increase of 60 meV in ϕ back to Q when the film was allowed to cool to room temperature. At room temperature once again the film was allowed to dissociate until the pressure became 10^{-8} torr and during this step there was a drop of 45 meV in ϕ back to F. The film was again warmed up to 50°C with the same rate as before and then at 50°C the pressure was increased up to 2×10^{-2} torr. A drop of 55 meV in ϕ, back to G during the temperature increase, and an increase of 50 meV to H during the pressure increase, was observed. Finally the film was allowed to dissociate at 50°C and a drop of 50 meV, back to G, was observed.

In the third set of experiments (details were shown in figures 4.g.

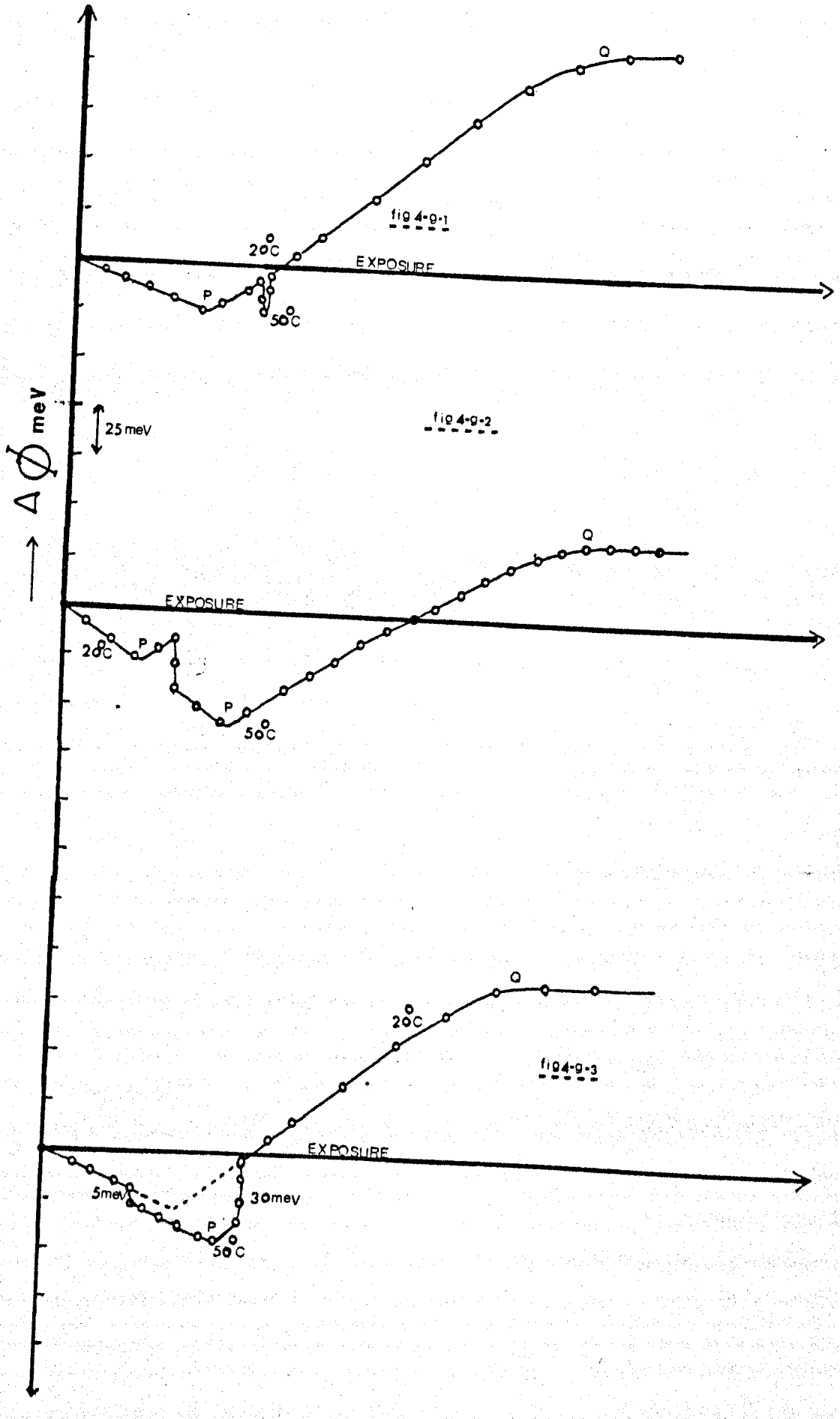
Q
fig 4-g-1
20°C
EXPOSURE
P
50°C
25 meV
fig 4-g-2
Δ Φ mev
Q
EXPOSURE
20°C
P
P
50°C
Q
20°C
fig 4-g-3
EXPOSURE
5mev
30mev
P
50°C

2,3). a) A sandwich film of thickness about 200 A^{o} was exposed to a hydrogen atmosphere at 20°C until a rise of 20 meV in ϕ after the minimum - P, was obtained, and then the pressure was reduced to 10^{-8} torr. No change of ϕ was observed. At this pressure the film was warmed up to 50°C at the same rate as in the previous experiment and a gradual drop of 20 meV with temperature increase was observed. Then the film was allowed to cool to room temperature and there was 20 meV increase in ϕ. At room temperature the film saturated and there was a further rise of 100 meV.

b) A few layers of Ti were deposited over the previous sandwich film and hydrogen was introduced until a rise of 10 meV in ϕ was obtained. At this stage the chamber was evacuated but there was no change of ϕ. Then the film was slowly warmed up to 50°C and there was a gradual drop of 20 meV with temperature increase. After ensuring a steady state of ϕ at 50°C, the pressure of hydrogen was increased until the film became saturated. During this step ϕ showed a sharp minimum, P after a drop of 10 meV.

c) Again several layers of Ti were deposited and hydrogen was introduced until a small drop of 10 meV in ϕ was obtained. The chamber was evacuated but no more change of ϕ was observed. Then the film was warmed up to 50°C and during this step a drop of 5 meV was observed. After ensuring a steady state for ϕ, hydrogen was introduced until ϕ passed the minimum P by 7 meV. Once again the chamber was evacuated and allowed to cool to room temperature, and a rise of 30 meV was observed when the temperature became steady at 20°C. Finally the film was saturated at 20°C and a rise of 90 meV was observed.

g) Anomaly in the variation of ϕ

At the start of an experiment with a fresh film, if a big dose, or few quick doses of moderate size were added, the work function showed a large increase above its initial value and a very long term decay.

For example a big dose of 10^{20} molecules was added to a fresh film of thickness about 100 A^o and the pressure in the chamber immediately after this dose was 2×10^{-1} torr. The work function suddenly increased by 210 meV and the resistance dropped by 22% of its initial value. However both parameters were no longer steady at the above values; ϕ decayed over six hours to become steady after 360 meV decrease. Meanwhile the resistance dropped slowly a further 5%. The same kind of effect was common when a few quick doses were added, especially shortly after the maximum. This kind of rise of about 70 meV in ϕ was easily reversible by allowing it to decay until a steady state was attained.

4.2 Discussion

(a) Variation of resistance R with atomic ratio r

The films studied have a thickness of 100 A^o or more, therefore they are sufficiently representative of bulk materials for their properties to be related to the phases for bulk samples. Different chemical phases are often accompanied by a different sequence of lattice packing and a different amount of interaction of conduction electrons due to the presence of the new entity, so that in general they will have different electronic properties. In the light of this, the phase boundaries of titanium/hydrogen can be identified at A, B and C (Fig. 4.a). The point A corresponds to the $\alpha/(\alpha + \gamma)$ boundary*, B corresponds to the $(\alpha + \gamma)/\gamma$ boundary and C corresponds to the $\gamma/(\gamma')$ boundary. The difference between our values and Azark *et al*'s (1970) x-ray work values for the bulk phase boundaries can be attributed to the different sensitivity of the techniques used in the two cases.

The part OA corresponds to the solution of hydrogen in H.C.P. titanium. The maximum percentage increase of resistivity is about 0.65% at the composition about r = 0.08, which is believed to be the boundary of $\alpha/\alpha + \gamma$. Our value of the composition for this boundary is very

*see Appendix G

much smaller than the value of Azark et al. (1970) [r = 0.15], however it is in very good agreement with the values of Wedler et al. (1966) [r = .060] and Surplice (unpublished) [r = 0.65]. The diffusion of hydrogen in titanium is very rapid (jump frequency $\sim 10^{12}$ sec^{-1}) and after each dose we allowed sufficient time for resistance to attain a steady value, therefore before each dose we can assume the film had a homogenous composition (in the macroscopic sense). In the solution phase every sorbed hydrogen atom (in the tetrahedral interstitial position) can behave like an additional scattering centre, therefore the increased scattering of conduction electrons can cause an increase of resistivity. In contrast to other metal hydrogen systems for Er, Y and Sc, the rate of the percentage increase of resistance of the Ti/H system in this work and in all other previous works (given in section 3.2) is very small.

The studies of Er/H (Singh et al., 1976), Y/H (Curzon et al., 1979) and Sc/H (unpublished) by the same method showed a very large percentage rate of increase of resistance. This indicates that the number of scattering centres (H,atoms) alone is not adequate for a quantitative explanation of the resistivity increase. The nature of the conducting electrons (e.g. effective mass, screening ability) along with the effect of hydrogen on the lattice spacing could be other important parameters.

The resistance drop after A indicates the titanium hydride is more conducting than titanium. This increase of metallic character could be due to the contribution of some different processes, e.g. 1) Formation of a new characteristic conduction band due to the presence of hydrogen nuclei in the lattice. 2) Changes in the degree of band overlap due to the structural transition (H.C.P.-F.C.C.). 3) Contribution of some more electrons to the metallic conduction band due to the ionization of hydrogen atoms. 4) Variation of non-isotropic conductivity of the polycrystalline sample. 5) Different amount of s-d scattering of electrons,

6) Effect of lattice expansion.

The relative importance of these parameters is not well understood. More discussion of this will be given later. At this stage let us assume that in the mixed phase some hydride patches of composition $TiH_{1.5}$ are precipitated and experimentally this process is accompanied by a measureable amount of resistance drop. So the mixed phase extended up to $r = 1.55 \pm 0.05$. Azark et al's (1970) value is 1.5 at room temperature. The fast diffusion of hydrogen could allow for the formation of a homogeneous composition (macroscopic sense) throughout the film, therefore for a first approximation we would expect a linear drop of resistance in the mixed phase, however experimentally this is not observed. Fletcher et al. (1970) have pointed out that the shape of the resistivity vs composition curve in the mixed phase is determined by the distribution of the two phases, and therefore in their case, it depended upon the manner of preparation of sample. We can say that it depends upon the manner of precipitation of the hydride patches. Further the sudden large drop of resistance around the mid part ($r = .5 - 1.2$) of the mixed phase seems to be a characteristic behaviour of the titanium-film/hydrogen system. The reason for this effect is not clear, however it cannot be due to either any basic process described previously, nor to contact problems, nor to selective sorption of the sample within this small range of composition.

The sudden and relatively rapid effect of each dose within the mixed phase indicates: 1) hydrogen from each dose immediately enters into the bulk and/or 2) adsorption of additional hydrogen from each dose pushes some already adsorbed hydrogen from surface sites into the bulk. After this the gradual drop of resistance to its steady state could be due to:1) a small amount of absorption of new hydrogen from the surface or gas phase via adsorption, or 2) some rearrangement of hydrogen within the hydride clusters, or both. The first case seems

to be the main one, because R takes longer time to reach a steady state near B than near A, and the sticking coefficient is smaller at B than at A (as discussed later).

Finally, most of the resistance drop is observed within this portion and the total amount of drop is independent of the roughness (Surplice, unpublished) and geometrical shape of the film. Therefore the reason for the change is something basic, not the polycrystalline nature of the sample.

The constant resistivity region from B to C is believed to correspond to the single-phase hydride of F.C.C. structure. In contrast to the mixed phase, there is no structural transition or formation of clusters, but the distribution of hydrogen is rather uniform (see section 3.2). Therefore the constant resistivity of this phase may be a result of a balance between some processes (more discussion given later). Here it is worth noting that the single phase of F.C.C. zirconium hydride shows an increase of resistivity with hydrogen content (Andrievskii et al., 1967; Bickel et al., 1970). Further, in this region every dose showed first a fast drop, and then a gradual increase to its original value. This could be due to the formation of another, better conducting, phase of hydride, at first, and then a gradual removal of these patches by either 1) diffusion of hydrogen to other patches with lower composition or 2) dissociation. Dissociation alone is not enough to explain this process (we can see the reason later). The composition at C, corresponds to $r = 1.78 \pm 0.05$.

After C the resistance showed a definite decrease and this region is believed to correspond to the F.C.T. structure of the single hydride. In other words the hydride with F.C.T. structure is a better conductor than F.C.C. It is worth noting that Gesi et al. (1963) also came to the same conclusion from their resistivity measurements as a function of temperature for a hydride sample of composition $TiH_{1.86}$. Further, this

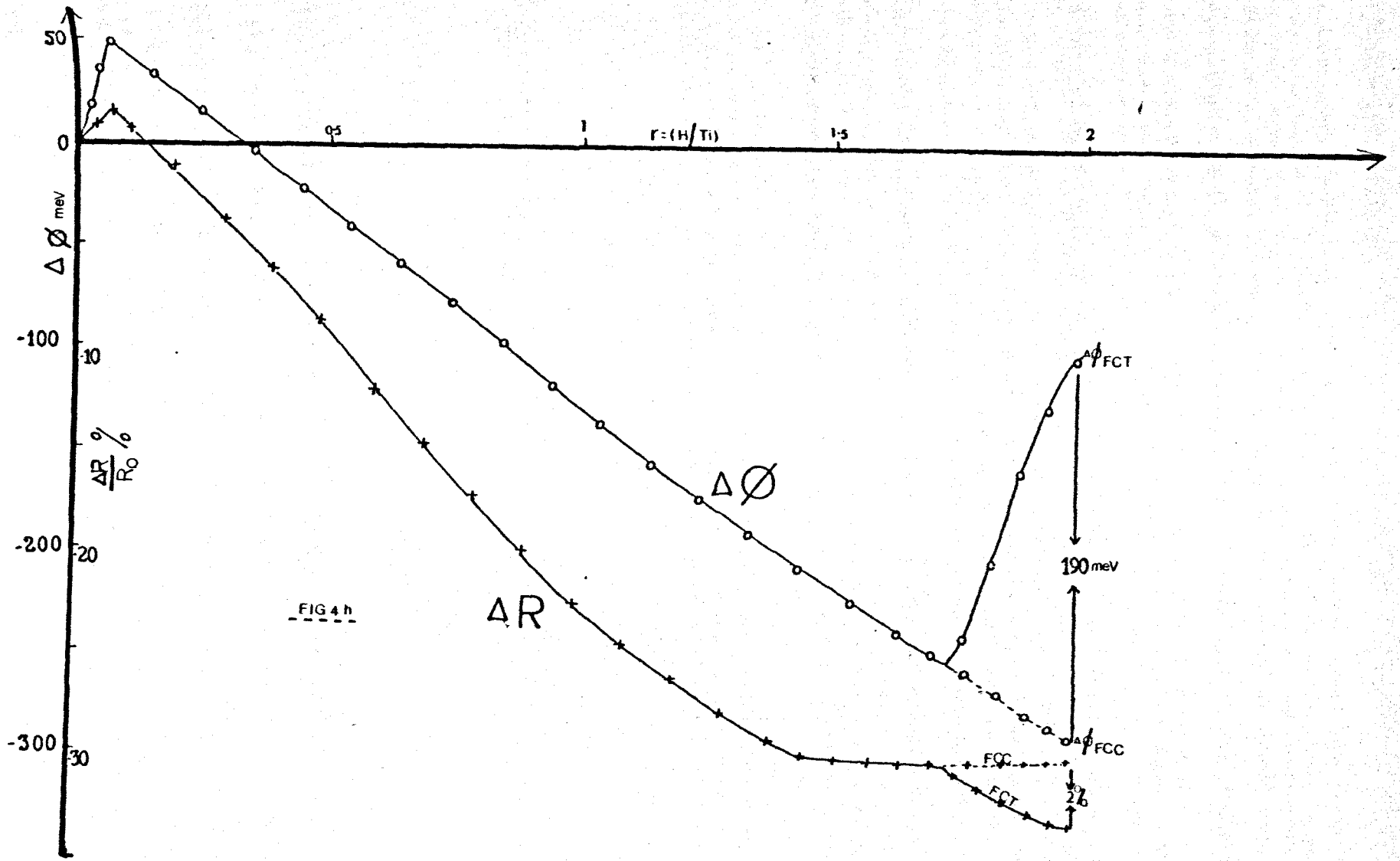
50
0
-100
-200
-300
10
20
30
0·5
1
r = (H/Ti)
1·5
2
Δ Ø mev
ΔR/R₀ %
ΔØ
ΔR
190 meV
ΔØ FCT
ΔØ FCC
FCC
FCT
2%

FIG 4 h

is also in agreement with study of Andrievskii et al. (1967) and Bickel et al. (1970) for the zirconium-hydrogen system. The better conductivity of F.C.T. hydride could be due to 1) change of electronic band structure 2) decrease of s-d scattering of conducting electrons (the relative merits of these processes will be discussed later).

The increase of resistance when the pressure of hydrogen is reduced to 10^{-8} torr is due to the dissociation of titanium dihydride, because the high composition hydride ($r > 1.90$) is unstable at 10^{-8} torr at room temperature (see table 4.4). Now we can understand why dissociation is not the only reason for the slow increase of resistance after the initial sharp drop for each dose in part B C. The dissociation up to 10^{-8} torr can raise the resistance only half way along the part CS, also the pressure in the part BC is higher than 10^{-8} torr. Therefore as mentioned previously, the significant process for that slow resistance increase is the redistribution of hydrogen to other parts of the film by diffusion.

In conclusion, the hydride of titanium is a better conductor than titanium. The conductivity - (σ) of F.C.T. dihydride is greater than the conductivity of F.C.C. dihydride of titanium (see extrapolation in the figure 4.h).

i.e. 1) $\sigma(TiH_2) \approx 1.4\ \sigma(Ti)$

2) $\sigma(Ti, HCP) < \sigma\ (TiH_2$ F.C.C.) $< \sigma\ (TiH_2$, F.C.T.)

b) Correlation of work function ϕ and resistance R with exposure

As explained previously, the region corresponding to OA is the solution phase. In this part we can assume for titanium that the Fermi level is unchanged (see section 3.1), therefore the variation of ϕ is governed only by surface potential part, consequently ϕ is sensitive only to surface conditions and the increase of ϕ up to M is purely due to the chemisorption of hydrogen atoms. The good coincidence of M and A indicates that the sorbed hydrogen was well distributed in all parts

of the film (because of the fast diffusion of hydrogen in titanium lattice). In general a negative surface potential can be the result of the adsorption of positively polarized atoms 'below' the surface or negatively polarized atoms above the surface. But the terms "above" and "below" are rather tentative depending on the relative size of sites and chemisorbed atoms. Further, negatively polarized atoms can chemisorb in both kinds of sites (if this is energetically possible) and can give either a net increase in ϕ or vice versa. Now it is well known that in transition metals hydrogen chemisorbs dissociatively as a negatively polarized species. The radius of a negative hydrogen ion is 1.36 A^{o}, which is very large to diffuse through the triangular holes between 3-titanium atoms in the H.C.P. structure. The radius of the holes is roughly equal to the covalent radius of hydrogen atoms ($\simeq$ 0.25 A^{o}). Our experiment indicates that hydrogen enters the lattice very rapidly, therefore its radius cannot be very large and therefore we assume the chemisorbed hydrogen carries only a fractional charge [i.e. $H^{-\delta}$, $\delta < 1$].

It is well established that low index planes have a high probability of being at the surface of a polycrystalline sample, therefore the most probable ones for H.C.P. titanium are (0001) $(10\bar{1}0)$ and $(1\bar{1}01)$. The recent x-ray work of Yasuhiro et al. (1978) showed that (0001) and $(1\bar{1}01)$ are the most probable planes at the surface of an evaporated Ti film in U.H.V. However for a first approximation suppose the above three low index planes have equal probability. These planes contain hollow sites [4-fold and 3-fold], bridge sites and top sites. In general a hydrogen atom on a top site would have a more negative charge than one on other sites (Bullett et al., 1977), and could give a larger increase of ϕ. But the observed change of ϕ for each dose is very small, which indicates that most of the hydrogen atoms were chemisorbed on the other sites.

If chemisorption on each of the other two types of sites corresponded

to an increase of ϕ then again we would expect a reasonably large total increase. The small value observed indicates that the two sites produce opposite effects. Therefore we suppose the adsorption of hydrogen on bridge sites corresponds to an increase of ϕ, and adsorption on hollow sites corresponds to a decrease of ϕ, but simultaneous adsorption (on both) can give a net increase of ϕ. This assumption predicts a radius for the chemisorbed hydrogen of about 0.6 - 0.75 A^{o}, and a charge 0.1 - 0.16 of an electronic charge (see Appendix A). This small value of charge is in agreement with the small experimental increase of ϕ. The upper limit for the charge comes from the hollow sites, but generally the charge of adatoms on bridge sites is more than on hollow sites (Bullett et al., 1977). Quantum mechanics shows that a 1s electron does not have a uniform radial charge distribution (the probability of finding the electron is greatest at approximately the Bohr radius $\sim$ 0.59 A^{o}). Therefore we can expect there to be more charge than 0.1e - 0.16e contained in a sphere of radii 0.6 - 0.75 A^{o}. Further, d-electrons can be distributed in five different electron lobes which are d_{xy}, d_{yz}, d_{zx}, $d_{x^2-y^2}$ and d_{z^2}. The energies of the electron states corresponding to the above lobes differ slightly in a crystal according to the crystal symmetry. For the H.C.P. lattice the d-band splits into 3 sub-bands and two of them are doubly degenerate for electrons, corresponding to dxy and $d_{x^2-y^2}$, d_{xy} and d_{xz} respectively (Moon, 1964). Altmann et al. (1957) have suggested that d_{xy} and $d_{x^2-y^2}$ are bonding electron lobes in the (0001) plane of the H.C.P. lattice. Further, d_{z^2} electron lobes are not directed towards any nearest neighbours in the lattice, therefore d_{z^2} corresponds to a higher energy state and the probability of occupation of d_{z^2} electron lobes is relatively low. In addition titanium has only two electrons out of a possible ten in the d-band, therefore we can conclude that the probability of one electron being in a d_{z^2} lobe is negligible and saturation of any one of these

lobes is impossible. The probability of chemisorption of an adatom on a particular site, depends on the nature of the electron lobes which are available there (Bond, 1969), and on the degree of their possible overlap with the adatom electron cloud. Further, high coordination sites are generally most preferable for bonding. In the light of all these facts it is obvious that the hollow and bridge sites are the more favourable ones for the chemisorption of hydrogen on the low index planes of titanium. The relative favourability of these two types depends on the planes; for example, on (0001) plane hollow sites are more favourable than bridge sites, while on $(10\bar{1}0)$ plane, bridge sites are more favourable than hollow sites.

Now we can give a simple explanation for the variation of ϕ after each dose in the part OM. From the mass spectrometer data we know that the doses at the start quickly disappear (2 sec), therefore the adsorption of hydrogen after this time is negligible. The sudden initial increase of R and more or less constant value of resistance later on, indicates a large portion of hydrogen going into the bulk at the time of the dose. This could be due to the action of electrostatic forces (see in Chapter 5). This does not mean that later on there is no diffiusion of hydrogen from surface sites to bulk, but the amount of hydrogen diffusing later has negligible effect on resistance. Generally diffusion has to take place via the hollow sites, so if there is no other process in operation then the adatoms in the hollow sites will have most chance of diffusing into the bulk. Therefore at the start of the experiment (doses near 0) for each dose a major fraction of the hydrogen can diffuse in an activated fashion into the bulk before we take our measurement (normally 5-10 sec) and the rest can be adsorbed on the energetically favourable hollow and bridge sites giving a net increase of ϕ. Later on a few more adatoms from hollow sites can diffuse slowly into the bulk, and by thus increasing the proportion left on the bridge sites this can give a gradual increase

of ϕ. Close to M, the same process can still be in action but we can expect more hydrogen atoms on surface sites. This will create strong repulsive forces between the adatoms, and this can give an equal tendency for adatoms to diffuse from bridge sites to hollow sites as from hollow sites to the bulk; so this situation gives effectively a gradual depopulation of the bridge sites, and therefore can give a gradual drop of ϕ after the initial increase. Alternatively we could say this drop of ϕ was due to the formation of a few "surface hydride" patches, but their formation did not affect the resistance.

After M, the net drop of ϕ for each dose indicates the existence of a new process, which is suspected to be hydride formation. Then the variation of ϕ is no longer governed by the surface potential part alone because hydride formation is generally accompanied by a change of Fermi level. Therefore in addition to the surface potential part the variation of ϕ has another contribution from the Fermi level shift which results from changes in the band structure. Further, during the hydride formation the lattice structure transforms from H.C.P. to F.C.C. This transformation can take place simply by sliding every third (0001) plane through one atomic distance, therefore the geometrical nature of the surface remains more or less unchanged. The conductivity of titanium and titanium hydride is of the same order of magnitude ($\sigma_{TiH_x} \approx 1.3\sigma_T$) i.e. no major change occurs in free electron density. Therefore for a first approximation we can assume that the change in surface potential due to the structural transformation is negligible. We can conclude that the hydride formed in the mixed phase region (F.C.C. structure $TiH_{1.5}$) has a lower work function or in other words its Fermi level lies above the Fermi level of the metal.

In our experiment we did not observe any difference in the variation of ϕ across the $(\alpha + \gamma)/\gamma$ phase boundary, in contrast to the marked change which we had observed at the previous $\alpha/(\alpha + \gamma)$ boundary.

Both the $(\alpha + \gamma)$ and γ phase have a lattice expansion and modification of band structure due to the introduction of hydrogen. Further, the change of lattice parameter with r, $(\frac{\Delta a}{\Delta r})$ has more or less the same order of magnitude on both sides of the $(\alpha + \gamma)/\gamma$ boundary (0.114 in $(\alpha + \gamma)$ phase, 0.105 in γ phase). But there are differences; during $(\alpha + \gamma)$ phase the H.C.P. structure of the titanium lattice transforms into F.C.C. structure, and the composition of the hydride patches stays constant at $TiH_{1.5}$, whereas the volume of the hydride increases continuously with r (see section 3.2). But the γ phase is entirely F.C.C. and its hydride composition increases steadily from r = 1.55 to 1.78. It is evident that these differences do not have much effect on the average variation of ϕ. But at the other boundary $\alpha/(\alpha + \gamma)$ there is a marked change in ϕ, so there the lattice expansion in the mixed phase and the modification of the band structure due to the precipitation of the hydride have major effects.

A simple model for the H.C.P./F.C.C. structural transition also indicates that its effect on the variation of ϕ would probably be small. Suppose H.C.P. Ti transformed into F.C.C. Ti at room temperature without any lattice expansion. The only difference would be the stacking sequence, and other features (neighbours, interatomic distances) would be the same, therefore the average interaction of the electrons with one another and with the ion cores would be more or less unchanged and the Fermi level could be the same. More or less same suggestion was made by Switendick in his band structure calculation (Switendick, 1970).

In our experiment we cannot tell if each dose causes the composition to change uniformly in all patches by a small fraction, or whether it causes a small change in the amount of hydride patches of local composition $TiH_{1.5}$, because the Kelvin capacitor measures the average value of ϕ. In the mixed $(\alpha + \gamma)$ phase of the Ti/H system the average composition changes due to the precipitation of increasing numbers of

hydride patches with the local composition $TiH_{1.5}$. But in the single phase (γ) the composition changes uniformly in all parts of the sample. The Kelvin capacitor is insensitive to these different methods of conversion in these two phases, so it is reasonable that we should observe a continuous variation of ϕ across the $(\alpha + \gamma)/\gamma$ boundary. However we can conclude two things: that the hydride patches do not form in layers but rather in well distributed "pillars", and the ϕ of F.C.C. hydride of titanium is less than the ϕ of H.C.P. titanium.

The gradual lessening of the initial increase of ϕ for each dose during the mixed phase is not due to any basic process; it simply reflects the sticking efficiency of the film. Close to M the sticking coefficient is high, therefore at the dose the surface suddenly gains a high population of chemisorbed hydrogen and that effectively increases ϕ. Then some H atoms gradually diffuse to energetically more favourable sites and some diffuse into the bulk, and in the meantime hydride precipitation reduces the average value of ϕ of the surface, therefore ϕ drops slowly to lower than its initial value. But close to N the sticking coefficient is small, therefore even at the start the Fermi level shift is dominant, so ϕ decreases without any initial increase. The gradual lessening of the initial increase could be due to the gradual decrease of sticking coefficient at the surface. This in turn could be due to the gradual change of surface patches from metal with a high sticking coefficient to hydride ($TiH_{1.5}$) with a lower one.

The relatively rapid resistance drop at the time of the dose again indicates some activated diffusion of hydrogen atoms from surface to bulk. The longer time taken to reach a steady value of R for a dose close to N could be due to the long "life" of each dose close to N and comparatively slow diffusion of hydrogen in the hydride.

In conclusion to this part, the total drop of 250-270 meV indicates that the Fermi level of $TiH_{1.5}$ (average) shifts to higher energy by this

amount (within our approximation of no change of surface potential). Further in the mixed phase the variation of ϕ is controlled by the transformation of metal patches into hydride patches of composition $TiH_{1.5}$, and the variation of the sticking coefficient has an effect on the variation of ϕ after each dose. Now we will see how the special feature of once again seeing an initial rise of ϕ after each dose helped to identify the boundary at point N.

As mentioned previously the diffusion of hydrogen, or its jumping frequency in the hydride, is smaller than in the metal (Korn et al., 1970; Stalinski et al., 1961). Therefore at the dose the possibility of the enhancement of hydrogen in the top few layers is high. However if we allow enough, time the hydrogen atoms diffuse to other parts of the film and give a homogeneous composition everywhere in the film. Therefore, suppose at the time of the dose a few patches in the top layers become F.C.T. hydride (which has high ϕ and low R) and later on they return to an average value (which corresponds to F.C.C. hydride) This kind of process can increase the ϕ from ϕ_1 to ϕ_2 and then drop to ϕ_3 ($< \phi_1$) as observed in the region NP. Therefore the Fermi level in the single phase region of F.C.C. hydride rises with composition, and the total rise varies 30-50 meV over a range of atomic ratio about 0.2. From the above explanation it is clear that the coincidence of N with B depends to a great extent on the equilibrium in mixed phase region. Otherwise we could observe the position N before the position B.

After P, the same sort of variation of ϕ indicates that the process which we proposed for the region NP is still in operation. This is reasonable, because both parts belong to the same single phase of hydride which has two different crystal structures. However, an increase of the steady value of ϕ, after each dose, indicates that the patches become stable at the surface due to the increase of average composition r of the hydride, which has a higher ϕ. Further, close to the

saturation, Q, the variation of ϕ becomes pressure dependent (see later in the discussion). The ineffectiveness of pressure variation, or dose introduction after Q, confirmed the saturation of the film at about $r = 2$ at a pressure 1.2×10^{-3} torr at room temperature. The good coincidence of Q with S indicates that the hydride corresponding to the higher value of ϕ is the better conductor.

In conclusion, the measurement of work function can be equally helpful as measurement of resistance to identify the phase boundaries. The Fermi level of the titanium hydrides lies above the Fermi level of titanium (H.C.P.). The Fermi level of the F.C.T. hydride lies below the Fermi level of the corresponding F.C.C. hydride (see extrapolation on Fig. 4.h). For example the structural transformation (F.C.C. → F.C.T.) at room temperature can lower the Fermi level of TiH_2 about 190 meV.

$$\text{i.e. } E_F(\text{Ti H.C.P.}) < E_F(TiH_2 \text{ F.C.T.}) < E_F(TiH_2 \text{ F.C.C.})$$

c) Pressure variation during the sorption of hydrogen by titanium

The constant pressure in region 1 (Fig. 4.c) indicates that almost all the input hydrogen molecules become sorbed. Therefore in this region the rate of flow is the rate-controlling process rather than sticking coefficient-S. So we cannot say anything particularly except that S is relatively large up to the end of this region which is about $r = 0.4$. This also agrees with the complete disappearance of a dose within 2-5 seconds in this region. Kasemo *et al.* (1979) have shown from their microbalance experiments that S decreases linearly up to $r = 0.3$ and after that remains constant until $r = 1.8$. But in our experiment in region 2 (Fig. 4.c) the pressure increases with a linear rate of increase, and the time taken for the sorption of doses gradually increases. So both things show the sticking coefficient is not constant but decreases slowly. This disagreement could be due to the formation of a high composition hydride, perhaps TiH_x ($x > 1.8$), at the surface

of their samples, but not on our sample. This is highly probable for two reasons: 1) Their samples were suddently exposed to a pressure 10^{-6} - 10^{-5} torr and this pressure is enough to establish an equilibrium with a hydride TiH_x ($x > 1.9$) (see table 4.4) but in our experiments the pressure increases gradually and even at the end of this region is about 10^{-7} torr. 2) They observed desorption of hydrogen from a sample with average $r = 0.66$ at pressure 5×10^{-10} torr, but our results shows dissociation is only possible for high compositions of hydride TiH_x ($x > 1.9$) at 10^{-8} torr, therefore the dissociation of $TiH_{0.66}$ is impossible even at 5×10^{-10} torr, since the pressure vs composition curve is very steep near saturation. So it seems clear that the surface of their sample suddenly became high composition hydride on exposure to 10^{-6} - 10^{-5} torr and had a low sticking coefficient. Both results for the region-3 indicate that in that region S is very low. Possibly this is due to the formation of hydride patches on all parts of the surface.

Flow experiments showed that the $\alpha/\alpha + \gamma$ boundary (A and M) corresponds to a composition $r = 0.067$, but the dose method gave $r = 0.045$. However both the values are in agreement with the observed small value of $r = 0.08$ in the experiments on resistance variation with atomic ratio-r. The difference is probably due to adsorption of some H before the first measurement was taken and the sensitivity of the mass spectrometer. Especially in the dose method, the mass spectrometer read a lower value of pressure because the films received hydrogen before the mass spectrometer. For the detailed calculation see Appendix B.

In conclusion the sticking coefficient decreases linearly in the mixed phase region and this could be due to the low value of the sticking coefficient of hydride patches. The atomic ratio-r at the $\alpha/\alpha + \gamma$ boundary, calculated from mass spectrometer measurements agrees with

the calibrated value from another experiment.

d) Sandwich film study

When hydrogen was allowed to react with sandwich films there was no resistance increase at the start of the experiment. This clearly shows that the starting composition of those films was beyond the solubility limit. The appearance of the ϕ vs exposure curves (Fig. 4.b and 4.d) also indicated that the starting features were missing, therefore even the surface of the film did not have the same nature as a fresh film. The sorption of hydrogen from the surrounding atmosphere (10^{-9} torr) was too little to explain the deviation from fresh film behaviour; therefore it must have been that some hydrogen had diffused from the hydride substrate and changed the composition of newly evaporated film. This is possible because the rate of diffusion of hydrogen in titanium (generally in all transition metals) is rapid and we have evidence of this rapidity from our fresh film experiments. Further, at the same time as this work was in progress, the same effect was recognized in different labs. by Malinski (1978) and Kasemo et al. (1979).

Let us assume that during the evaporation of titanium, hydrogen from the substrate diffuses up and forms a homogeneous composition through all parts of the composite film. However we cannot say that the diffused hydrogen occupies all the surface sites (hollow sites and bridge sites), and adsorption of hydrogen on these sites could increase ϕ (like a fresh film) at the start. However this increase was not observed in most experiments (see table 4.2), which could be due to the decrease of ϕ, due to a rise of Fermi level being dominant, which would also agree with the starting composition being well after the solution phase. Only two or three films (see table 4.2) showed an initial increase of ϕ. This may have been due to an anomaly such as a few unconverted metal patches at the surface or the existence of some

surfaces which had a small surface diffusion rate, but the cause is not well understood. Further, one of these films (Ti 39/2) (see fig. 4.d) showed two maxima which correspond to two different flow rates, and this indicates that there are two processes in operation. However in most of the films one process is dominant, which is Fermi level shift.

To check the merit of our assumption we have made some calculations for a simple model which is given in Appendix C. The calculated results for selected films are presented in table 4.3. The estimated atomic ratios ($r = {}^{H}/_{Ti}$) for the starting composition of a sandwich film, r_1, r_2 and r_3 are derived from ϕ measurement, thickness calculation via resistance measurement, and calculation of percentage drop of R respectively. The good agreement of r_1 and r_2 (except for Ti 31/2) supports our model's validity. In the case of Ti 31/2, before the evaporation of this film, the whole U.H.V. system had been baked up to 250°C, which could have caused more dissociation than we had assumed in the model (i.e. $r = 1.8$) therefore the calculated value of r_2 would be too high. Overall the very good agreement of r_1 and r_2 support the formation of a homogeneous composition, especially because r_1 can show only the nature of the surface, but r_2 is the average for the bulk. However r_3 shows random deviations. From figure 4.a it is evident that the % drop of resistance used in r_3 is not a useful parameter for calculation in the mixed phase.

The tables 4.1 and 4.3 indicate a great deal of variation in the amount of initial exposure. This is due to the different amounts of evaporation in each experiment. Even if we evaporate the same thickness of film on the substrate, the amount of evaporation outside the substrate (i.e. on the wall of the chamber) is completely different because this depends on the position and the orientation of the titanium filament, as it is difficult to have these features exactly the same each time.

In conclusion, the hydrogen atom diffuses rapidly to the top layer and forms a hydride of average composition in all parts of the film.

e) Study of dissociation of titanium hydride

The dissociation of titanium hydride has recently been recognized at room temperature (Surplice & Kandasamy, 1978; Kasemo & Tornquist, 1979). Previous values for dissociation pressure P_d of titanium hydride have been extrapolated from high temperature work, but those extrapolations are not valid, because they were extended from one phase to another by crossing the boundaries. Those extrapolated values for P_d are very low. Previous workers who assumed those values were correct often created some unrecognized experimental problems owing to the dissociation of their samples in x-ray, magnetic susceptibility and N.M.R. studies, as has recently been pointed out by Surplice and Kandasamy (1978) [for details see Appendix 1], our data for P_d which were given in table 4.4 show a rapid change of P_d with r which agrees qualitatively with a report of Stalinski et al. (1961) that at 200°C P_d was 10^{-2} torr for $1.6 \leq r \leq 1.93$ and 1 torr for $r = 1.93$. It would be unreasonable to extrapolate our order of magnitude data for r=1.9, but extrapolation of our data for $r = 2$, gives $P_d = 12.5$ torr at 200°C. For each phase of a gas/solid system $\log P_d = \frac{A}{T} + B$, but the coefficients A and B for a single phase are constant only if the composition is constant (Müller et al., 1968). The form of this equation means that the calculated value of P_d at a particular temperature is quite sensitive to small changes in A and B, consequently the values A and B calculated from our data are not so very different from those published previously (McQuillan, 1950; Beck, 1960; Gibb et al., 1951).

In the present work it was noticed that the variation of ϕ with time was linear when the pressure P was increasing but non-linear when it was decreasing. Since the Kelvin capacitor is sensitive to only a few

atomic layers near the surface, the change in the behaviour of ϕ vs t indicated that different reaction kinetics were in operation. The following model gives a qualitative explanation for the difference. When the pressure is continuously and slowly increasing, the composition of the hydride at the surface depends on the pressure above the film [i.e. in equilibrium]. However, when the pressure is decreased above a film which has r = 2 throughout its volume, then the surface does not reach a steady state until H atoms have stopped diffusing up to it from the lower parts of the film, consequently the H concentration in the surface layer decreases non-linearly.

Consider a small patch of titanium dihydride inside the bulk. We can represent the dissociation kinetics of the patch by the equation

$$TiH_2 \underset{K_1^1}{\overset{K_1}{\rightleftharpoons}} TiH_x + (2-x)\, H_B \underset{K_2^1}{\overset{K_2}{\rightleftharpoons}} TiH_x + (2-x)\, H_S \underset{K_3^1}{\overset{K_3}{\rightleftharpoons}} TiH_x + \left(1 - \frac{x}{2}\right) H_2(g)$$

where H_B - hydrogen atom in bulk

H_S - hydrogen atom at the surface

$H_2(g)$ - hydrogen molecules in gas phase

The step $H_S + H_S \rightarrow H_2(S)$ has been omitted because it is very rapid; for $r \geq 1.8$ the surface will be covered by the adsorbed H atoms at all times, and every H atom diffusing up to the surface will very rapidly find a neighbour to recombine with. The reaction constants are represented by K_1, K_2, K_3 and K_1^1, K_2^1, K_3^1. The first three of them are forward reaction constants and the others are the corresponding reverse reaction constants. Forward reactions can be described as follows. The first step represents the dissociation of dihydride into lower composition hydride and hydrogen atoms, which is in equilibrium with its parent hydride all through the volume of the patch. The second step represents the diffusion of dissociated hydrogen to the surface. The

third step represents the recombination of surface hydrogen atoms into hydrogen molecules in the gas phase. Suppose the pressure above the film falls to 10^{-7} torr at r = 2, this is far lower than the dissociation pressure, then the first step becomes very rapid so this is not the rate-limiting process. If the space above the film is continuously pumped so that the desorbed molecules of hydrogen are removed, then in the third step the forward reaction is dominant. In other words, as soon as the hydrogen atoms diffuse to surface from the bulk they can recombine and escape from the surface. Therefore the second step becomes the overall rate-limiting process. In contrast to the case above, if the pressure drops slowly then it is very hard to say which one step is the rate-limiting one. However the slow drop of ϕ observed experimentally indicates that the pressure drop due to the absorption by the wall will be the rate-limiting process.

The compositions of equilibrium with pressure 10^{-8} torr for different temperatures (20°C, 50°C and 70°C) do not differ much from one another. However, the increased amount of drop of ϕ at higher temperatures shows that the amount of dissociation is more at high temperature, as generally expected. Further a large drop of pressure (10^{-3} - 10^{-8} torr) indicates that the pressure vs composition curve is very steep close to the saturation.

In conclusion, the dissociation pressure of titanium dihydride at room temperature is very much greater than previously expected, and the pressure vs composition curve is very steep close to the saturation. Some of the anomalies in the previous works were due to the problem of dissociation.

f) Comparative study at 50°C and 20°C.

Basically these experiments were conducted to find out the relative positions of the γ/γ' phase boundary around the transition temperature

310°K (≃ 370°) which had been proposed by early workers (see Section 3.2). The measurement of ϕ was selected in preference to resistance R, because of its high sensitivity (especially for sandwich films) around the investigated region. Further these experiments involved heating and cooling processes therefore measuring only ϕ avoided any possible confusion between the variation of film resistance and contact resistance. The reproducibility of these experimental results was excellent in all repeated cycles. In the first experiment (Fig. 4.g) the drop of ϕ, when the temperature of the sample was increased from 20°C to 50°C is in general agreement with other results for metals (Holze et al., 1979). There is no other data available for metal hydrides to compare them with our result. Christmann et al. (1974) and Holze (1975) observed changes of $\phi \sim 10^{-4}$ eV K^{-1} for Ni samples in their C.P.D. measurements. Our value for TiH_2 is $\sim 2 \times 10^{-3}$ eV K^{-1}, which is relatively high. It is worth noting here that for the same range of temperature in the F.C.C. hydride phase region (part C of third experiment) a change of ϕ of 1.6×10^{-4} eV K^{-1} was observed, therefore the higher value might be the characteristic of F.C.T. TiH_2. The variation of ϕ with temperature depends on many physical variables and is very difficult to estimate separately. Our films were condensed on substrates at about 75°C during the evaporation and then they were brought to room temperature gradually, these warmings would have little effect on the surface of the film. In the case of F.C.T. TiH_2, the temperature increase has an effect on the degree of tetragonality (Azark et al., 1970) and this can have a large effect on the position of the Fermi level. In other words the large drop of ϕ could be a reflection of a change in the degree of tetragonality with temperature increase. Further, the increase of ϕ with composition at 50°C as well as at 20°C, shows that the F.C.T. phase is stable even at 50°C, which is higher than the previously proposed transition temperature, 310°K.

Once again the second experiment (Fig. 4.g.2) confirmed the existence of F.C.T. hydride at 50°C. Further, two simple estimations from our results indicate that the F.C.T. TiH_2 could be stable up to 110-120°C (see Appendix D). This experiment shows the change of ϕ (i.e. $\frac{d\phi}{dT}$) for TiH_2 during the temperature change 20 → 50°C is higher than the corresponding change of ϕ for a lower composition hydride ($\sim TiH_{1.9}$). This is clear from figure 4.g.2. This might indicate either a different amount of change in tetragonality at these two compositions, or the position of the Fermi level is in the decreasing part of the density of states curve for F.C.T. titanium hydride. The x-ray work of Azark et al. (1970) at 183°K and 295°K showed that there is not much difference in the change of tetragonality for compositions TiH_2 and $TiH_{1.9}$. Therefore this experiment could be an indication that the position of the Fermi level is in the decreasing part of the density of states curve. Now we will see how this is possible. Suppose in F.C.T. hydride of titanium, the Fermi level is in the decreasing part of the density of states curve, and it is moving to lower and lower parts of the curve due to the modification of energy (we can see later), when the composition of the hydride increases. When the temperature rises the Fermi level shifts higher and the electrons occupy some of the higher energy states; then to populate a given number of energy states the Fermi level has to move by a large amount if it lies in the lower part of density of states curve for TiH_2. Experimentally a larger shift was observed for TiH_2 than for lower composition hydrides $TiH_{1.9}$. Therefore it is clear that the Fermi level in the F.C.T. hydride probably lies low down in the decreasing part of the density of states curve.

The third experiment clearly shows that the position of the minimum P in the ϕ vs composition curve is shifted to the high composition part with a temperature increase. A simple estimation indicates that the shift is equivalent to $\Delta r = 0.075$ for the temperature increase from 20°C

to 50°C (see Appendix D).

In conclusion the transition temperature for F.C.T. into F.C.C. structure of TiH_2 is higher than the previously predicted value 310°K. The Fermi level in the F.C.T. hydride probably lies in the decreasing part of the density of states curve. At 50°C the phase boundary γ/γ' moves to r = 1.85 from its room temperature (20°C) value of r = 1.78.

g) Anomaly in the variation of ϕ

In principle all compositions of the Ti/H system will have ϕ less than its value at the position M in the plot. The reason for the observed high value after M for some fresh films is not well understood and we can describe this as an anomaly in our results. Further, the instability of this high value of ϕ indicates it corresponds to a metastable state of the Ti/H system. This could be due to the formation of some high composition complex (for example TiH_3 or TiH_4) at the surface.

4.3 Phenomenological model

In this section a phenomenological model for the Ti/H system is suggested which agrees with the generally accepted properties of the conduction band of transition metals. It can account qualitatively for the changes of work function and resistance with atomic ratio, and for the F.C.C./F.C.T. transition.

a) Conduction band of transition metal

It is well known that transition metals have overlapping broad s-bands and narrow d-bands. The s-band can accommodate only two electrons per atom but the d-band accommodates ten electrons per atom, thus the density of states of the d-band is very high. Band structure calculations for these metals indicate that d-bands lie near the Fermi level (Ashcroft et al., 1976), therefore there is no reason to expect them to have a free-electron type Fermi surface or a parabolic density of states function.

Part of their Fermi surface is mainly s-like and is thus in a region of k-space having a low density of states, and part is mainly d-like and this has high density of states.

Generally all these features are reflected in the band structure calculations for these metals. However Lopez (1979) has remarked that the characterization of states, their energetic location and related band positions greatly depend on the potential and geometrical parameters used in the calculation. Therefore the band structure calculations do not adequately represent the real nature of the various types of electron bands, because of the choice of computing parameters. But the band structure calculations may give a rough idea about the general features of the energy bands of the metal or metal hydride which are considered below.

The tight binding approximation is generally considered as the best method for energy band calculations for transition metals. This approximation establishes the first order energy shift when the atoms are brought close together in a crystal, in terms of overlap integrals. Physically this term in the band theory represents the effect of neighbours, and depends strongly on first and second nearest neighbours (Haydock et al., 1972). This term contains two main parts which are 1) transfer term (or bonding part), 2) crystal field integral. The transfer integral term will include an exchange term, a correlation term and a spin interaction term. The crystal field integral represents the effect of the non-spherical electrostatic field due to the neighbours. Among the s, p, d and f electrons, s and p electrons are collective, therefore the transfer term is more effective for them than the crystal field term. However, f electrons are completely screened from the surrounding by overlying s and p electrons [e.g. 4 f electrons are screened from the surrou ings by the 5 s and 5 p electrons]. Consequently the f electrons have no effect on the surroundings [i.e. they are localized]

and therefore the crystal field term is dominant for them. But d-electrons are not screened completely, they have some influence on the surroundings therefore d-electrons are intermediate between the case of collective electrons and localized electrons. Cotton et al. (1972) mentions that the d-block transition metals are very sensitive to their environment and they are also able to influence it very significantly. Further, Goodenough (1960) has proposed that the d-electrons can exist simultaneously both as collective and localized electrons, therefore both terms in the energy shift part are important for d-electron metals, and neglecting either of them gives an extreme case of the real situation.

Most of the band theory calculations rest on the assumption that the interaction between the atoms is so large that electrons can be shared equally by all like atomic nuclei, so in the integral only the transfer term is effective and the crystal field term is negligible. Matheiss (1972) has pointed out that the crystal field effect can be extended to energy band theory by means of semi-intuitive arguments. Mott (1964) has pointed out that the density of states of (B.C.C. - F.C.C.) transition metals should have a minimum at the centre of the band, however for an F.C.C. metal the minimum is less predominant (Beeby, 1966). A number of workers have suggested that the d-band should really be double, consisting of an upper part capable of holding four electrons and a broader lower part holding six electrons, per atom. The origin of the separation of these "sub bands" is not clear but has been ascribed either to crystal field effect or bonding effect (Williams, 1966). Matheiss (1972) has pointed out that the crystal field splitting is associated, not with energy separation at the centre of the Brillouin zone, but rather with the difference between the average e_g and t_{2g} band energies. Mott et al. (1957) have suggested that the anisotropy of the electrostatic field around an atom in a metal splits the 3d band into a higher energy and lower energy group. But Friedel (1969) has

fig 4-i-1

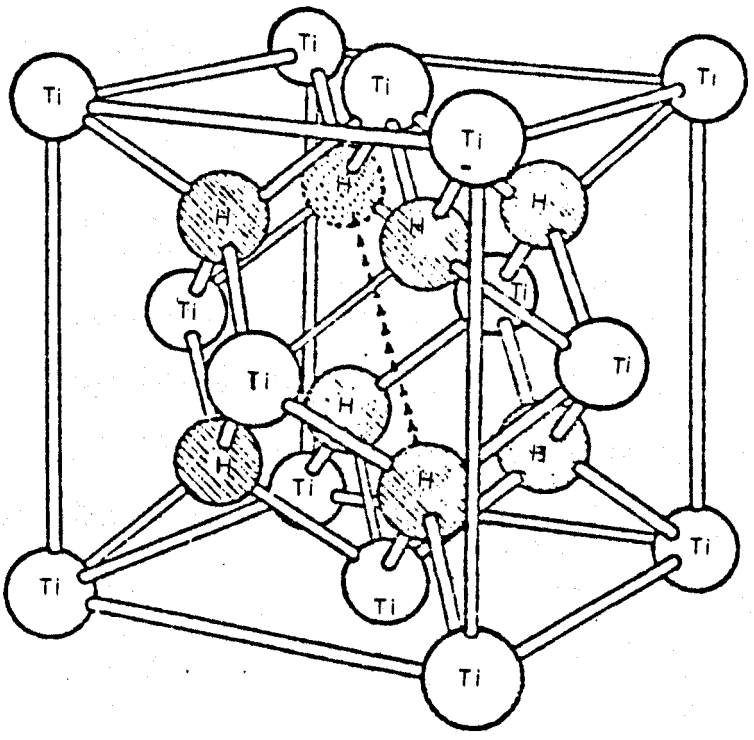

fig 4-i-2

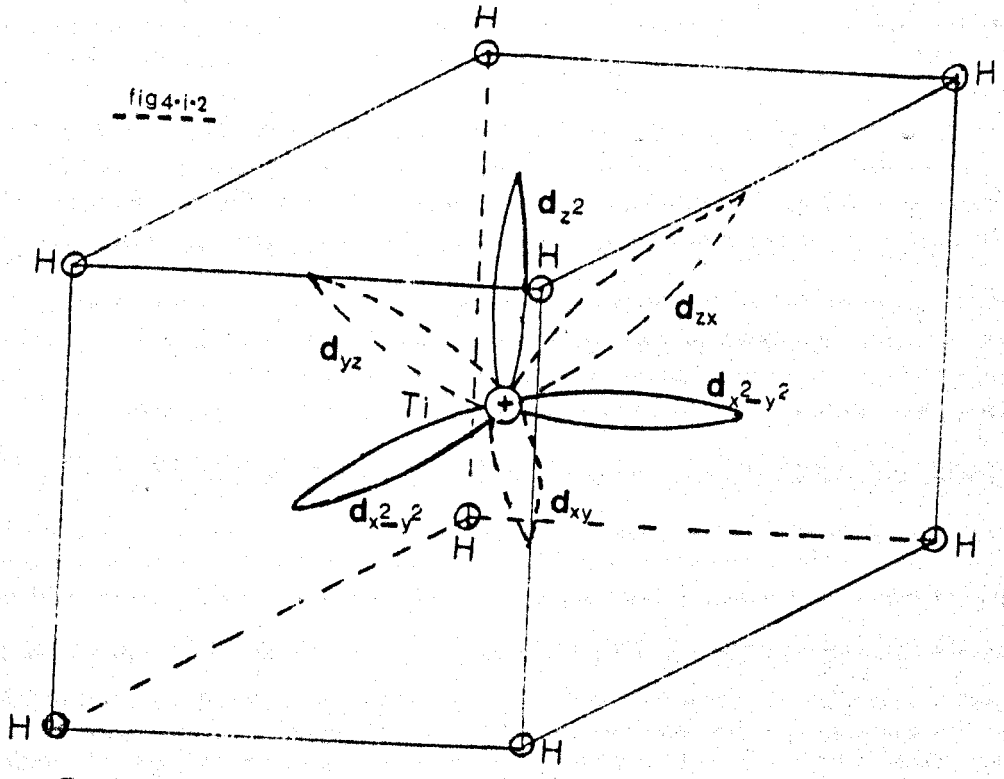

In TiH_2 each Ti atom is surrounded by 8 hydrogen atoms. 9 more XY symmetry d-electron (lobes) and 3 more X^2-Y^2 symmetry d-electron lobes are not shown for clarity.

remarked that the crystal field effect in 3d transition metals is negligible compared with the band width, and so this splitting should not be important for these elements. However, neutron diffraction experiments on Fe (Shull, 1963) and on Ni (Mook et al., 1966) indicate that there is a reasonable amount of crystal field splitting. A number of workers (Callaway, 1961; Hodges et al., 1966) have suggested that in a crystal field of cubical symmetry the d-band splits into a triply degenerate t_{2g} band and a doubly degenerate e_g band. Callaway et al. (1960) suggested that a crystal field with cubical symmetry lowers the energy of electron states with symmetry xy, yz and zx - (t_{2g}) with respect to the energy of electron states with symmetry $(x^2 - y^2)$ and $(3z^2 - r^2)$ - (e_g). Slater (1965) has suggested that the d-band of transition metals contains a bonding type wave function in the lower part of the band, and an anti-bonding type wave function in the upper part of the band, and net bonding arises from the d-electrons as well as s-electrons.

b) Conduction band of titanium (F.C.C.)

Now we will start to consider the conduction band of titanium while keeping all this information in mind. In titanium hydride the hydrogen atoms are contained in a metal "cage" of F.C.C. structure as shown in figure 4.i.1. In the F.C.C. lattice every metal atom is surrounded by twelve nearest neighbours, which are placed along the diagonal of the cubic faces of a unit cell, and by six next nearest neighbours which are placed along the edges of the unit cell. The t_{2g} atomic orbitals [or xy symmetry electron orbitals] are directed towards the nearest neighbours and the e_g atomic orbitals [or $x^2 - y^2$ symmetry electron orbitals] are directed towards the next nearest neighbours. It is generally believed that the overlap of t_{2g} orbitals is large therefore they form a broad electron band and are responsible for bonding and for electrical conductivity. But the overlap of e_g orbitals is slight, therefore they form a narrow electron band, and are responsible for the

magnetic nature of the metal (Bond, 1969).

In F.C.C. titanium the next nearest neighbours are separated about 4.4 A^{o}, and the nearest neighbour distance is about 3 A^{o}. Goodenough (1960) has mentioned for 3d metals, that if the interatomic distance equals to 2.9 $\pm$ 0.1 A^{o} or less, then d-electrons behave like collective electrons, but if the distance is more than 2.9 $\pm$ 0.1 A^{o}, then d-electrons behave like localized electrons. Quantum mechanics predicted for the hydrogen atom that, the expectation value of probability of the 3d-electron occupation is about 10.5 atomic units [5.5 A^{o}] from the nucleus, but we can expect a lower value for titanium because of its higher nuclear charge. Therefore without loss of generality, we can treat the d-electrons of titanium as collective, but with a relatively more localized nature for electrons in e_g atomic orbitals. In other words, we can imagine for titanium that the t_{2g} band is wider than the e_g band and in each band anti-bonding electrons occupy the high energy part of the band. Weinberg *et al.* (1972) have pointed out that in F.C.C. metals the electron orbitals pointing towards the next nearest neighbours are of higher energy than the electron orbitals pointing towards nearest neighbours.

Titanium has only two d-electrons per atom therefore the d-electrons are not even enough to fill more than half of each sub band e_g or t_{2g} separately. Therefore the probability of two electrons occupying the same electron lobe is always small. So the Coulomb repulsion between the electrons is very small even in the t_{2g} orbitals which are expected to have a large overlap. Further electrons in t_{2g} atomic orbital will have more attractive potential than in e_g atomic orbital, because of the close position of the atomic centres. Therefore we can conclude that the t_{2g} band is extended to lower energy than the e_g band in such a way as to accommodate the bonding electrons. Also we can say that the t_{2g} band is extended to higher energy than e_g band because of the large overlap of anti-bonding electron orbitals. On the grounds of the

fig 4-i

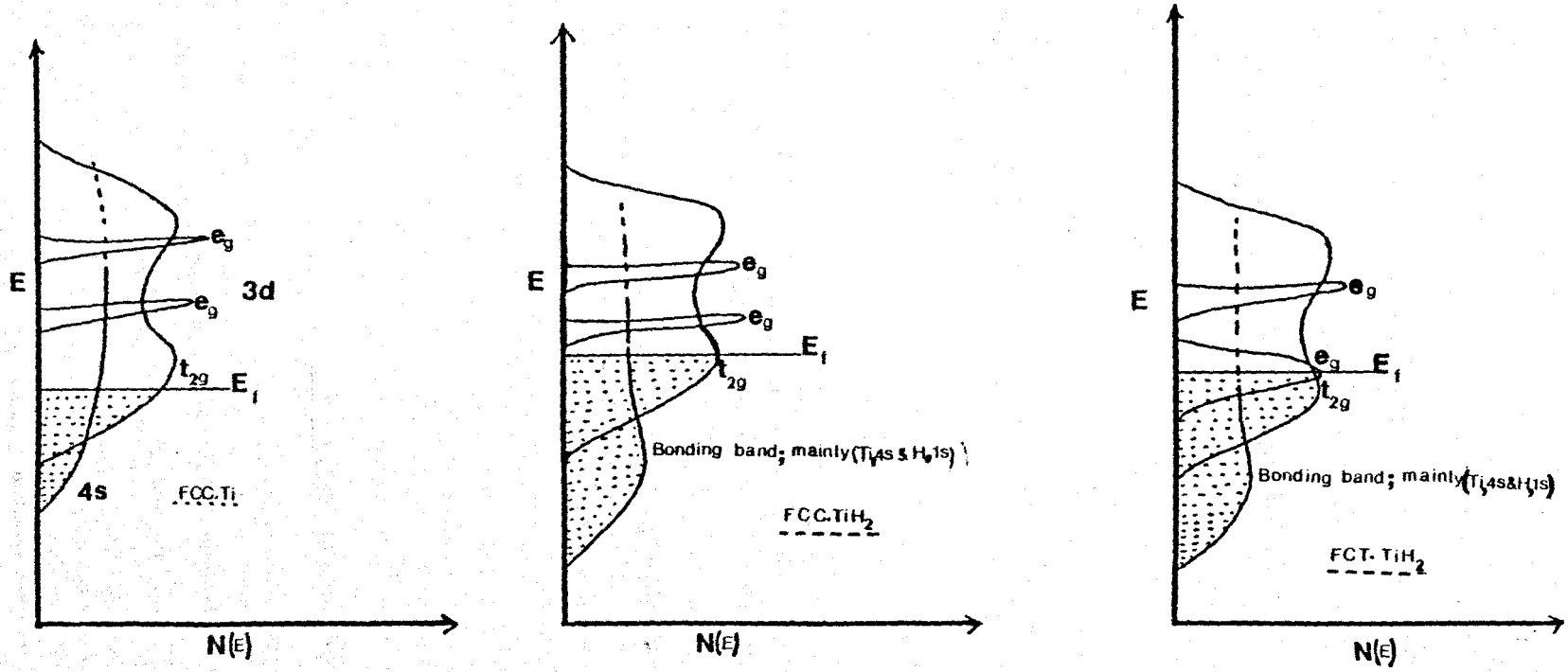
E
e_g
3d
e_g
t_{2g}
E_f
4s
FCC.Ti
N(E)
E
e_g
e_g
E_f
t_{2g}
Bonding band; mainly(Ti_{4s} & H_{1s})
FCC.TiH_2
N(E)
E
e_g
e_g
E_f
t_{2g}
Bonding band; mainly(Ti_{4s}&H_{1s})
FCT. TiH_2
N(E)

fig 4-k

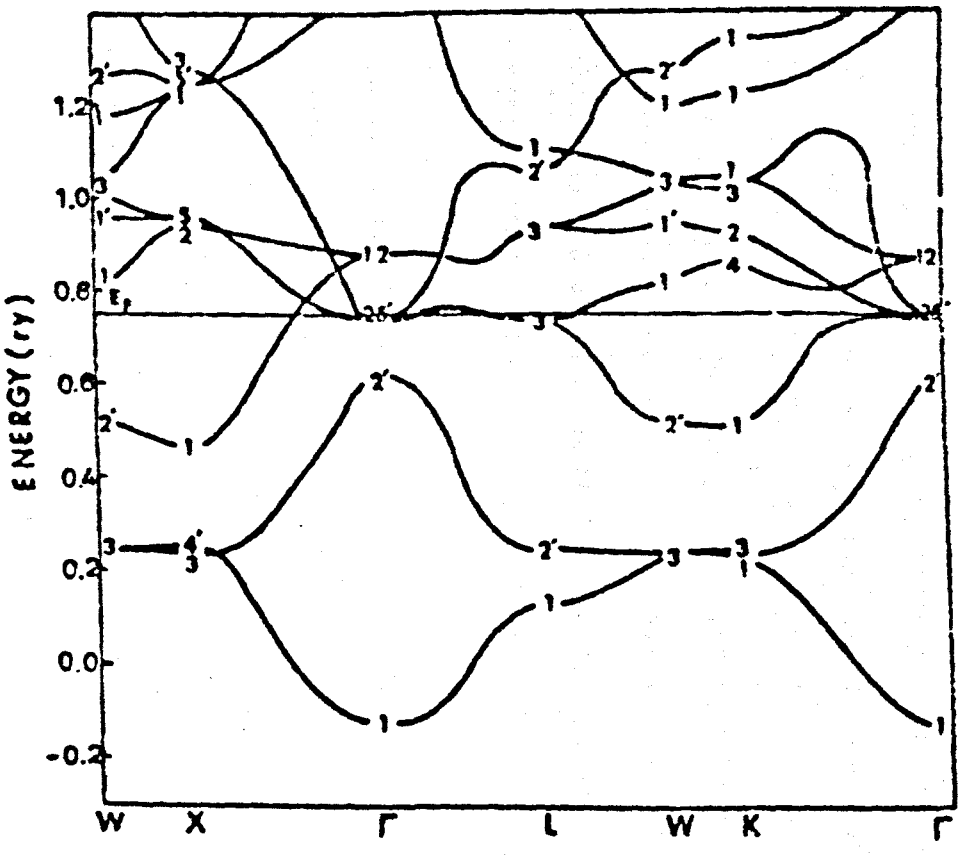

Fig. Energy Bands for Cubic Titanium Dihydride

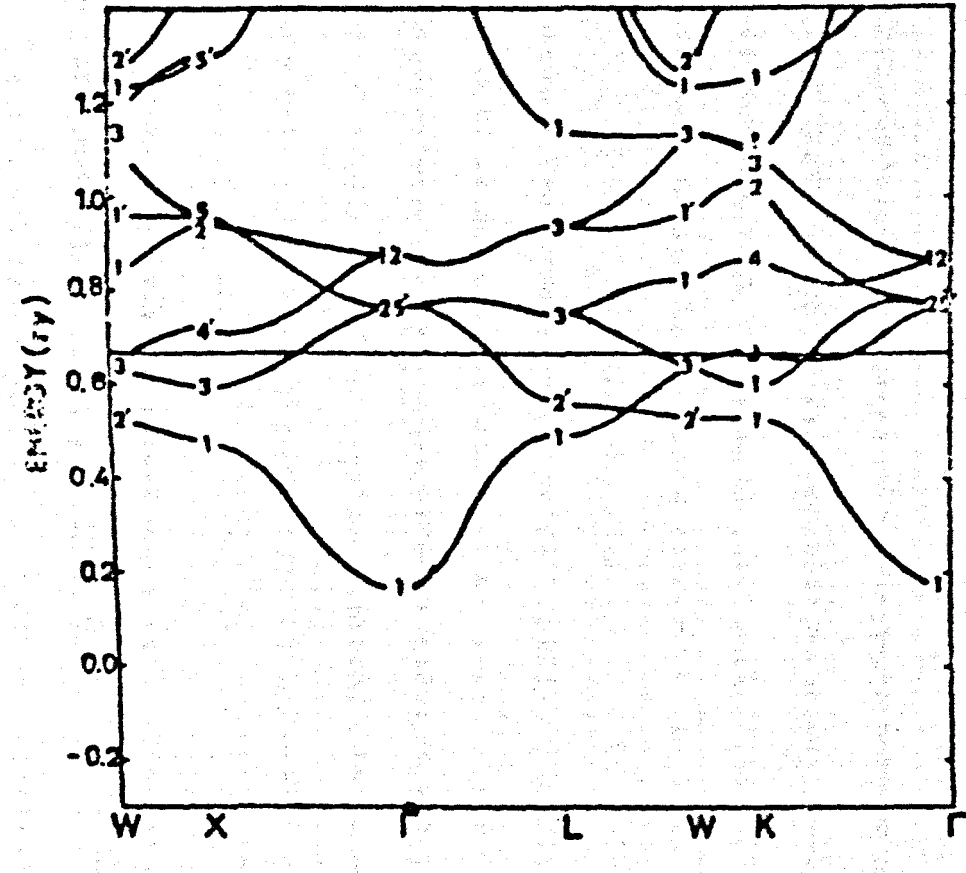

Fig. Energy Bands for Cubic Titanium

above ideas we can propose a band model for F.C.C. titanium lattice as shown in fig. 4.j. The relative position of the t_{2g} and e_g bands is not critical. The 4s band generally shows overlap with the 3d band, but their relative overlap is also uncertain. However Hirohiko et al. (1979) cluster claculation suggests that the population of the 4s orbital is only about 50%.

The above picture is in agreement with the crystal field effect, if we assume that the Ti^{2+} ions are placed in a sea of free electrons (4s electrons), and with the general features of band structure calculations for F.C.C., 3d metals. These calculations show that electron wave functions with a t_{2g} nature (Γ_{25}', X_3, K_3, K, and W_3) have a lower energy than the electron wave functions of e_g nature (Γ_{12}, X_2, K_4, W_2'). All these features are reflected in the band structure calculations of Switendick (1976) for F.C.C. titanium, shown in figure 4.k. Finally the proposed band structure indicates the existence of a minimum about the mid part of the band (4 - 6 electron per atom). The exact position of the minimum depends on the relative position of the e_g and t_{2g} bands, therefore this can vary from metal to metal. In the same way the degree of overlap of the metal s-band and d-band can vary from metal to metal.

Recently Korn (1978) has proposed a phenomenological model for the Ti-H system, in which he has assumed a bonding band with four d-electrons, and an anti-bonding band with six d-electrons. Further he suggested that the hydrogen atoms in metal hydrides seem to compensate electronically for electrons of less than four in number in the d-band. According to his suggestion all group III B elements can form trihydrides but group VB elements can only form monohydrides. But ScH_3 does not exist, V and Nb can form hydrides having a composition more than monohydride (Müller et al., 1968). This indicates that his idea was too simple. Further, instead of four bonding electrons, Mott (1964) has suggested five bonding electrons. In addition to this, his model

predicted a continuous rise in Fermi level E_F with hydrogen concentration, even in F.C.T. hydride. This is contradictory to our experimental results, especially for the F.C.T. hydride phase.

c) The effect of hydride formation on the conduction band

Now we will start to consider the effect of hydride formation in our model. If we introduce hydrogen atoms to the titanium lattice, after certain concentration (solubility limit) the hydrogen interacts with the electron states of the metal and other hydrogen atoms. This strong interaction can lower the energy of the many-electron states. In other words, this interaction lowers many unoccupied high lying states to well below E_F. However the relative amount of drop of various states depends on the degree of interaction of these states. We can say that there is more lowering of potential energy for free-electron type states (s and p states), because they are more dispersive. But for d-electrons the lowering of potential depends on how near their electron lobes are to the positions of the hydrogen atoms: the lowering of energy is more for the states which have appreciable wave function amplitudes at the hydrogen sites.

Generally the effect on these d-states is small. To understand this situation we imagine that instead of hydrogen being in the tetrahedral voids of an F.C.C. lattice of titanium, they are placed at vertices of a cube and a titanium atom is placed at the centre, as shown in figure 4.i.2. Then 12 lobes of t_{2g} orbital which have xy symmetry are pointed towards the mid points of the 12 edges of the cube and lobes of e_g orbitals which have $(x^2 - y^2)$ symmetry are directed towards the mid points of the faces of the cube. It is obvious that the position of hydrogen is closer to the projection of t_{2g} electron lobes than the projection of e_g electron lobes, but none of them are directly pointed towards the hydrogen atom. Therefore the effect on the d-electron

states is small compared with effect on the other electrons with free electron nature. But we can say that relatively the effect is more on the t_{2g} electron states than e_g electron states. Therefore t_{2g} electron states will shift slightly downward. This also indicates that the bonding between d-electrons of Ti and s-electrons of hydrogen is more probable via t_{2g} electrons than e_g electrons. In conclusion we can say that in the conduction band of the hydride the higher energy part retains the d-character of the metal band but lower energy part has a completely new feature with more free electron (s and p) nature. Generally the lower part contains mostly bonding and anti-bonding states of H with H and bonding states of H with metal.

Now we will see how changes of Fermi level are possible, when the hydride starts to precipitate. The position of the Fermi level can be affected by structural transition, expansion of lattice and formation of new conduction band. As we concluded previously the structural transition (H.C.P. → F.C.C.) will have negligible effect. Lattice expansion generally reduces the overlap of the electron orbitals. This can reduce the band width and can increase the potential energy of the conducting electrons. In other words, energy bands with bonding nature will shift to higher energy due to lattice expansion. Therefore effectively this can raise the Fermi level.

The presence of hydrogen atoms in the titanium lattice lowers the many electron states, also the number of electrons in the overall band is increased by one more electron for every hydrogen atom present in the lattice. The appearance of extra electron states (i.e. so called hydrogen-derived states) below the Fermi level of titanium can lower the Fermi level. But if the hydrogen-derived states can accommodate only a fraction of the electrons of hydrogen, then the rest of them will occupy higher energy states of metallic nature. This will raise the Fermi level. The relative strength of these three effects is not clear in

the present situation. However we can say that according to the relative strength of these effects in titanium hydride the Fermi level can rise or drop. Suppose effectively these three effects raise the Fermi level, then the work function will drop. This is the simplest explanation for the author's data for the change of ϕ with hydrogen concentration in the mixed ($\alpha + \gamma$) and F.C.C. single hydride phases. The author's experimental result and his proposed model are qualitatively in agreement with Switendick's theoretical calculations (Switendick, 1976).

d) F.C.C./F.C.T. phase transition and the conduction band

Now we will consider how the continued addition of hydrogen to the titanium lattice could cause it to transform from F.C.C. to F.C.T. Suppose the Fermi level in F.C.C. titanium hydride rises with increase of composition (r) and reaches the high density of states part of the conduction band. Generally a high value for density of states corresponds to the existence of degeneracy in the electron states. The Jahn-Teller theorem says that distortion of the lattice can lower the energy of the degenerate electron states. Previously this effect has been proposed as a possible reason for the structural transition by various workers (see section 3.2).

However another explanation can be given for this phase transition as follows. Suppose that the high density states corresponds to the start of overlap of e_g bands with t_{2g} bands at lower energy. Then when the Fermi level reaches the energy at which overlap is starting, some of the electrons start to go into the e_g band. This band is derived from the overlap of electron states which have wave functions with $(x^2 - y^2)$ symmetry, in other words overlap of d_z^2 and $d_{x^2-y^2}$ electron lobes. Now the question is, which of these two lobes is energetically more probable for occupation by electrons. Electrons in d_z^2 electron

lobes have magnetic quantum number m = 0 but those in $d_{x^2-y^2}$ electron lobes have magnetic quantum number m = 2. Phillips et al. (1967) have suggested that the interaction of an s electron is stronger for d-electron with m = 0 and shifts the energy of d-electrons states with m = 0 to relatively lower energy. Therefore the electrons in the e_g band could first occupy the d_{z^2} electron lobes which are pointed along the z-axis. Further, the d-electron wave function can generally be divided into six wave functions, in which three of them have xy symmetry, which are linearly independent, and the other three have $(x^2 - y^2)$ symmetry which are linearly dependent (Hameka, 1975). The $(x^2 - y^2)$ symmetry wave function can be written as two linearly independent wave functions which correspond to d_{z^2} and $d_{x^2-y^2}$ electron lobes. The d_{z^2} electron lobes correspond to the linear combination of two $(x^2 - y^2)$ symmetry wave functions, but $d_{x^2-y^2}$ corresponds to only one (x^2-y^2) symmetry wave function. Therefore we can say that there is more probability for the electron being in the lobes d_{z^2} than $d_{x^2-y^2}$.

Suppose when the bands start to overlap then some of the electrons of the hydrogen atom start to flow to the d_{z^2} electron lobes. The existence of electrons in this lobe can increase the binding forces in the direction in which d_{z^2} electron lobes are pointed. This asymmetrical situation can give a distortion of the lattice, as observed in titanium hydride, because generally the binding forces are attractive and attractive forces give a compressional strain along the line of action and an extensional strain along the orthogonal plane.

Now we will consider the effect of distortion on the band structure. The separation of nearest and next-nearest neighbours increases in the xy plane, but reduces in other planes due to this structural transition. Therefore the energies of the states corresponding to d_{xz}, d_{yz} and d_{z^2} shift relatively downward, but the energies of the electron states corresponding to d_{xy} and $d_{x^2-y^2}$ shift relatively upwards. In other

words the average potential can remain unaffected, but the energy of the different electron states can be rearranged due to the structural transition. The upward shift of the electron states corresponding to $d_{x^2-y^2}$ electron lobes is less important since these states are vacant even in F.C.C. hydride. The shift of the electron states corresponding to d_{xy}, d_{xx}, and d_{zy} electron lobes, in the t_{2g} band, more or less gives an unchanged situation because of the opposite movement of the d_{xy} to the other two states, and the broad nature of the t_{2g} band. The downward shift of electron states corresponding to d_{z^2} electron lobes is more important and is relatively large. The volume change of the unit cell during the structural transition is negligible (Azarkh et al., 1970), therefore for a first approximation we can neglect the kinetic energy change of the conduction electorns during the transition. Therefore we can say that some of the electrons which populate high energy states for F.C.C. structure [i.e. at Fermi level] depopulate and occupy the additionally derived d-electron states at low energy during the structural transition. This situation can lead to a shift of Fermi level to lower energy. It is also obvious that the general features of the density of states can change, and the Fermi level can lie in decreasing part of the density of states curve, as we concluded previously. Finally in our discussion we have mentioned that the structural transition can arise due to extra population of electrons in one direction. Generally there is no physical reason to prefer one specific direction in space than any other direction. However co-operative effects between neighbours can lead to one preferred direction, at least within a grain.

e) General application of the model

Now we will consider the effect of temperature on the stability of F.C.T. structure for high composition hydrides. The temperature

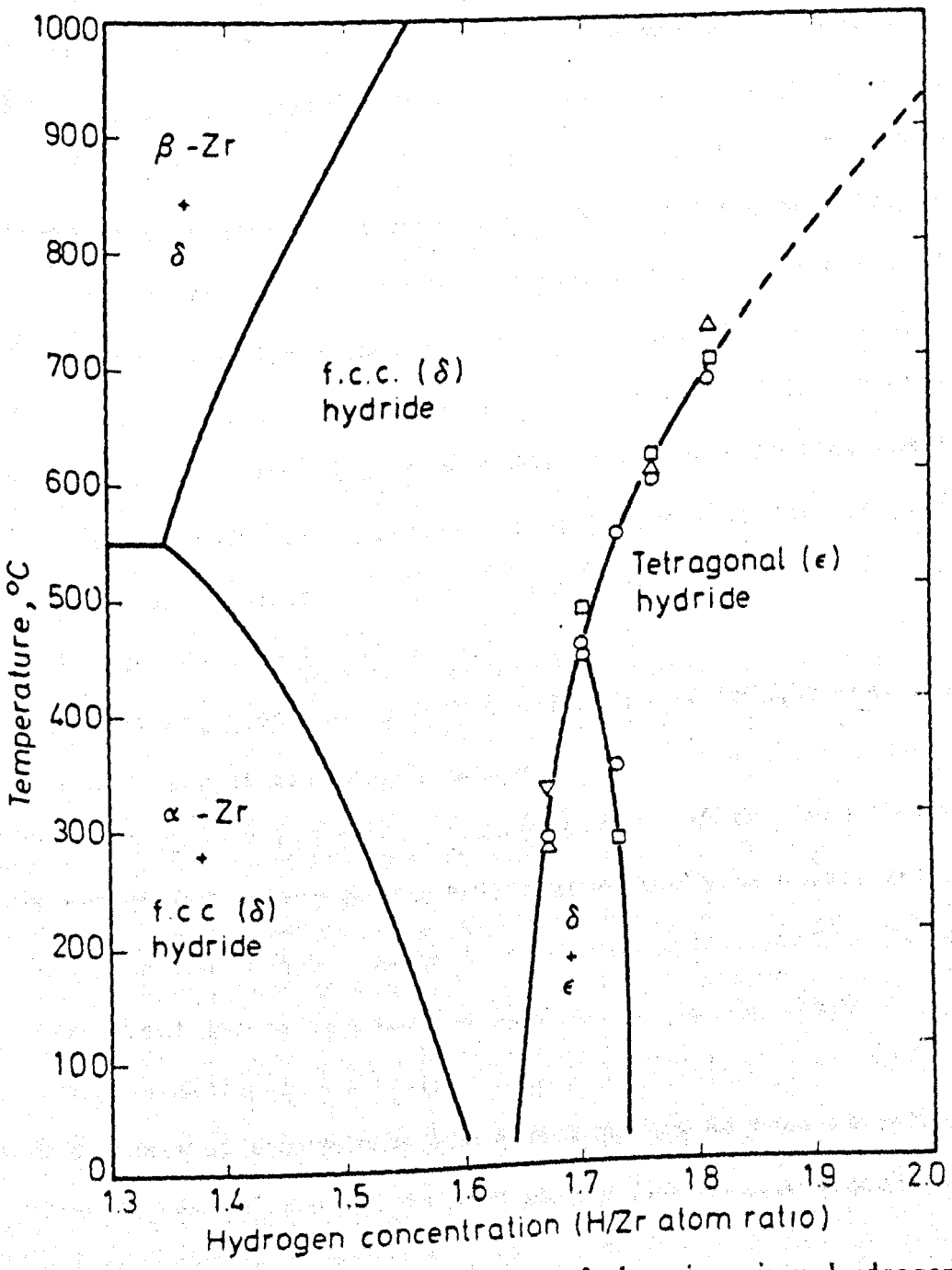

Figure 4-1 Partial phase diagram of the zirconium-hydrogen system. (From Moore and Young , by courtesy of the North Holland Publishing Co.)

increase will give lattice expansion and a reduction in the tetragonality ($^{c}/_{a}$) for a particular composition in the F.C.T. hydride phase. Generally lattice expansion can shift the Fermi level to a higher energy. Reduction of tetragonality shifts the electron states corresponding to d_z^2 electron lobes to higher energy, and consequently the Fermi level will shift to higher energy. The effect of tetragonal change could be very much larger than lattice expansion. The temperature increase can gradually shift the Fermi level to higher energy and depopulate the d_z^2 electron lobes. Therefore at a certain temperature the d_z^2 electron lobes become vacant so above this temperature (known as transition temperature) the F.C.T. structure is unstable. It is obvious from the above discussion that the transition temperature is a strong function of tetragonality and therefore is a function of composition. In other words, the transition temperature will increase with composition.

Further, from the above discussion it is obvious that the extension of F.C.T. structure along both dimensions of the phase diagram depends on the amount of electrons in the d-band. If the amount of electrons is relatively high then the F.C.T. structure will exist even at low concentrations and be stable even at high temperature. The number of d-electrons can be increased either by adding high valency metal atoms such as vanadium or by lowering the d-band relative to other bands as in the case of zirconium. In zirconium the 4d band is relatively lower in energy than the 5s band due to the smaller screening by the inner 3d-electrons.

The above suggestion from our model is in agreement with the observed boundaries of the F.C.T. structure for Zr/H and TiV/H systems (Moore et al., 1968; Nagel et al., 1975) Zr belongs to the same chemical group as Ti. For comparison the high composition part of the phase diagram of the Zr/H system is given in figure 4.1. It is obvious from

the figure that the transition temperature gradually increases with composition even to more than 1000°C for Zr/H system so we can expect a similar nature for the titanium hydrogen system. Therefore our estimation for the transition temperature of 120°C (see Appendix E) for TiH_2 [which is relatively higher than previous values (37°C)] is reasonable.

Further the band structure calculations of Switendick's and Kulikov et al. (see section 3.2) are in agreement with our estimation of 190 meV for the Fermi level drop when F.C.C. TiH_2 deformed into F.C.T. TiH_2 at room temperature (see the extrapolation in figure 4.h).

We can also estimate a value for the ionization of hydrogen in F.C.C. hydride, from our data and with assumption of rigid band approximation. The detailed estimation is given in the appendix F. The small estimated value (0.14e) compared to Switendick's (1976) calculated value for ionization of hydrogen in F.C.C. hydride, which is 0.425e, indicates our rigid band approximation is wrong. Further Switendick's (1976) band structure calculations indicate that during the hydride formation the metal's electron states, especially those of a free electron nature, are reduced in energy by even 5 eV. Therefore in addition to the previously considered higher energy states these lowered electron states - N_2 also become filled by the electrons from hydrogen after ionization. Consequently the real amount of ionization is greater than we calculated for the electron states - N_1. This explanation is qualitatively in agreement with a higher value of ionization as given by Switendick for $(N_1 + N_2)$.

f) Resistance variation and the model

Now we will see from our model how we can account for the variation of resistance with atomic ratio. In the first instance, the large drop of resistance in the mixed phase ($\alpha + \gamma$) and the constant resistance value for the single phase (γ) of the Ti/H system suggest that, the

structural transition (H.C.P.-F.C.C.) is the major process controlling the resistance variation during the formation of hydride. But the information given in table 4.5 shows (in the case of Ce) 30% drop of resistance even without any structural transition. Therefore the structural transition is not the only reason for a resistance drop. However, a higher percentage drop of resistance (than Ce) in the case of all other metals (except Ti, Yb and Pd) indicates that a structural transition has a reasonable effect. The possible next major factor is the nature of the conduction band which is formed during the hydride formation. As we discussed previously, the new band has a more free-electron nature, therefore this will give an increase of conductivity. This could be the reason for the higher conductivity of CeH_2 than Ce. But in the case of the Ti/H system this process is common for both mixed ($\alpha + \gamma$) and single (γ) phases. If there is no other process, especially in the single phase of F.C.C. titanium hydride, then we can expect a resistance drop even in the single phase (γ). But it is not observed experimentally, in contrast a more or less constant resistance is observed in this phase. This suggests the existence of some other processes which have the opposite effect on resistance variation, so that the net variation of resistance with atomic ratio is negligible. Other possible processes are s-d scattering of conducting electrons, and the effect of lattice expansion, especially on the band overlap.

The effect of s-d scattering depends on the position of the Fermi level. This could have a reasonably large effect for titanium hydride, because the Fermi level lies near the maximum of the density of states of the d-band. Both these processes will give an increase of resistance and also are common for both phases. The effect of these processes could be the reason for the relatively smaller drop of resistance for the Ti/H system than for other metal/hydrogen systems

given in table 4.5. Further Pd, and Yb show resistance increases during the hydride formation which suggests that, in addition to above factors already discussed, the vacant electron state in the conduction band is also an important factor. In the case of the titanium/hydrogen system plenty of electron states in the conduction band are unfilled. Therefore there would not be any effect due to this "hole" factor in the case of the Ti/H system.

Tenatively we can conclude that the resistance drop in the mixed phase is predominantly due to structural transition and the net effect of other processes (which are lattice expansion, s-d scattering and modification of conduction band) is negligible. This is the reason for the negligible resistance change in the F.C.C. single hydride phase. Further, the proposed effect due to the variation of non-isotropic conductivity in section 3.4(a) could be very small and may be the reason for the slight variation of the total drop of resistance between the different films.

Metal	Structure of Metal	Structure of hydride (MH_2)	$\approx \Delta R/R_0$	Refs.
La	Hex	F.C.C.	- 65%	a
Nd	Hex	F.C.C.	- 60	a
Er	H.C.P.	F.C.C.	- 80-75	a, b
Gd	H.C.P.	F.C.C.	- 52	a
Ho	H.C.P.	F.C.C.	- 76	a
Y	H.C.P.	F.C.C.	- 70	c
Sc	H.C.P.	F.C.C.	- 70	d, g
Ti	H.C.P.	F.C.C.	- 30	e
Ce	F.C.C.	F.C.C.	- 30	a
Yb	F.C.C.	orthorhombic	+ 2050	a
Pd*	F.C.C.	F.C.C.	+ 901	f
Zr	H.C.P.	F.C.C.	- 55	g

Table 4.5

* For monohydride

a - R. C. Heckman. Report (1969) SC-RR-69-571.
b - J. Müller and N. A. Surplice. J. Phys. D. 1977.
c - A. E. Curzon and O. Singh. Thin solid films 57 (1979) 157.
d - Savin, W. I, Markin, VYa, Mychlovskii, Vu. G.
e - This work.
f - R. J. Smith, D. A. Otlerson. J. Phy. Chem. sol. 31 (1970) 187.
g - to be published (Kandasamy, K. and Surplice, N. A.).

Now we will consider the variation of resistance in the F.C.T. phase (γ') of Ti/H system. As we have proposed, modification of the conduction band and changes in the amount of s-d scattering can affect the resistance variation. Structural deformation (F.C.C. → F.C.T.) is small and continuous, and can increase the overlap of bands in some direction but can reduce it in some other direction. Therefore we can say that its net effect is small. However the deformation brings the Fermi level to a position at which the density of states is low. This can reduce the probability of scattering of a conduction electron into a localized electron (i.e. s-d scattering) and this can drop the resistance. Therefore the conductivity increase in the γ' phase is mostly due to the reduction of s-d scattering.

In conclusion of this chapter, the hydrides of titanium are better conductors than titanium metal. The diffusion of hydrogen in the titanium lattice is considerably faster than the diffusion of hydrogen in titanium hydride. The dissociation pressure of titanium hydride is relatively large ($\sim 10^{-3}$ torr) at room temperature. The position of the Fermi level shifts to higher energy during the formation of titanium hydrides. The structural transition from F.C.C. to F.C.T. lowers the Fermi level. In F.C.T. titanium hydride the Fermi level lies in the decreasing part of the density of states curve. The determination of chemical phase boundaries of metal hydrogen systems from $\Delta\phi$ is quite possible if the behaviour of the parameters (such as lattice constant) which affect the position of the Fermi level are known.

CHAPTER 5

Titanium - oxygen study

5.1 Metal - oxygen system:

The interaction of oxygen with metal surfaces (i.e. oxidation) is a very complicated subject and much literature about it is available. A review of the subject was given by Lawless (1974). However present ideas about the physical processes which are involved in oxidation are often debatable. Oxygen unlike hydrogen, has a low rate of diffusion in most metal lattices and a strong interaction with metal surfaces, which often creates experimental problems in trying to perform well defined studies. However most of the techniques of surface science have been used. As with hydrogen, the different states of interaction of oxygen with metal surfaces can be classified as adsorption, solution and compound formation; but unlike hydrogen, identification of these stages for most metals is very difficult. However an initial fast interaction and a final slow interaction are observable. Generally adsorption is the precursor state of oxygen interaction with a metal. Chemisorption of oxygen is thermodynamically possible on all metal surfaces except gold. Generally chemisorbed oxygen can take the form either O^- or O_2^- or O^{2-}. However near room temperature dissociative chemisorption of oxygen is most probable and in most cases it is believed that there is partial ionization of oxygen on chemisorption. This initial process is very sensitive to the condition of the metal surface and the nature of the crystal faces. The interaction of oxygen can end with the adsorption process if the activation energy for adsorption or bulk compound formation is too high (e.g. Mo, W, Pt, Pd).

In most metals the surface structures that are formed as a result of oxygen adsorption lead to a rearrangement of the surface atoms. In

the published literature two commonly proposed mechanisms for this rearrangement are place exchange, and reconstruction of the metal surface. Place exchange involves the interchange of metal and oxygen atoms; the energy for this process was considered to be derived from the heat of adsorption, and the idea was based on the minimization of surface dipole-dipole interaction. Generally all the metal oxides are interstitial alloys, so we can say that the interstitial positions for oxygen in metal lattices are more energetically favourable than the substitutional positions. But place exchange will leave the oxygen in substitutional positions in metal lattice, therefore in this respect place exchange processes are less favourable. Further in the past literature we meet several different working hypotheses for the place exchange mechanism (Hall et al. 1971, Kirk et al. 1968, Simmons et al. 1967, Eley et al. 1960) but they only explain temporarily some particular result which was observed by their authors. Therefore the general validity of this mechanism is debatable.

The reconstruction idea is based on the principle that a reconstructed surface is thermodynamically more stable than unperturbed surface. Reconstruction involves movement of metal atoms laterally or longitudinally. Generally the solubility of oxygen atoms in most metal lattices is very small (few PPM). During chemisorption some oxygen atoms can penetrate the top layer of the metal surface, so the amount of penetrated oxygen atoms can easily exceed the solubility limit in the top few layers of the metal (perhaps in first two layers), and therefore precipitation of a metal oxide or suboxide is possible in these surface patches. This new oxide compound will generally have a different crystal structure, which could be a distorted one due to the influence of the underlying massive metal. So the reconstruction of the surface layer could be the manifestation of compound formation in the surface region.

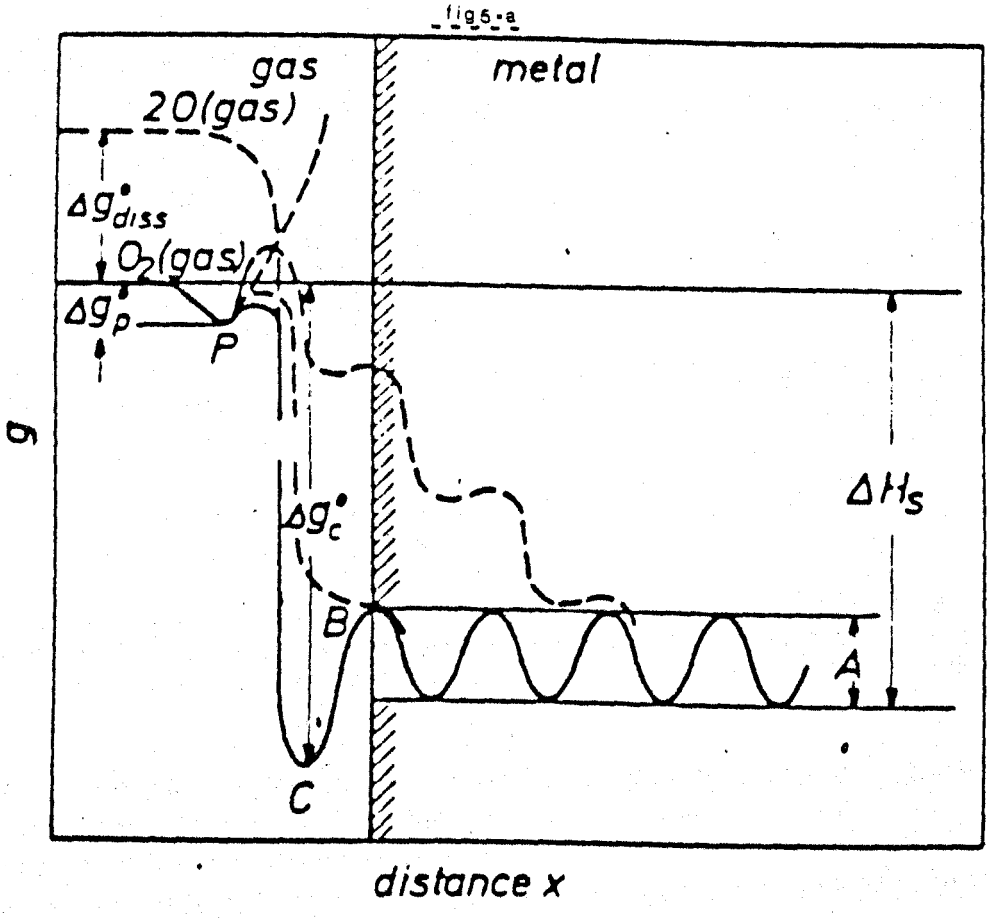

Free energy vs. distance diagram and reaction path in sorption systems

The sticking coefficient of oxygen on most metal surfaces is unity, and constant up to the adsorption of several monolayer equivalents (Fromm 1977). Fromm (1977) has proposed a model for the sorption of oxygen by metals, which is given in the fig. 5.a and his phenomenology is as follows, metal surfaces have two types of adsorption sites (1) with energy (Δg_c) lower than the energy of bulk adsorption - (ΔH_s) (2) absorption sites with energy (Δg_c) greater than the energy of the surface barrier (ΔH_s-A) (see fig. 5.a). Therefore the dissociative chemisorption of oxygen on the 2nd type of site leads to the penetration of oxygen atoms into the bulk interstitial sites. He further suggested that the energy of the second type of adsorption sites will increase with the amount of adsorbed atoms, and reach the energy of dissociation. At this state the surface becomes saturated. In other words, we can say that at the later state of adsorption, dissociative chemisorption of oxygen on the metastable surface sites can lead to the penetration of oxygen into the bulk, even without any thermal activation. The degree of penetration depends on the metal and the crystal face of the surface. The energy of the metastable adsorption state will increase with adsorption and will reach a situation at which further dissociative adsorption of oxygen is replaced by molecular adsorption. Delchar et al. (1967) have suggested that the electrostatic repulsion between the adatoms accounts for the observed low activation energy for the penetration of oxygen into Ni surfaces. Further in their study they have concluded that the chemisorbed oxygen atom bonded covalently so the effective radius of oxygen for penetration is its covalent radius which is 0.66Å. Gallagher et al.(1979) have pointed out that when oxygen is chemisorbed significant amount of the oxygen 2p electron weight is on neighbouring metal -Ni atoms and the effective radius for the penetration is that of the remaining oxygen

core which is comparatively small. Therefore we can conclude that the penetration of oxygen atoms into the metal is not impossible but depends on the nature of the surface barrier, on the amount of ionization of chemisorbed oxygen and the size of interstitial region.

Measurements of the changes of the work function and resistance of metals during their interaction with oxygen have been very helpful for understanding oxidation processes (Colmenares 1975). Oxidation can also be studied by observing changes in L.E.E.D. pattern, and changes in secondary electron spectrum of the metal (A.E.S., U.P.S., X.P.S.). Measurements of work function (ϕ) changes have been widely used. An increase of ϕ during the interaction of oxygen is generally interpreted as due to chemisorption of oxygen on the metal surface. A decrease of ϕ is generally believed to be due to incorporation of oxygen atoms in the metal (Hofmann et al. 1979, Gerwinner et al. 1978, Lawless 1974, Roberts 1970). The word "incorporation" as used in the literature seems to have several meanings; e.g. diffusion of oxygen from surface to bulk, or from one site to another site with reduction of ϕ, or chemisorption at deeper sites, or shortening of the metal-oxygen bond. The ambiguous use of this word often makes complications, therefore in this thesis its usage is generally avoided.

In many cases (e.g. Mo(100), Al(111), Ta(110) Nb(110), Er(Poly) etc.) a drop of ϕ was observed at the start of oxygen adsorption (for low exposure). Different types of explanation were given by various workers for this drop. Klemperer (1962) explained it on the basis of oxygen atom being pulled into the metal surface. Brearley et al. (1977) assumed it was due to the chemisorption of oxygen atoms in the deeper surface sites. Hofmann et al. (1979) have suggested it was due to the penetration of oxygen atoms to the immediate subsurface region. However one thing clear is that an initial drop of ϕ is a possible phenomenon

for an oxygen-metal system. Fehrs et al. (1967) found that this state is stable against a high temperature flash for the Ta(110)/O_2 system. But Hofmann et al. (1979) observed the reversal of this effect (i.e. increase of ϕ) when the oxygen supply for Al(111) was stopped. The reason for this observation is not well understood.

Moderate exposures of oxygen on many metal surfaces (Al, Nb, Ta, Fe, Co, Mn, Ni, W, Pt, Pd, etc.) gave increases of ϕ and these were generally interpreted as due to the chemisorption of oxygen in the electronegative form. Different rates of increase of ϕ with exposure were observed for different crystal surfaces of Cu (Delchar 1971). For some metals (e.g. W, Pt, Rh) the work function increase was stable (Lawless 1974) but it was unstable for others (e.g. Er, Ni). Stopping the oxygen supply to the surface of these latter metals gives a decay of ϕ in this region (Brearley et al. 1977, Roberts 1970). Further for large exposures some metals (Cu, Ni, Fe, Co, Mn, Al, Th, etc.) showed a drop of ϕ after an initial increase. Different ideas were proposed by different workers for this type of drop. For Cu/O_2 system Benndrof et al (1978) suggested that reconstruction or "incorporation" was the reason for the drop of ϕ. Hall et al. (1971) in their work on Co/O_2 and Mn/O_2 systems have suggested that penetration of oxygen atoms below the surface was the reason for this drop. However the formation of oxide has been suggested as the reason for Th/O_2 system by Riviere (1965), for Fe/O_2 system by Brucker et al. (1976), for Ni/O_2 system by Krishnan et al. (1976) Benndrof et al (1980) and for Al/O_2 system by Hofmann et al. (1979). On the basis of the phase diagrams, the formation of oxide at least within the top few layers, seems to be the most likely reason for this change of sign of the work function variation. The formation of oxide is in most cases accompanied by a structural change therefore the reconstruction idea also supports

the formation of oxide, since reconstruction is some form of structural change.

Only a limited amount of literature is available for resistance changes due to the interaction of oxygen with metal surfaces. In addition to the uncertainty about the physical processes which are involved in oxygen adsorption, there are uncertainties in the theoretical interpretation of resistance variations during gas adsorption which hinders an understanding of these studies. Generally, the sorption of oxygen by a metal increases the electrical resistance. Reasons such as a reduction of the number of conducting electrons of the metal due to their participation in the chemisorption bond, a demetalization of the top few layers of metal sample, changes in the scattering properties of the surface on adsorption, and effects due to the adsorption of oxygen in grain boundaries, have all been proposed to account for resistance changes due to the sorption of oxygen (Murgulescu et al. 1971, Blinakov et al. 1972). Singh et al (1974) have suggested the effect of changes in the geometrical parameters of films for the resistance change of Er films on oxygen adsorption. Surplice et al. (1975) have proposed a columnar model for metals that is only about a monolayer of oxygen atoms, however this model does not explain all the properties of the clean metal. A sudden step-type increase of film resistance on the introduction of oxygen doses was observed for Er and Ti (Singh 1971) and for Ag (Murgulescu et al. 1966). Further Murgulescu et al. (1966) have observed an increase in the percentage change of resistance when the adsorption temperature increased. A change of slope of resistance versus dosage was observed for Al/O_2 by Huber et al. (1966). At present the explanation for the variation of resistance during oxygen sorption stands unresolved, and a new model is needed for the general explanation of the subject.

L.E.E.D. studies in this field are numerous but the predictions are still doubtful due to the lack of theoretical knowledge. Widely observed experimental features due to the interaction of oxygen with metal surfaces are differently ordered L.E.E.D. structures, and a reduction in intensity of the L.E.E.D. pattern of clean metal surfaces. However different explanations for these features were given by different workers. Further Hopkins et al. (1971) have mentioned that L.E.E.D. studies are not able to detect the physisorbed state of oxygen because of the desorption effect of the L.E.E.D. beam. A recent study of Martinson et al. (1979) for Al crystal faces indicated the different behaviour of these faces ((111), (110), (100)) for oxygen adsorption. In conclusion, even in the lack of a complete theory L.E.E.D. studies have indicated the different states of oxygen interaction with a metal and their dependence on temperature and on the crystal face.

In recent years spectroscopic studies such as X.P.S, S.X.A.P.S, A.E.S and S.I.M.S have also become widely used in this field. Because of their high sensitivity for surface effects, these techniques are often preferred but they do not yet seem to distinguish unambiguously between the different states of oxygen in the metal lattice. Their identification of the characteristics of oxygen interaction with metals basically depends on the chemical shift which is observed, by these techniques. There are some doubts about the relative contribution to the observed shift from the chemical environment and from relaxation processes, which creates some difficulty in the determination of chemical structures (Martinson 1979). Further Hofmann et al. (1979) have mentioned that there would not be any difference in the chemical shifts due to the position of oxygen above the surface layer (chemisorbed state) or below the surface layer at interstitial positions (e.g. dissolved state) Recently Joyner et al. (1979a) have said these

techniques can only reveal information about a surface which is in equilibrium with low pressure gas and it is not feasible to make time-continuous studies. For high pressure studies two-chamber systems are commonly used but these systems can easily cause the loss of any weakly sorbed oxygen. However recently some special high pressure versions of the X.P.S technique has been developed by Joyner et al. (1979b). Generally like other studies S.I.M.S also indicates different states of interaction of oxygen but the lack of theory prevents conclusive explanation. In conclusion the interpretation of the electronic processes which are involved in oxidation needs a good theoretical understanding of these spectroscopies and a combination of several techniques such as X.P.S S.I.M.S and $\Delta\phi$ measurement.

Finally it is a general belief that at low pressures, isolated nuclei of oxide form randomly on the surface of the metal and the growth of oxide expands into other parts of metal. However, the nature of this process is not well understood. There are a number of theories which have been proposed to explain oxide growth (Cabrera and Mott 1949, Uhliq 1956). Generally these theories are too simple for the real situation. In recent years the effects on oxide formation of defects, dislocations, grain boundaries and solution of oxygen have been receiving attention. The solubility of oxygen in different metal lattices varies from a negligible amount to as high as 30 at %. The phase diagram of many metal-oxygen systems in unknown. Further the electrical properties of most metal oxides are complicated and very sensitive to defects, vacancies and temperature. Most of the oxides of transition metals are semi-conductors at intermediate temperature but metallic at high temperature.

In conclusion the physical processes which are involved in the interaction of oxygen with metals are not yet well understood. Combined studies using several experimental techniques will probably be necessary

to provide sufficient data before an adequate theory of oxidation can be developed. However the metal Ti which is being studied in this thesis is one of a few metals which sorb comparatively large amounts of oxygen. So for the oxidation of Ti films it is important to know the O/Ti phase diagram.

5.2 Titanium - oxygen system

A large number of studies using a variety of techniques have been conducted for this system, because of its importance in electronics, optics and refractories. However most of them are not comparable with our work because of the nature of the experiment. Some of them were conducted at high temperature and in some of them the specimens were prepared by either evaporating the metal in an oxygen atmosphere or evaporating samples of oxide. Further room temperature studies can be divided into two groups which are (1) specimens prepared at room temperature and (2) specimens prepared at high temperature. These two groups differ remarkably because of the distribution of oxygen in the metal lattice which greatly depends on the oxygen diffusion rate and in turn on the method of preparation. Therefore a critical consideration of these factors, along with the limits of detection of the techniques, are very important for a clear understanding of the physical processes which are involved in the oxidation of titanium. The studies with specimens prepared at high temperature may be able to resolve the physical nature of the different phases of titanium-oxygen alloys. The O/Ti system at room temperature has numerous phases which have been revealed by X-ray and neutron crystallography of bulk samples. There are several types of solutions for atomic ratios r (= O/Ti) from 0 to 0.5, and solid oxide phases for $r > 0.5$ (Andersson et al. 1957, Holmberg 1962, Yamaguchi et al. 1966, Wahlbeck and Gilles 1966, Arai

fig 5-b

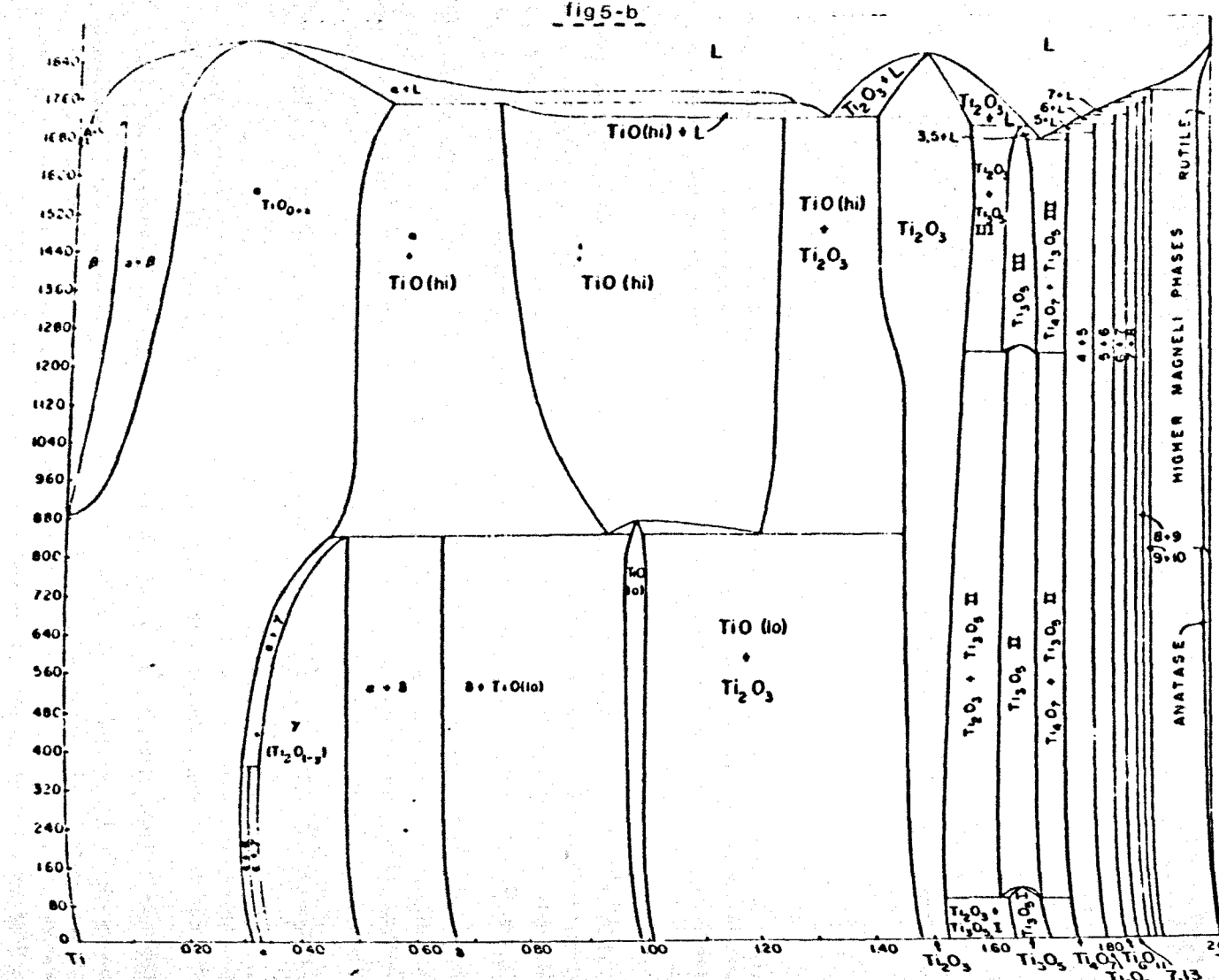
L
α+L
TiO(hi) + L
Ti2O3 + L
3.5+L
7+L
6+L
5+L
β
α+β
TiO(hi)
TiO (hi)
TiO (hi) + Ti2O3
Ti2O3
Ti3O5 II
Ti4O7 + Ti3O5 II
4+5
5.6
6.7
7.8
8+9
9+10
HIGHER MAGNELI PHASES
RUTILE
ANATASE
α+γ
γ (Ti2O3-y)
α+β
β + TiO(lo)
TiO (lo) + Ti2O3
Ti4O7 + Ti3O5 II
Ti3O5 II
Ti3O5 I
Ti
020
040
060
080
100
120
140
160
180
200
Ti2O3
Ti3O5
Ti4O7
Ti6O11
Ti5O9
7.13
TiO2

and Hirabayashi 1976, Geraghty et al. 1977). The low temperature part of the phase diagram was reported by Roy et al. (1972), which is shown in the fig. 5.b. Wells (1975) has mentioned that H.C.P. titanium takes oxygen up to r = 0.5 in three distinct phases; A random solid solution phase followed by two ordered structural phases, with preferential occupancy of certain octahedral interstitial positions in the lattice of oxygen. Beyond this composition the H.C.P. structure of titanium breaks down and oxide of the structure of ε - TaN will form in the range $Ti\,O_{0.68}$ - $Ti_{0.75}$ at low pressure and at low temperature (< 900°C) (Wells 1975). Obviously this oxide structure is deficient in oxygen, however Libowitz (1965) pointed out that titanium deficiencies are more stable at low temperatures. This is followed by a wide ranging phase of TiO with NaCl structure, at low temperature. Every sixth site of each type of ion is unoccupied in this defect structure. These phases are followed by Ti_2O_3 with a corundum structure, at ordinary temperature (< 200°C). Then Ti_3O_5 and no fewer than seven distinct phases of type $Ti_n\,O_{2n-1}$ (n = 4 .. 10) are observed in the range $TiO_{1.75}$-$TiO_{1.9}$. There are three forms of TiO_2 (rutile, brookite, anatase) known, but anatase is the stable form at low temperature (Wells 1975). Further TiO_2 is a white compound but Ti_2O_3 is black.

Now we will consider some physical properties which are observed in the case of oxide specimens which are prepared at high temperature, so these specimens may be considered as having a uniform composition all through. The composition range from r = 0 to 0.5 is the most investigated portion of this system; electron, neutron and x-ray diffraction works showed that the lattice parameters a,c and ratio c/a of H.C.P. titanium increases with composition up to r = 0.5 (Yamaguchi 1969) and oxygen occupies octahedral interstitial sites (Yamaguchi et al. 1970). Resistivity measurements (Arai et al. 1976, Filion et al. 1975,

Wasilewski 1962, Pearson 1958) were all in agreement about the increase of resistivity in the composition range r = 0 - 0.3. Filion et al. 1975 showed that at room temperature the resistivity increases up to a composition r = 0.33 by 500% and then drops to the initial resistivity around the composition r = 0.5. The same feature was observed by Arai et al. (1976) at $4^{o}K$. Further they have explained that the increase of resistivity is due to the scattering of conducting electrons by dissolved oxygen atoms, and the decrease of resistivity after r = 0.33 is due to the ordered arrangement of oxygen atoms in the titanium lattice. In the ordered structure oxygen atoms fill every octahedral site in every second layer of H.C.P. structure. Further Arai et al. (1976) work showed that at room temperature magnetic susceptibility decreases with composition in the range r = 0 - 0.5 and they concluded from this that the density of states at the Fermi level decreases with oxygen content. Further X.P.S work by some authors showed a gradual shift of Ti 2p and 3p peaks towards higher binding energy with increasing oxygen content, and this has been interpreted as a shift of energy levels of the metal core to higher energy. Pearson's (1958) studies have showed that the resistivity of TiO. is of the same order as the resistivity of the solid solution phase. Further his work indicated that the resistivity increases slowly with oxygen content within the composition range r = 0.7 - 1.2. This is in agreement with Bernus et al. (1972) study. Further their study showed that within the composition range r = 0.8 - 1.2 the lattice parameter slightly decreases with oxygen content. Also Ti_2O_3 is a P-type semiconductor at room temperature and TiO_2 is an insulator. Therefore from above results we can tentatively conclude that at room temperature the resistivity of the Ti/O alloy increases with oxygen content up to r = 0.33, then decreases (perhaps to just above the resistivity of pure titanium) to a minimum value between composition range r = 0.5 - 0.7, and

FIG 5-C

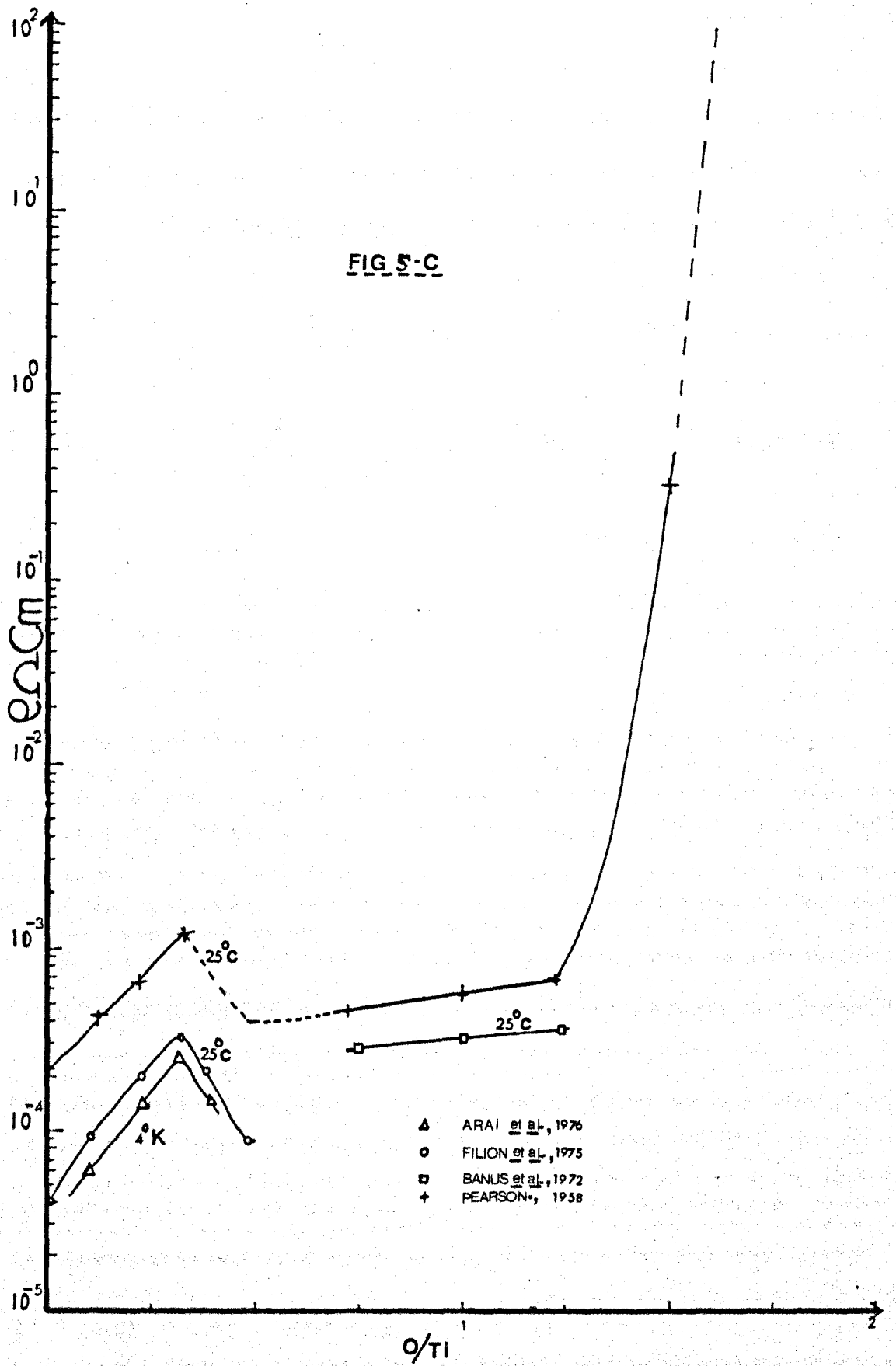
10^{2}
10^{1}
10^{0}
10^{-1}
10^{-2}
10^{-3}
10^{-4}
10^{-5}
Ωcm
25°C
25°C
25°C
4°K
ARAI et al., 1976
FILION et al., 1975
BANUS et al., 1972
PEARSON, 1958
1
2
O/TI

then increase of resistivity in the monooxide phase is slight, but beyond this the increase could be rapid (see some results in the fig. 5.c.)

Now we will consider sorption studies in which specimens were prepared at room temperature. It is well recognised that at room temperature and low pressure titanium sorbs several monolayers of oxygen (Lawless 1974). So under these conditions oxygen is chemisorbed dissociatively and diffuses into the bulk. This effect was recognised recently for titanium films (Fromm et al. 1978, Kameso et al. 1978, Müller 1977) and for a single crystal plane of (0001) (Fukuda et al. 1980). Further Duppel and Fromm (1976) have pointed out that the structure and orientation of Ti films does not play a major role in their oxidation. The sticking coefficient - S for oxygen on titanium films at room temperature is constant and nearly unity until the equivalent of more than ten monolayers have been sorbed (Fromm 1977). In all surface studies on Ti/O system, the formation of "oxide" (oxygen compound) has been suggested (Eastmann 1972, Bassett et al. 1973, Smith 1973, Müller et al. 1974, Nyberg 1975, Johansson et al. 1977, Porte et al. 1977, Shih et al. 1977, Dawson 1977, Fukuda et al. 1978, 1980 and Wall et al. 1980). However all these studies were not certain about the chemical nature of the oxygen compound and unable to distinguish between the different states of oxygen in the titanium lattice (which are solid solution or oxides such as Ti O, Ti_2O_3, Ti_3O_5 and Ti O_2) Generally, a fast interaction region defined as the chemisorption region was observed prior to "oxide" formation. The boundary between these two regions (i.e. chemisorption and "oxide" region) was indentified as about 10L exposure by Fukuda et al. (1978) from the observed changes in A.P.S and secondary electron yield, and by Andersson et al. (1975) from their S.X.A.P.S. It is noteworthy here that Fukuda et al. (1978) work function measurements indicated that the boundary (about 10L) corresponded to an increase of

ϕ about 300 - 400meV, but the total increase up to the constant ϕ value at 2000L is about 1.2eV. In a S.I.M.S experiment of Dawson (1977) this boundary was predicted at 3L, however his electron induced desorption studies indicated that the chemisorption region coexists with an "oxide" region - even at high exposures (> 50L). Benninghoven et al. (1978) have also suggested the coexistance of chemisorption and "oxide" phases from their S.I.M.S, A.E.S and X.P.S. study. Further there is a large range of scattered information given for the thickness of the oxygen compound (from $6A^{o}$ - $30A^{o}$) this could be due to the different limits of the technologies which were used in these surface studies (e.g. 10 - $15A^{o}$ for U.P.S, 15 - $25A^{o}$ for X.P.S (Henrish et al. 1978) and a relatively large value for ellipsometry) and experimental conditions such as pressure (e.g. pressure varies from 10^{-6} to 40 torr in these studies).

The formation of TiO, TiO_2 and another oxide (Ti_2O_3 or Ti_3O_5) were suggested by Porte et al. (1977), and in their work the films were exposed up to 40 torr oxygen. The formation of TiO_2 has also been suggested by Eastmann (1972) and Platau et al. (1977) but their films were only exposed to low pressure oxygen (perhaps < 10^{-4} torr). Further Eastmann (1972) found evidence for TiO_2 after an exposure of only 100L (1L = 10^{-6} torr sec) but Platau et al. (1977) work had not definitely found it even at 3000L exposure although they suggested the possibility of TiO_2 after 3000L. It is noteworthy here that in the recent U.P.S. experiment of Henrich et al. (1978) on vacuum fractured $TiO_{1.15}$, the specimens resembled TiO_2 only after an oxygen exposure of 10^{8}L. Bassett et al. have also mentioned that it was only after an exposure of 5×10^{5}L that the Auger spectrum of their titanium specimens resembled that of vacuum cleaved TiO_2. The microbalance experiments of Kasemo et al. (1978) showed very thin films (<$5A^{o}$) were only able to sorb oxygen up to a maximum (average) atomic ratio 1.5 (i.e. Ti_2O_3), however their thicker

films were able to sorb as much as 43 monolayers of oxygen after 5000L exposure. The transmission electron diffraction work by Stolz et al. (1974) indicated TiO was the most commonly formed "oxide" in their sorption experiment. Further Shih et al (1977) have also pointed out from their L.E.E.D and A.E.S. data that the "oxide" formed after an exposure of 100L on Ti (0001) is TiO not TiO_2. Further some interesting information in Shih et al. (1977) study was the change of slope of the plot, A.E.S. oxygen peak height Vs exposure, after the formation of ½ monolayer L.E.E.D pattern P(2 x 2) at about 1.2L. This is an indication for the dominancy of some new effect over chemisorption at this exposure 1.2L. This is also in agreement with other studies (Andersson et al. 1975, Fukuda et al 1978, Dawson 1977) which observed some changes at low exposures ($\sim$ 5L). These studies have suggested this change as the formation of "oxide". It is noteworthy here that the recent A.E.S study of Wall et al. (1980) on polycrystalline titanium agreed qualitatively very well with Shih et al. (1977) work on Ti(0001), however Wall et al. (1980) have suggested the formation of TiO only after 1000L. On account of all this information and the large solubility of oxygen in titanium (Lawless 1974) we can probably conclude that the new effect which gave changes in the observations at low exposures in all studies was the diffusion of oxygen into the bulk and its becoming soluble at octahedral interstitial sites.

Previously work function changes - $\Delta\phi$ due to the exposure of oxygen on titanium samples have been measured only at pressures < 10^{-3} torr. and exposure < 10^{-2} torr sec (10^4L) (Fukuda et al. 1978, Muller 1977, Brearley et al 1977, Smith 1973). Smith's work was conducted at 391°C, the others' work at room temperature. All works agree in the large increase of work function ϕ (> 1eV) due to the sorption of oxygen. At the start a small reduction of ϕ for low exposures was commonly observed

(Müller 1977, Brearley et al. 1977). At large exposures a decay of ϕ after each dose of oxygen was noticed by Müller (1977). The increase of ϕ was not monotonic at large exposures (Fukuda et al 1978, Müller 1977). Some interesting observation from Smith's study are (1) constant ϕ for long exposure time after a rapid initial increase at a particular pressure. (2) The amount of increase of ϕ increases with pressure and (3) the rate of change of ϕ with exposure also increases with pressure. These all indicate the attainment of a dynamical equilibrium between two processes, because they are all pressure dependent. Obviously one is chemisorption, and the other one is probably diffusion of oxygen atoms into the bulk. Further Fukuda et al. (1978) observed decrease of ϕ to the value for a clean titanium, but no change in the A.P.S spectrum of oxygen, when they heated the specimen up to 400°C after increasing ϕ up its maximum value. To explain this observation they suggested solution of oxygen into the bulk. Smith (1973) also observed a return of ϕ to the clean surface value from its high value due to oxygen exposure when he pumped out the oxygen above the film, but he suggested it was due to desorption of oxygen atoms. However it is appropriate to note here that the removal of chemisorbed oxygen from titanium is much more difficult even by ion bombardment (Dawson 1977).

Resistance measurements have previously been used in studies of the sorption of oxygen by titanium by Fehlner (1966), Kawasaki et al (1967), Singh et al (1974) and Lehoczky et al (1979). These workers observed a large increase of resistivity. Lehoczky et al (1979) have pointed out that the dominancy of anion diffusion (i.e. oxygen diffusion) in the oxidation of titanium is in agreement with previous workers Brennan et al. (1960) and Stevels (1957). Fehlner (1966) has observed a rapid initial resistance increase followed by rather slow increase. On the basis of this observation he separated the chemisorption regime with a fast increase

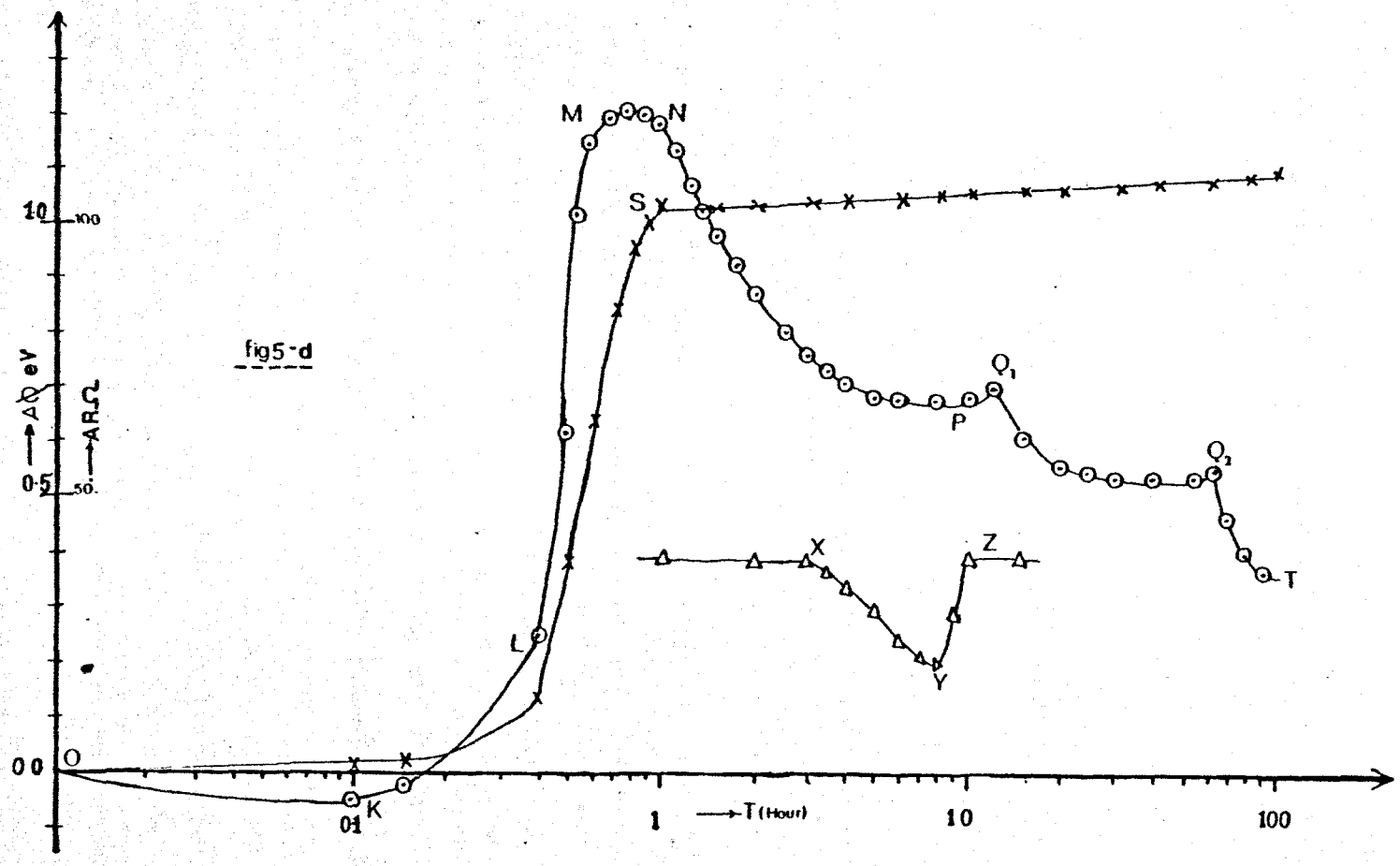
fig5-d
10
100
0·5
50
0·0
0·1
1
10
100
T (Hour)
ΔQ eV
ΔR Ω
O
K
L
M
N
S
P
Q1
Q2
T
X
Y
Z

of resistance from the oxide regime with a slow increase. Singh et al. (1974) have observed a sudden step type increase of resistance on the addition of an oxygen dose. Surplice et al (1975) have shown that the effect of oxygen in the grain boundaries was not an adequate explanation for the resistance increase due to oxygen interactions with titanium films.

From the above descriptions it is clear that the mechanism involved in the interaction oxygen is not straightforward. But there is definitely diffusion of oxygen beyond 15-25A^{o} thickness (range of detection limit of U.P.S and X.P.S) even at low exposures. Therefore the effect of interstitial oxygen, along with the nature of oxygen diffusion have become important parameters for consideration, and for explanation of experimental results. It is also obvious that the word "oxide" in surface science studies is rather flexible and in the past has been used for different purposes by various workers.

5.3 Results

The general pattern of the changes in work function ϕ and in film resistance R with time are shown for the continuous flow method in figure 5.d. Parts O.K.M and O.S correspond to the fast stage of the reaction. A very slow rate of flow of gas or a very small dose, reduced ϕ at point K to less than the work function of the clean film. The change of R near K was small, and not reproducible from film to film. Continuing at the same rate of flow soon produced a large increase in ϕ at L, and reproducible changes of R, and ϕ continued to increase up to its maximum value at M which was 1.0 ± 0.2eV greater than the work function of the clean film. The effect of addition of equal doses of gas at equal intervals is shown in fig. 5.e. Immediately after each dose ϕ and R increased rapidly during the short time taken for the oxygen pressure to fall to 10^{-9} torr, which was < 5 sec per dose up to points

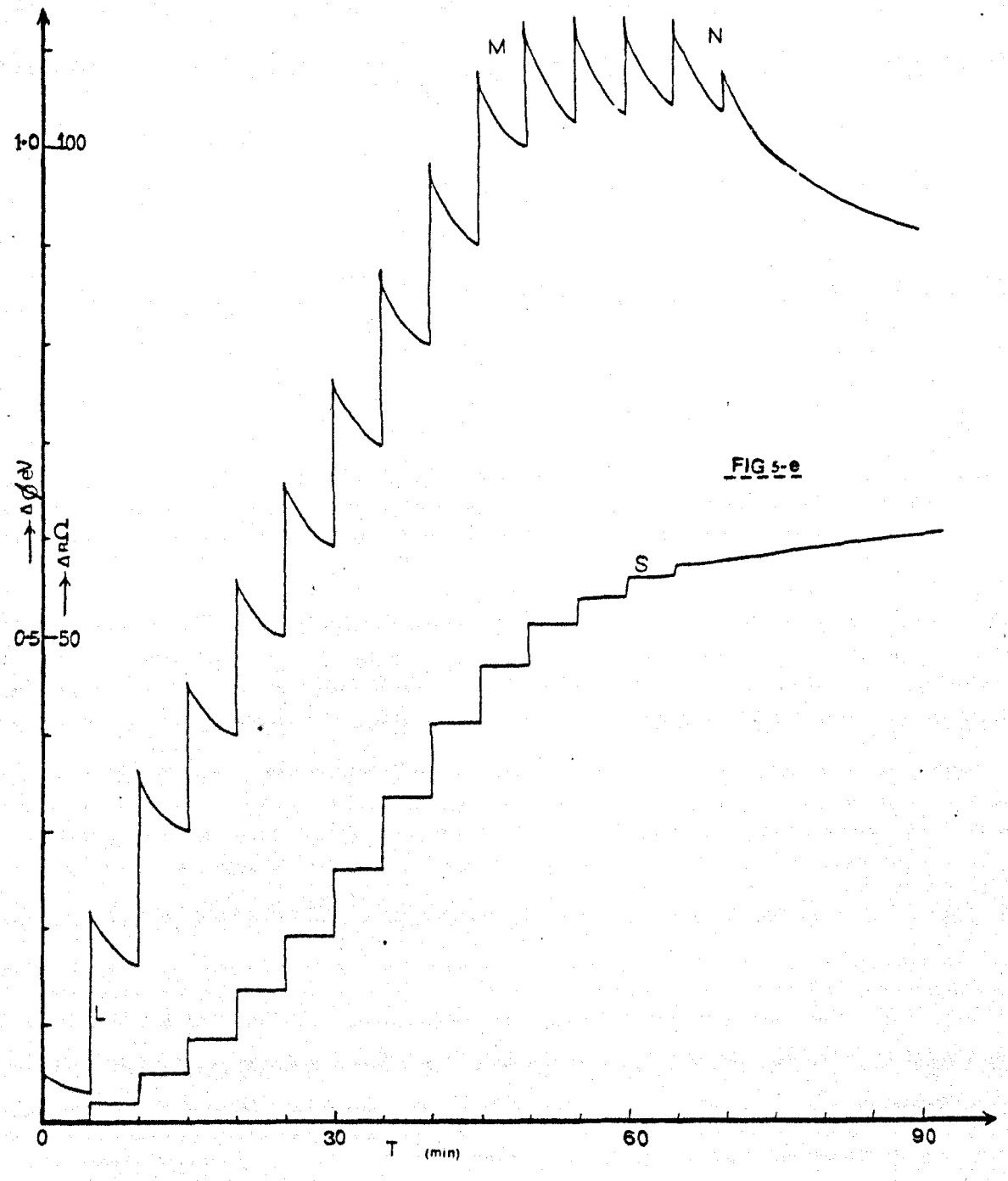

FIG 5-e

Table 5.1

Film	R_o	$\left(\frac{\Delta R_o}{R_o}\right)_M$	$\Delta\phi_M$ (meV)	T_M (min)	Q_M torr sec	$\Delta\phi_{MP}$ (meV)	$\Delta\phi_U$ (meV)	$\Delta\phi_V$ (meV)	P_{max} (torr)	Q_{EXPT} (10^5 torr sec)	T_{EXP} (hour)
Ti 46/3	505	6	1010	90	0.27	500	130	–	5	9.0	90
47/1	550	–	900	45	0.14	690	140	70	4_{-2}	3.0	86
48/2	500	–	1100	35	0.11	650	–	450	3×10^{-2}	0.14	130
48/3*	460	–	1020	120	0.40	>500	–	–	10^{-3}	–	10
48/4	400	15	1080	20	0.06	720	–	370	10	20	60
49/1	560	–	1020	6	0.02	600	250	–	5	7.5	48
50/1	550	–	1000	32	0.1	520	–	–	5	1.5	15
51/1	430	22	950	10	0.03	660	200	–	1	2.5	75
51/2	500	7	800	40	0.1	950	–	–	1	0.7	100
51/3*	410	4.0	800	60	0.2	>540	–	–	2×10^{-3}	–	5
51/4	300	3.0	1170	120	D	900	120,100	–	4_{-3}	10	110
52/1*	205	12	850	360	D	>500	–	–	10^{-3}	–	30
53/1*	505	14	1070	240	D	–	–	–	10^{-3}	–	5
53/2*	405	>12	>750	–	D	–	–	–	–	–	–
55/1*	575	>28	>550	–	D	–	–	–	–	–	–
55/2*	575	>28	>700	–	D	–	–	–	–	–	–
56/1*	520	37	820	120	D	>300	–	–	10^{-3}	–	15
59/2*	430	–	1010	90	D	–	–	–	–	–	–
60/2	490	27	945	30	0.1	>500	–	–	2×10^{-3}	–	2
60/3	400	12	1065	30	D	>300	–	–	2×10^{-3}		1
60/4	340	12	840	60	D	>300	–	–	10^{-3}		1
61/4	105	14	1220	105	D	–	–	–	–	–	–
62/2	180	21	1110	60	0.2	600	–	–	10^{-2}	–	2
62/3	–	–	1030	80	D	–	–	–	–	–	–
62/4	–	–	1040	13	0.04	–	–	–	–	–	–
72/1	145	45	860	20	0.06	–	–	–	–	–	–
74/3	440	23	1135	20	0.06	–	–	–	–	–	–

* Stopped halfway

For clarity see figs 5.d, 5.e, 5.f.

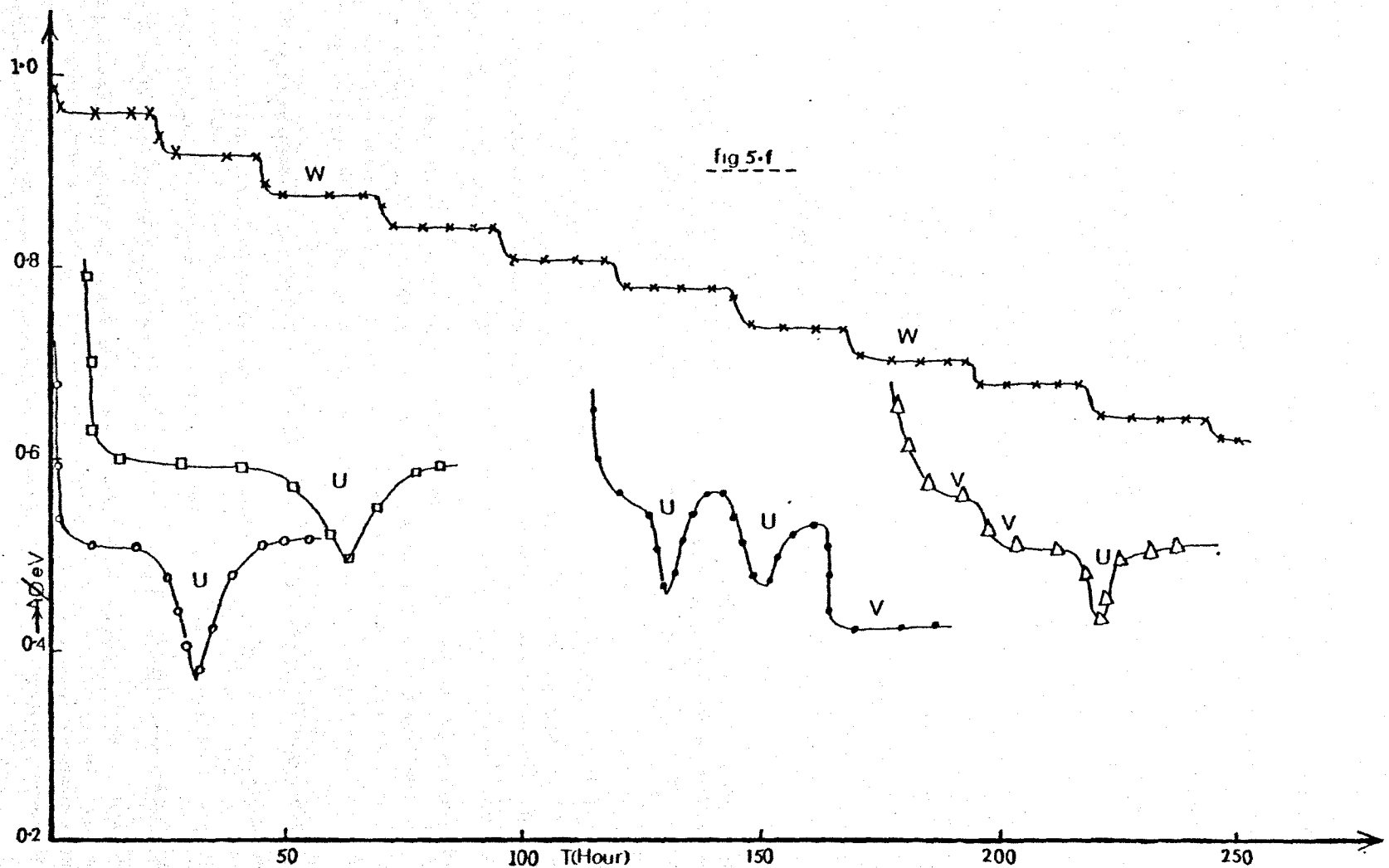

fig 5·1

M and S on the curves but lengthened to 60 sec per dose by point N. After each increase R stayed constant, but ϕ decreased slowly for several minutes to reach a new equilibrium value. The rapid increase of ϕ, its subsequent decrease, and its initial rate of decrease, were all greatest near M. The increment in R was usually greatest about half way between O and S.

At M the equilibrium pressure P_1 was about 10^{-4} torr (certainly 10^{-3}torr) and it was independent of the time taken to go from O to M (4 - 120 min). If the gas was added slowly to keep the pressure $P \leqslant P_1$ then ϕ stayed almost constant for a while from M to N, as in fig. 5.d. The subsequent decrease after N depended on having $P \geqslant 10^{-4}$ torr, independent of the total exposure to oxygen over the range 10^{-2} - 4 x 10^{-1} torr sec.

During the slow stage of the reaction which followed there was relatively little increase in R during many hours at $10^{-3} < P < 5$ torr, but ϕ decreased considerably under the same conditions. The rate of change of ϕ increased slightly with P and although the observed change at 10^{-4} torr was only 0.1eV in 2 days it is possible that it might have decreased by 0.5eV if we had waited long enough. When the pressure was kept approximately constant ϕ eventually approached asymtotically to a steady value at exposures $420 < q < 10^6$ torr sec. (points P and T fig. 5.d). However, if the pressure was suddenly increased as at points Q in fig. 5.d, there was slight temporary increase in ϕ before the slow decrease began again at a slightly faster rate.

There were several ways that ϕ of a particular film could change at high exposures (4.8 x 10^3 - 10^6 torr sec), as shown in fig. 5.f. The commonest type of change was a slow fall of $\sim$ 0.1eV followed by slow recovery which could be repeated, and is shown as U on the curves. Another common change was a permanent decrease V, of 0.1eV. For one film only there was a succession, W of smaller decreases which occurred at intervals

of 12 - 20 hours during 10 days. All three types of change occurred spontaneously whether the film was in daylight or darkness, so they were not due to photo desorption effects nor photoelectronic transitions in the oxide. Although it is possible that the Au reference electrode might slowly have adsorbed oxygen at 1 - 10 torr over 100 hours we feel sure that these comparatively rapid changes U, V, W were owing to changes in the Ti film. The contact potential difference between the Au and the oxidised Ti-film remained constant when the pressure was increased from 5 - 60 torr and left there for an hour. If the reaction chamber was evacuated before reaching N in an experiment this had no effect on ϕ. However, if it was evacuated after N, at X in fig. 5.d then ϕ was reduced by 0.1 - 0.2eV for as long as the film remained in vacuum, and if oxygen was re-admitted, as at Y, then ϕ returned to almost its pre-evacuation value. A summary of the experimental results are given in the table 5.1.

5.4 Discussion

The simplest explanation of our data can be given on the basis of the Ti/O phase diagram and possibility of oxygen diffusion into the titanium lattice. The penetration of oxygen to a great depth in the titanium lattice has been proposed by a large number of workers to account for their results obtained by various techniques. It is generally believed that the penetration of oxygen into the metal lattice occurs by place exchange (Lawless 1974). We found that up to the point S on the R-curve, the gas pressure fell rapidly to 10^{-9} torr after each dose, and the resistance increased rapidly after each dose then quickly became constant. So any exchange of places would have to happen in a few seconds; but if this is so then why does ϕ decay for a long time after the initial increase for each dose? The recent works of Kasemo et al 1978, Lohoczl et al. 1979 and Fukuda et al. 1978, 1980, also suggest that the place exchange

mechanism is not able to explain their results. We think that electrostatic repulsion between the oxygen atoms is the most likely driving force for the diffusion of oxygen atoms from surface sites to bulk, and from one interstitial site to another in the bulk. The detailed discussion will be given later in this chapter. Now we will assume that the oxygen atoms diffuse into the bulk after dissociative chemisorption on the surface. The presence of oxygen atoms in interstitial sites will lead to the formation of oxides (probably low oxides first) if the local concentration of oxygen exceeds the solubility limit. Generally precipitation of oxide is accompanied by a change in position of the Fermi level. This will reflect as a change of slope in the $\Delta\phi$ curve; so we believe that the slope change at N (fig. 5.d) corresponds to the start of oxide precipitation, at least in the patches at the top layers. The coincidence of N and S is reasonable. A corresponding change in the R curve is generally to be expected, one seems obvious from the given plot in the fig. 5.c, however, we do not believe that the variation of resistance beyond S is completely due to the precipitation of oxide, but we believe that it is the combined effect of oxide precipitation in the top layers and a rather slow rate of solution of oxygen in the lower layers of the film; we can see the merit of this statement now. A decrease in oxygen concentration across the film thickness is generally to be expected in a sorption experiment like ours because of the low rate of diffusion of oxygen in the metal lattice. Therefore it is obvious that in the top layers the oxygen concentration is greater than in low lying layers, so in those top layers the oxygen concentration will first exceed solubility limit and oxide start to precipitate (perhaps initially a low-oxide $\sim$ Ti O). When the surface patches become oxides generally, all the sorption mechanisms such as sticking rate and diffusion of oxygen into the bulk become different. We believe from our experiments that when this happens only a slow rate of

sorption takes place and a fraction of the sorbed oxygen stays in the top oxide layers and increases their concentration of oxygen or, in other words, gradually converts them to higher oxides such as Ti_2O_3, Ti_3O_5. The other fraction diffuses through the oxide layers and helps to thicken the oxide layers and to increase the extent of oxygen solution in the metal lattice. So now it is clear that the variation of R beyond S is a combined effect of oxide formation in the top layers and solution of oxygen in the lower layers.

Before S on the R-curve, the resistance increase is purely due to the solution of oxygen in the titanium lattice. The relatively large increase of resistance in this region is consistent with the possible large amount of scattering of conduction electrons by interstitial oxygen. There is a qualitatively similar resistance increase for a dose of oxygen on titanium and for a dose of hydrogen on titanium, scandium or erbium (in their solution phase). This also supports our conclusion that oxygen diffuses into the bulk and becomes soluble at the interstitial viods of titanium.

Now we will discuss the observed changes in ϕ. In the early stages the ϕ drop in the part OK on fig. 5.d corresponds to dissociative chemisorption of oxygen on the deep surface sites. The O adatoms would form dipoles with their negative poles away from metal, but it is generally accepted that such dipoles could reduce ϕ if they were in sufficiently deep hollows in the metal surface. A simple model for this effect is that the hollow should be deep enough to conceal a spherical adatom of covalent radius r but not one of radius 2r, where r is assumed to be the Friedel screening radius; and this suggests that ϕ could be reduced about 0.1eV by O adatoms in the pyramidal hollows with 5 nearest neighbours in Ti $(10\bar{1}1)$ (Surplice et al, 1978). Another possible hollow is the one with 4 nearest neighbours in the valleys in Ti $(1\bar{1}00)$.

For convenience we will call both types of hollow D sites. Adsorption on these two types of D sites would give a coverage of $^1/3$ of monolayer if the film surface consisted of equal areas of the 3 principal H.C.P. phases (0001, $1\bar{1}00$, $10\bar{1}1$). Müller (1977) found that ϕ was reduced by 120 meV by an oxygen coverage 0.5 monolayer on his Ti films. The small value of exposure ($^1/3$L) is in agreement with our observation that the observed drop of ϕ is for a small for a slow rate of flow of oxygen. Our proposal of chemisorption of oxygen on D sites at the early stage of exposure is consistent with the idea that high coordination sites are more attractive for chemisorption of gas atoms, since D sites are the high coordination sites in the principal planes (0001, $1\bar{1}00$, $10\bar{1}0$) of H.C.P. lattice. Small and non reproducible changes of R within this region are probably due to surface scattering effects and perhaps local annealing owing to the high heat of adsorption. So we think there is little or no penetration of O into the metal lattice in this region.

The comparatively large increase in R from the second dose of gas in fig.5.e and from L onwards in figs. 5.d and 5.e indicates a major fraction of the oxygen atoms diffuse into the bulk and they become scattering centres for conduction electrons. Generally if W_S is the surface potential and E_F is the position of the Fermi energy then the change in work function $\Delta\phi$ is given by $\Delta\phi = \Delta W_S + \Delta E_F$ (in energy units). The change of ϕ up to N (i.e. in solution phase) is mainly due to ΔW_S since ΔE_F due to lattice expansion (if any) in solution phase is usually small and negligible compared to ΔW_S. Then the initial increase of ϕ for each dose is due to adsorption of oxygen on the various surfaces, and the decay following this (fig. 5.d) is due to the rearrangement of adsorbed oxygen from initially adsorbed sites to energetically favourable sites, which have been left vacant by other oxygen atoms which have

diffused into the bulk at each dose. (A clear picture of this process will be given later). The same processes are effective up to N or a little beyond N, where the surface sites more or less become completely filled. After this, these processes become insensitive for a dose of usual size (10^{18} atoms). Comparison of our result with Müller's (1975) work shows that the oxygen atoms started to diffuse into the bulk even at low exposures about 1L. Shih et al. (1977) work also indicates that before 1L exposure oxygen atoms started to diffuse into the bulk from (0001) surface of H.C.P. Ti, since it was only after their crystal had been exposed to 1.2L of oxygen that they observed 1/4 monolayer L.E.E.D pattern, but titanium surfaces generally have sticking coefficient unity. Evidently oxygen diffuses into the bulk even at low exposures ($\leq$ 10L) and we believe that the observed changes within this range of exposure in some spectroscopic studies (Fukuda et al. 1978, Dawson 1977, Benninghoven et al. 1977 and Anderson et al. 1975) are due to the penetration of oxygen to form solution of oxygen atoms in the titanium lattice, not the formation of any oxide.

The significant experimental parameter at N is pressure, not the amount of oxygen exposure. This is obvious from the data given in the table 5.1. If the pressure rises above 10^{-4} torr patches of solid oxide start to precipitate in the surface layer. This does not mean that 10^{-4} torr is the pressure for the formation of oxide, i.e. it does not have any thermodynamical significance, but it is a pressure well able to create a dynamical situation in our experimental condition, in such a way that the oxygen concentration in the top layers exceeds the solubility limit. Therefore the work function change after N is mainly due to ΔE_F. The gradual drop in ϕ of over 600meV is therefore due to the conversion of metal patches into oxide patches (perhaps lower oxide patches), within the depth-detection limit of the Kelvin

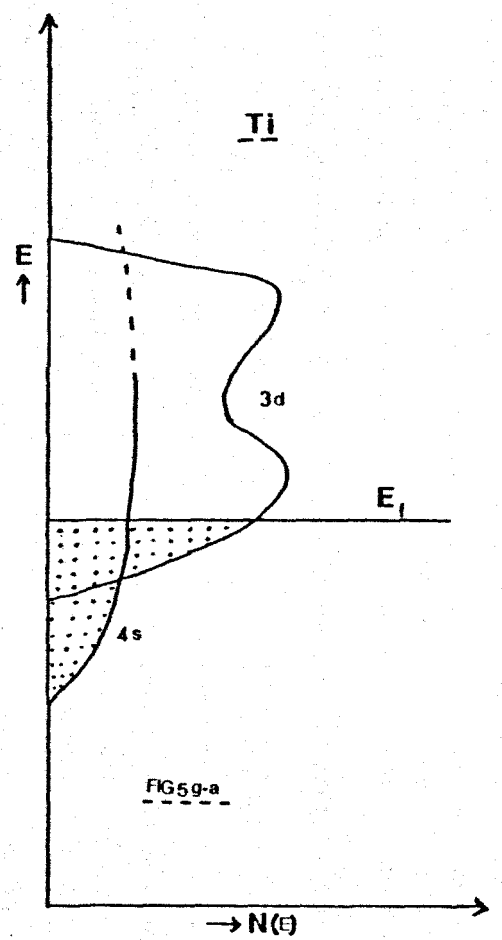

FIG5g-a

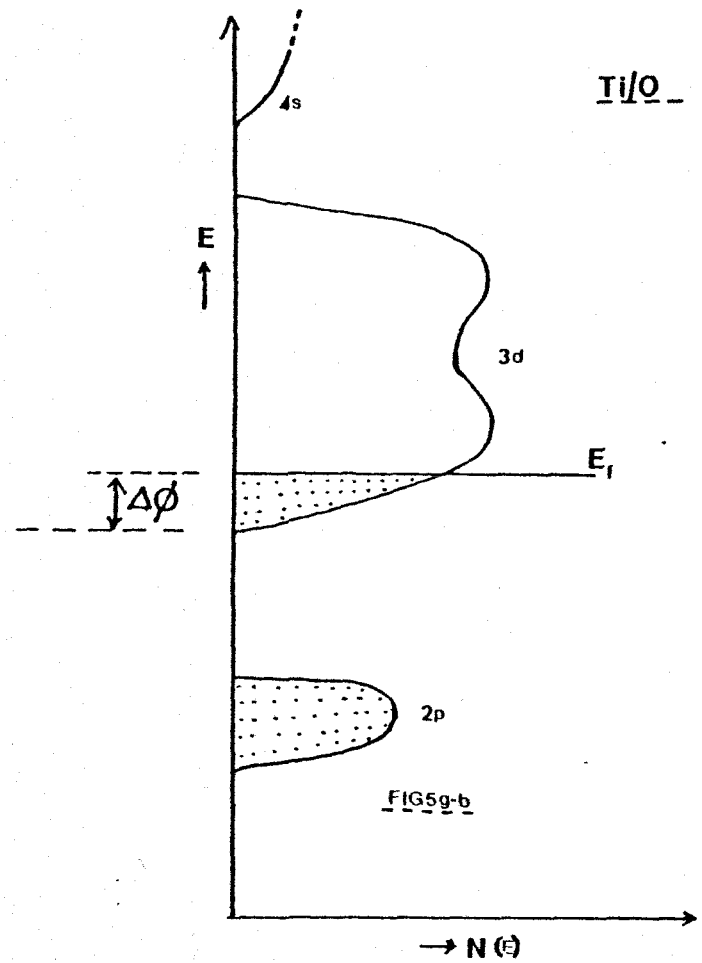

FIG5g-b

capacitor. A similar effect was observed by Riviere (1965, 64) for O/U and O/Th beyond the solubility limit. In the later stages of our experiment frequentlywe have observed some further changes of ϕ (U,V type). This indicates that the oxide formed at the start is unstable during a long exposure to oxygen, therefore evidently this oxide cannot be titanium dioxide, probably it could be a lower oxide, perhaps TiO. The changes (U and V) of ϕ may correspond to the formation of higher oxides such as Ti_2O_3, Ti_3O_5, TiO_2 or the conversion of oxygen-deficient TiO into titanium deficient TiO. However this work is not conclusive, because the changes in the Fermi level may be complicated for two reasons: firstly by the band bending at the oxide metal interface (Riviere 1965), secondly because the Kelvin method should detect changes at greater depth in the oxide than in the metal owing to the much larger screening distance (e.g. Debye length) in the former. Unfortunately the nature of the processes which control the resistance variation in our experiment did not allow us to determine the nature of the oxide formed on the film. However one thing we can conclude is that the work function of oxygen-covered oxide patches is less than that of oxygen-covered metal. Therefore for the first approximation we can conclude that the Fermi level is shifted to higher energy during the formation of titanium oxide. We can appreciate this from a simple model given in the fig. 5.g.

Generally in titanium the 3d band overlaps well the 4s band. In the oxide the oxygen occupies the intersitial sites, because of its high electronegativity, thus it effectively behaves like negative charge centres in the titanium lattice. The interaction of oxygen atoms with the metal electrons raises the energy of the metal electron states. However the degree of interaction is different for different electrons of the metal. The metal electron states most sensitive to this inter-

TiO

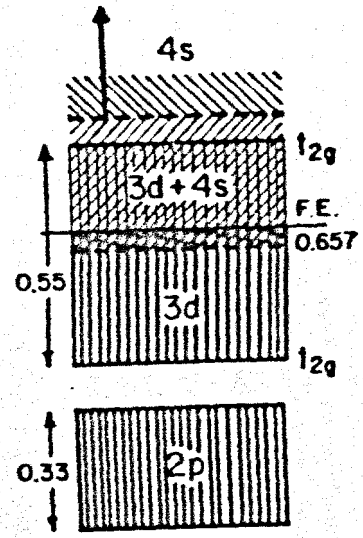
4s
3d+4s
t2g
F.E.
0.657
0.55
3d
t2g
0.33
2p


0.13
2s

fig5-h

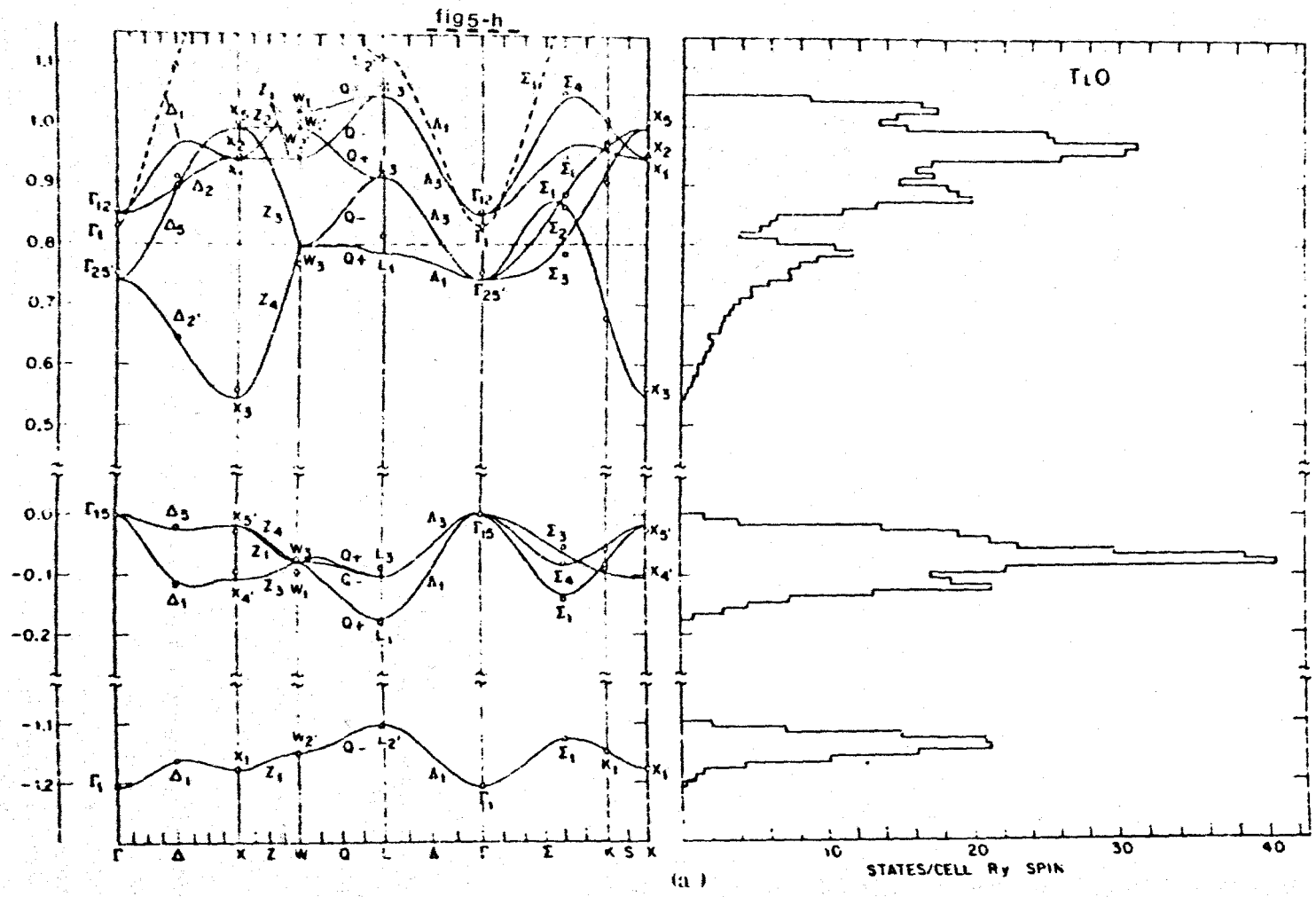
TiO
STATES/CELL Ry SPIN
10
20
30
40
Γ Δ X Z W Q L Λ Γ Σ K S X

(a)

action are those which have an appreciable wave function amplitude at the oxygen sites. The free electrons such as 4s electrons, generally have more amplitude so their energy states are raised by a relatively large amount; but localized electrons such as 3d-electrons generally have less amplitude so their energy states are raised by a relatively small amount. But in the presence of one or two oxygen atoms per unit cell, (e.g. TiO or TiO_2) the interaction between their electrons is also possible, therefore the 2p electrons of the oxygen form an energy band and generally this will have lower energy than the 3d band of metal electrons, as shown in the fig. 5.g.b. The 2p band of oxygen electrons can accommodate two more electrons for every oxygen atom. Therefore for the minimization of total energy, the electrons from high energy metal bands are transfered to 2p bands. Generally we can expect that all the states in 4s band become vacant; however this 4s band is not fully filled in titanium (fig. 5.g.a.) therefore some electrons from 3d band are also transfered to 2p band. But the Fermi level drop due to this process is relatively small because of the high density of d-electron states. For the first approximation we can conclude that the Fermi level shift is mainly due to the interaction of oxygen with the metal electrons, which will shift it to higher energy, in other words, will reduce the work function as we observed in our work. This model is consistent with the work function change after N, which also supports the idea that the oxides started to precipitate only after N, not before that. For comparison with our model, the band structure calculations of Ern and Switendick (1965), Maththeiss (1972) for TiO also given in the Fig. 5.h. The relative positions of the energy bands in our model are not critical, they can overlap in low oxides but become separated in high oxides. Further splitting of 3d band is also possible due to the crystal field effect of oxygen atoms.

After N some of the adspecies are only weakly bound to the surface (perhaps they are O_2^-). If the chamber is evacuated after N as at X in fig. 5.d, ϕ drops as these adspecies are adsorbed, and when oxygen is admitted again at Y they are readsorbed and ϕ returns to almost its previous value. The temporary change of ϕ with the pressure shown at two points Q in fig. 5.d also suggests there are some weakly bound adspecies. It seems that the sudden increase of pressure at Q temporarily increases the number of weakly bound species and ϕ rises, but the increased pressure also increases the rate of growth of the oxide (Lehoczky et al. 1979), which soon has a larger effect and ϕ drops again until a new steady state is reached at T. An alternative explanation for the decrease of ϕ from Q to T could be that different oxides are being formed at the higher pressures. The drop of ϕ in the form of steps (W type) could be due to the formation of some oxide patches as one unit, however the significance of this variation is not well understood.

In conclusion during the whole of the fast stage of the oxidation of Ti at room temperature oxygen atoms dissolve in the Ti lattice and do not form a layer of oxide. A solid oxide does not precipitate until the pressure > 10^{-4} torr and this is the start of the slow stage in oxidation. The oxide which precipitate first is not Ti O_2 but one of the lower oxides. The Fermi level shifts to higher energy in the oxide of titanium.

5.5 Mechanism for the penetration of oxygen atoms into the titanium lattice.

In general all faces of a crystal will have different kinds of sites for the adsorption of gas atoms. The principal planes of the H.C.P. lattice all have adsorption sites with 1-fold, 2-fold and 3-fold coordination, in addition to previously identified D sites, we will call

them A, B and C sites respectively. It is impossible to fill all these sites on a face simultaneously because of the size of the oxygen adatom compared to the lattice spacing. So if the adatoms are mobile, then the sites will tend to be filled in order of increasing adsorption energy. Generally the chemisorption bond between oxygen and metal is not purely ionic. Further Grubanov et al. (1977) quantum mechanical calculation shows that the Ti-O bond is mainly covalent even in a TiO crystal. Therefore any expectation of a size of adatom equivalent to O^{--} can be ruled out. At present we do not have any experimental value for the size of chemisorbed oxygen atoms on titanium faces. However Jona (1977) estimated 0.78 A^{o} and 0.74 A^{o} for the radius of the oxygen adatom on Fe(001) and Ni(001) faces respectively. Also he estimated 0.62 A^{o} for the radius of nitrogen on Ti(0001) face. Therefore without loss of generality let us assume a slightly higher value about 0.80-0.90 A^{o} for the radius of oxygen adatoms in titanium faces. Simple geometrical considerations show that even on the mostly closely packed (0001) face, oxygen adatom with the assumed radius can fill all the C-sites (if they are preferable energetically). The adsorption energy generally increases with the coordination number and with how preferable the nature of the electron lobes is for the bonding. Therefore the adsorption energy will be slightly different even for the same type of site on different crystal planes, because of the different directions of the Ti orbitals which are available at each plane. On the basis of this phenomenology for example we can expect C sites to be sites of higher adsorption energy than B sites or A sites on (0001) and $(10\bar{1}1)$, but B sites to have higher adsorption energy C or A sites on $(1\bar{1}00)$. Whatever the order is it is not critical, but let us assume the presence of sites in two different broad categories. One category say G_1 with high adsorption energy, the other category say G_2 with slightly lower adsorption energy. Adsorption

Fig 5i

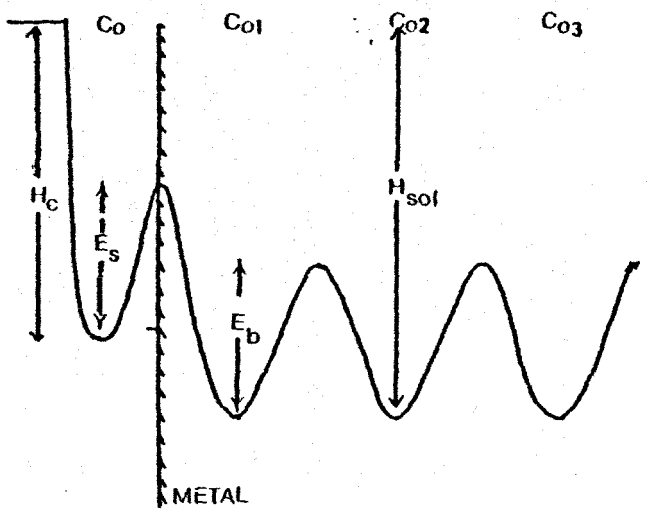

CLEAN STATE

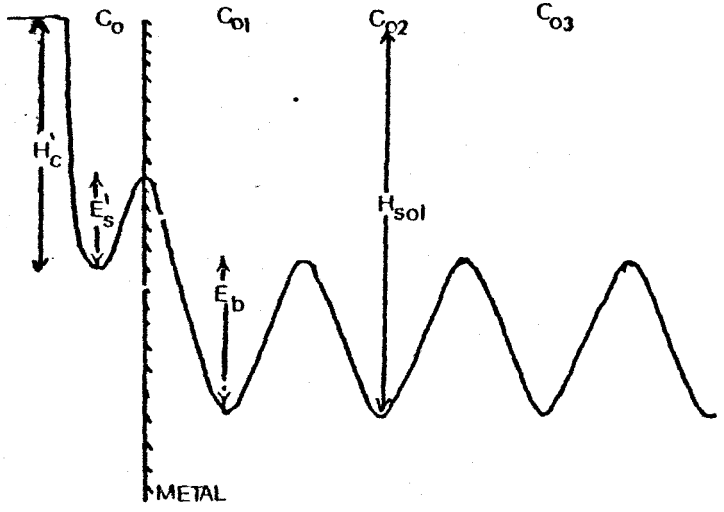

ADSORBED STATE

of oxygen on G_1 and G_2 is possible if other factors such as geometry allow it but chemisorbed atoms on G_2 will be in a metastable state against the site G_1. There are two kinds of C site, closed and open: the closed sites have a Ti atom below them in the second plane of the lattice, but the open sites are at ends of channels which run right through the crystal. Shih et al. (1978) have mentioned that there is only a slight difference in terms of probability for adsorption, however the diffusion of oxygen atom is easier through an open C-site because the octahedral intersitial site lies below it. Penetration can also take place through D sites because they are also the termination of channels which contain octahedral interstitial sites.

The reasonably large size of oxygen chemisorbed at the surface and dissolved in the bulk interstitial sites compared to aperture available for diffusion encouraged workers to believe in a large barrier against the diffusion. Theoretical calculation by Beck et al. (1975) gave a smaller value for the rate of diffusion of oxygen atoms in the titanium bulk than the experimentally observed value. Further Surplice et al. (1975) have described how sorption of oxygen at grain boundaries is not adequate to account for the large percentage increase of R. We found the way that R changes with time is significant; there is one rapid rise, which suggests a single rapid sorption process and no sign of any other change that could correspond to the slow decrease of ϕ. It shows that the oxygen penetrates unexpectedly quickly, in an activated manner into the Ti lattice. Therefore we begin to understand the possibility of oxygen penetration into the lattice of titanium and the energy process involved in terms of the model which is given in the fig. 5.i. This model differs in certain respects from Fromm's model (1977) which was described in fig. 5.a. We believe that the potential barrier for the penetration of oxygen from surface to bulk is slightly

higher than the one for the bulk diffusion of oxygen, because the concentration of electrons at C-sites on the surface is higher than the concentration of electrons at the same place inside the bulk, due to the surface effect. It is obvious that these barriers are dependent on the direction of diffusion in H.C.P. titanium and on the type of surface sites (C,D). However in the model we are not taking any account of these parameters.

In general the rate of penetration is proportional to exp.(-E/RT), where E is known as activation energy or potential barrier for the penetration. For the penetration of oxygen from surface to bulk $E=E_s$ but for the diffusion of oxygen in the bulk $E=E_b$ (fig. 5.i). Therefore the rate of penetration can be altered by varying the height of potential barrier-E. We think that the electrostatic repulsive energy between two oxygen adatoms can alter E. In other words, the height-E also depends on the concentration gradient across the aperture, and the diffusion is activated in the low concentration direction. Koiwa et al. (1969) have estimated that in Ti-O solution, the repulsive energy between oxygen atoms is 2 KCal / mole for a separation a_o ($\simeq 5A^o$) in the direction perpendicular to the plane (0001) but is 10 KCal/mole for a separation $C_0/2$ ($\simeq 2.5\ A^o$). Therefore we can appreciate the order of magnitude of these data in our explanation. For simplicity let us consider a thick patch with (0001) face at the surface. If we count the number of octahedral sites down the channel in the C-direction from the surface then we can say C_0- open C-site for adsorption, C_{01}- octahedral site between 1st and 2nd layer, C_{02}- -octahedral site between 2nd and 3rd layer and so on. The presence of an oxygen atom in C_{01} can reduce the E_b for the penetration of an oxygen from C_{02} to C_{03} by about 10 K Cal/mole. A simple estimate indicates this can increase the rate of diffusion as much as 10^4 times. Similarly the presence of an oxygen atom in C_{03} can increase E_b

for the penetration of oxygen C_{02} to C_{03}. Therefore it is clear that the concentration gradient is the main mechanism for diffusion of oxygen in bulk. The same mechanism is valid for the penetration of oxygen from surface to bulk. Further, we can expect a strong interaction between the oxygen atoms, because at the surface the interaction between the electrons of oxygen occurs in free space. It is also clear that the concentration of oxygen in the underlying layers has an effect on the penetration of oxygen.

Now we will see how this hypothesis explains the variation of R and ϕ in the solution phase at low exposures, i.e. shortly after K, suppose only a few G_1 sites are filled. On the addition of a dose some more G_1 sites and a few G_2 sites can become populated at the same time this can raise the electrostatic repulsive energy, which can cause a rapid penetration of oxygen into the first layer, consequently the diffusion of oxygen down into the bulk. These two processes can happen almost simultaneously within a few seconds after each dose, and can give effectively a rapid increase of ϕ and R. At the end of this state some sites, especially open C sites and D sites, are left vacant because the oxygen from them has gone into the bulk and the pressure has dropped to a very low value ($\simeq 10^{-9}$ torr) so there is then no chance for further penetration of oxygen atoms and the repulsive energy becomes less because of the temporary reduction of oxygen concentration on the surface. One thing only can happen, the adsorbed oxygen atoms on sites of type G_2 are in a metastable state relative to sites G_1, therefore they can gradually diffuse to G_1. This is effectively the same as diffusion from A to C or B and B to C, so it corresponds to decrease of ϕ. After each dose there is a greater concentration of oxygen in the top layers and at the surface. In other words, at the steady state after each dose more and more sites of G_1 become filled so the steady value

of ϕ after each becomes higher and higher, close to M most of the G_1 sites have become filled, but the oxygen concentration in the top layers is less than the solubility limit. The amount of adsorption and the amount of penetration becomes less, consequently the pressure starts to rise. Therefore a little more adsorption and some slow penetration is possible for some time after each dose. In other words, close to S, the increase of R becomes smaller and less rapid. However after M the equal increases and decreases of ϕ indicate that the amount of adsorption on G_2 sites is more or less equal to the amount of penetration from G_1 sites. This situation seems to extend up to N until the oxygen concentration in the top layers gradually exceeds the solubility limit. It is also clear that a big dose, or a fast flow, can instantly populate all the G_1 sites and consequently can give a large amount of penetration of oxygen into the bulk. This can raise the oxygen concentration in the top few layers above the solubility limit before some of them diffuse to lower layers. In other words, in small dose or in slow flow experiments the part N can appear after a large exposure, but in big dose or fast flow experiments this point can appear after even a small exposure. This can explain scattered values for the exposure before the maximum of ϕ (Table 5.1). Also our experience is in agreement with Gimzewski et al. (1979) suggestion in their X.P.S. study for Sc/O_2. They have pointed out that low pressure exposure over a long time will favour dissolution but high pressure exposure in short time will give a high local oxygen concentration and allow nucleation of the oxide.

In conclusion, the electrostatic repulsion between the oxygen atoms on the surface and in the bulk is the main mechanism for the penetration of oxygen into titanium films. In a sorption experiment of our type oxygen penetration gradually establishes a concentration gradient. The

depth of penetration or amount of oxygen sorbed before the slow oxidation state starts depends to a large extent on the rate of introduction of oxygen to the titanium surface.

CHAPTER 6

Titanium - water vapour study

6.1 Introduction:

The interaction of water with surfaces is of fundamental interest in many branches of science. Water vapour is one of the major residual gases in U.H.V. which will contaminate the metal surfaces and the gas phase under investigation, and interact with active components such as filaments. But so far surface science has paid little attention to sorption studies of water vapour. In many cases the mechanisms, final reaction products, and the surface structure resulting from interaction of water vapour with metal surfaces, remain unresolved problems. However the increasing amount of research in the last couple of years is an indication of the growing interest of scientists and for the future development of this study.

Among the surface science techniques X.P.S. has mostly been used in sorption studies of water vapour (Fuggle et al. 1975, Padalia et al. 1976, Gimzewski et al. 1977, 1979, Norton et al. 1977, Eberhardt et al. 1978, Hopster et al. 1979 and Nornes et al. 1979). However other techniques such as L.E.E.D (Ibach et al. 1980, Dwyer et al. 1977, Walerian et al. 1976), U.P.S. (Fujiwara et al. 1977), S.I.M.S (Benninghoven et al. 1977), N.I.S (Renouprez et al. 1979), microbalance (Sharma et al. 1979, Zabov et al. 1975), and work function measurement (Dowson et al. 1980, Watanable 1977, Kruger et al 1972, Fort et al. 1972, Batt et al. 1970, Suhrmann et al. 1968) have also been used. There have been only a few works conducted on single crystal planes; X.P.S. studies of Norton et al. 1977 on Ni(100) and of Eberhardt et al. (1978) on Al(100) (110) and L.E.E.D studies of Ibach et al. (1980) on Pt(100) of Dwyer et al. (1977) on Fe(001) and of Walerian et al. (1976) on Fe(111). However these studies do not yet seem to have given

additional information over polycrystalline samples in this field.

Generally these studies have suggested that water adsorption on metal surfaces is by dissociative chemisorption at room temperature. Blyholder et al. (1975) have reasoned thermodynamically about the possibility of dissociative adsorption of water vapour on Ni surfaces. A large amount of hydrogen emission was detected by Fuggle et al. 1975, and Eley et al. (1960) in their sorption studies of water vapour. The S.I.M.S study of Benninghoven et al. (1977) on vanadium surfaces suggested the presence of oxygen-bonded and hydroxyl-bonded species on the metal. But the S.I.M.S study of Hopster et al. (1979) on Ni indicated only the presence of NiOH clusters. The X.P.S. study of Norton et al. (1977) on Ni suggested the formation of $Ni(OH)_2$ or NiO(OH) on the surface. The further formation of oxides covered with a hydroxyl complex on Sc and Fe was suggested by Gimzewski et al. (1979, 1977); on the rare earth metals Lu, Yb, Tm, Er, Ho, Dy and Tb by Padalia et al. (1976) and on Al, Mg, Cr and Mn by Fuggle et al. (1975), after room temperature water sorption experiments. Dwyer et al. (1977) have suggested that the adsorbed H_2O molecules on Fe(001) are mobile, but not the adsorbed OH species. Further Padalia et al. (1976) have suggested bulk oxides of rate earth metals adsorb water vapour and form surface hydroxides at room temperature.

Suhrmann et al. (1968, 1964) studies on Cu, Fe and Ni films, Dowson et al. (1980) work on Pt tips and Watanable's (1979) study on Fe(100) face have all indicated that water vapour sorption is accompanied by a reduction of work function. Further Fort et al. (1972) and Batt et al. (1970) works on Al surfaces indicated that the sorption of water vapour gives an initial drop of ϕ, and this is followed by an increase at high exposures at room temperature. The initial drop of ϕ is generally attributed to the adsorption of H_2O or OH species with positive dipoles

away from the surface. The increase of ϕ at high exposures is interpreted as due to the adsorption of a second layer of H_2O by Fort et al. (1972). A resistance increase was observed by Suhrmann et al. (1968, 1964) when the water vapour was sorbed by Cu, Fe and Ni films at room temperature.

At present there is no work available for H_2O on titanium surfaces at room temperature. At high temperature (> 650°C) Motte et al. (1976) have suggested from their weight gain and S.E.M. techniques that the oxidation of titanium in water vapour occurs in two stages. The U.P.S and L.E.E.D study of Lo et al. (1978) on TiO_2 surfaces indicated a drop of ϕ by 800meV and disordered adsorption for water vapour exposure of 10^5L. However the same authors' study on a titanium-rich TiO_2 surface showed only an effective drop of 400meV for the same amount of exposure at room temperature (Lo et al. 1978). Further they have suggested that water vapour adsorption on TiO_2 surface is molecular but on titanium-rich TiO_2 surface is dissociative. The X.P.S study of Sharma (1979) on rutile (TiO_2) surfaces suggested the existence of chemisorbed OH and H_2O species. However the recent E.S.D and E.L.S studies of Knotek (1980) indicated only the dissociative adsorption of water vapour, not molecular H_2O.

In conclusion, dissociative chemisorption of water vapour occurs at room temperature and the formation of oxides and the coexistance of H, H_2O, and O species at the surface are generally predicted. However the complete picture of water vapour interaction is not yet well understood. A broad study is necessary for the correct conclusion to this study.

6.2 Results

The results given below are divided into four sub-headings which are (a) Water vapour sorption on clean titanium films (b) Water vapour

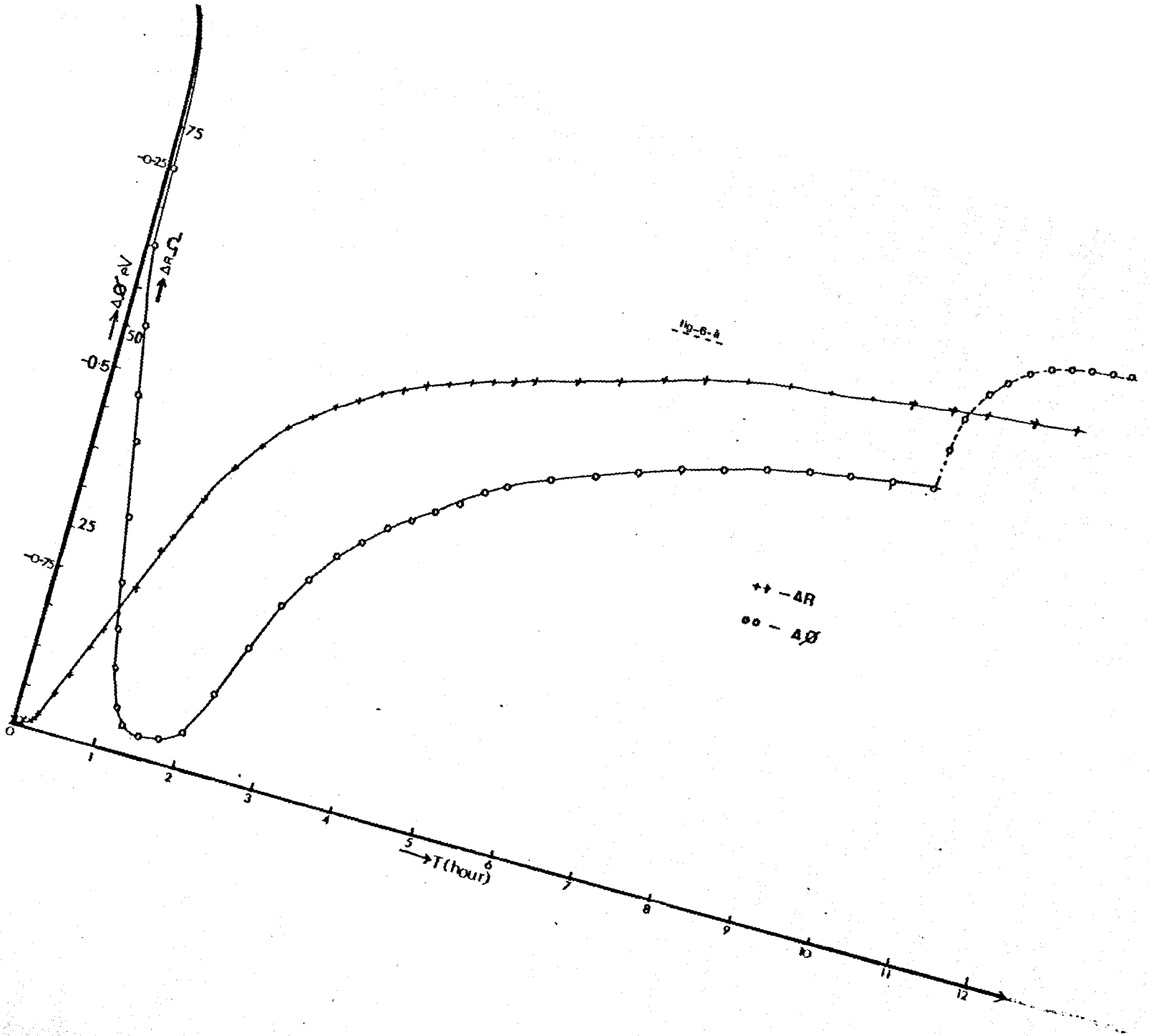
Fig-6-4
75
-0·25
50
-0·5
25
-0·75
0
1
2
3
4
5
6
7
8
9
10
11
12
T (hour)
++ — ΔR
oo — ΔØ

sorption on titanium films with presorbed oxygen (c) oxygen sorption on titanium films which had presorbed water vapour and (d) sorption of oxygen and hydrogen mixture by titanium films. The last three types of experiments were conducted in order to understand the mechanisms involved in the interaction of water vapour with titanium films.

(a) Water vapour sorption on clean titanium films.

The general features of ϕ and R variations for water vapour exposure are shown in fig. 6.a and fig. 6.b, and a summary of the data is in table 6.1. At the start ϕ drops rapidly by 200-300meV to A for small exposures, and then becomes slower up to B. The total drop of ϕ at B is 750-950meV. Beyond B ϕ is almost constant up to C, at which point the total pressure has risen to 10^{-2} torr. After C ϕ increases first rapidly, and then gradually becomes constant. The increase was about 500-600meV at saturation, D. The variation of resistance at the start is very small and unpredictable until to ϕ drops to A: sometimes a small increase, sometimes a small drop, sometimes hardly any variation. Beyond this region the resistance increases relatively rapidly up to P and then becomes slower and slower until Q. After Q the increase of R is steady but small. The coincidence of P with B and Q with C is reasonable. The total increase of R at P varies from 10-15% of the initial film resistance. The removal of water vapour by pumping has no effect on R in the entire region of study, but it has effect on ϕ after B. Beyond B an increase of ϕ was observed on pumping out water vapour, but this increase was small (50-75meV) within the region BC and large (200-250meV) after C.

In a dose experiment 2 or 3 small doses (10^{15} molecules) are enough to cover the range up to A. In this range ϕ drops in a step-like fashion for each dose. Many moderate sized (10^{16}-10^{17} molecules) doses,

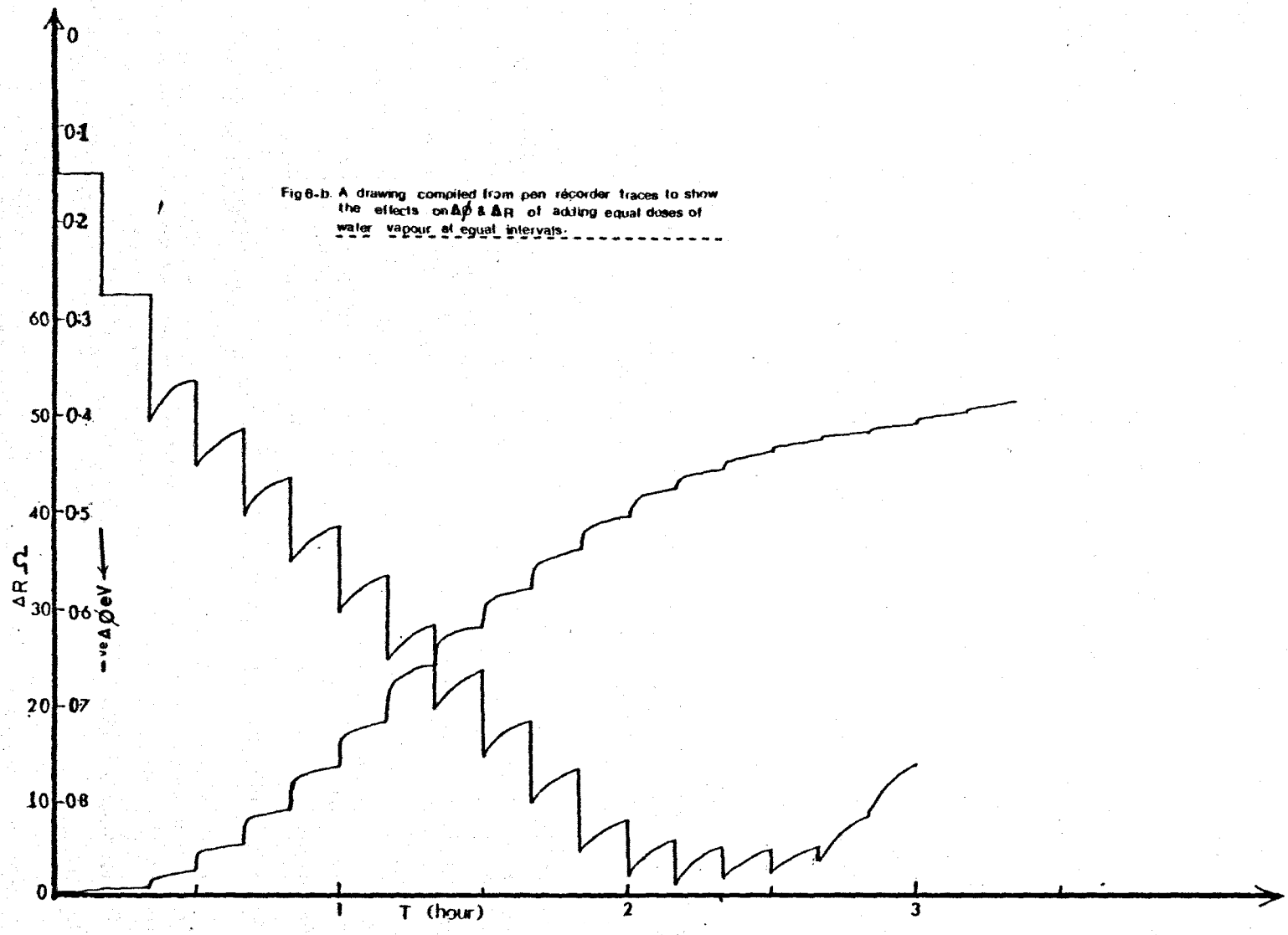

Fig 6-b. A drawing compiled from pen recorder traces to show the effects on ΔØ & ΔR of adding equal doses of water vapour at equal intervals.

Table 6.1

Film	$\Delta\phi_o$ (meV)	$\frac{\Delta R}{R_o}$	T (min)	P (10^{-3} torr)	$\Delta\phi$ (meV)	$\frac{\Delta R}{R_o})_{sat}$	T_{sat} (hour)	P_{sat} (10^{-2} torr)	ϕ Pump
Ti 62/5	975	–	100	6	535	–	6.5	3	255
62/6	1095	–	80	6	605	–	8	4	200
62/7	1065	–	30	6	>535	–	–	–	100 *
63/2	575	–	200	6	>100	–	–	–	200 *
63/3	670	5.5	20	8	415	11.5	5	2	150
63/4	600	4.4	30	8	500	17.0	5	150	130
63/5	615	2.5	150	6	460	8.0	20	1	–
64/1	890	–	50	10	720	–	23	10	105
65/1	830	17.3	120	10	>370	>35	–	–	140 *
65/2	950	10.5	150	8	>310	>13	–	–	– *
65/3	750	7.0	300	7	>350	>13	–	–	135 *
65/4	>650	>6.6	–	–	–	–	–	–	0 *
66/1	>670	>22.5	–	–	–	–	–	–	0 *
66/2	800	7.0	180	5	–	–	–	–	30 *
70/3	790	5	5	–	–	–	–	–	50 *
70/4	740	5	20	10	>300	>7	–	–	190 *
70/5	800	5	12	10	520	7	3	4	–
70/6	850	3	12	5	>30	4	–	–	60 *
71/2	910	–	300	10	>300	–	–	–	– *
73/1	>650	>12	–	–	–	–	–	–	– *
74/7	915	7	23	5	–	–	–		50 *

* Not saturated. For clarity see fig. 6.1.

more than twenty, are needed to cover from A to B and each dose gives a sudden drop of ϕ which is followed by a slower increase of 20-30 meV in over 10 minutes. In the meantime, the resistance increases suddenly at the dose by 4-5 ohms, then more slowly by 1-2 ohms. The variation of R is slightly larger at the toe of the curves, then becomes smaller and smaller especially after P, and finally becomes ineffective after Q. Within the region BC the initial drop of ϕ at the dose has become small (20-30 meV) and equal to the slow increase that follows it. After C with the same size of doses, the initial drop of ϕ disappeared.

Mass spectrometer experiments showed that even for the first dose there was a large increase of mass peak-2 at the dose. After each dose up to A this mass peak disappeared quickly, but after A it took a long time for complete disappearance. In another experiment a mixture of hydrogen/water vapour was introduced to the reaction chamber and the variation of ϕ and R indicated that our technique was not sensitive to the presence of hydrogen in the mixture. In a blank experiment, a titanium film saturated with water vapour was exposed to hydrogen and no adsorption was detected within the limits of our experimental technique.

(b) Water vapour sorption on titanium films which had pre-sorbed oxygen.

There were four experiments conducted on films which had pre-adsorbed different amounts of oxygen. Clean films were exposed to oxygen until ϕ increased by 400meV in experiment 1, by 600meV in experiment 2, and up to its maximum ($\Delta\phi$ = 1.1eV) in experiment 3, but in experiment 4 until the surface was covered with oxide patches. The corresponding resistance increase was 2.5% in experiment 1, 9.8% in experiment 2, 25.5% in experiment 3 and 70% in experiment 4. The general features of the variation of ϕ are shown in the fig. 6.c. Experiment 1 and experiment 2 showed a broad minimum like water vapour sorption on clean titanium films

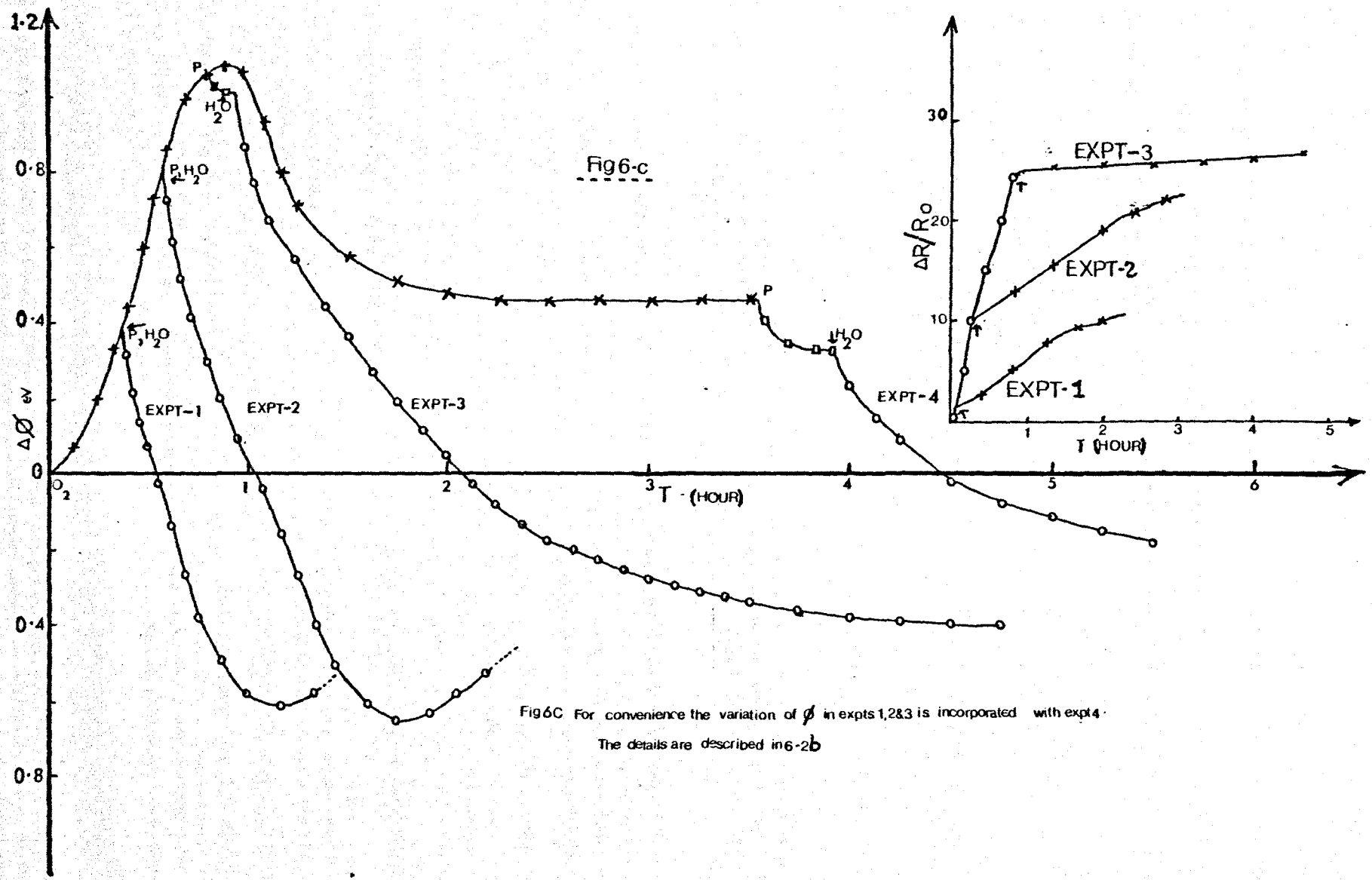

Fig 6C For convenience the variation of ϕ in expts 1,2&3 is incorporated with expt 4.
The details are described in 6-2b

(see fig. 6.a) but not experiment 3 and experiment 4.

Water vapour exposure in experiment 1 and experiment 2 gave a rapid drop of ϕ to 1.020eV and 1.230eV respectively at the start, then a gradual increase to a constant value, which lay below the clean film value ϕ_o. The additional resistance increase at the minimum of ϕ was 7.7% and 3.8% respectively. In experiment 3 ϕ dropped at the start, then more gradually to a steady value of ϕ below the clean film value ϕ_o. A total drop of 1.350meV in ϕ and an additional increase of 4% in R were observed. In experiment 4 ϕ dropped gradually below the clean film value ϕ . A total drop of 550meV in ϕ and no resistance change were observed in this experiment. The emission of hydrogen in all four experiments was noticed by using the mass spectrometer, but the amount of emission was less in experiment 4. The variation of ϕ for each dose of water vapour in experiments 1 and 2 was exactly the same as for water vapour sorption on clean titanium films. In the initial part of the experiment 3 where ϕ dropped rapidly, the variation of ϕ for the addition of water doses was like water vapour on clean films, but near saturation ϕ dropped in a step-like fashion. In experiment 4 throughout the experiment ϕ dropped in a step-like fashion.

(c) Oxygen sorption on titanium films which had presorbed water.

There were four experiments conducted with different amounts of water vapour presorbed on titanium films. The general features of the variation of ϕ and R are shown in the fig. 6.d. In all experiments the variation of ϕ and R was qualitatively like the case of oxygen sorption by clean titanium films (described in Chapter 5). The total increase of ϕ up to its maximum was different in each experiment, and the value of ϕ at the maximum decreased with increasing amounts of presorbed water vapour. The mass spectrum indicated the emission of water vapour when oxygen was added

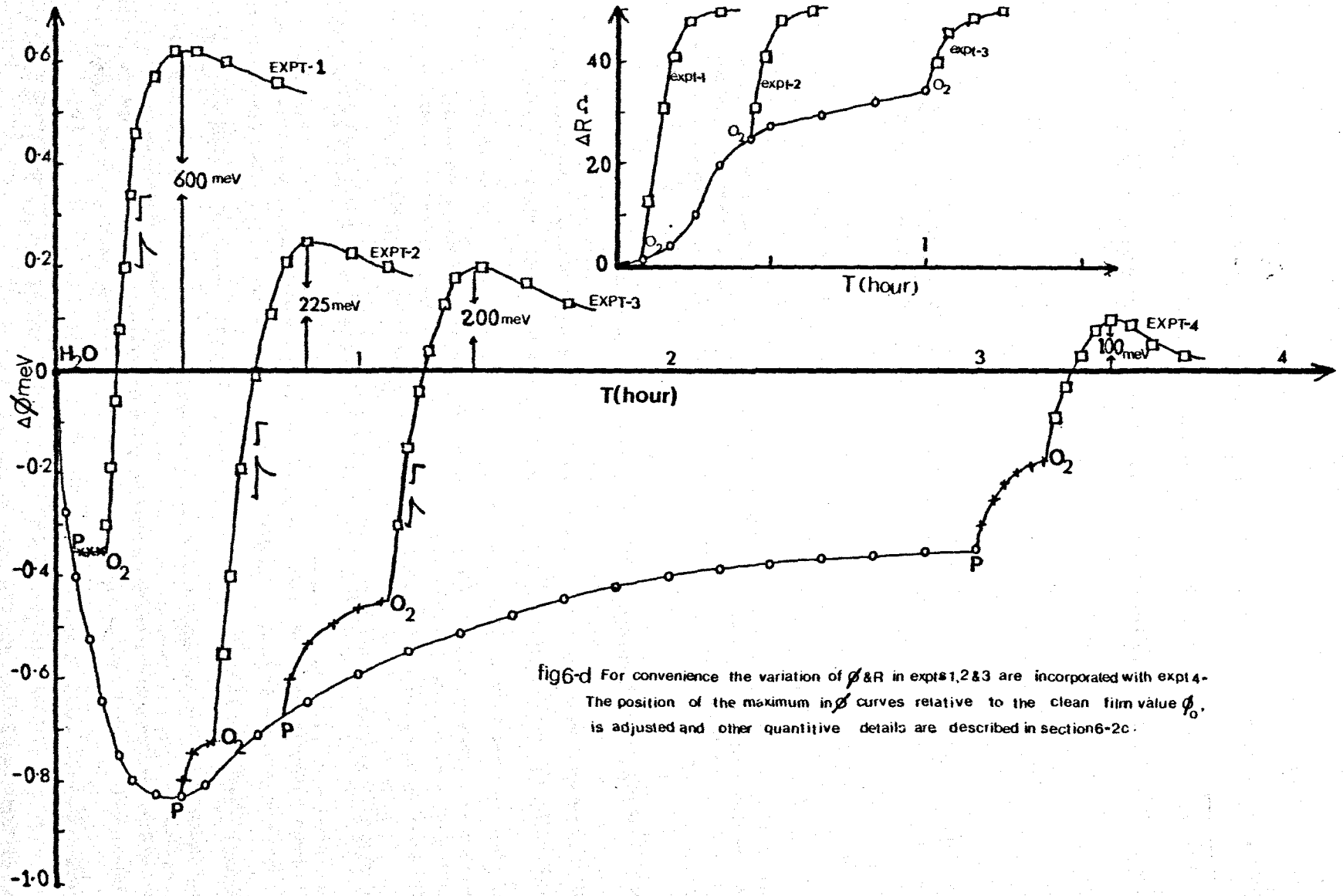

fig6-d For convenience the variation of ϕ &R in expts 1,2 &3 are incorporated with expt 4- The position of the maximum in ϕ curves relative to the clean film value ϕ_0, is adjusted and other quantitive details are described in section 6-2c.

to the system.

Clean titanium films were exposed to water vapour until ϕ had dropped by 310meV in experiment 1, down to the minimum ($\Delta\phi$ = 850meV) in experiment 2, and until an increase of 350meV after the minimum in experiment 3 and until ϕ had become steady after this increase in experiment 4. Then water vapour was pumped; there was no change of ϕ in experiment 1, but a change of 75meV in experiment 2, a change of 200meV in experiment 3 and a 250meV change in experiment 4 were observed. Then oxygen exposure gave a maximum in the ϕ curve after increases of 910meV in experiment 1, 1.0eV in experiment 2, 475meV in experiment 3 and 280meV in experiment 4 (for clarity see fig. 6.d). The increases of R after water sorption and after water followed by oxygen, were respectively 2% and 24% in experiment 1, 5% and 15% in experiment 2, and 8% and 7% in experiment 3. In all experiments the total pressure at the maximum of ϕ was about 10^{-3} torr, which is noticeably higher than the oxygen pressure at the maximum of ϕ for the clean films, which was about 10^{-4} torr.

(d) Sorption of oxygen and hydrogen mixture by titanium films.

There were three experiments conducted for mixtures of O_2 and H_2 with different atomic ratios (H/O) 1, 2 and 10. The variation of ϕ was exactly the same as for oxygen sorption on clean titanium films, however the total pressure at the maximum was about 10^{-3} torr, which is higher than the pressure of ϕ maximum in the pure oxygen sorption experiments (described in Chapter 5). The qualitative features of the resistance variation were also the same as in oxygen sorption on clean films, except in the experiment with (H/O) ratio 10. In the experiment with atomic ratio 10, the resistance dropped for a large part of the experiment i.e. until ϕ had risen up to 700meV. To further understand the roles of the oxygen and oxide in the sorption of hydrogen three experiments under each

category were conducted. In the first category clean films were exposed to oxygen until ϕ increased by 400-500meV, then the oxygen was pumped out, and hydrogen introduced. These films sorbed a large amount of hydrogen and ϕ and R dropped. However the same type of experiment with films saturated in an oxygen atmosphere of 10^{-2}torr (i.e. oxide film) did not show any changes of ϕ and R nor any sign of sorption during more than one hour.

6.3 Discussion

It is generally accepted that for the clear understanding of any surface studies one should have information either from combined studies using different techniques or reliable data from other workers. At present within the knowledge of the author, there is no other data available on sorption of water vapour by titanium films at room temperature. Therefore as a starting step here the author tries to give a very simple explanation in terms of the dissociation of water vapour, the absorption of some dissociated species, and the formation of hydroxyl and oxygen complexes at the surface, which are consistent with his data and the general nature of the system.

The dissociative chemisorption of water vapour on metal surfaces is a generally observed phenomena at room temperature. The emission of hydrogen after each dose in the author's experiments further suggests the dissociation of water vapour on titanium films. There are only two possible direct ways for the dissociation of water molecules

$$H_2O_{ad} \rightarrow H_{ad} + OH_{ad} \rightarrow OH_{ad} + \tfrac{1}{2}H_2(g) \rightarrow \text{Process 1}$$

$$H_2O_{ad} \rightarrow H_{ad} + H_{ad} + O_{ad} \rightarrow O_{ad} + H_2(g) \rightarrow \text{Process 2}$$

If the dissociation of all adsorbed water molecules occurs by process 2, then the situation is similar to the hydrogen and oxygen mixture with

atomic ratio H:O = 2:1. Therefore, we can conclude from the dissimilar variation of ϕ during water sorption and during the sorption of the oxygen-hydrogen mixture, that not all the adsorbed water molecules are dissociating by process 2. Further it is obvious that the energy for process 2 is greater than the energy for process 1. Therefore we can argue that not all adsorption sites on the surface are suitable for process 2. Only on certain sites, especially those with high coordination can the dissociation of watermolecules by process 2 be possible. Further oxygen sorption on water-presorbed titanium films (section 6.2.b) indicates, from the emission of water vapour (mass no. 18) that chemisorbed water molecules are also present on the surface. These are not physisorbed water molecules because they are stable against pumping below 10^{-7} torr. Therefore let us assume the possibility of both molecular and dissociative chemisorption via process 1. It is also obvious from the effect of removing water vapour beyond point B on the ϕ curve that a few water molecules became physisorbed at higher pressures, and the amount of physisorbed water molecules increases with exposure at high pressure (beyond C).

The behaviour of the H atoms removed from the water molecules by dissociation is not well understood. An initial emission, and then a gradual sorption of hydrogen was abserved by the mass spectrometer from the start. The blank experiment indicates there is no sorption of hydrogen by water-saturated titanium films. Further we can justify from the sorption of hydrogen by titanium films which have already dissolved oxygen (section 6.2.d), that the presence of a small amount of OH species did not prevent the interaction of dissociated hydrogen with titanium films. Therefore tentatively we can conclude that from the start some hydrogen can be sorbed by titanium films but the relative effect is very small, compared with the effect of either oxygen or the hydroxyl species.

During the initial stage of the experiments i.e. up to A on the curve of ϕ vs exposure, the rapid change of ϕ and the corresponding unpredictable variation R are due to pure chemisorption, mainly dissociative chemisorption by process 1. The step-like drop of ϕ and the quick disappearance of mass peak 18 in this region in dose experiments indicates that the sticking coefficient is reasonably high. The drop of ϕ indicates the positive pole of the dipole OH is directed away from the surface; in other words, the chemisorption bond is via the oxygen atom. The process 2 may be possible on certain sites which could be D sites (described in Chapter 5, Section 5.4), therefore adsorption of oxygen on these sites gives a drop of ϕ which is small (see section 5.4).

Beyond this region a large and definite increase of resistance indicates the penetration of some scattering centres with a large scattering cross-section. In this work they could be oxygen or hydroxyl species. We can argue that the bulk interstitial are high energy sites for OH species because of their dipole nature. Therefore we can conclude that some oxygen species started to diffuse into the bulk after A. However oxygen sorption on water presorbed on titanium films, showed a maximum in the variation of ϕ (Fig. 6.d) and a large increase of R in all four experiments, like oxygen sorption on clean films. This indicates that even near saturation of Ti-films by water vapour, the concentration of oxygen in the top layers of the film has not exceeded the solubility limit. In other words the amount of oxygen penetration in water vapour sorption experiments is generally small, this is also in agreement with the relatively small increase of R for a moderately sized dose of water vapour compared to a similar dose of oxygen on clean titanium films.

The solution of oxygen in the titanium lattice can have an effect on the position of the Fermi level and in turn on the work function, but generally this is small therefore we can ignore it at this stage. The

slow rate of drop of ϕ after A could be an indication of a new process at the surface. Since the mass 18 peak also takes a long time to disappear, the slow rate of drop of ϕ could be partially due to a low sticking cooefficient for water vapour after A. Further, the drop of ϕ for a dose of moderate size is small compared to the drop of ϕ at the start. This could be due to the presence of more oxygen on the surface, therefore we have to account for the generation of more oxygen: Now we will see how that is possible.

Generally adsorption with high sticking coefficient takes place on high energy sites but adsorption on low energy sites, will have a low sticking coefficient for a particular adsorbent system. Therefore suppose before A adsorption takes place on high energy sites, dissociatively mostly by process 1, and after A on low energy sites non-dissociatively. For example, on (0001) plane of H.C.P. titanium dissociative chemisorption can occur at the start on 3-fold (C-sites), but later molecular chemisorption can take place on 1-fold sites (A-sites). Chemisorption on the 2-fold sites (B sites) is not possible at a later stage, because of geometrical reasons. For chemical reasons, the chemisorption bond forms via an oxygen atom. The structure of water molecule is triangular with angle H.O.H about 106°, therefore the projection of hydrogen is not perpendicular to the surface plane. In this situation the separation between a hydrogen atom in the OH species, which are on the high energy sites, and any hydrogen atom in the water molecules which are on the low sites is comparatively small; Therefore there is the possibility for these two hydrogen atoms to come within the attractive potential of one another, so they can combine and leave as hydrogen gas. Quantum mechanics indicate that the attractive potential of H_2 is very deep for separation between the H atoms from 0.6 A° to 1.2 A° (Pimentel et al. 1970). Therefore the above phenomenology is possible in most close-packed planes. For a

Fig 6-e

Ti(0001) + H_2O

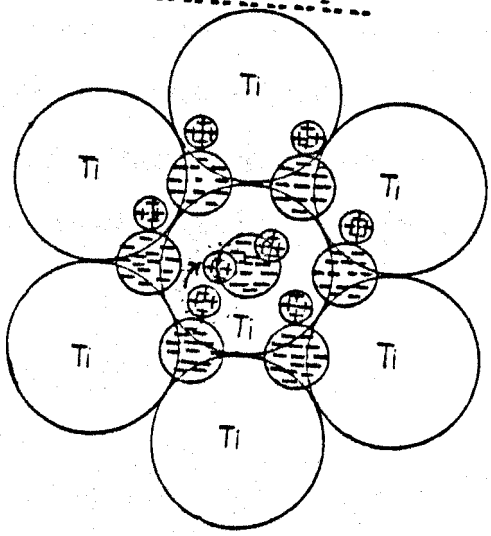

Fig 6-f

Ti (0001) + $H_2O(v)$

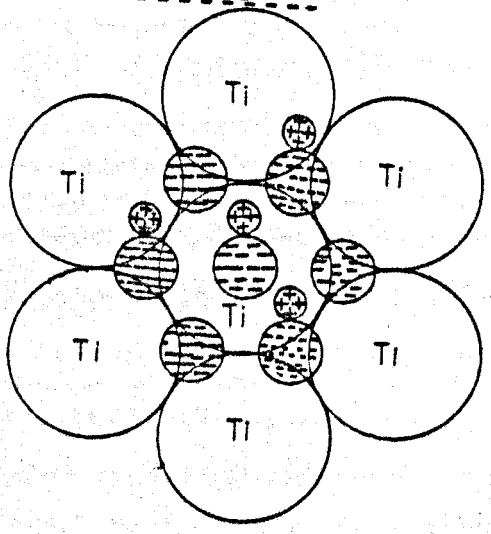

$TiO(OH)_2$

simple example the situation on (0001) plane is shown in the fig. 6.e. As soon as one hydrogen of the water molecule is removed, for symmetry reasons the projection of the other hydrogen atom becomes perpendicular to the surface, therefore further combination is impossible. Simultaneous removal of both hydrogens from water molecule is obviously a high energy process, therefore we can ignore that possibility. Therefore in conclusion the generation of more oxygen atoms can take place at the surface as follows.

$$OH_{(ad)} + H_2O_{(ad)} \rightarrow O_{(ad)} + OH_{(ad)} + H_{2(g)} \quad \text{- Process-3}$$

After A, at each dose water vapour molecules become chemisorbed at low energy sites and become dissociated by process-3. In the meantime the electrostatic repulsive force drives a large percentage of the oxygen which is produced by process-3 from high energy sites to bulk interstitial sites, as described in Chapter 5. All these processes can happen within a short time, and can give effectively a drop of ϕ and an increase of R at the time of the dose. Later, the OH species on the low energy sites (produced by process-3), can diffuse gradually to high energy sites which have been left vacant by the oxygen atoms which have diffused into the bulk; this process corresponds to a gradual increase of ϕ in the later stages of each dose. The low sticking coefficient of water vapour may still allow some new adsorption even in these later stages but it seems that if so it did not modify the qualitative variation of ϕ. However it could be the reason for the very slow increase of R in these later stages because additional adsorption could keep the repulsive force large enough to continue to drive appreciable numbers of oxygen atoms into the bulk.

The same mechanism is in operation up to C; but after B, the equality of the drop of ϕ and increase of ϕ is an indication that the amount of the adsorbed species equal to the amount diffused into the

bulk. We might argue also that the more or less constant ϕ value at the end of each dose between B and C is due to the existence of an equilibrium between two species: those giving an increase of ϕ on adsorption, e.g. oxygen and those giving a drop of ϕ on an adsorption e.g. OH, H_2O. The corresponding variation of R between P and Q indicates that the amount of oxygen atoms which is diffusing into the bulk is becoming less and less after each dose. The further increase of ϕ when the gas is removed by pumping, is an indication for the weakly bound H_2O or OH species..

The increase of ϕ after C might be simply attributed to relative increase of the amount of oxygen at the surface. But we believe that this is not the reason because from oxygen sorption on films which had presorbed water (section 6.2.c), we know that the concentration of oxygen in the top layers had not exceeded the solubility limit even in experiment 4 (section 6.2.c). Therefore if the increase of ϕ after C was due to more oxygen atoms on the surface, then we could expect some extra penetration of oxygen and in turn a comparable amount of increase in R. This is not observed. In contrast to this, a sudden break in the variation of R indicates the increase of ϕ is due to some new process (fig. 6.a). This could be the formation of some complex compound at the surface, with a layer structure, perhaps $TiO(OH)_2$, which increases the value of ϕ. In other words when the pressure rises to 10^{-2} torr at C, sorption processes establish a dynamical state in such a way as to precipitate a complex compound, at least in a few surface patches. This also agrees with the relatively fast increase of ϕ at C. It seems that the complex patches are inert for further sorption of water vapour and all the surface patches are gradually converted to this complex compound as ϕ becomes constant. The possibility of having the complex $TiO(OH)_2$ on the (0001) plane is shown in the fig. 6.f as a simple example.

It is obvious that the macroscopic ratio O:OH at the surface patches is an important parameter for the formation of a complex compound. This could be the reason why experiment 1 and 2 for water sorption on films that had presorbed oxygen, showed a minimum in the ϕ Vs exposure curve (fig. 6.c) but experiment 3 and 4 did not. Suppose in experiment 1 and 2, the concentration of oxygen is low, then adsorption of water vapour can drive some oxygen inside the bulk which is indicated by the resistance increase, and it can also create some more oxygen atoms as in the case of water adsorption on clean films. Therefore it is possible to establish gradually the composition which is suitable for the formation of the complex compound. So the qualitative variation of ϕ with exposure agrees with our explanation. However, the slightly high value of ϕ at the minimum, compared to clean film experiments (section 6.2.a), could be due to the change in the features of the surface after oxygen sorption. Suppose in experiment 3 and 4, the concentration of presorbed oxygen is high. The variations of ϕ and R show only a little oxygen diffuses into the bulk in experiment 3 but none, or very little, in experiment 4. In other words, most of the surface sites are already occupied by the oxygen atoms. Therefore it is very hard to find enough sites for water adsorption, to form the complex compound. Therefore in these experiments water vapour becomes adsorped with the positive pole of the dipole directed outwards and reduces the value of ϕ . However the adsorption of the water vapour in experiments 3 and 4 may be different because basically they are different substrates; in experiment 3 the substrate is oxygen presorbed on titanium film, in experiment 4 it is titanium oxide. But, from mass spectrometer observations we can say that, in both experiments water vapour adsorption is dissociative on at least a few sites.

In oxygen sorption on water vapour presorbed on titanium films, the

mass spectrometer indicates some chemisorbed water molecules are removed by the oxygen atoms. But the value of ϕ at the maximum of the ϕ Vs exposure curve is remarkably decreased with the amount of presorbed water vapour. This indicates that there is some unremoved species that will reduce ϕ. Probably these species are OH, because it can bind relatively strongly with the surface at high energy sites. The reduction of ϕ seems very sensitive to the amount of presorbed water in experiment 1 and 2: e.g. $\Delta\phi$ at the maximum for oxygen sorption on a clean film is about 1.1eV but in experiment 1 it is 600meV and in experiment 2 it is 225meV. This could be an indication for the nature of the water vapour adsorption. Suppose at low exposures H_2O adsorption takes place at high energy sites, mostly in dissociated form, then removal of these species is difficult. Therefore the amount of oxygen adsorption is very sensitive to the surface, in turn so is ϕ at the maximum. But at high exposures especially after C (experiments 3 and 4) oxygen can be adsorbed only on a few sites, those from which it can desorb weakly bound water molecules, so the maximum value of ϕ becomes less sensitive to the amount of presorbed water.

In conclusion, water vapour sorption reduces the work function of the film. Mostly the adsorption takes place in the dissociated form and oxygen diffuses into the bulk: At high pressures ($> 10^{-2}$ torr) the surface becomes passive for the further sorption of water vapour and hydrogen, but not for oxygen. Oxygen sorption on water vapour presorbed on the films removes weakly bonded water molecules and gives further penetration of oxygen inside the film. Water vapour adsorption on oxygen presorbed on the films depends on the amount of oxygen presorbed. Formation of a complex component may occur but this is not possible if a film has presorbed a large amount of oxygen. In all cases weakly adsorbed water molecules exist at high exposures.

CHAPTER 7

Work function, summary and suggestions for further work

7.1 Work function of titanium films

The H.C.P. structure has 3 low index planes which are (0001), $(10\bar{1}1)$ and $(10\bar{1}0)$. In general these are the most probable crystal faces at the surface of a film. A Kelvin probe measures the average C.P.D. value of all crystal faces which exist at the surface of a film. The amount of different crystal faces at the surface can vary film to film, therefore it is reasonable to observe different C.P.D. values. The data for the titanium films evaporated on glass substrates is given in table 7.1 and the statistical distribution is plotted in figure 7.a. The C.P.D. values for Ti 17/1, Ti 27/1, Ti 35/1 and Ti 36/1 are omitted from the discussion since these are far outside the distribution of the other values.

Recent calculation of Feibelman et al. (1980) predicted the work function of Ti(0001) face is 3.8 eV. But our C.P.D. values ranged from + 400 mV to -900 mV. If we take the work function of the gold reference to be constant at 4.4 eV (Surplice et al., 1975) then the average work fork function of the titanium films varies from 4.0 eV to 5.3 eV. This is in agreement with previous works of D'Arcy (1971), Anderson et al. (1971) and Eastman (1970). This large difference is not surprising since there is evidence that the crystal faces of a metal can differ in work functions by more than 1 eV (Rivière, 1969). However here the nature of the statistical distribution is surprising. It is reasonable to assume that about 60 samples are enough to show the statistical distribution. The distribution shown in figure 7.a is not a normal distribution but seems to represent three different sub-distributions, one has a sharp peak around -650 meV, another has a peak around +225 mV, and the third one is a broad distribution ranging from 0 to -500 meV. Recent work by Igasaki et al. (1978) indicates that

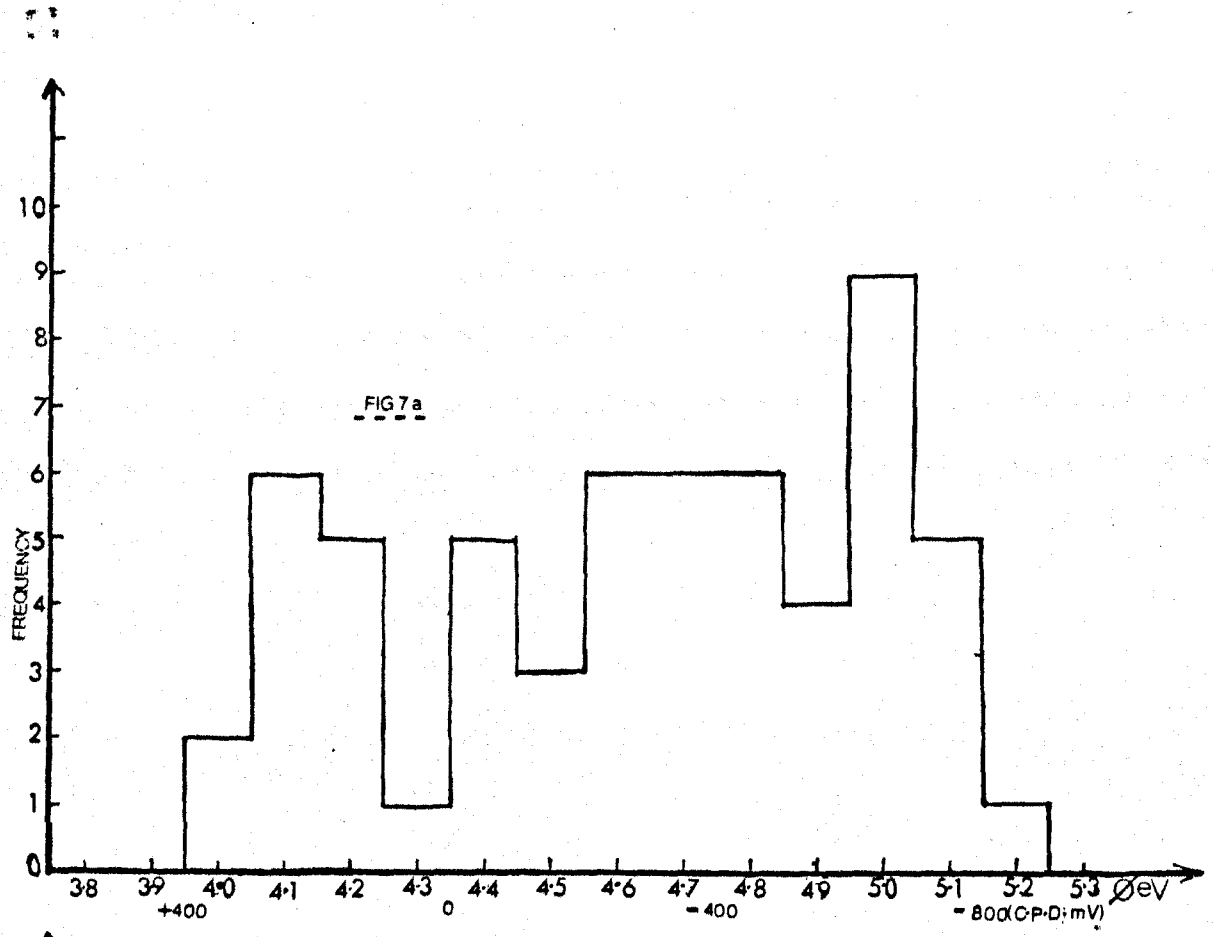
FREQUENCY
0
1
2
3
4
5
6
7
8
9
10
3·8
3·9
4·0
4·1
4·2
4·3
4·4
4·5
4·6
4·7
4·8
4·9
5·0
5·1
5·2
5·3
Øev
+400
0
-400
-800(C·P·D·mV)

FIG 7a

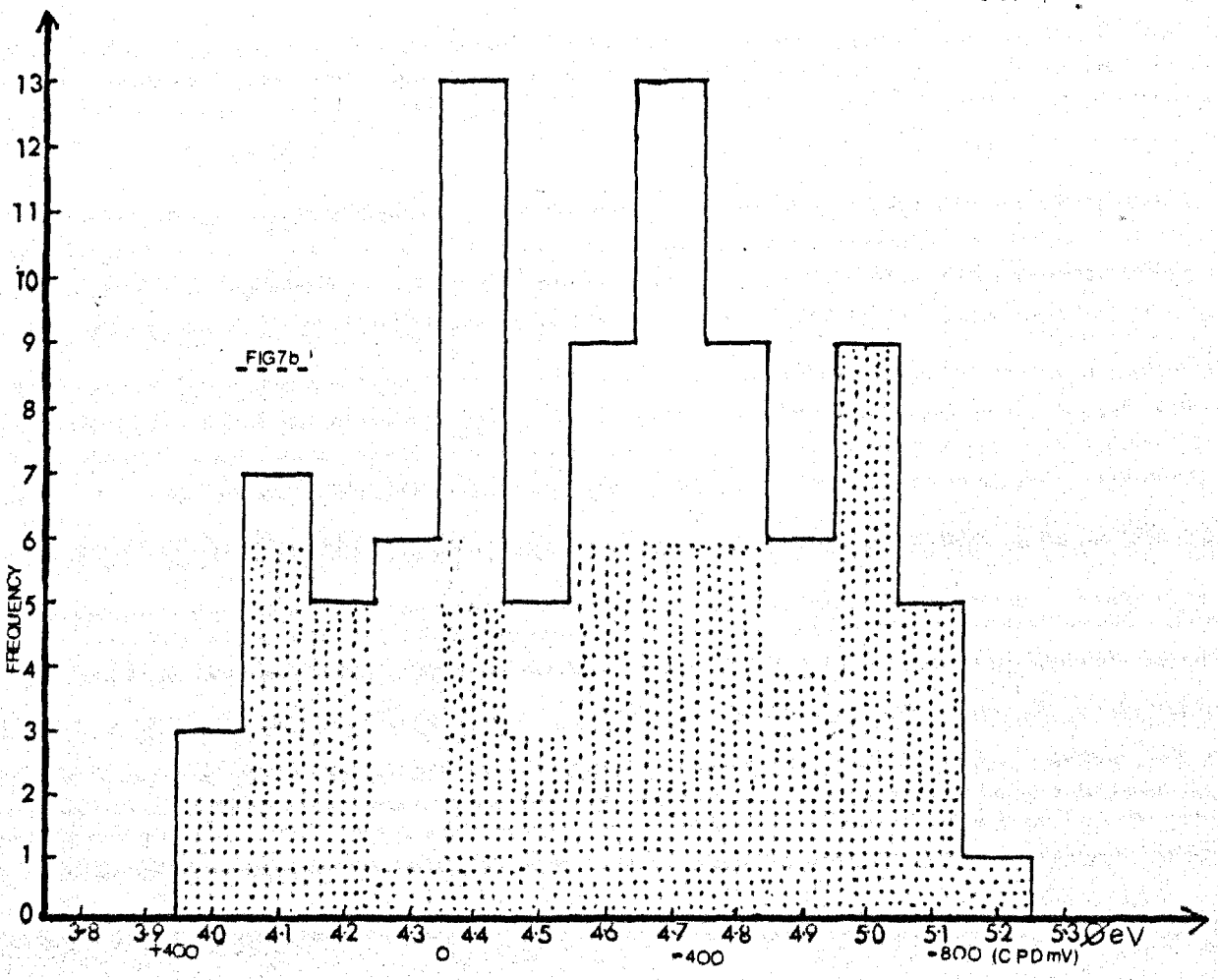
FREQUENCY
0
1
2
3
4
5
6
7
8
9
10
11
12
13
3·8
3·9
4·0
4·1
4·2
4·3
4·4
4·5
4·6
4·7
4·8
4·9
5·0
5·1
5·2
5·3
Øev
+400
0
-400
-800 (C P D mV)

FIG 7b

Table 7.1

Film	CPD(mV)	Film	CPD(mV)	Film	CPD(mV)
Ti 11/1	- 65	Ti 34/1	-425	Ti 57/1	- 35
12/1	-615	35/1	-1390	58/1	+ 90
13/1	-400	36/1	-1580	59/1	-690
14/1	+235	37/1	-440	60/1	-325
15/1	+165	38/1	-225	61/1	-450
16/1	+265	39/1	-650	62/1	+110
17/1	+735	40/1	-590	63/1	-490
18/1	-300	41/1	-340	64/1	-210
19/1	only R	42/1	+300	65/1	- 50
20/1	"	43/1	-150	66/1	-100
21/1	"	44/1	-645	67/1	+100
22/1	"	45/1	-290	68/1	-450
23/1	-620	46/1	-650	69/1	-520
24/1	-720	47/1	-725	70/1	+200
25/1	+265	48/1	-700	71/1	+120
26/1	+235	49/1	-900	72/1	+400
27/1	-1240	50/1	-400	73/1	-120
28/1	-780	51/1	-610	74/1	-260
29/1	-200	52/1	-600	75/1	- 10
30/1	-480	53/1	-800	76/1	-260
31/1	-400	54/1	-640	77/1	+210
32/1	-710	55/1	-600		
33/1	-400	56/1	+310		

Table 7.2

Film	CPD(mV)	Film	CPD(mV)	Film	CPD(mV)
Ti 48/2	-250	Ti 56/2	- 10	Ti 60/5	-100
48/3	-440	58/2	-370	61/2	-255
48/4	+330	59/2	-330	61/3	+130
48/5	-370	59/2[1]	-100	61/4	0
49/2	- 80	53/3	-325	61/5	+250
51/2	-520	59/4	-150	61/6	- 50
51/3	-525	60/2	-305	62/3	- 80
51/4	-440	60/3	-180	62/4	0
53/3	-250	60/4	-350	62/5	-395
55/2	-500				

their titanium films which were evaporated on glass substrates consisted predominantly of (0001) faces for evaporations at low substrate temperatures (< 300°C). In other words it is possible that the films consist predominantly of one low index face which depends on the evaporation conditions. In our experiment the relative position of the titanium filament and glass substrate was not the same in all evaporations. A slight change in the direction of evaporation could probably grow preferentially one of the low index faces over most of the patches at the surface, therefore the C.P.D. would be weighted mainly to one of the low index faces. If this is so, then we can say that the three distributions correspond to the predominancy of three low index faces.

If we assume that the sub-distributions described previously are each due to the predominancy of the one low index face of H.C.P. structure then the distribution around -650 mV (say distribution 1) must be due to the dominancy of the (0001) face; since this is the most closely packed face it will have the highest work function. The distribution around +225 mV (say distribution 2) must be due to the dominancy of the $(10\bar{1}0)$ face; since $(10\bar{1}0)$ is the most openly packed face of the three it will have a lower work function. The third distribution (say distribution 3) must be due to the dominancy of $(10\bar{1}1)$ face. The faces $(10\bar{1}1)$ and $(10\bar{1}0)$ can have two orientations and in general the different orientations of the same face will have different work functions, so this could be the reason why distributions 2 and 3 are more broad than distribution 1.

It is interesting to see here that if we include the C.P.D. values for titanium films (> 100A°) evaporated on titanium oxide substrates (i.e. sandwich films in titanium/oxygen study), then the corresponding distribution is shown in figure 7.b and additional data is given in table 7.2. It is obvious that there is no C.P.D. value corresponding

to distribution 1, i.e. face (0001). Further almost all this data is spread within distribution 3 and has two peaks around -50 mV and -350 mV (which are less intense in the distribution 7.a). These two separate peaks could correspond to the two different orientations of $(10\bar{1}1)$ face. In general the titanium are further apart in the oxide than in the metal, therefore the separation of Ti atoms in an oxide substrate is not well suited to grow (0001) face which could be the reason why there is no C.P.D. value within the distribution 1. It is impossible to grow the metal with Ti atoms above both the titanium atom and the oxygen atom in the oxide substrate, since the Ti-O separation is about 2 A^{o} in all oxides, which is too small for the titanium lattice.

7.2 (a) Titanium-hydrogen study

This study confirmed that a) titanium hydride is a better conductor than titanium, b) the Fermi level in titanium hydride lies at higher energy than in titanium, and c) the titanium dihydride is unstable in high vacuum at room temperature. The resistivity of the titanium films drops by 30% of its initial resistivity when the titanium is converted into titanium dihydride at room temperature. In the meantime the Fermi level effectively rises by about 100-125 meV. The dissociation pressure of titanium dihydride is 2×10^{-3} torr at room temperature, below this pressure the dihydride is unstable and dissociates until the pressure establishes equilibrium with a lower compositions hydride. Further the chemical phase boundaries $\alpha/(\alpha + \gamma)$, $(\alpha + \gamma)/\gamma$ and γ/γ' appear at atomic ratios of 0.08, 1.55 and 1.77 respectively at room temperature. In addition to this the major deductions of this study are a) F.C.T. titanium hydride is a slightly better conductor than F.C.C. titanium hydride, b) the Fermi level in F.C.C. hydride lies at higher energy than in F.C.T. hydride, c) the Fermi level in F.C.T. hydride occurs in the decreasing part of the density of states curve,

d) some of the previously observed anomalies with high composition hydrides can be due to the dissociation of these hydrides, e) hydrogen in titanium diffuses rapidly and the sandwich films used in this study were therefore partially hydrided, f) the sticking coefficient of hydrogen on titanium films is high and decreases linearly across the mixed phase ($\alpha + \gamma$) and g) F.C.T./F.C.C. structural transition temperature of titanium dihydride is about 110°C ($\simeq$ 383°K) which is higher than the previously predicted value 310°K.

(b) Titanium-oxygen study

The interaction of oxygen with titanium films can be divided into two regions. An initial rapid interaction region is followed by a slow interaction region. In the rapid interaction region the work function increases by 1.1 eV and that is mainly due to the change in surface potential. In the slow region the work function decreases by more than 700 meV and this mainly corresponds to a Fermi level shift. Meanwhile the resistance increases in both regions, though relatively very little in the slow region. The increase of work function corresponds to adsorption of oxygen atoms but in the meantime a large amount of oxygen penetrates into the bulk and forms a solution phase. The author believes that the main driving force is the electrostatic repulsion between the oxygen atoms. The drop of work function in the slow region corresponds to oxide formation at the top layers of film. The oxide which is formed at first is not TiO_2 but it is one of the low composition oxides, perhaps TiO. Finally, in the slow interaction region some weakly bonded oxygen atoms also exist at the surface of the film.

(c) Titanium-water vapour study

The interaction of water-vapour with titanium films is accompanied by the emission of large amounts of hydrogen and an increase of film

resistance and an initial drop of work function by about 900 meV followed by 500 meV increase. The interaction can be divided into three regions. The first region mainly corresponds to pure adsorption of water vapour and in this region the resistance almost constant but the work function drops rapidly about 400 meV. In the region two the resistance increases relatively rapidly and the work function drops slowly. The increase of resistance is due to penetration of oxygen atoms which are formed from the dissociative adsorption of water molecules. In the third region the work function reaches a steady value after a gradual increase, and the increase of resistance becomes slow probably due to reduction in the amount of oxygen penetration. The author believes the third region corresponds to the formation of a hydroxyl complex at the surface which is passive for the further sorption of water vapour. Finally in the third region some water molecules become weakly adsorbed and removal of species on pumping increases the work function by 200-250 meV.

7.3 Suggestions for further work

It is clear from the qualitative explanation for the titanium/hydrogen system given in this study that there are many physical processes operating during the interaction of hydrogen with transition metals. It is not possible to make an experimental investigation of one of these processes on its own. But it seems possible to select studies for which one process would be absent; e.g. in the Ce/H system there is no structural transition and in Sc/H system there is no lattice expansion in the mixed phase and in the hydride phase. It would therefore be interesting to conduct the same studies for a collection of transition metal hydrides (Sc, Zr, V, Ce, Er, Yb, and Th) to explore this problem. Further work function measurements would be an experimental test for the band structure calculations (which seems

correctly to have replaced the previous chemical models and the rigid band approximation).

In the case of oxygen studies it seems very unlikely that our method could be used to prepare a sample of titanium oxide of homogeneous composition, and so the results would always be very complex to explain. However it might be a useful method for other transition metals which form only a few fairly widely spaced oxygen-metal phases. It could help other surface techniques such as the various electron spectroscopies to identify the different oxygen compounds of transition metals, like titanium.

APPENDIX A

Suppose the radius of the hydrogen ion ($H^{-\delta}$) is r and the radius of metallic titanium is R. If the centre of the chemisorbed hydrogen ($H^{-\delta}$) atom lies below the surface then ϕ will drop.

Therefore the maximum radius of $H^{-\delta}$ to give a drop of ϕ on 3-fold hollow site is given by the equation

$$(R + r_{max})^2 = (R^2 + \frac{4}{3} R^2) \rightarrow \text{see fig. A}$$

$$\therefore \quad r_{max} = 0.5\ R$$

$$\simeq 0.725\ A^{\circ} \qquad R = 1.45\ A^{\circ}$$

Assume a uniform distribution of charge around the nucleus; one electronic charge distributed in a sphere of radius equal to radius of a negative hydrogen ion which is $1.36A^{\circ}$. Therefore the charge distribution within the sphere of radius with $0.725\ A^{\circ}$ is δ (say)

$$\text{Then} \quad \delta_{max} = (\frac{0.725}{1.36})^3 e$$

$$= 0.16e \qquad \text{ie } H^{-0.16}$$

Maximum radius of $H^{-\delta}$ to give an increase of ϕ on the bridge sites is given by the equation

$$R^2 + R^2 = (R + r_{min})^2 \rightarrow \text{see fig. B}$$

$$r_{min} = 0.414\ R$$

$$\simeq 0.6\ A^{\circ}$$

$$\text{Charge on the H atom} \quad \delta_{min} = (\frac{0.6}{1.36})^3 e$$

$$\delta_{min} = 0.09e$$

$$\simeq 0.1e \qquad \text{i.e. } H^{-0.1}$$

APPENDIX B

From kinetic theory of gases, number of impinging gas molecules on the one cm^2 area of film in one sec is given by

$$N = \frac{3.535 \times 10^{22} P(\text{torr})}{\sqrt{MT}}$$

M - molecular weight

T - temperature degree Kelvin

$\therefore$ For hydrogen at room temperature $20^{\circ}C$

$$N = 14.60 \times 10^{20} \quad P(\text{torr}) \quad \text{molecules of } H_2$$

$$= 29.2 \times 10^{20} \quad P(\text{torr}) \quad \text{atoms of hydrogen}$$

(a) In continuous flow experiment; the film was at a pressure 10^{-9} torr for 90 min to reach the boundary $\alpha/\alpha+\gamma$

$\Sigma N = N.t = N_T$ = total number of impinging atom

$$N_T = 15.768 \times 10^{15} \text{ atoms}$$

assume sticking coefficient $S = 0.17$ Kasemo et al (1979)

$\therefore$ no. of sorbed atoms $= N_S = N_T.S$

$$N_S = 2.68 \times 10^{15} \text{ atoms}$$

No. of Ti atoms in 120 A° thickness $= \frac{120}{3} \times 10^{15}$ atom

$$N_M(\text{say}) = 40 \times 10^{15} \text{ atom}$$

$$r = \frac{N_S}{N_M} = 0.067$$

(b) In dose experiment; Total exposure before maximum

$\alpha/\alpha+\gamma$ boundary $= 3.1.L = \int p\,dt$

then $N_T = 29.2 \times 10^{20} \int p\,dt$

$$= 90.52 \times 10^{14} \text{ atoms}$$

$$N_S = N_T.S \simeq 1.5 \times 10^{15} \text{ atoms}$$

No. of titanium atoms in 100 A° film $\simeq 33 \times 10^{15}$ atom

$\therefore$ $r = 0.045$

APPENDIX C

Assume the average distribution of hydrogen atoms is in all parts of the sandwich film, then its initial resistance is not the parallel resistance of a pure titanium film (which is newly evaporated) and a hydrided substrate film, but rather the resistance of a partially hydrided composite film. We can identify three different resistance values which are :

1) Resistance of a pure titanium film - R_o

2) Initial resistance of a sandwich film - R_x

3) Resistance of a saturated film - R_S

Then from the fresh film's experimental results

$$\frac{R_o - R_S}{R_o} = \frac{\Delta R}{R_o} = 30\%$$

$$\text{where } R_o = R_S + \Delta R \qquad (1)$$

$$\therefore \quad \frac{R_o}{\Delta R} = \frac{R_S + \Delta R}{\Delta R} = \frac{100}{30} \qquad \text{from equation one}$$

$$\frac{R_S}{\Delta R} = \frac{70}{30}$$

$$\Delta R = 0.43\, R_S$$

$$R_o = R_S\,(1 + 0.43) \qquad \text{from equation one}$$

$$R_o = 1.43\, R_S \qquad (2)$$

For every sandwich film we can measure R_S and R_x but not R_o. However we can calculate R_o by using R_S and equation 2. If we know the value of R_o, then $(R_o - R_x)$ will give the drop of resistance due to the presence of hydrogen from the substrate film.

$\frac{R_o - R_x}{R_o}$ will give the percentage drop of resistance.

From a curve of the percentage drop of resistance vs composition we can estimate the initial composition of the sandwich film, but this clearly depends on which curve we choose from fig. 4.a. In the table 4.2 the mean estimate is represented as $r_3(av)$. In all experiments we know that the hydride dissociated until r = 1.9 at room temperature and 10^{-8} torr. However during the degassing of the titanium filament at its evaporation, the temperature of the substrate film can rise (possibly up to $75^{o}C$) and the base pressure can drop to 10^{-9} torr. Therefore for a first approximation we can assume that at the end of the evaporation the substrate film effectively has r = 1.8. Further we know the values of R_o measured for the substrate film and calculated for the sandwich film. Therefore, we can estimate the thickness of the substrate film $-d_1$ and the sandwich film d_2 from the resistance vs thickness curve fig. 2.f. From these data the possible initial composition of a sandwich film is given by $(d_1 \times 1.8)/d_2$. These values in the table 4.2 are represented as r_2.

From M to P the observed average drop of ϕ is about 300meV (Fig. 4.b) and the average composition changes from 0.08 to 1.78. The drop in ϕ is almost linear in this region, therefore the change of r corresponding to 1meV drop is 5.666×10^{-3}. Suppose a sandwich film experiment gives only ϕ_d meV drop then due to "sandwich effect" we missed $(300-\phi_d)$meV. This corresponds to a composition change = $5.66 \times 10^{-3} \times (300-\phi_d)$

$\therefore$ The starting composition of the sandwich film = $0.08 + 5.66 \times 10^{-3}$ $(300-\phi_d)$. and this is represented as r_1 in the table 4.2.

APPENDIX D

The change in the composition Δr at the minimum P due to temperature increase from $20^{\circ}C$ to $50^{\circ}C$ can be estimated from parts (b) and (c) of the third experiment described in section 4.1.F.

From Part (b):

Generally the increase of ϕ near the saturation is about 150meV for $\Delta r = 0.22$

$$\frac{\Delta r}{\Delta \phi} = \frac{0.22}{150} \quad \Delta r_{20} \text{ corresponds to 10meV rise (see Fig. 4.g).}$$

$$\therefore \quad \Delta r_{20} = \frac{0.22}{150} \times 10 = 0.017$$

For first approximation we can assume rate of drop of ϕ $(\frac{\Delta \phi}{\Delta r})$ between M and P at $50^{\circ}C$ is the same as at $20^{\circ}C$

$$\therefore \quad \frac{\Delta \phi}{\Delta r} = \frac{300}{1.7} \text{ meV}$$

Δr_{50} corresponds to 10meV drop

$$\Delta r_{50} = \frac{1.7}{300} \times 10 \simeq 0.056$$

$$\therefore \quad \Delta r \simeq r_{20} + r_{50} = 0.017 + 0.56$$

$$\Delta r \simeq 0.073$$

From Part (c):

See Fig. 4.g, 90meV increase corresponds to Δr^{1}_{20}

$$\Delta r^{1}_{20} = \frac{0.22}{150} \times 90$$

$$= 0.132$$

at $50^{\circ}C$, generally we can expect an average of 100meV increase of ϕ, $\therefore$ 93meV increase could correspond to $\Delta r = 0.132$ see Fig. 4.g.

$$\therefore \quad \Delta r^{1}_{50} = \frac{0.132}{93} \times 100$$

$$= 0.142$$

$$\Delta r = 0.22 - \Delta r^{1}_{50}$$

$$\therefore \quad \Delta r = 0.22 - 0.142$$

$$= 0.078$$

$$\therefore \quad \Delta r_{(av)} = 0.075$$

APPENDIX E

We can estimate the transition temperature in two ways

(1) The increase of ϕ near saturation due to the presence of F.C.T hydride, is 150meV at 20°C, but is 100meV at 50°C. In other words a temperature increase 30°C is able to reduce the ϕ increase by 50meV.

Suppose T_c is the transition temperature at which no F.C.T hydride exists. In other words the ϕ increase is equal to zero. Therefore we can say that the temperature increase $(T_c - 20)$ will reduce the ϕ by 150meV

$$\therefore \quad \frac{T_c - 20}{150} = \frac{50-20}{50}$$

$$T_c = 110^{\circ}C$$

(2) Suppose at 20°C the F.C.C. hydride exist up to saturation

Then the extrapolation will give an additional drop of

$$\phi \simeq \frac{300}{1.7} \times 0.22\text{meV}$$

$$= 40\text{meV}$$

$$\frac{\Delta\phi}{\Delta T} \text{ for F.C.C single phase hydride} = \frac{5}{30} \text{ meV/ } ^{o}C$$

$$\frac{\Delta\phi}{\Delta T} \text{ for F.C.T single phase hydride} = \frac{60}{30} \text{ meV/ } ^{o}C$$

Suppose T_c^{o} C is the transition temperature at which the Fermi level of F.C.C and F.C.T dihydride are the same. Then there is no preference for F.C.T structure over F.C.C. structure. In other words F.C.C is stable up to saturation.

$$\therefore \quad (T_c - 20)\ \frac{5}{30} + 190 \quad (T_c - 20)\ \frac{60}{30}$$

$$T_c \approx 120^{o}C$$

APPENDIX F

Estimation for ionization in F.C.C titanium hydride.

Let us assume the rigid band approximation is valid. Then we can say that the observed Fermi level rise ($\Delta\phi$) in our experiment is due to the occupation of Ti band by electrons from hydrogen atoms. Therefore if we calculate the number of electron states N_1 within the energy range of ΔE_F ($=\Delta\phi$) in Ti then we can estimate the ionization of hydrogen δ.

To estimate N_1 - the electron state we would have to know N(E) within the range ΔE_F, but this is unknown. But if we know the $N(E_F)$ for $TiH_{1.75}$ then we can estimate an upper limit for the number of states and ionization.

Ducastelle et al. experimental estimation for $N(E_F)$ for $TiH_{1.75}$ is 0.80 states /eV atom, which is in agreement with the calculated values of Gupta's (1979) Kulikov et al. (1978), and Switendick's (197) for F.C.C TiH_2.

Therefore if we assume Ducastelle et al. value

Then $N_1 = 0.80 \times 0.300$ states

$$\delta = \frac{N_1}{1.75} \simeq 0.14$$

$\therefore$ Ionization of hydrogen = 0.14e.

APPENDIX G

An alternative hypothesis is that the phase-boundary occurs at 0.1 atomic % (Vitt et al 1971) which could not be observed in these experiments. An alternative explanation for point A might be saturation of surface and grain boundary sites by hydrogen.

REFERENCES

Altmann,S.L., Coulson, C.A. and Hume-Rothery, W. 1957 Proc Roy Soc (Lon) A240, 145

Anderson, P.A. 1941 Phy Rev 59, 1034

Anderson, P.W. 1961 Phy Rev 124, 41

Anderson, J.R. and Thompson, N. 1971 Surf Sci 26, 397

Andersson, S., Collen, B., Kuylenstierna, U. and Magnelli, A. 1957 Acta Chem Scand 1, 1641

Andersson, S. and Nyberg, C. 1975 Surf Sci. 52, 489

Andrievskii, R.A. Boiko, E.B. and Ioffe, R.B. 1967 Inorg Metals (U.S.S.E.) 3, 1385

Arai, T. and Hirabayashi, M. 1976 J.Phy Soc Jap 41, 1236

Ashcroft, N.E. and Mermin, D.N. ed Dorothy Garbose 1976 Crane, U.S.A.

Auger, P. 1925 J. Phys Radium 6, 205

Azarkh, Z.M., Funin, V.N. and Yureva 1967 Sov Phy Solid State 9, 1066

Azarkh, Z.M. and Gavrilov, P.I. 1970 Sov Phy cryst 15, 231

Bagchi, A., Gomer, R. and Penn, D.R. 1974 Surf Sci 40, 555

Baker, F.A. 1965 Mass Spect Symp AEI MS10, 51

Baker, M.M. and Rideal, K.E. 1954 Nature 1974, 1185

Baloock, M. Cardillo, M.J., Miller, D.R. and Stickney, R.E. 1974 Surf Sci 46, 358

Banus, M.D., Reed, T.B. and Strauss, A.J. 1972 Phy Rev 135, 2775

Baskin, E.M., Chaplik, A.V. and Entin, M.V. 1976 Sov Phy JETP 36, 566

Bassett, P.J. and Gallon, T.E. 1973 J Electron Spectra & Rel Phenom 2, 101

Batt, R.J. and Mee, C.H.B. 1970 Appl Optics (U.S.A.) 9, 79

Beacker, J.A. 1961 in Actes du Deuxiene congr intern catalyse Paries, 1977

Beavis, L.C. 1969 J. Less Common Metal 19, 315

Beck, D.E. and Miyazaki 1975 Surf Sci 48, 493

Beck, R.L. 1960 U.S.A.E.C. Report LAR-10 Denver Research Institute

Beeby, J.L. 1966 Phy Rev 141, 781

Benndrof, C., Egert, B., Keller, G., Siedel, H. and Thieme, F. 1978 J. Vac Sci & Tech 15, 1806

Benndrof, C., Egert, B., Nobl, C., Siedel, H. and Thieme, F. 1980 Surf Sci 92, 636

Benninghoven, A., Ganschow, O. and Wiedmann 1978 J. Vac Sci Tech 15, 506

Benninghoven, A., Muller, K.H., Plog, C., Schemmer, M. and Steffens, P. 1977 Surf Sci 63, 403

Bickel, P.W. 1960 U.S.A.E.C. Report NAASR 4173

Bickel, P.W. and Berlincourt, T.G. 1970 Phy Rev 82, 4807

Blyholder, G. 1975 J. Chem Phy 62, 3139

Blyholder, G. and Sheets, R.W. 1975 J Catalysis 39, 152

Bliznakov, G.M., Lazarov, D.L., Manev, S.G. 1972 Comptes rendus del'Academk bulgare

Bond, G.C. 1969 Surf Sci 18, 11

Bouwman, R., Lippits, G.J.M. and Sachtler, W.M.H. 1972 J. Catal 25, 350

Brearley, W. and Surplice, N.A. 1977 Surf Sci 64, 372

Brennan, D., Hayward, D.O. and Trapness, B.M.W. 1960 Proc Roy Soc (Lon) A256, 81

Brocker, F.J. and Wedler, G. 1971 Surf Sci 26, 454

Brucker, C.F., Rhodin, T.N. 1976 Surf Sci 57, 536

Brüning, H. and Sieverts, A. 1933 Z Phys Chem (Leipzig) 163 (Part A) 409

Bullett, W. and Cohen, M.L. 1977 J Phy C 10, 2083

Butz, R. and Wagner, H. 1977 Surf Sci 63, 448

Butz, R. and Wagner, H. 1977 Appl Phys 13, 37

Cabrera, N. and Mott, N.F. 1949 Rep Prog Phys 12, 163

Callaway, J. and Edwards, D.M. 1960 Phy Rev 118, 923

Callaway, J. 1961 Phy Rev 121, 1351

Christmann, K., Schöber, O, Erth, G. 1974 J Phys Chem 6o, 4719

Christmann, K. Schöber, O. and Newmann, M. 1974 J Chem Phy 60, 4528

Christmann, K., Erth, G. and Pignet, T. 1976 Surf Sci 54, 365

Christmann, K, Behm, R.G., Erth, G., Van Hove, M.A. and Weinberg, W. 1979 J Chem Phy 70, 4168

Colmenares, C.A. 1975 Prog Solid State Chem 9, 105

Conarad, H., Erth, G. and Latt, E.E. 1974 Surf Sci. 41, 435

Cotton, F.A. and Wilkinson, G. 1972 Adv Inorg Chem. Inter-Science

Crossland, W.A. and Pritchard, J. 1964 Surf Sci 2, 217

Culver, R.V. and Tompkins, F.C. 1959 Adv Catal 61

Curzon, A.E. and Singh, O. 1978 J Phy F 8, 1619

Curzon, A.E. and Singh, O 1979 Thin Solid Films 59, 157

D'Arcy, 1971 Ph.D. Thesis Univ of Keele

Dawson, P.H. 1977 Surf Sci 65, 41

Dawson, P.T. and Peng, Y.K. 1980 Surf Sci 92, 1

Delchar, T.A., Eberhagen and Tompkins, F.C. 1963 J. Sci Inst 90, 135

Delchar, T.A. and Tompkins, F.C. 1977 Surf Sci 8, 165

Delchar, T.A. and Tompkins, F.C. 1968 Trans Fara Soc 64, 1915

Delchar, T.A. 1971 Surf Sci 27, 11

Delchar, T.A. and Tompkins, F.C. 1975 Trans Fara Soc 64, 1915

de Boer, J.S.W., Krusmeyer, H.J. and Burhoven-Jaspers, N.C. 1973 Rev Sci Intru 44, 1003

Demuth, J.E. and Rodin, T.N. 1974 Surf Sci 45, 249

Demuth, J.E. 1977 Surf Sci 67, 369

Dowdin, D.A. "in Chemisorption" Ed Gayner, W.E. 1958 Butterworths, London.

Dooley, G. and Hass, J.W. 1970 J. Chem Phys 52, 993

Ducastelle, F., Caudron, R. and Costa, D. 1970 J. de Phys 31, 57

Duess, H. and Van Der Avoird 1973 Phy Rev 86, 2441

Dus, R. 1973 Surf Sci 42, 324

Dus, R. 1975 Surf Sci 52, 440

Dus, R. and Lisowski, W. 1976 Surf Sci 61, 635

Duppel, H. and Fromm, E. 1976 Z. Metalld 67, 40

Dwyer, D.J., Simmons, G.M. and Wei, R.P. 1977 Surf Sci 64, 617

Djubua, B. Ch., Kullashew, D.K. and Gorshkova, L.V. 1966 Sov Phy Solid State 8, 882

Eastman, D.E. 1970 Phy Rev B2, 1

Eastman, D.E., Cashion, J.K. and Switendick, A.C. 1971 Phy Rev lett 27, 35

Eastman, D.E. 1972 Solid State Commu 10, 933

Eberhardt, W. and Kunz, C. 1978 Surf Sci 75, 709

Eggleton, A.E.J. and Tompkins, F.C. 1952 Trans Fara Soc 48, 738

Eley, D.D. and Wilkinson, P.R. 1960 Proc Roy Soc (Lon) A254, 339

Eley, D.D. and Norton, P.R. 1966 Disc Fara Soc 41, 135

Eley, D.D. and Moore, P.B. 1978 Surf Sci 76, L599

Ern, V. and Switendick, A.C. 1965 Phy Rev 137, A1927

Fain, S.C., Corbin, L.V. and McDavid, J.M. 1976 Rev Sci Instru 47, 354

Fassaert, D.J.M. and Van Der Avoird 1976, Surf Sci 55, 313

Fehlner, F.D. 1966 Nature 210, 1036

Fehrs, D.L. and Stickney, R.F. 1967 Surf Sci 8, 267

Feibelman, P.J. and Hamann, D.R. 1980 Phy Rev 821, 1385

Filion, A., Nerov, J.P. and Giraud, D.E. 1975 J. Phy E 5, 468

Fletcher, R., Ho, N.S. and Manchester, F.D. 1970 Metal Phys Suppl 1, 559

Fort, T. Jr. and Wells, R.L. 1972 Surf Sci 32, 543

Fowler, R.H. 1931 Phy Rev 38, 45

Friedel, J. 1969 in "Phys of Metal 1: Electron" ed Ziman, P.M., 340

Friedel, J. 1972 Ber Bun Phy Chem 76, 828

Fromm, E. and Mayor, O. 1978 Surf Sci 74, 259

Fromm, E. 1977 Proc 7th intern Vac cong & 3rd intern conf Solid Surf (Vianna) 889

Fuggle, J.C., Watson, L.M., Fabian, D.J. and Affrossmann, S. 1975 Surf Sci 49, 61

Fugiwara, K. and Ogata, H. 1979 Surf Sci 86, 700

Fukai, Y., Kajama, S., Tamaka, K. and Matsumto, M. 1979 Solid State Comm 19, 507

Fukuda, Y., Elam, W.T. and Park, R.L. 1978 Appl Surf Sci 1, 278

Fukuda, Y., Honda, F. and Rabalais, J.W. 1980 Surf Sci 91, 165

Gallagher, J.G. and Haydock, R. 1979 Surf Sci 83, 117

Gesi, K., Takagi, Y. and Takeuchi, T. 1963 J. Phys Chem Jap 18, 309

Gesi, K., Takagi, Y. and Takeuchi, T. and Noguchi, S. 1964 in "nuclear metallurgy intern symp" ed Weber J.T., Chiott, P. and Minev, W. (AIME) NY, P45

Geraghty, K.G. and Donaghey, L.E. 1977 Thin Solid Films 40, 375

Geus, J.W. 1964 Surf Sci 2, 48

Gewinner, G., Peruchetti, J.C., Talgle, H. and Kalt, H. 1978 Surf Sci 78, 439

Gibb, T.R.P. Jr. 1962 Proc Inorg Chemistry Vol 3. Interscience N.Y.

Gibb, T.R.P. Jr. 1963 Adv Chem Ser 39, 99

Gibb, T.R.P. Jr., McCharry, J.J. and Bragdon, R.W. 1951 J. Amer Chem Soc 73, 1751

Gimzewski, J.K., Padalia, B.D., Affrossman, S.A., Watson, L.M. and Fabian, D.J. 1979 Surf Sci 80, 298

Goodenough, J.B. 1960 Phy Rev 120, 67

Graham, T. 1866 Phil Trans Roy Soc 156, 415

Grimley, T.B. 1967 Proc Roy Soc 90, 751

Gubanov, V.A., Kumaev, E.Z. and Shveikin, G.P. 1977 J. Phy Chem 38, 201

Gundry, P.M. and Tompkins, F.C. 1968 Surface potential, in "experimental methods in catalic research" ed Anderson, R.B. Academic Press

Gupta, M. 1979 Solid State Comm 29, 47

Gurney, R.W. 1935 Phy Rev 47, 479

Guse, M.P., Blint, B.A. and Kurz, A.B. 1977 Intern J Quant Chem 11, 725

Hall, C.G. and Mee, C.H.B. 1971 Surf Sci 28, 598

Harries, L.A. 1968 J. Appl Phy 39, 1419, 1428

Hass, G.A. and Thomas, R.E. 1966 Surf Sci 4, 64

Hass, T.W. 1968 J. Appl Phy 39, 5854

Hawson, A.C. and Newns, D.M. 1974 Jap J. App Phys Suppl 2 Pt 2, 121

Hayes, F.H., Hill, M.P., Lechini, M.A. and Pathica, B.A. 1965 J. Chem Phy 42, 2919

Haydock, R., Heine, V. and Kelly, M.J. 1972 J. Phy C 5, 2845

Hayward, D.O. and Trapnell, B.M.W. 1964 Chemisorption 2nd edn Butterworths, London

Heckman, R.C. 1969 U.S.A.E.C. report No SS-R.R-69-771

Hemeka, H.F. 1975 Quantum theory of chemical bond, Hafner Press P77

Henrich, V.E., Zeiger, H.J. and Reed, T.B. 1978 Phy Rev 19, 4121

Hill, R.V., Stephanakos, E.K. and Tinder, R.F. 1971 J. Appl Phy 42 4296

Hillig, W.B. 1953 Ph.D. Thesis Univ of Michigan

Hirohiko, A. and Shosuke, I. 1979 J. Phy Soc Jap 46, 1194

Hodges, L., Ehrenreigh, W. and Lank, N.D. 1966 Phy Rev 152, 55

Hofmann, P., Wyrobisch, W. and Bradshaw, A.M. 1979 Surf Sci 80, 344

Hohenberg, P. and Kohn, W. 1964 Phy Rev 136B, 864

Holze, J. and Schrammen, P. 1974 J. Appl Phy 3, 353

Holze, J. and Porsch, G. 1975 Thin Solid Films 28, 93

Holze, J. and Schulte, F.K. 1979 Solid Surf Phys Vol 85 Springer tracts in modern phys, Springer Verlag - Berlin Heidelberg N.Y.

Holmberg, B. 1962 Acta chem Scand 16, 1245

Hopkins, B.J., Mee, C.H.B. and Parker, D. 1956 Brit J. Appl Phy 15, 865

Hopkins, B.J. and Davies, D.E. 1959 Brit J. Appl Phy 10, 498

Hopkins, B.J., Williams, C.B. and Wilmer, P.C. 1971 Surf Sci 25, 633

Hopster, H., Bundle, C.R. 1979 J. Vac Sci & Tech 16, 548

Huber, E.E. Jr and Kirk, C.T. Jr. 1966 Surf Sci 5, 47, 447

Ibach, H. and Lehwald 1980 Surf Sci 91, 187

Igasaki, Y. and Mitsuhashi, H. 1978 Thin solid films 51, 33

Irving, P.E. and Beevers, C.J. 1971 Metallurgical Trans 2, 613

Ito, T. and Kadowaki, T. 1977 Proc 7th Intern Cong and 3rd Intern Conf Solid Surfaces (Vinna) Vol 2, 972

Jepsen, R.L., Francis, A.B., Rutherford, S.L. and Kiezmann, B.E. 1960 Trans A.V.S. Soc Symph 7, 45

Jewsbury 1977 J. Phy C, 10, 681

Johnson, K.H. 1977 Intern J Quant Chem Symph 11, 39

Johansson, L.I., Hagstrom, A.L., Platau, A. and Karlson, S.E. 1977 Phys status solidi (b) 83, 77

Jona, F. 1977 Surf Sci 68, 204

Jones, R.O., Jennings, P.J. and Painter, G.S. 1975 Surf Sci 53, 409

Joyner, R.W., Roberts, M.W. and Yates, K. 1979 Surf Sci 87, 501

Joyner, R.W. and Roberts, M.W. 1979 Chem Phy Lett 60, 459

Kachalkin, A.K., Krumshkin, Z.V., Petrukhin, V.I., Suvorov, V.M., Horvath, D., Yuttandov, I.A. 1977 Zh Eksh Teor 735, 1975

Kaminsky, M. 1965 Atomic and Ionic Impact Phenomena on Metal Surfaces Springer Verlag N.Y.

Kasemo, B. 1977 Proc 7th Intern Vac Cong and 3rd Intern Conf Solid Surf (Vinna) vol 11 899

Kasemo, B. and Torquist, E. 1979 Appl Surf Sci 3, 307

Kasemo, B. and Tornquist, E. and Johnansson, P.K. 1979 Chem Phys Lett 68, 416

Kawasaki, K., Sugita, T. and Ebesawa, S. 1967 Surf Sci 7, 502

Kirk, C.T. Jr. and Huber, E.E. Jr 1968 Surf Sci 30, 263

Klemperer, D.F. 1962 J App Phys 33, 1532

Knapp, A.G. 1973 Surf Sci 34, 289

Knotek, M.L. 1980 Surf Sci 91, L17

Kohn, W. and Sham, L.T. 1965 Phy Rev 140A 1133

Koiwa, M. and Hirabayashi, M. 1969 J. Jap Phy Soc 27, 807

Korn, C. and Zamir, D. 1970 J. Phy Chem Sol 31, 489

Korn, C. 1977 Hydrides for energy storage Proc Intern Symp ed Anderson, A.F., Macland 1978, p119

Korn, C. 1978 Phy Rev B17, 1707

Konishi, R. and Koto, S. 1976 J. Jap APP Phy 15, 1237

Krishman, N.G., Delgass, W.G. and Robertson, W.P. 1976 Surf Sci 57, 1

Krueger, W.H. and Pollack, S.R. 1972 Surf Sci 30, 263

Kucherov, R., Markin, V. Ya, Savin, W.I. and Tapulskii, W.D. 1978 Izvestiya Akad Wauk S.S.S.R. Neorg Meter 14, 1678

Kulikov, V.I., Bonzunov, V.N. 1978 Phy Stat Sol (b) 86, 83

Kulikov, V.I. and Bonzunov, V.N. 1978 Izvestiya Akad Nauk S.S.S.R. Neorg Meter 14, 1659

Lang, N.D. and Williams, A.R. 1975 Phy Rev Lett 34, 531

Lang, N.D. 1973 Solid State Phys 28 ed Ehrenreich, H., Seity, H. and Turnball, P. Academic Press N.Y. London

Lang, B., Joyner, R.W. and Somarzai, G.A. 1972 Surf Sci 30, 454

Languir, I. 1916 J. Am Chem Soc 38, 2221

Languir, I. 1932 J. Am Chem Soc 54, 798

Lawless, K.R. 1974 Report Prog Phys 37, 231

Lenning, G.A., Craighead, C.M. and Jafee, R.I. 1954 AIME Trans 200, 367

Lennard-Jones, J.E. 1932 Trans Fara Soc 28, 28

Lagare, P., Claire, L.H., Sotto, M. and Maire, G. 1980 Surf Sci 91, 175

Lewis, R. and Gomer, R. 1969 Surf Sci 17, 333

Libowitz, G.G. 1958 Acta meta 6, 133

Libowitz, G.G. 1965 Prog solid state chem, vol 2, ed Reiss

Libowitz, G.G. 1965 The solid state binary metal hydrides ed Benjamins, W.A., N.Y.

Libowitz, G.G. and Park, J.G. 1969 J. Chem Phy 50, 3557

Libowitz, G.G. 1972 Solid State Chemistry, Inorganic Chemistry series 10, ed Roberts, L.E.J. Butterworths Univ Park Press

Lo-Wei-Jen, Yip-Wah-Chung and Somoryai, G.A. 1978 Surf Sci 71, 199

Lohoczky, S.L., Lederich, R.J. and Bellina, J.J. Jr. 1978 Thin Solid Films 55, 125

Lopez, F., Aguilar 1979 Phys Solidi Status (b) 9, 1971

Madey, T.E. 1972 Surf Sci 29, 571

Madey, T.E. and Yates, J.T. 1970 Coll intern C.N.R.S. Paries 187, 155

Madey, T.E. and Czyzeucki, J.T. and Yates, J.T. 1975 Surf SCi 48, 465

Magee, C.B. 1967 Denver Research Institute

Malinowski, M.E. 1976 J. Nuclear Mater 63, 386

Malinowski, M.E. 1978 J. Nuclear Mater 71, 368

Malyuchkov, O.T. and Finkelshekin, B.N. 1959 Dokl Akad Nauk S.S.S.R. 127, 822

Martinson, C.W.B. and Flodstrom, S.A. 1979 Surf Sci 80, 306

Matheiss 1972 Phy Rev 5, 290, 306

McQuillan 1950 Proc Roy Soc (Lon) Ser A 204, 309

Melius, C.F., Moskowitz, J.E., Mortola, A.P., Backlbe, M.B. and Ratner, M.A. 1976 Surf Sci 59, 279

Mignolet, J.C.P. 1955 Rec Tran Chim Phys Bas 74, 68

Mignolet, J.C.P. 1957 J. Chem Phy 54, 19

Miller, R.J. and Satterthwaite, 1975 Phy Rev Lett 34, 144

Mints, R.I., Melikhim, V.P. and Rartenskii, M.B. 1975 Sov Phy Solid State 10, 2330

Monnier, R, Pendev, J.P., Langreth, D.C., Wilkins, J.W. 1978 Phy Rev B18, 659

Moon, R.M. 1964 Phy Rev 136, P195

Mook, H.A. and Shull, C.A. 1966 J. Appl Phy 37, 1034

Moore, K.E. and Young, W.A. 1968 J. Nucl Mater 34, 125

Mott, N.F. and Stevens, K.W.H. 1957 Phil Mag 2, 1364

Mott, N.F. 1964 Adv Phy 13, 325

Motte, F., Coddet, C., Sarrazin, P., Azzopardi, M., Besson, J. 1976 Oxidation of metals 10, 113

Mueller, W.M., Blackledge, J.P. and Libowitz, G.G. 1968 Metal hydrides Academic Press N.Y.

Müller, A. and Benninghoven, A. 1974 Surf Sci 41, 493

Müller, E.W. 1943 Z Phys 120, 261

Müller, J. 1977 Surf Sci 69, 708

Müller, J. and Surplice, N.A. 1977 J. Phys D 10, 213

Murgulescu, I.G. and Nonescu, N.I. 1966 Rev Roumaine Chem 11, 1035

Murgulescu, I.G. and Ionescu, N.I. 1971 Thin solid film 7, 355

Nagel, H. and Gorelzki, H. 1975 J. Phy Chem Solid 36, 431

Nathan, R. and Hopkins, L.J. 1974 J. Phy E 7, 851

Nemchenko, V.F., Savin, V.I. and Charnelskii, V.G. 1975 Izvestiyo Akad Nauk S.S.S.R. Neorga Mater 11, 649

Newns, D.M. 1969 Phy Rev 178, 1123

Newns, D.M. 1970 Phy Rev B1, 3304

Nornes, S.B. and Meisenheimer, R.G. 1979 Surf Sci 88, 191

Norton, P.R., Tapping, R.L., Goodale, J.W. 1977 Surf Sci 67, 13

Nyberg, C. 1975 Surf Sci 52, 1

Oxley, A.E. 1922 Proc Roy Soc (Lon) A101, 264

Padalia, B.D., Gimzewski, J.K., Affrossman, S., Lang, W.C., Watson, L.M. and Fabian, D.J. 1976 Surf Sci 61, 468

Parker, D.S. 1960 U.S.A.E.C. report APEX-558

Parks, C.D. and Bos, B.G. 1970 J. Solid State Chem 2, 61

Pauling, L. and Ewing, F.J. 1948 Ibid 70, 1660

Pearson, D. 1958 J. Phy Chem Solid 5, 316

Phillips, J.C. and Muller, M.F. 1967 Phy Rev 155, 594

Pimentel, G.C. and Spratley, R.D. 1970 Chemical Bonding Clarified through Quantum Mechanics, 2nd Printing Holden-Day Inc

Pinto, H., Korn, C., Goren, S. and Shakleed, H. 1979 Solid State Comm 32, 397

Platau, A., Johansson, L.I., Hagstrom, A.L., Karlessons, E. and Hagstrom S.B.M. 1977 Surf Sci 63, 153

Porte, L., Demosthenous, M. and Duc, T.M. 1977 J. Less-Comm Metals 59, 183

Pritchard, J. 1965 Trans Fara Soc 51, 437

Prude, J.A. and Tsong, I.S.T. 1971 Trans Fara Soc 67, 297

Reichardt, J.W. 1972 J. Vac Sci Tech 9, 548

Renouprez, A.J., Foucl1oux, P,, Candy, J.P. and Tomkinson, J. 1979 Surf Sci 83, 285

Rivière, J.C. 1965 Brit J. App Phys 15, 1341

Rivière, J.C. 1965 Mass Spect Symp AEIMS 10, 1

Rivière, J.C. 1965 Brit J. Appl Phys 16, 1507

Rivière, J.C. 1967 Nuovo Cim Suppl 5, 407

Rivière, J.C. 1968 in "Solid State Surf Sci" Vol 1 ed Green, M. (Decker, NY) Chap 4, pp179

Roberts, J.K. 1935 Proc Roy Soc (Lond) A152, 445

Roberts, M.W. 1970 Recent Prog Surf Sci 1

Roy, R. and White, W.B. 1972 J. Crystal Growth 13-14, 78

Rye, R.R., Bradford B.D. and Canlier, P.G. 1973 J. Chem Phy 59, 1963

Satchler, W.H.M. and Dargelo, G.H.J. 1959 J. Chem Phy 54, 27

Satchler, W.H.M. and Dargelo, G.J.H. 1960 Z Physik Chem NF 25, 69

Satchler, W.H.M. and Dargelo, G.J.H. 1966 Surf Sci 5, 221

Schwarz, J.A. and Polizzotti, R.S. and Burton, J.J. 1977 Surf Sci 67, 10

Schaieffer, J.R. and Gomer, R. 1971 Surf Sci 25, 315

Schodt, M. and Walton, A.J. 1977 Phy Lett 60A, 53

Sham, L.J. and Kohn, W. 1966 Phy Rev 145, 561

Sharma, S.P. 1979 J. Vac Sci & Tech 16, 557

Shih, H.D., Jona, F., Jepsen, D.W. and Marcus, P.M. 1976 J. Phy C 9, 1405

Shih, H.D. and Jona, F. 1977 Appl Phys 12, 311

Shull, C.G. 1963 Electronic structure and alloy chem of the transition elements (Interscience, Publishers, Inc. N.Y.) 69

Sidhu, S.S., Heaton, L. and Zauberis, D.D. 1956 Acta Crystallag 9, 607

Sidhu, S.S., Satyamurthy, N.S. Compos, F.P. and Zauberis, P.A. 1963 Advan Chem Ser 39, 87

Simmons, G.W., Mitchell, D.F. and Lawless, K.R. 1967 Surf Sci 8, 130

Singh, B., Muller, J. and Surplice, N.A. 1974 Thin Solid Films 21, 255

Singh, B., Surplice, N.A. and Muller, J. 1976 J. Phy D 9, 2087

Singh, B., 1971 Ph.D. Thesis, University of Keele

Singh, S. 1976 Ph.D. Thesis, University of Keele

Slater, J.C. 1965 Quantum theory of molecules and solids Vol 2
McGraw-Hill Inc

Smith, T. 1973 Surf Sci 38, 292

Somarajai, G.A. and Morgan, A.E. 1968 Surf Sci 12, 501

Somenkov, V.A., Zembianov, M.G., Kost, M.E., Chernoplekov, H.A.
and Cherlkov, A.A. 1968 Doklady Akad Nauk S.S.S.R. 18, 156

Stalinski, B. 1972 Ber Bun Phy Chem 79, 724

Stalinski, B. and Buganski, Z. 1960 Bull Akad Polan Sci Ser Sci Chim
8, 243

Stalinski, B., Coogan, C.K. and Gutowsky, H.S. 1961 J. Chem Phy 24, 1191

Stalinski, B. and Zogal, O.J. 1967 Collg Int C.N.R.S. No. 157, 483

Stevels, J.M. 1957 Handbook of Phys Vol 20, 550 ed Flugg, S.

Steinberg, R. and Alger, D.L. 1973 J. Vac Sci & Tech 10, 246

Stolz, M. and Dittman, R. 1974 Prakt Metalogv 11, 311

Stranski, I.Z. 1928 Phy Chem 139, 259

Suhrmann, R., Mizushima, Y., Hermann, A. and Wedler, G. 1959
Z. Physiks Chem (Frankfurt) 20, 332

Suhrmann, R., Hermann, A. and Wedler, G. 1962 Z. Physik Chem (Frankfurt)
35, 155

Suhrmann, R., Heras, J.M., Viscido der Heras, A. and Wedler, G. 1964
Ber Bun Phy Chem 68, 990

Suhrmann, R., Heras, J.M., Viscido de Heras, L. and Wedler, G. 1968
Ber Bun Phy Chem 72, 1968

Surplice, N.A. and Kandasamy, K. 1978 J. Phy D 11, L15

Surplice, N.A. and D'Arcy, R.J. 1970 J. Phy E 3, 477

Surplice, N.A. and Brearley, W. 1975 Surf Sci 52, 62

Surplice, N.A., Müller, J. and Singh, B. 1975 Thin Solid Films 28, 179

Switendick, A.C. 1970 Solid State Commun 8, 1463

Switendick, A.C. 1975 Hydrogen in metals ed Vaziroglu, T.W. Plenum N.Y.

Switendick, A.C. 1976 J. Less-Comm Metals 49, 283

Tamm, P.M. and Schmidt, L.D.J. 1970 J. Chem Phy 52, 1150

Tamm, P.M. and Schmidt, L.D.J. 1971 J. Chem Phy 54, 4725

Taylor, T.N. and Estrup, D.T. 1974 J. Vac Sci & Tech 11, 244

Thomas, W. (Kelvin) 1898 Phil Mag 46, 82

Tompkins, H.G. 1977 Surf Sci 62, 293

Trapnell, B.M.W. in "Chemisorption" ed Garner, W.E. 1955 (Butterworth, London)

Ubbelohde, A.R. 1937 Proc Roy Soc (Lon) A159, 295, 306

Uhliq 1956 Act Metal 4, 541

Venema, A. 1959 Vacuum 9, 54

Vitt, R.S. and Kanji, O 1971 Metal Trans 2, 608

Wahlbeck, P.A. and Gilles, P. 1966 J. Amer Ceram Soc 49, 180

Watanabe, M. 1977 Nippon Kagaku Kaishi 12, 1762

Wall, W.E., Ribarsky, M.W. and Stevenson, J.R. 1980 J. Appl Phys 51, 661

Wallase, W.E. 1961 J. Chem Phys 35, 2159

Walerian, A. and Hans Joachim, M. 1976 Thin Solid Films 34, 103

Wasilewski, R.J. 1962 Trans AIME 222, 8

Weaver, J.H., Rosei, R. and Paterson, D.T. 1979 Phy Rev B19, 4855 and Refs therein

Weaver, J.H., Knapp, J.A., Eastman, D.E., Paterson, D.T. and Saterthwaite, C.B. 1977 Phy Rev Lett 39, 639

Wedler, G. and Strothenk, H. 1966 Z. Physik Chem N.F. 48, 86

Weinberg, W.H. and Merrill, R.D. 1972 Surf Sci 33, 493

Wells, A.F. 1975 Structural Inorganic Chem, Clarendon Press, Oxford

Westlake, D.G., Satterthwaite, C.B. and Weaver, J.H. 1978 (Nov) Phys Today, Nov 2

Williams, D.E.G. 1966 Mag Prop of Matter, Camelot Press Ltd, U.K.

Winger, E. and Bardeen, J. 1935 J. Phy Rev 48, 84 Longman Green & Co. Ltd

Wollan, E.O., Cable, J.W. and Koehler, W.C. 1963 J. Chem Phy Solid 24, 1141

Worsham, J.E., Wilkinson, M.K. and Shull, C.G. 1957 J. Phy Chem Solids 3, 303

Yakel, H.L. Jr. 1958 Acta Crystallogr 11, 46

Yamaguchi, S. 1969 J. Phy Soc Jap 27, 155

Yamaguchi, S., Koiwa, M. and Hirabayashi, M. 1966 J. Phy Soc Jap 21, 2096

Yamaguchi, S., Hiraga, H. and Hirabayashi, M. 1970 J. Phy Soc Jap 28, 1014

Yasuhiro Igasaki and Hiroji Milsuhashi 1978 Thin Solid Film 51, 33

Yoshinori Takahashi 1977 J. Phy Soc Jap 43, 1350

Zabov, E.V. and Tuerrdokhleb, S.K. 1975 Deposited Doc VINITI 2254

Zamir, D. and Colts, R.M. 1964 Phy Rev 134A, 666

Zemlyanov, M.G., Parshin, P.P., Rumyamsov, A.U., Tkach, K.G., Mayer, J. and Sudnik Hrgnkuwiz 1978 Report J.T.N.R.R.-14, 116625

Zisman, W.A. 1932 Rev Sci Inst 3, 367